INFORMATION TO USERS

This manuscript has been reproduced from the microfilm master. UMI films the text directly from the original or copy submitted. Thus, some thesis and dissertation copies are in typewriter face, while others may be from any type of computer printer.

The quality of this reproduction is dependent upon the quality of the copy submitted. Broken or indistinct print, colored or poor quality illustrations and photographs, print bleedthrough, substandard margins, and improper alignment can adversely affect reproduction.

In the unlikely event that the author did not send UMI a complete manuscript and there are missing pages, these will be noted. Also, if unauthorized copyright material had to be removed, a note will indicate the deletion.

Oversize materials (e.g., maps, drawings, charts) are reproduced by sectioning the original, beginning at the upper left-hand corner and continuing from left to right in equal sections with small overlaps.

Photographs included in the original manuscript have been reproduced xerographically in this copy. Higher quality 6" x 9" black and white photographic prints are available for any photographs or illustrations appearing in this copy for an additional charge. Contact UMI directly to order.

UMI®

Molecular Mechanisms Underlying Pattern Formation

in the Mouse Somatosensory Cortex

by

Raja' M. Abdel-Majid

Submitted in partial fulfillment of the requirements for the degree

of Doctor of Philosophy in Anatomy and Neurobiology

at

Dalhousie University

Halifax, Nova Scotia

November 1999

DALHOUSIE UNIVERSITY

FACULTY OF GRADUATE STUDIES

The undersigned hereby certify that they have read and recommend to the Faculty of

Graduate Studies for acceptance a thesis entitled "Molecular Mechanisms Underlying

Pattern Formation In The Mouse Somatosensory Cortex"

by   Raja' Abdel-Majid

in partial fulfillment of the requirements for the degree of Doctor of Philosophy.

Dated: _____ November 10, 1999 _____

External Examiner _____

Research Supervisor _____

Co-Research Supervisor _____

Examining Committee _____

_____

_____

ii

DALHOUSIE UNIVERSITY

iii

Dedication

I dedicate this dissertation to my husband, Omar Arafa, and my daughter, Rama Arafa, without whom I would have not been able to accomplish my goals. I am deeply grateful to Omar for his continuous support, encouragement and patience. He always reached out to help me in all aspects of my life in the past four years. To my little girl, I dedicate this dissertation with all my love.

Table of Contents

List of Figures

List of Tables

Abstract

Somatotopic maps are a fundamental feature in the organization of somatic sensory systems in the mammalian central nervous system. A striking example of these maps is present in the rodent cortex. Periphery-related patterns are evident in histological sections of layer IV of the primary somatosensory (SI) cortex in what is known as "barrels". The objective of the studies presented in this dissertation was to identify molecular and cellular mechanisms that underlie pattern formation in the cerebral cortex using the barrel field.

Barrelless (*brl*) mutant mice fail to develop neuronal arrangements of barrels in their SI cortex. High resolution linkage and physical maps and candidate gene analysis strategies were followed to isolate and identify the *brl* gene. We identified adenylyl cyclase type I gene (*Adcy1*) as the gene disrupted in *brl* mutants. These results provide the first evidence for the involvement of cyclic nucleotide signaling pathways in pattern formation of the SI cortex and additionally argues that neuronal activity plays a role in the formation of periphery-related patterns in the SI cortex.

In order to investigate whether cAMP-dependent protein kinase (PKA) acts in the same developmental pathway as *Adcy1*, we examined the SI cortex of five PKA null mutant mice (*Prkar1b, Prkar2a, Prkar2b, Pkaca,* and *Pkacb*). Our results reveal the presence of normal barrels in the SI cortex of all knockout mice, except for one that displayed poorly-formed barrels. These results suggest that *Adcy1* acts in the thalamocortical afferents, whereas PKA acts on layer IV cortical neurons.

Since neurotrophins have recently been implicated in synaptic plasticity during development, we investigated their role in the development of barrels in the SI cortex. Our results indicate that intracortical injections of exogenous brain-derived neurotrophic factor and neurotrophin-3 can produce a barrelless phenocopy, and that absence of neurotrophin-4/5 in knockout mice results in poorly-formed barrels. Collectively, these results indicate a new role for neurotrophins in pattern formation of the cerebral cortex.

List of Abbreviations and Symbols

°C	degrees Celsius
μg	microgram
μl	microliter
+ve	positive
3' UTR	3' untranslated region
5,7-DHT	5,7-dihydroxytryptamine
5-HT	serotonin
5-HT_{1B}	serotonin receptor subtype 1B
5-HT_{2A}	serotonin receptor subtype 2A
A	anterior
AC	adenylyl cyclase, protein
AC1	adenylyl cyclase type I, protein
AChE	acetylcholinesterase
Adcy1	adenylyl cyclase type I gene
Adcy1^{brl}	*Adcy1* mutation in *brl* mutant mice
AHC	selective media for growing YACs
ALBSF	anterolateral barrel subfield
AMP	adenosine monophosphate
AMPA	α-amino-3-hydroxyl-5-methyl-4-isoxazolepropionate

Anneal. temp.	annealing temperature
APV	2-amino-5-phosphonovaleric acid
ATP	adenosine triphosphate
b.p.	base pair
B6	C57BL/6J mouse strain
BDNF	brain-derived neurotrophic factor
brl	barrelless
BSA	bovine serum albumin
C	catalytic
Cα	catalytic subunit of the PKA enzyme, alpha isoform
Cβ	catalytic subunit of the PKA enzyme, beta isoform
Ca^{2+}/CaM	Ca^{2+} and calmodulin
CaM	calmodulin
CaM kinase II	Ca^{2+}/Calmodulin-dependent protein kinase II
Camk2a	Ca^{2+} calmodulin-dependent protein kinase II a gene
Camk2b	Ca^{2+} calmodulin-dependent protein kinase II b gene
cAMP	3', 5'-adenosine cyclic monophosphate
cDNA	complementary DNA
cM	centiMorgan
CNG	cyclic nucleotide gated channels
CNS	central nervous system
CO	cytochrome oxidase

CP	creatine phosphate
CPK	creatine phosphokinase
D11Mit#	Whitehead Institute micorsatellite markers, e.g. *D11Mit2*
DAB	diaminobenzidine
DTT	dithiothrietol
E #	embryonic day, e.g. E10
ETn	early retrotransposon
EUCIB	European Collaborative Interspecific Mouse BackCross
Ewsh	Ewing sarcoma homologue
F#	forward primer, e.g. F1
FGF2	fibroblast growth factor 2
FISH	fluorescence in situ hybridization
fmole	femtomole
FP	forepaw
G protein	guanosine triphosphate binding protein
GAP-43	growth associated protein-43
GDB	genome database
Gk	glucokinase activity
GTP	guanosine triphosphate
HP	hindpaw
IBMX	3-isobutyl-1-methyl-xanthine

Igfbp1	insulin-like growth binding protein 1
Igfbp3	insulin-like growth binding protein 3
Ikaros	zinc finger protein, subfamily 1A, 1
kb	kilo base pair
KO	knockout
LAMP	limbic system-associated membrane protein
LDS	lauryl dodecyl sulfate
LGN	lateral geniculate nucleus
Lif	leukemia inhibitory factor
LJ	lowerjaw
LTD	long-term depression
LTP	long-term potentiation
M	medial
Maoa	monoamine oxidase A gene
MAOA inhibitor	monoamine oxidase A inhibitor
mg	milligram
ml	milliliter
mm	millimeter
mRNA	messenger ribonucleic acid
Nfh	neurofilament, heavy polypeptide
ng	nanogram
NGF	nerve growth factor

Nissl	cresyl violet stain
NMDA	N-methyl-D-aspartate receptor
NMDA ε	NMDA receptor regulatory subunit 2, type ε
NR1	NMDA regulatory subunit 1
NR2	NMDA regulatory subunit 2
NT-3	neurotrophin-3
NT-4/5	neurotrophin-4/5
NT-6	neurotrophin-6
NT-7	neurotrophin-7
Ntf5	neurotrophin-4/5 gene
ODC	ocular dominance columns
P#	postnatal day
PB	phosphate buffer
PBS	phosphate-buffered saline
PCR	polymerase chain reaction
PFGE	pulse-field gel electrophoresis
PKA	cAMP-dependent protein kinase
Pkac2a	protein kinase, cAMP dependent catalytic, type II alpha
Pkac2b	protein kinase, cAMP dependent catalytic, type beta
PKC	protein kinase C
PLC-β	phospholipase C-β
PLC-β-1	phospholipase C β-1

PMBSF	posteromedial barrel subfield
pmole	picomole
POm	posterior medial nucleus of the thalamus
Prkar1b	protein kinase, cAMP dependent regulatory, type I beta
Prkar2a	protein kinase, cAMP dependent regulatory, type II alpha
Prkar2b	protein kinase, cAMP dependent regulatory, type II beta
R	regulatory
R#	reverse primer, e.g. R1
RFLP	restriction fragment polymorphism
RIα	regulatory subunit of the PKA enzyme, alpha isoform
RIβ	regulatory subunit of the PKA enzyme, beta isoform
RIIα	regulatory subunit of the PKA enzyme, alpha isoform
RIIβ	regulatory subunit of the PKA enzyme, beta isoform
SDS	sodium dodecyl sulfate
SI	primary somatosensory cortex
SII	secondary somatosensory cortex
STS	sequence-tagged site
TBE	tris-borate-EDTA buffer
TCAs	thalamocortical afferents
Tcn-2	transcobalamin 2
Tg	transgenic
Trk	tyrosine kinase

TTX	tetrodotoxin
V	trigeminal
VB	ventrobasal complex of the thalamus
YAC	yeast artificial chromosome
YNB	yeast nitrogen base
YPD	yeast extract-peptone-dextrose

Acknowledgments

Chapter 1

Introduction

1.1 Functional Localization in the Cerebral Cortex

The adult mammalian cerebral cortex is divided into numerous regions, each of which is functionally distinct and has its own cytoarchitecture and connectivity. Brodmann (1909) divided the human cerebral cortex into 52 areas based on size, shape, density and connections of neurons in each of these areas. Similarly, the cerebral cortex is divided into functional areas such as sensory, motor, and association cortices.

Despite the fact that some differences exist between areas in the neocortex, some basic features and characteristics are shared among them. For instance, the neocortex is organized into six layers with neurons in layers V and VI projecting to subcortical regions and neurons in layer IV receiving inputs from the thalamus. On the basis of these similarities in structure and function it was proposed that different areas of the neocortex share a common principle of organization (Lorente de Nó, 1938; 1949; Mountcastle, 1978; Powell, 1981). If this is true, then the question is: when and how does the structural and functional specification of cortical areas happen?

1.2 Development of the Central Nervous System

The development of the vertebrate central nervous system (CNS) starts at the gastrula stage of embryogenesis. The dorsal mesoderm of the gastrula induces the overlying ectoderm to form a sheet of neuroectodermal cells, the neural plate. The neural plate folds to give rise to the neural tube and the neural crest. The anterior part of the neural tube undergoes a series of swellings and flexures that form different regions of the brain, while the caudal part retains its simple tubular structure to form the spinal cord.

Neural crest cells migrate away from the neural tube to form the peripheral nervous system.

During development cells undergo numerous cell divisions that will increase cell numbers, a process called proliferation, followed by the generation of cellular diversity, a process called differentiation. Differentiated cells are then organized into tissues and organs that are formed in an orderly fashion, a process called morphogenesis. The regulation of these processes is under the control of intrinsic, predetermined "genetic" factors in addition to extrinsic influences from the environment.

1.2.1 Cortical Development

Neocortical cells are generated in the pseudostratified telencephalic neuroepithelium that lines the ventricular zone (Sauer, 1935; Fujita, 1963; Rakic, 1974; Bayer and Altman, 1991). These cells, known as germinal, progenitor, or precursor cells, give rise to all the neurons and glia in the brain. As symmetrical division continues, progenitor cells migrate away from the ventricular zone to form the subventricular zone and take over the production of committed cells. Corticogenesis starts with the first asymmetric division to produce neurons that migrate towards the pial surface along the processes of radial glia (Rakic, 1972; 1978; 1981) to form the preplate or the primordial plexiform zone (Marin-Padilla, 1971). The preplate is then divided into two layers: the superficial marginal zone (future layer I) and deep subplate (Luskin and Shatz, 1985a; 1985b). The cortical plate lying between the marginal zone and the subplate thickens as new waves of migrating cells move through the subplate and take their position forming

deeper layers first (Berry and Rogers, 1965; Lund and Mustari, 1977, Bayer and Altman, 1991).

1.2.2 Pattern Formation

Differentiated cells are not randomly distributed. They are spatially arranged in an orderly manner to form specific patterns that can be generated by mechanisms that involve cell-to-cell interaction. Three different general mechanisms have been proposed to explain how patterns are formed: induction, positional information, and prepattern.

Induction is a mechanism by which a signal from one cell type or tissue influences the proliferation, differentiation and morphogenesis of neighboring cells. Spemann and Mangold (1924) were the first to draw attention to the presence of a specific region (dorsal lip of the blastomere) that is important for the formation of the whole embryo. Using differently pigmented embryos from two species of newt they were able to identify the origin of tissues in the embryo. Transplanted gastrula tissue developed according to its new environment with the exception of the dorsal lip. It continued to be a blastopore lip and induced gastrulation and embryogenesis in the surrounding tissue. In another set of experiments, Spemann (1938) transplanted ectoderm of a frog gastrula into the mouth region of a salamander gastrula. He found that the mesoderm was able to induce a piece of ectoderm of another species; however, tissue developed according to genetic information present in the ectoderm. This was the first set of experiments that revealed the importance of extrinsic influences on the development of an embryo and on patterning. In vertebrates, induction plays a greater role than in invertebrates, where in the

latter, development depends mainly on lineage rather than on an interaction with a neighboring cell.

In the hypothesis known as "positional information", Wolpert (1969) proposed that each cell has intrinsic information about its position and can interpret its position with reference to other cells in the system. The best studied example of positional information is the morphogenesis of the vertebrate limb (Weiss, 1939; Wolpert, 1977). Basically, there are two regions that determine the formation of a limb, the zone of polarizing activity (ZPA) and the progress zone. Depending on the position of a cell in the ZPA it will either form a thumb or index finger (anteroposterior axes) and depending on the time that the cell spends in the progress zone it will form either a radius or a digit (proximodistal axis). It is believed that positional information is achieved by a gradient of morphogens (molecules that induce morphogenesis) and cells will respond differently depending on their position in the gradient.

The "prepattern" hypothesis was first described by Stern in 1968. He proposed that a certain gene, a pattern gene, controls the onset of differentiation and hence patterning. In order to explain how a pattern gene can affect patterning, he hypothesized that during development there are spatial differences between differentiated cells, a prepattern, that precedes the final morphological pattern. Moreover, intrinsic and extrinsic factors can enhance differences between prepatterns or even create new ones. Accordingly, different genotypes will respond differently to a prepattern or can have different prepatterns.

1.2.3 Development of Regional Specialization

At early stages during development, the immature cortex seems to be uniform and the area-specific features observed in the mature cortex are not present. So when and how does regional specialization occur? Two hypotheses were proposed to answer this question. In one extreme, cortical areas are entirely prespecified in the neuroepithelium of the ventricle zone. In other words, there is a fate-mosaic or "protomap" in the progenitor cells of the ventricular zone and the characteristics of each area are genetically determined (Rakic, 1988). This protomap is translated via radial glial scaffolding in the form of ontogenetic columns. In the other extreme, the cortical plate is a homogenous "protocortex" and area specific features are imposed on it by outside influences (O'Leary, 1989). Accordingly, characteristics of an area result from an interaction between the immature cortex and the extrinsic signals, most probably thalamocortical afferents. Of course, neither of these extremes is probably completely true. Both authors recognize the contribution of both genetic and extrinsic factors in the development of regional specialization in the neocortex with the protomap concept giving more weight to genetic factors and the protocortex concept giving more weight to extrinsic signals as a major event in the formation of area-specification in the cortex.

Several lines of evidence support the protomap, or radial unit, hypothesis. Immunostaining experiments revealed that precursor cells produce segregated pools of cells, either neurons or glia, when an antibody marker against radial glial cells was used (Levitt and Rakic, 1980; Levitt et al., 1981; Levitt et al., 1983). Retrovirus gene transfer experiments, which utilize the infection of a single progenitor cell with a retrovirus that

carries a specific marker that enables the visualization of these cells by histochemistry, revealed the presence of clones of different sizes that contained only neurons or glia (Luskin et al., 1988; Price and Thurlow, 1988; Walsh and Cepko, 1988, Parnavelas, 1990). Consistent with the protomap hypothesis, McConnell (1988a; 1988b) has provided evidence for laminar commitment at an early stage during development. In these experiments, she manipulated the environment through which the cortical neurons migrate in order to determine the role of extrinsic signals. For instance, neurons that would normally migrate to layers V and VI were transplanted into an environment in which neurons migrate to superficial layers. Neurons in this case migrated to layers V and VI, suggesting that postmitotic neurons are committed to a specific lamina and extrinsic cues do not change their fate. In subsequent studies, McConnell and Kaznowski (1991) determined the time at which these neurons become committed; this decision is made during the mid S-phase of the final cell division. More recently, two studies have reported that distinct patterns in the cerebral ventricle and in the cortical plate are present in a region-specific and lamina-specific pattern as observed from the expression of molecules that are intrinsic to the cortex such as ephrins and cell-adhesion surface molecules (Miyashita-Lin et al., 1999; Donoghue and Rakic, 1999).

Although the bulk of evidence supports the protomap hypothesis, some studies disagree with this model and instead provide evidence favoring the protocortex model. Retrovirus-labeling indicated that the same progenitor cell can produce clones that are widely distributed in the neocortex and are scattered over many areas (Walsh and Cepko, 1992). These results are consistent with the results of O'Rourke (1992) who reported that

only 80% of labeled newborn neurons migrated radially and the rest migrated tangentially from one functional region into another. Perhaps the most compelling evidence was provided by heterotopic transplantation. Schlaggar and O'Leary (1991) have demonstrated that the specific features of the immature cortex are not set at birth and that certain areas of the cortex can develop architectural features that are normally associated with other cortical regions. In the first set of experiments, they transplanted a piece of late-embryonic occipital cortex to the sensorimotor cortex of a newborn rat and retrogradely double labeled layer V projection neurons using two different dyes injected into the pyramidal decussation and the superior colliculus (Stanfield et al., 1982; Stanfield and O'Leary, 1985; O'Leary and Stanfield, 1989). Results revealed that in mature animals, layer V pyramidal neurons of the transplanted visual cortex maintained the corticospinal projections which are usually lost during development. In another set of studies, they evaluated the plasticity of area-specific features. Heterotopical transplants were again used, but this time they looked at the anatomical organization of the transplant (Schlaggar and O'Leary, 1991). The results of these experiments revealed that the transplant developed cytoarchitectonic features that were similar to their new location and not to the donor. These results, along with results from the first set of experiments, indicate that area-specific features are not determined at birth in the developing neocortex, and that extrinsic signals play an important role in cortical regionalization.

In the last few years a new hypothesis for cortical specification has emerged. Levitt and colleagues (1993) has proposed the "progressive acquisition of phenotype" concept. It states that the cerebral wall has fated uncommitted precursor cells and that

their initial position is controlled genetically. Later on extrinsic signals will guide the choices of differentiated neurons by progressively limiting the choices that these cells can make. Such a hypothesis was deduced from their results of cortical transplantation along with the identification of a molecular marker for the limbic system, limbic system-associated membrane protein (LAMP) (Levitt, 1984; Levitt et al., 1986, Zacco et al., 1990). LAMP is only expressed in developing limbic cortical areas but not in the developing neocortex (Horton and Levitt, 1988). Transplanting perirhinal cortex or sensorimotor cortex from E12 rat fetuses, which contains only precursor cells, followed by immunostaining for LAMP revealed that cells differentiated according to their new location and not according to their origin (Barbe and Levitt, 1991; 1992). On the other hand, if the same experiments were repeated with a transplant from E15 or older rat fetuses, it was found that cells differentiated according to their origin. Taken together, these results indicate that developmental time is very important in controlling the cell's fate to a particular phenotype.

1.2.4 Generation of Neural Connections

The function of the central nervous system depends on the precise pattern of connections that neurons make among themselves and with their targets. Once a cell has differentiated into a neuron rather than a glial cell, it is faced with more decisions. It has first to extend an axon, select its pathway, select its correct target and lastly refine the connections with its target "address selection" (for review see Goodman and Shatz, 1993). Genetics establish the initial pattern of neuronal connections which is then modified by neuronal activity, a process that continues throughout life (Purves et al.,

1986; Bailey and Chen, 1989). Generation of precise neuronal connections during development can be explained by two mechanisms: activity-dependent and activity-independent mechanisms. The first two processes, pathway selection and target selection, do not depend on neuronal activity while address selection is activity-dependent.

1.2.4.A Pathway Selection

Pathway selection is the process wherein axons travel along a route to a particular region in the embryo. A good example of pathway selection is found in the neuromuscular junction system. Motor axons can find their appropriate muscle target even when activity is blocked (Twitty and Johnson, 1934; Twitty, 1937) or when functional neurotransmitter receptors are ablated (Westerfield et al., 1990). Several mechanisms have been proposed for the specificity of axonal growth including contact guidance, gradient of adhesivity, axon-specific migratory cues, specific growth cone repulsion, and multiple guidance cues.

1.2.4.B Target Selection

After axons reach the correct area, they have to recognize a specific target in that area to form specific connections. The best studied example of target selection is retinal axons in frogs and fish in which retinal axons from each eye project to the opposite side of the optic tectum. Sperry (1951) has demonstrated that retinal axons send a pioneering axon to a specific site within the tectum which precedes other axons and acts as a guide for them. Later on, he proposed that axons and their matching targets have a chemical identification tag that can connect them in a selective manner (Sperry, 1965). Recently, it has been demonstrated that retinal axons express receptors for fibroblast growth factors

where they are rapidly diminished upon arrival to the tectum, hence slowing their growth and allowing them to find their targets (McFarlane et al., 1995). It has been proposed that retinal axons can find their targets based on gradients of adhesivity (Marchase et al., 1976; Gottlieb et al., 1976; Walter et al., 1987; Cox et al., 1990; Baier and Bonhoeffer, 1992).

1.2.4.C Address Selection

The initial patterns that are formed between neurons and their targets are then refined and remodeled, a process called "address selection". As described above, motoneurons and muscles do not require activity for the development of connections; however, activity-dependent mechanisms are required in the refinement of motor projections. Initially, motoneurons form several synapses with a muscle fiber, an activity-independent mechanism, but during development branches of motor axons retract such that one muscle fiber is innervated by one motor axon. This refinement of connections is an activity-dependent process (Redfern, 1970; Brown et al., 1976; Purves and Lichtman, 1980).

Most of our knowledge about activity-dependent mechanisms during development comes from studying the visual system. In the visual system of vertebrates, retinal axons send projections to the tectum (in lower vertebrates) or to the thalamus (in mammals). Retinal axons initially project to their targets in an activity-independent manner to form a coarse topographic map using molecular and cellular cues such as cell adhesion molecules, extra cellular molecules and diffusible factors. Once retinal axons reach their target, they form arbors that extend over a wide area followed by retraction and

remodeling to restrict their axonal arborization which will refine the topographic map, events that require activity (for review see Constatine-Paton et al., 1990; Shatz, 1990). Blockade of retinal neural activity during the period of refinement by tetrodotoxin (TTX, a poison that blocks action potentials by blocking voltage-sensitive sodium channels) in fish, frog, chick, and rodents prevents the fine refinement of retinotectal projections, although coarse topographic maps are still retained (Harris, 1980; Meyer, 1982; 1983; Schmidt and Edwards, 1983; Harris, 1984; Fawcett and O'Leary, 1985; Kobayashi et al., 1990).

The best studied example of activity-dependent mechanisms in cortical development come from studies of the visual cortex of higher mammals. In the adult visual cortex, inputs from the lateral geniculate nucleus (LGN) from each eye are segregated in layer IV onto cortical cells that are driven by one eye or the other. These eye-specific domains are the anatomical basis of ocular dominance columns (ODC). Electrophysiological recording confirmed that the majority of cortical neurons in layer IV will respond exclusively to stimulation of one eye only (Hubel and Wiesel, 1963; Hubel et al., 1977; Shatz and Stryker, 1978). The pattern of ODC in layer IV is not evident at birth as LGN afferents are overlapped, and appears during development during a period of LGN axonal remodeling and retraction to form the adult pattern of eye-specific domains (Rakic, 1977; LeVay et al., 1978; 1980). Activity-dependent mechanisms play a role in segregation of LGN axons and formation of ODC in the visual cortex where blocking activity from both eyes by intraocular injections of TTX prevents the segregation of retinogeniculate

afferents of the thalamus (Shatz and Stryker, 1988) and the formation of ODC in cortical layer IV (Stryker and Harris, 1986).

The above findings implicate neural activity in the formation of ODC, but do not explain how activity permits the segregation of LGN axons in layer IV. The answer to this question was provided by the pioneering studies of Hubel and Wiesel (1970; 1977) in which they determined that the spatial and temporal pattern of neuronal activity between both eyes plays a major role in the formation of ODC. Changing the pattern of activity during the critical period by monocular deprivation, closure of one eye by eyelid suture at birth, results in a dramatic physiological and anatomical shift in ODC in the visual cortex in favor of the open eye (Hubel and Wiesel, 1970; Hubel et al., 1977; Shatz and Stryker, 1978); however, binocular deprivation does not result in the same dramatic effects on ODC in the cortex (Wiesel and Hubel, 1965). Stryker and Strickland (1984) provided direct evidence for the importance of patterned activity and competition between LGN axons from both eyes in the formation of ODC. In these experiments, they blocked retinal activity in both eyes by TTX and then electrically stimulated the optic nerve. Their results revealed that when both optic nerves were synchronously stimulated ODC did not form, but when they were stimulated asynchronously ODC were formed. At the cellular level it has been proposed that N-methyl-D-aspartate (NMDA) receptors play an important role in mediating activity-dependent refinement of topographic maps in the retinotectal pathway (Meyer, 1983; Schmidt and Edwards; 1983; Cline et al., 1987; Schmidt, 1990; Simon et al., 1992) and in the mammalian visual cortex (Tsumoto et al., 1987; Fox et al., 1989; Miller et al., 1989; Fox and Daw, 1993).

1.3 The Somatic Sensory System

The somatic sensory system processes information such as touch, vibration, pressure, pain and temperature derived from different parts of the body (Kaas and Pons, 1988; Kaas, 1990), thus allowing animals to respond to external and internal stimuli exerted on the body. The somatosensory system has two components: the spinal somatosensory pathway, which transmits sensory information from the upper and lower parts of the body; and the trigeminal somatic sensory system which deals with sensory information arising from the face. In humans, sensory information arriving into the cortex is processed in four distinct regions corresponding to Brodmann's areas 3a, 3b, 1 and 2. Area 3b is generally termed the primary somatosensory cortex (SI) and responds primarily to cutaneous stimuli. Electrophysiological mapping studies in humans and primates revealed that the somatosensory cortex contains an orderly representation of peripheral receptors, known as somatotopic maps (Kaas, 1983; Corsi, 1991). In humans, inputs from the periphery are represented in specific locations in the neocortex, hence the term homunculus or "the little man", moreover, segregated inputs are represented in proportion to the degree of innervation. Thus, in humans, heavily innervated areas such as the face, tongue and thumb have the largest representation in the somatosensory cortex. Similar distortion has been observed across species. For example, the rodent brain devotes a substantial area of the somatosensory cortex to the representation of the large mystacial vibrissae on the snout area, while raccoons over-represent their paws.

Somatic sensory information is processed first in the primary somatosensory cortex (SI) and is then distributed to other cortical regions including the secondary

somatosensory cortex (SII), the motor cortex, and subcortical regions such as the thalamus. The SII cortex receives divergent information from the SI cortex and sends projections in turn to the limbic system.

1.4 The Primary Somatosensory Cortex in Rodents

A striking example of somatotopic maps is present in the SI region of the parietal cortex of rodents (area 3 in the mouse [Caviness, 1975]). Sections parallel to the pial surface through layer IV of the SI cortex reveal cytoarchitectonic features termed "barrels" (Woolsey and Van der Loos, 1970). Barrels are the somatotopic representation of the sinus hairs and mystacial vibrissae on the face and other parts of the body. This region of layer IV is called the "barrel field" and the cortical region that contains the barrel field is called "barrel cortex". The total area of the barrel field in the mouse ranges between 2.1 and 2.8 mm^2 and consists of the anterolateral (ALBSF), posteromedial (PMBSF), lower jaw, forepaw and trunk barrel subfields (Figure 1.1).

1.4.1 General Appearance of Barrels

Barrels in the ALBSF are the cortical representations of the sinus hairs on the contralateral side of the muzzle area, while barrels in the PMBSF represent the contralateral large mystacial vibrissae (whiskers). Barrels in the ALBSF region are circular in shape, small and are randomly packed, whereas barrels in the PMBSF are elliptical, larger and organized in an orderly fashion (Woolsey and Van der Loos, 1970). This dissertation will be focusing only on barrels present in the PMBSF which represent the contralateral mystacial vibrissae.

Figure 1.1 A schematic drawing showing the area of the primary somatosensory cortex (SI; gray area) in the mouse brain (top) and the barrel field in a flattened section of layer IV of the SI cortex (bottom). The barrel field consists of several subfields that represent the sinus hairs on the face and different parts of the body. Barrels in the PMBSF are the largest and are arranged in oval rings, while barrels in the ALBSF are circular and are randomly distributed. Abbreviations: HP, hindpaw; FP, forepaw; LJ, lowerjaw; PMBSF, posteromedial barrel subfield; ALBSF, anterolateral subfield. Arrows indicate section orientation; A, anterior; M, medial.
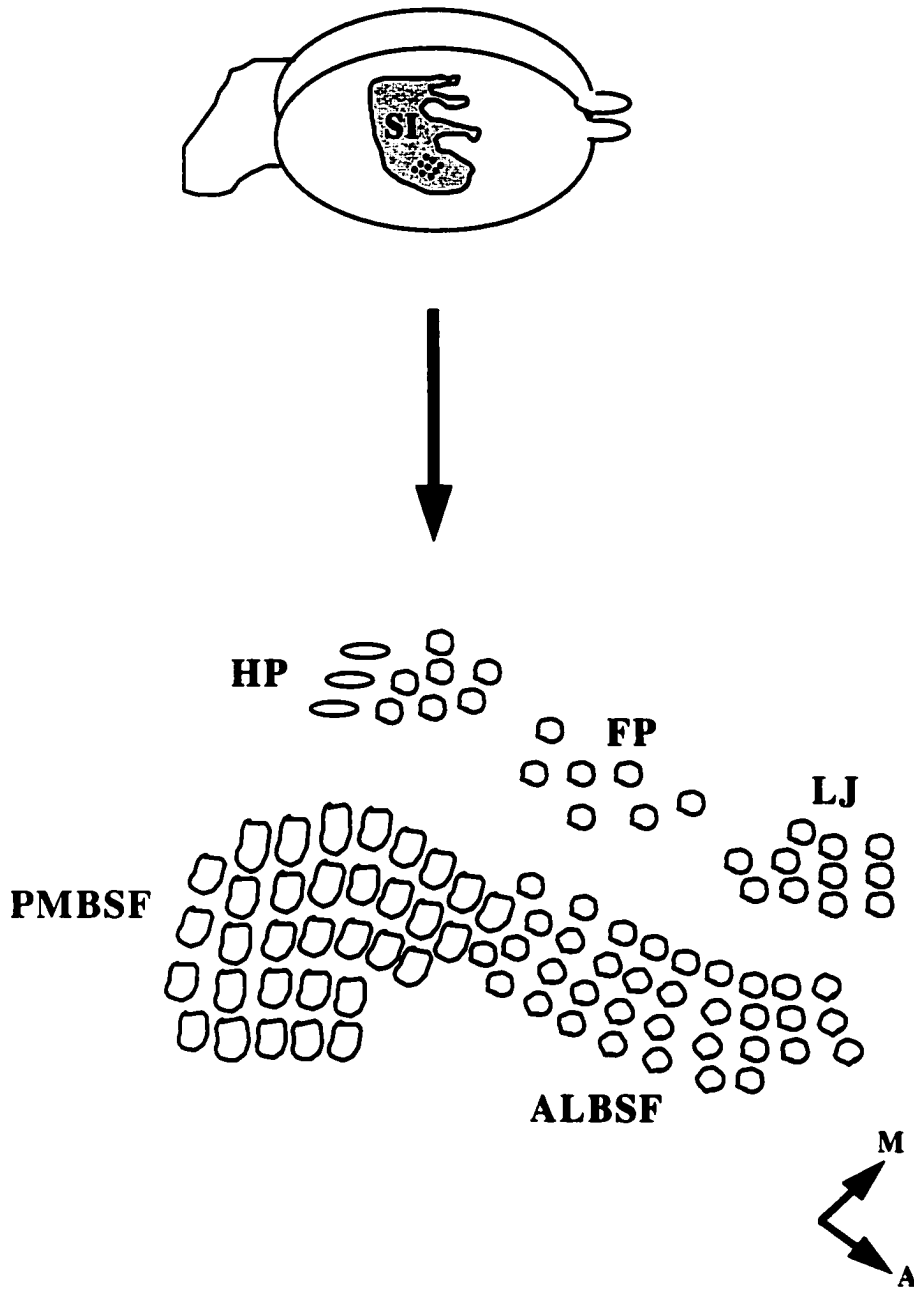
Figure 1.1

In cresyl violet (Nissl) sections cut parallel to the pial surface overlying the SI

cortex barrels have the appearance of oval-shaped rings (Figure 1.2A). Neurons in a

barrel are arranged in a cell-dense ring surrounding a cell-sparse center "hollow", and are

separated from each other by hypocellular "septa" (Woolsey and Van der Loos, 1970).

The density of neurons in the hollow is reduced by about 50% relative to the sides,

whereas the density of synapses is higher by 40% (White, 1976). The 34-40 barrels

present in the PMBSF are the largest in the barrel field (150 - 380 μm) and occupy 40%

of the total barrel field area. In coronal sections, barrels have a columnar appearance with

the barrel walls tapering at the most superficial and deepest regions of layer IV (Figure

1.2B). It is due to this anatomical shape that barrels derived their name.

1.4.2 Types of Barrels

Among all species examined to date, barrels were found to be present only in

rodents, lagomorphs and some suborders of marsupials (Weller, 1972; Woolsey et al.,

1975b; Rice and Van der Loos, 1977; Rice, 1985; Rice et al., 1985; Waite et al., 1991,

Weller, 1993; Waite et al., 1998). Other species such as carnivores and primates lack

barrels in their SI cortex (Feldman and Peters, 1974; Rice 1985b; Sur et al., 1980; Rice et

al., 1993). Three types of cytoarchitectonic barrels have been identified in various

species: hollow, solid and indistinct. Hollow barrels are present in the mouse where

neurons in the barrel wall surround an area of lesser cell density (Woolsey and Van der

Loos, 1970). Solid barrels are present in the rat SI cortex where the center of the barrel

contains cell dense clusters (Welker and Woolsey, 1974; Weller, 1972). Finally,

Figure 1.2 Nissl-stained sections cut parallel to the pial surface through layer IV of the mouse SI cortex (A) and in the coronal plane through the PMBSF (B). **A.** 50μm-thick sections cut tangential to the pial surface overlying the SI using vibratome and stained with cresyl violet (Nissl) stain. Barrels in the PMBSF are arranged in cylindrical rings "sides" surrounding a cell-sparse center "hollow" and separated from each other by hypocellular "septa" (arrow heads). Scale bar = 400 μm. **B.** In coronal sections, barrels have the appearance of columnar organization that spans the whole thickness of layer IV. Barrels derive their name from their appearance in this orientation where the septa appear to be wider at the upper and lower aspects of layer IV (arrow heads). Abbreviations: PMBSF, posteromedial barrel subfield; ALBSF, anterolateral barrel subfield. Barrel rows are lettered A-E. Scale bar = 200 μm.
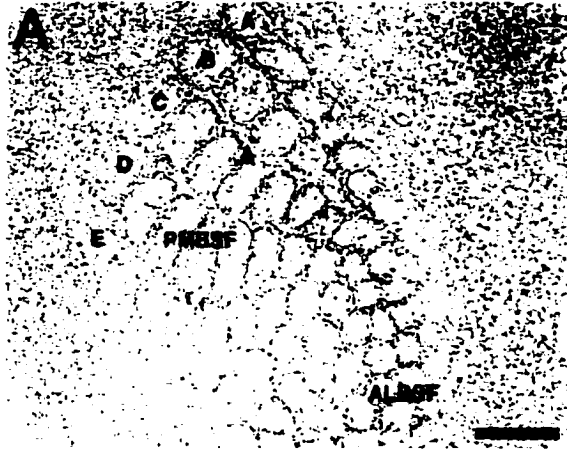
Figure 1.2

indistinct barrels were identified in some species such as the gray squirrel, flying squirrel and rabbit (Woolsey et al., 1975b; Rice et al., 1985). In these species barrels were hard to discern and septa were always absent. Their presence was identified by superimposing adjacent sections, and by correlating the anatomical results with the electrophysiological recording results from this area (Woolsey, 1958).

1.4.3 Organization of the Mouse PMBSF

There is an isomorphic relationship between the distribution of the mystacial vibrissae in the whisker pad and cortical barrels. Barrels are arranged in five rows (A-E) (Woolsey and Van der Loos, 1970) with the larger elements of each row lying caudally and the smaller ones rostrally (Figure 1.3). Caudally, the rows are bordered by a set of four large, straddling barrels denoted α, β, γ, δ. In most mice, rows A and B have four units each, row C has 6 units, row D has 7 units, and row E has 8 units (Woolsey and Van der Loos, 1970). Barrels in the C row are the largest and are composed of about 2000 neurons (Pasternak and Woolsey, 1975; Curcio and Coleman, 1982) with myelinated and unmyelinated axons concentrated in the barrel sides and septa (White, 1976).

1.4.4 Neuronal Components of the Barrel Field

The majority of neurons in the barrel field are stellate cells. These cells are divided into two classes on the basis of their dendritic morphology: Class I (spiny) stellate cells and Class II (smooth) stellate cells (Lorente de Nó, 1922; Woolsey et al., 1975a; Simons and Woolsey, 1978; Harris and Woolsey, 1981; Simons and Woolsey, 1984). Class I stellate cells have small somata and spiny dendrites, while Class II cells

Figure 1.3 A schematic drawing representing the mouse whisker pad on the snout (left) and corresponding barrels in the PMBSF of the contralateral SI cortex (right). Barrels are arranged into rows and arcs (white arrows) that replicate the distribution of whiskers in the periphery, and each barrel is stimulated by its whisker. Barrels are arranged in five rows (A-E) and straddled posteriorly by four large elements (α, β, γ, δ). Rows A and B contain 4 units (A1-A4), row C contains 6 units (C1-C6), row D contains 7 units (D1-D7) and row E contains 8 units (E1-E8). Barrels in row E lie more medially (black area) and the straddlers (hatched area) lie more posteriorly.
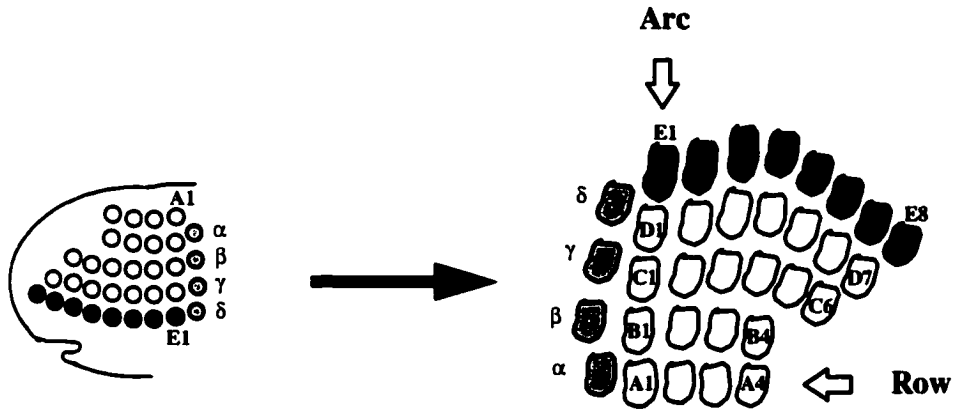
Whisker pad   **Cortex**

Figure 1.3

have larger somata, and smoother and longer dendrites. Both types of cells are present in the barrel hollow as well as in barrel sides. These two classes are further subdivided (a, b, c, d) on the basis of the orientation of their dendrites and the location of their somata with respect to the parent barrel (Woolsey et al., 1975a).

Class II stellate cell axons are long, thick, highly branched and are directed towards the pial surface as compared to Class I neuronal axons that are thin and directed towards the white matter (Harris and Woolsey, 1983). As for dendritic morphology, neurons that are present in the barrel hollow have radial dendritic fields while neurons present in the barrel side have an eccentric dendritic tree directed toward the barrel hollow (Woolsey et al., 1975a; Harris and Woolsey, 1983; Greenough and Chang, 1988). Both axons and dendrites of the two types of stellate cells terminate into barrel boundaries (Harris and Woolsey, 1983; Simons and Woolsey, 1984). Only 15% of neurons have dendrites extending to neighboring barrels (Woolsey et al., 1975a; Simons and Woolsey, 1984). In cells where dendrites extended to adjacent barrels, it was found that their axons also extended to adjacent barrels (Harris and Woolsey, 1983). The above organization of processes suggests that the majority of neurons in a barrel respond to stimulation of one whisker while the minority of neurons respond to stimulation of neighboring whiskers. These anatomical results have confirmed the one-to-one functional relationship between the whisker and its barrel and suggest a closer functional relationship among barrels in the same row than barrels of different rows (Welker, 1971; Simons, 1978; Simons and Woolsey, 1979).

1.4.5 Inputs to the Barrel Field

The barrel field receives massive input from cortical and subcortical structures. Some of these afferents are related to processing somatosensory information from the whiskers while others are thought to modulate the activity and, hence, response of neurons in the barrel field .

1.4.5.A Thalamocortical Inputs

Vibrissal information is conveyed to the barrel field via thalamocortical afferents arising in the ventrobasal (VB) complex (or ventral posterior nucleus) and posterior medial (POm) nucleus of the thalamus. Thalamocortical afferents (TCAs) arising from VB (Killackey, 1973; Killackey and Leshin, 1975; Wise and Jones, 1978; Jensen and Killackey, 1987a) terminate into layer IV of the SI cortex forming periphery-related clusters (Lorente de Nó, 1922; Killackey, 1973; Killackey and Leshin, 1975). Labeling of individual VB afferents revealed that they terminate mainly in two layers of the barrel cortex: in the barrel hollow of layer IV (Figure 1.4) extending into layer III and into the border of layers V and VI (Wise and Jones, 1978; Keller et al., 1985; Bernardo and Woolsey, 1987; Jensen and Killackey, 1987a; Agmon et al., 1993).

TCAs to the barrel field form asymmetrical synapses in the barrel hollow (White, 1976; White, 1978; Keller et al., 1985; Keller and White, 1987; Lu and Lin, 1993; White et al., 1997) that are found on dendritic spines and shafts of spiny and smooth stellate cells (White, 1976; Hersch and White, 1981; Benshalom and White, 1986; White et al., 1997). They exert an excitatory influence, through glutamate (Tsumoto, 1990; Agmon and O'Dowd, 1992), on their postsynaptic cortical cell targets (Carvell and Simons, 1988;

Figure 1.4 A schematic drawing representing the termination of the thalamocortical afferents (TCAs) from the ventrobasal complex and serotonergic (5-HT) inputs from dorsal raphe nucleus into layer IV of the SI cortex. TCAs (solid lines) terminate into the hollow of the barrel forming dense clusters of terminal arborizations that are confined within the barrel domains. They synapse on neurons present in the barrel hollow, which have radially dendritic orientation, and on neurons in the barrel sides, which have eccentric dendritic orientation. Similarly, serotonergic inputs (dotted lines) to layer IV of the SI cortex during the first two weeks of postnatal life form dense clusters of arborizations that matches the pattern of the TCAs termination.

TCA

5-HT
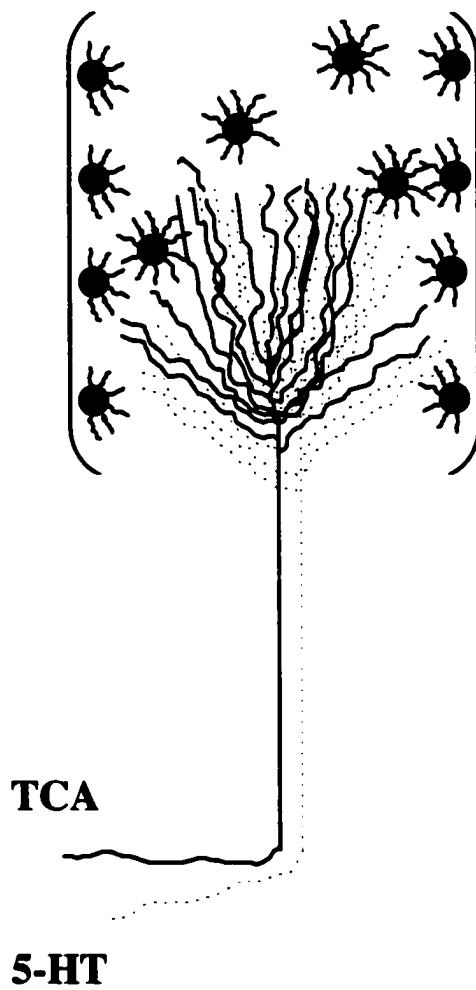
Figure 1.4

Agmon and Connors, 1992). These excitatory synapses are functional at birth (Kim et al., 1995) and activity can be evoked in the SI cortex by peripheral stimulation in neonatal rats (McCandlish et al., 1993; Landers and Sullivan, 1999).

Projections from the POm nucleus to the barrel field terminate in the septa between barrels in a complementary pattern to that of VB afferents (Koralek et al., 1988; Chmielowska et al., 1988; 1989; Lu and Lin, 1993). Projections of the POm nucleus to the barrel field are topographically organized; that is, there is an orderly relationship between projection neurons in the POm nucleus and their cortical target (Nothias et al., 1988; Fabri and Burton, 1991).

1.4.5.B Serotonergic Input

Serotonergic afferents innervate the cortex starting at embryonic day (E) 16 (Lidov and Molliver, 1982; Lauder, 1990) and continue through early postnatal life (Fujimiya et al., 1986; D'Amato et al., 1987; Hohmann et al., 1988; Rhoades et al., 1990). The barrel field receives transient serotonergic hyperinnervation during the first two weeks of perinatal life (Fujimiya et al., 1986; D'Amato et al., 1987; Aitken and Tork, 1988; Rhoades et al., 1990; Blue et al., 1991; Erzurumlu and Jhaveri, 1992). By postnatal day (P) 1 whisker row patterns start to emerge and by P2 whisker-related patterns are identified. Serotonergic innervation arises mainly from the dorsal raphe nucleus in the brainstem (Bennett-Clarke et al., 1991) and serotonin (5-HT) immunoreactivity matches the pattern of the thalamocortical afferents (Fujimiya et al., 1986; D'Amato et al., 1987; Rhoades et al., 1990).

There is a temporal and spatial relationship between the TCAs and serotonergic terminals (Figure 4); TCAs transiently express 5-HT$_{1B}$ receptor (Leslie et al., 1992; Bennett-Clarke et al., 1993; Mansour-Robaey et al., 1998), serotonin transporter (Bennett-Clarke, 1996; Lebrand et al., 1996; Bruning and Liangos, 1997) and genes encoding serotonin transporter and vesicular monoamine transporter (Lebrand et al., 1996; 1998). Furthermore, the distribution of 5-HT$_{1B}$ receptor during development closely matches serotonin immunoreactivity (Leslie et al., 1992).

In the SI cortex 5-HT plays a critical role in the formation of cytoarchitectonic barrels. Increased 5-HT levels, by either genetic manipulation or pharmacological treatment, in the first week of postnatal life results in the absence of barrels from the SI cortex of mice (Cases et al., 1995; 1996; Vitalis et al., 1998), whereas destruction of serotonergic afferents by the neurotoxins p-chloramphetamine or 5,7-dihydroxytryptamine in neonatal rats delays barrel formation and reduces barrel size (Blue et al., 1991; Bennett-Clarke, 1994; Osterheld-Haas et al., 1994; Osterheld-Haas and Hornung, 1996; Rhoades et al., 1998). Changes in barrel size were attributed to 5-HT effect on the growth of the thalamocortical afferents via the 5-HT$_{1B}$ receptor (Bennett-Clarke, 1994; 1995; Cases et al., 1996; Rhoades et al., 1998; Lotto et al., 1999; Lieske et al., 1999).

1.4.5.C Other Inputs

In addition to the thalamocortical and serotonergic afferents, the barrel field receives extrinsic inputs from the basal forebrain and locus coeruleus. Cholinergic afferents from the basal forebrain neurons terminate into the septa between barrels

(Lysakowski et al., 1989), while noradrenergic afferents from locus coeruleus terminate within barrel hollows (Lidov et al., 1978). Both of these inputs modulate the activity of neurons in the barrel field. Cholinergic inputs enhance cortical response to sensory input and play an important role in plasticity of the barrel field (Sachdev et al., 1998; Zhu and Waite, 1998). Noradrenergic inputs, on the other hand, modulate the plasticity and morphology of barrel neurons (Levin et al., 1988).

The barrel field also receives intrinsic inputs from other layers in the barrel cortex. For instance, corticothalamic efferents, arising from neurons in the infragranular (V/VI) and supragranular (II/III) layers, send axon collaterals that terminate in barrel hollows (Wise and Jones, 1977; Hersch and White, 1981; White and Hersch, 1982; White and Keller, 1987; Chmielowska, 1988; 1989). Ipsilateral corticocortical projections arising from cells in layers III and V project to the SII cortex, motor cortex and adjacent areas in layer IV (Wise and Jones, 1976; Akers and Killackey, 1978; Chapin et al., 1987; Olavarria et al., 1984; Fabri and Burton, 1991; Kim and Ebner, 1999). The barrel field also receives projections from the contralateral barrel field, SII cortex and motor cortex through the callosal pathway that terminate in the septa between barrels (White and DeAmicis, 1977; Akers and Killackey, 1978; Olavarria et al., 1984; Welker et al., 1988).

1.5 Anatomy and Development of the Whisker-to-Barrel Pathway

The whisker-to-barrel trigeminal pathway starts with the hair follicle of the mystacial vibrissae on the muzzle area. The spatial distribution of the mystacial vibrissae at the periphery is replicated through the pathway by the topographic organization of the afferents and neuronal somata to give rise to whisker-related patterns. Whisker-related

patterns emerge in sequence during development appearing first in the brainstem trigeminal nuclei, then in the thalamus and lastly in the SI cortex. In the trigeminal (V) brainstem complex whisker-related patterns are referred to as "barrelettes" (Belford and Killackey, 1979a; Ma, 1991). In the thalamus, they are referred to as "barreloids" (Van der Loos, 1976) and in the cortex they are called "barrels" (Woolsey and Van der Loos, 1970). They appear in a peripheral-to-central order where they are evident in the brainstem trigeminal complex nuclei at birth (Chiaia et al., 1992b) and at two days of postnatal life (P2) in the thalamus (Belford and Killackey, 1979b) and lastly they appear in the cortex at P3 in mice and rats (Rice and Van der Loos, 1977; Rice et al., 1985; Senft and Woolsey, 1991).

1.5.1 Mystacial Vibrissae

The mystacial vibrissae are motile, highly sensitive and are a means by which the rodent explores the surrounding environment (Vincent, 1912; Welker, 1964; Carvell and Simons, 1990). Each hair follicle of the mystacial vibrissae is innervated by a bundle of 100 - 200 myelinated sensory fibers (Lee and Woolsey, 1975; Renehan and Munger, 1986; Rice et al., 1986; Rice, 1993; Rice et al., 1993) and each of these peripheral fibers innervates a low-threshold mechanoreceptor and responds to stimulation of a single whisker (Zucker and Welker, 1969; Jacquin et al., 1986). These follicular nerves form the infraorbital nerve, a branch of the maxillary subdivision of the trigeminal nerve. Primary afferents transmit information regarding velocity, amplitude, duration, frequency and direction of hair deflection (Zucker and Welker, 1969; Gottschaldt et al., 1973; Gibson and Welker, 1983; Lichtenstein et al., 1990).

1.5.2 Trigeminal Ganglion

The cell bodies of the peripheral afferents lie in the Gasserian trigeminal ganglion (Dörfl, 1985). V ganglion cells appear between E10.5 and E13.5 in the rat (Forbes and Welt, 1981; Rhoades et al., 1991) and between E9 and E12 in the mouse (for review see Davies, 1988a; 1988b). V ganglion peripheral and central projections are topographically organized when they start to grow toward their targets, the whisker pad and the brainstem V nuclei (Erzurumlu and Jhaveri, 1992). Peripheral axons arrive at the whisker pad by E11 in the mouse and by E13 in the rat (Van Exan and Hardy, 1980; Erzurumlu and Killackey, 1983; Scarisbrick and Jones, 1993). By E14, whisker row patterns can be distinguished in the rat snout (Erzurumlu and Jhaveri, 1992). Similarly, central processes of V ganglion cells reach the brainstem at E13 and by E14 whisker row patterns are distinguished in the spinal V nucleus (Erzurumlu and Jhaveri, 1992).

Natural cell death (~ 55%) in the V ganglion neurons occurs between E14 and birth (Davies and Lumsden, 1984) and plays an important role in formation of whisker-related patterns in the brainstem. A 36% increase in the number of surviving V ganglion cells following injections of nerve growth factor (NGF) into rat fetuses at E15 and E18, results in the loss of whisker-related patterns in the brainstem at birth, whereas a 53% decrease in V ganglion cells at birth following fetal injections of antibodies to NGF or its receptor, did not have any effect on these patterns (Henderson et al., 1992).

1.5.3 Brainstem

The central processes of the V ganglion neurons terminate on second order neurons in the ipsilateral trigeminal sensory complex in the brainstem (Belford and

Killackey, 1979a; 1979b; Erzurumlu et al., 1980; Hayashi, 1980; Erzurumlu and Killackey, 1983; Bates and Killackey, 1985). Second order neurons in the brainstem appear between E12 and E15 (Miller and Muller, 1989), and then migrate to their appropriate position in the brainstem between E12 and E21 (Al-Ghoul and Miller, 1989).

Vibrissal representations in the brainstem trigeminal complex of rodents "barrelettes" are present in the nucleus principalis, and in the interpolaris and caudalis subdivisions of the spinal nucleus but not in the oralis subdivision of the spinal nucleus (Belford and Killackey, 1979a; Durham and Woolsey, 1984; Ma and Woolsey, 1984; Ma, 1991). Barrelettes become obvious by E20 in the interpolaris V nucleus and at birth in the principalis V brainstem nucleus (Chiaia et al., 1992c). At all times the pattern is more distinct in the interpolaris V brainstem nucleus than in the principalis nucleus due to the wide septa between the stained patches.

In transverse sections, barrelettes appear as clusters of neurons, the "sides", surrounding relatively cell-free "hollows" when stained with cresyl violet (Nissl), and as patches of intense staining when stained using histochemical techniques (Belford and Killackey, 1979a; 1979b; Ma and Woolsey, 1984; Ma, 1991; 1993). The majority of neurons that form the barrelette sides have dendrites that are predominantly directed toward the barrelette hollow (Ma, 1991). A small fraction of neurons that form the barrelette sides in the interpolaris and caudalis subdivisions of the spinal nucleus give rise to dendritic arbors that extend into adjacent barrelettes (Ma, 1991).

1.5.4 Thalamus

Second order neurons in the trigeminal nuclei send projections to the contralateral

VB of the thalamus (Smith, 1973). Thalamic neurons appear between E14 and E16 in the

mouse (Angevine, 1970) and axonal outgrowth starts at E16 (Catalano et al., 1991). VB

receives projections mainly from the principalis nucleus of the trigeminal complex

(Erzurumlu and Killackey, 1980; Erzurumlu et al., 1980; Feldman and Kruger, 1980;

Peschanski, 1984; Chiaia et al., 1991; Williams et al., 1993) and to a lesser degree from

the spinal trigeminal nucleus (Chiaia et al., 1991a; Williams et al., 1994). Projections

from the trigeminal complex are topographically organized in the VB nucleus and form

discrete structural and functional units called "barreloids" (Van der Loos, 1976, Belford

and Killackey, 1979a; Land and Simons, 1985). Barreloids are best seen in transverse

oblique sections using either Nissl stain or histochemical techniques (Van der Loos,

1976; Belford and Killackey, 1979a). Diffuse staining in VB is evident at P0, and row-

related patterns emerge at P1 and lastly whisker-related patterns are obvious at P2 as

revealed by succinic dehydrogenase histochemistry (Belford and Killackey, 1979b).

The trigeminal projection to the POm nucleus has been described recently (Chiaia

et al., 1991a; Williams et al., 1994). Projections from the spinal trigeminal nucleus

terminate in the POm nucleus of the thalamus, while projections from nucleus principalis

are less intense. The spinal nucleus also projects to the superior colliculus (Feldman and

Kruger, 1980; Killackey and Erzurumlu, 1981; Cadusseau and Roger, 1985; Rhoades et

al., 1988) which in turn projects to the POm nucleus (Roger and Casdusseau, 1984).

Single-whisker somatotopy is lost in the POm nucleus as a result of divergence of multiple inputs from the trigeminal complex (Chiaia et al., 1991a; 1991b).

1.5.5 SI Cortex

Third order neurons in the VB nucleus send projections to the ipsilateral somatosensory cortex (Wise and Jones, 1978) to terminate in a somatotopic pattern that mirrors the whiskers arrangement. Cortical neurons appear between E15 and E17 (Miller, 1988) and differentiation starts before birth and continues during the first few days of postnatal life (Rice and Van der Loos, 1977; Senft and Woolsey, 1991; Catalano et al., 1991). Barrels appear at P4 postnatally and the septa between barrels appears two days later (Rice and Van der Loos, 1977; Senft and Woolsey, 1991). The POm nucleus projects to the septa between barrels in layer IV, and to the supragranular (II/III) and infragranular (V/VI) layers (Lin et al., 1987; Koralek et al., 1988, Chmielowska, 1989).

As noted above, there is a highly ordered relationship between the distribution of whiskers in the periphery and their corresponding whisker-related patterns in the trigeminal somatosensory pathway. This morphological and physiological one-to-one relationship between the whisker and its barrel has offered scientists a great system to understand mechanisms that underlie pattern formation in the central nervous system, and provides a rich source for studying development and plasticity in newborns and adults. In doing so, the whisker-barrel model becomes a valuable model to provide scientists with answers to general questions such as how the brain obtains its anatomical and functional regionalization.

1.6 What Makes a Barrel?

An important, yet, unresolved question is how barrels in the SI cortex are formed. Is barrel formation dependent on intrinsic factors that are specified in the cortex, i.e. genetic factors, or is it dependent on extrinsic factors that are imposed on the developing cortex from the periphery. Numerous studies revealed that clustering of TCAs and intact innervation from the periphery are necessary for barrel formation.

1.6.1 Thalamocortical Afferents

The somatosensory cortex is exposed to thalamocortical inputs early in development and barrel formation is dependent on their growth in layer IV. TCAs are topographically organized from the time that they exit the thalamus at E16 and during their radial growth through cortical layers (Catalano et al., 1996). At birth, they are present in layers VI and V and at P2 they are in the deeper aspects of the trilaminar cortical plate, the site of future layer IV, and lastly they form dense clusters of terminal arborization in layer IV at P3 (Lorente de Nó, 1922; Killackey, 1973; Killackey and Leshin, 1975; Waite, 1977; White and DeAmicis, 1977; Hersch and White, 1982; Keller et al., 1985; Bernardo and Woolsey, 1987; Jensen and Killackey, 1987a). TCAs terminate in a precise order without an initial overgrowth of axonal terminals (Rice and Van der Loos, 1977; Wise and Jones, 1978; Dawson and Killackey, 1985; Erzurumlu and Jhaveri, 1990; Catalano et al., 1991; Agmon et al., 1993, Agmon et al., 1995; Catalano et al., 1996). Dense clusters of TCAs terminating in the barrel hollow have been visualized using different histochemical stains including cytochrome oxidase histochemistry (Wong-

Riley, 1980; Land and Simons, 1985; Figure 1.5) and succinic dehydrogenase histochemistry (Belford and Killackey, 1979a).

A role for thalamocortical afferents in barrel formation has been established by several studies. Elimination of the thalamic axons before they invade layer IV resulted in the absence of barrels without any effect on the laminar organization of the cortex in rats (Wise and Jones, 1978). On the other hand, normal cortical barrels form after transplantation of late-embryonic visual cortex to the position of the SI cortex in neonatal rats (Schlaggar and O'Leary 1991). More recently, Schlaggar and O'Leary (1994) provided compelling evidence that in the SI cortex of rats TCAs are arranged in a periphery-related pattern at birth. Using acetylcholinesterase (AChE) histochemistry as an early transient marker for the thalamocortical afferents (Kristt, 1979; Robertson, 1987), the authors revealed that at birth row-related patterns are evident in the presumptive SI cortex and by 24 hours postnatally clusters of AChE-reactive fibers in the barrel hollow are in place.

Although the above studies provide evidence for the importance of the TCAs in initiating barrel formation, none of them was successful in demonstrating how TCAs are segregated into periphery-related patterns, or why the somatotopic organization of the TCAs, although present in other species (Waite et al., 1991; 1996), does not result in the formation of cytoarchitectonic barrels in their cortices.

1.6.2 Innervation from the periphery

Differentiation of cytoarchitectonic barrels depends on the growth and proper clustering of TCAs which in turn depends on an intact pathway from the periphery.

Figure 1.5 A section through layer IV of an adult mouse that was processed for cytochrome oxidase (CO) histochemistry. CO staining reveals the presence of CO-dense clusters that are confined to the barrel hollow and are coincident with the thalamocortical afferents' termination in layer IV of the SI cortex. Abbreviations are the same as in Figure 1.2 legend. Scale bar = 400μm.
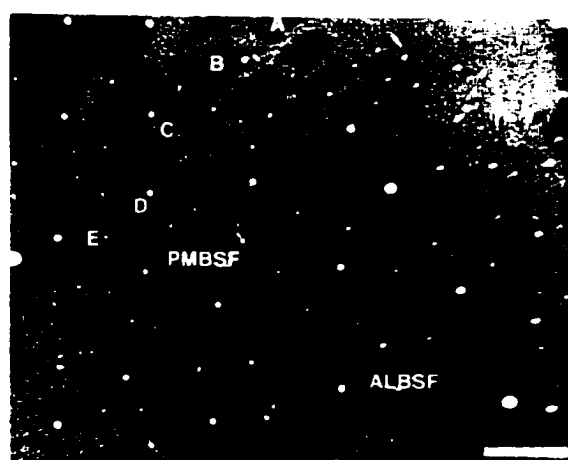
Figure 1.5

Numerous studies in the past two decades have demonstrated the importance of an intact anatomical pathway from the periphery in the emergence of whisker-related patterns in subcortical and cortical regions. Since periphery-related patterns develop in a peripheral-to-central order, there is a defined critical period at each of these synaptic relays during which these patterns are most susceptible to change. The critical period for barrel formation ends by P5; manipulation of the pathway after this period does not produce a change in the structure of barrels (Woolsey and Wann, 1976; Jeanmonod et al., 1981).

Van der Loos and Woolsey (1973) were the first to provide evidence for the importance of periphery innervation and intact trigeminal pathway in barrel formation. In their study, they cauterized either the whisker follicles in row C, or all rows except for row C, at birth. Examination of the barrel field in adolescent mice revealed that in every case cauterization of a follicle caused absence or shrinkage of cortical barrels corresponding to the damaged body surface with an expansion of adjacent rows. The morphological changes in row C barrels were attributed to reorientation of dendrites of its neurons towards adjacent active rows (Harris and Woolsey, 1981).

Subsequent studies in mice and rats confirmed the above findings. Neonatal lesions of the vibrissae follicle or transection of the infraorbital nerve result in the loss of segregation of trigeminal afferents and loss of whisker-related patterns corresponding to the lesioned peripheral receptors (Woolsey and Wann, 1976; Killackey et al., 1976; Killackey and Belford, 1979; Woolsey et al., 1979; Killackey and Belford, 1980; Steffen and Van der Loos, 1980; Jeanmonod et al., 1981; Waite and Cragg, 1982; Durham and Woolsey, 1984; Jensen and Killackey, 1987b; Chiaia et al., 1992a; 1992b; 1992c;

Killackey et al., 1994; Watanabe et al., 1995; Chiaia et al., 1996; 1997; Higashi et al., 1999). Whisker trimming (Verley and Axelrad, 1977) or plucking (Weller and Johnson, 1975), without causing damage to the follicle, does not produce any changes in the appearance of barrels. However, it has been reported that neuronal activity is reduced in the deprived barrels (Durham and Woolsey, 1978; Wong-Riley and Welt, 1980; Land and Simons, 1985).

1.6.3 Intrinsic Cortical Factors

As noted above, numerous studies have indicated the dependence of barrel formation on thalamocortical afferent clustering which in turn is dependent on an intact innervation from the periphery. The question remains of whether the manifestation of cortical barrels is completely under the control of extrinsic factors such as TCAs, or whether molecular cues that are specified in the developing SI cortex, i.e. intrinsic factors, play a role in the arrangement of TCAs and in barrel formation. For several years, this issue has been the subject of debate between scientific groups.

Cooper and Steindler (1986) reported the existence of a lectin marker for glycoconjugate molecules which are expressed by glial cells in the cortex and delineate barrel boundaries prior to the differentiation of cortical barrels. Delineation of boundaries was transient, appearing as early as late P2 and disappearing by the end of the second postnatal week. Accordingly, the authors proposed that molecular cues that are intrinsic to the cortex influence patterning of the TCAs and differentiation of barrels. Subsequent studies have provided evidence for the role of intrinsic factors in formation of whisker-related patterns in the cortex. Using immunocytochemistry, extracellular matrix

molecules such as tenascin, tenascin-binding protein and neurocan or adhesion molecules such as N-cadherin were reported to delineate barrel boundaries between 24 and 48 hours, before cytoarchitectural barrels are visible in the cortex by Nissl stain (Crossin et al., 1989; Steindler et al., 1989; Steindler et al., 1990; Jhaveri et al., 1991; Mitrovic et al., 1994; Watanabe et al., 1995; Huntley and Benson, 1999).

With the advent of sensitive techniques for axonal tracing, subsequent studies revealed that TCAs are arranged in periphery-related pattern at birth, two days before the delineation of barrel boundaries by these glycoconjugates (Erzurumlu and Jhaveri, 1990; Jhaveri et al., 1991; Schlaggar and O'Leary, 1994), hence suggesting that extrinsic factors guide the differentiation of barrels and patterning in the SI cortex. However, it is still conceivable that glial and cortical cell molecules might play a role in barrel formation where they act as barriers between barrels by their action as inhibitors of neurite outgrowth (Silver et al., 1987; Oakley and Tosney, 1988; Snow et al., 1990).

1.6.4 Activity-Dependent Mechanisms

While several studies have established the importance of an intact pathway from the vibrissae in barrel formation, there is still some controversy regarding the role of neuronal activity-dependent mechanisms in establishing cortical barrels. Purves and his colleagues (1994) proposed that barrels arise from induction and intercellular recognition as opposed to ocular dominance columns that arise as a result of activity-dependent mechanisms. They hypothesized that induction mechanisms occur at each level of the trigeminal pathway which will establish positional information through intercellular and trophic interaction with targets. According to this model activity does not play a role in

establishing cortical barrels in the SI cortex but it does play a role in influencing the size

of barrels during development (Riddle at al., 1992; 1993). In support of this hypothesis,

blocking neuronal activity in the infraorbital nerve of newborn rats by TTX did not have

an effect on whisker-related patterns in the brainstem, thalamus and cortex (Henderson et

al., 1992). Similarly, silencing neuronal activity in the cortex for the first two weeks of

postnatal life by either TTX or N-methyl-D-aspartate (NMDA) antagonists did not

prevent the appearance of whisker-related patterns in the cortex and subcortical structures

(Chiaia et al., 1992d). Moreover, blockade of activity did not affect the cortical

reorganization that usually occurs after vibrissae follicle damage or infraorbital

transection at birth (Chiaia et al., 1994).

The aforementioned studies clearly suggest that activity in the trigeminal pathway

is not necessary for formation of whisker-related patterns. However, in the past few years

a new line of evidence started to emerge implicating activity and NMDA receptors in

barrel formation. Schlaggar and his colleagues (1993) provided evidence for the role of

postsynaptic activity in structural plasticity in the SI cortex; pharmacological blockade of

NMDA and non-NMDA receptors by 2-amino-5-phosphonovaleric acid (APV) with

concomitant lesioning of row C follicles blocks cortical changes that normally occur after

denervation. Recently, it has been reported that blocking postsynaptic activity, by

application of APV, during the critical period of barrel formation disrupts the one-to-one

relation between vibrissae and its barrel and the columnar organization of projections to

supragranular layers in a barrel column (Fox et al., 1996). The requirement for a

functional NMDA receptor in the formation of whisker-related patterns in the trigeminal

brainstem complex has been reported (Li et al., 1994; Kutsuwada et al., 1996). Both studies reported that in mice lacking the R1 or R2 regulatory subunits of the NMDA receptor, barrelettes fail to develop. Unfortunately, these mutants die shortly after birth which prevents the assessment of barrels in their cortices; however it is unlikely that barrels will develop if whisker-related patterns were absent in lower parts of the pathway.

In support of activity-dependent mechanisms at the thalamocortical synapses in the developing SI cortex, Malenka and colleagues (Crair and Malenka, 1995; Feldman et al., 1998) reported that long-term potentiation and long-term depression can be induced in the barrel cortex of rats only during the first postnatal week, a developmental period that correlates with the synaptogenesis of thalamocortical afferents. Moreover, activation of NMDA glutamate receptors was very important for generating long-term potentiation (LTP). Loss of LTP by the end of the first week of postnatal life was accompanied by a decrease in NMDA synaptic currents and a change in NMDA receptor properties. More recently, it has been reported that developing thalamocortical synapses express postsynaptic kainate and AMPA (α-amino-3-hydroxyl-5-methyl-4-isoxazolepropionate) receptors, and that activity-dependent mechanisms regulate the expression of kainate receptors (Kidd and Isaac, 1999).

In parallel with the above studies, it has been reported that serotonergic activity during the critical period plays an important role in barrel formation. A nine-fold increase in 5-HT during the critical period of barrel formation resulted in the absence of barrels from the SI cortex of mice deficient in monoamine oxidase A (the enzyme that degrades 5-HT) (Cases et al., 1995; 1996). This was replicated by the use of a drug that inhibits

monoamine oxidase A activity. On the other hand, depletion of 5-HT from the cortex by systemic application of neurotoxin delays barrel formation and reduces the size of thalamocortical afferents zones (Bennett-Clarke et al., 1994).

1.7 Barrelless Mice (*brl*)

A spontaneous mutation in a mouse line bred at Université de Lausanne (Switzerland) for normal mystacial vibrissae has generated mice that lack cytoarchitectonic barrels in layer IV of their SI cortex as revealed by cresyl violet (Nissl) staining (Welker et al., 1996; Figure 1.6). Other than the absence of barrels, barrelless (*brl*) mutants did not show cytoarchitectonic abnormalities in their SI cortex at any postnatal stage, nor did they suffer from any obvious neurological or behavioral disorder. Additionally, whisker-related patterns in the thalamus "barreloids" were poorly formed while barrelettes in the brainstem were normal as revealed by cytochrome oxidase histochemistry (Welker et al., 1996).

Despite the absence of barrels from layer IV, somatotopy in the SI cortex was still preserved as seen in 2-deoxyglucose mapping and in physiological recordings. However, axonal tracing of individual TCAs following injections of dextran into VB revealed an overgrowth of TCA arbors in layer IV of *brl* mutant mice in contrast to wild-type animals in which TCA arbors terminate in barrel domains (Welker et al., 1996).

In the laboratories of Drs. Neumann and Guernsey, efforts were made to map and isolate the gene responsible for the *brl* phenotype. The *brl* phenotype is an autosomal recessive trait and the *brl* locus was mapped to the proximal region of chromosome 11

Figure 1.6 Nissl-stained tangential section (50μm) through layer IV of the SI cortex of the barrelless (*brl*) mutant mouse. The pattern of cell dense specialization present in wild-type mice (Figure 1.2) is not present in the *brl* cortex, instead layer IV neurons are uniformly distributed. Scale bar = 400 μm .

Figure 1.6

tightly linked with the microsatellite marker *D11Mit226* (Welker et al., 1996). Three

strategies were used to isolate the *brl* gene by positional cloning: fine resolution genetic

linkage mapping, physical mapping and candidate gene analysis. Construction of a high

resolution genetic linkage map around the *brl* locus was initiated by my colleague D. S.

Smallman who mapped the *brl* locus to an interval of 2.2 centiMorgan (cM; Figure 1.7).

Evaluation of candidate genes was initiated by Dr. W. Ourednik who ruled out Ca^{2+}

calmodulin-dependent protein kinase IIb (*Camk2b*) as a candidate for *brl* by sequencing

the coding region of the gene. Together these strategies offer powerful tools in isolating

the *brl* locus.

1.8 Objectives and Overview of Research Plans

The objective of studies presented in this dissertation is to isolate and characterize

the gene responsible for the *brl* phenotype, and to attempt to determine how this mutation

gives rise to the barrelless phenotype. This was achieved by construction of high

resolution linkage and physical maps in the region of interest and evaluation of candidate

genes. In order to isolate the *brl* locus a high resolution genetic map was constructed

around the *brl* region (chapter 2). The second step of positional cloning was initiated by

the use of *brl* flanking markers to screen genomic libraries to pull out genomic DNA

fragments that contains the region of interest (chapter 3). A physical map was constructed

in the *brl* region and candidate genes for *brl* were identified (chapter 3). Adenylyl cyclase

type I gene, a gene that was mapped to the *brl* critical region, was evaluated as a

candidate gene for *brl* (chapter 4). The initial goals were to characterize the *brl* gene and

its product(s) and to determine the pathogenesis of the barrelless phenotype from the
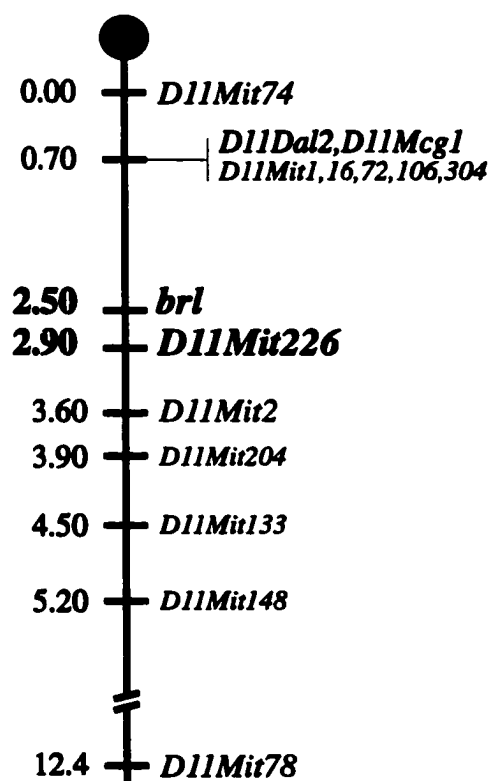
Figure 1.7 A genetic linkage map in the region of the barrelless (*brl*) locus in proximal mouse chromosome 11. The numbers on the left represent map distances in centiMorgan (cM), and the numbers on the right represent the Whitehead institute microsatellite markers. The *brl* (bold) locus is tightly linked with the microsatellite marker *D11Mit226* (bold). The *brl* locus is mapped to a 2.2 cM interval. The centromere is represented by a black circle.

barrelless mutation. Once adenylyl cyclase type I gene was identified, the next set of short-term goals were more sophisticated than they would have been if *brl* was an unknown gene with no sequence homology to a known gene. At that point we were more interested in determining the pathogenesis of the *brl* phenotype, and to construct a pathway for molecules that play an important role in barrel formation. Thus, the roles of cAMP-dependent protein kinase (chapter 5) and neurotrophins (chapter 6) were investigated. In doing so, some of the molecular and cellular mechanisms that underlie patterning in the cerebral cortex can be revealed. Understanding how patterns are formed is of great importance since the function of the central nervous system depends on the arrangement and the connections that neurons form among themselves and with their targets. In addition, abnormalities in patterning in humans usually lead to mental retardation and neurological disorders.

Chapter 2

Evaluation of Ca^{2+}/Calmodulin-Dependent

Protein Kinase II b

2.1 Introduction

Ca^{2+}/Calmodulin-dependent protein kinase II (CaM kinase II) is an oligomeric multifunctional isozyme that is involved in the regulation of diverse physiological conditions in response to an increase in intracellular Ca^{2+}. It is present in most tissues but most abundant in the brain, constituting approximately 0.3% of total brain protein (Bennett et al., 1983). In the telencephalon it comprises ~ 2% of the total hippocampal protein compared to 0.1% in the pons/medulla region (Erondu and Kennedy, 1985). The holoenzyme is composed of 8-12 subunits. Five distinct, but closely related, subunit isoforms have been cloned termed α, β, β', γ, and δ. Each is encoded by a separate gene except for the β' which is a splice variant of the β mRNA.

CaM kinase II purified from brain contains α, β, and β' subunit isoforms which vary widely in composition during development and in different regions of the brain (Sugiura and Yamauchi, 1992; Burgin et al., 1990; Kelly et al., 1987; Erondu and Kennedy, 1985). The ratio of α and β subunits, for example, in the adult rat forebrain is 3-4:1 compared to 1:4 in the cerebellum (McGuinness et al., 1985; Miller and Kennedy, 1985). At birth, the β subunit is the predominant isozyme which declines after the second week of postnatal life (Sahyoun et al., 1985; Weinberger 1986). The change in isozyme composition during development is due to the increase in the α subunit expression. Moreover, CaM kinase subcellular localization changes during development from being predominantly cytosolic to particulate (Kelly and Vernon, 1985; Sahyoun et al., 1985; Weinberger and Rostas, 1986). The enzyme is activated by binding of Ca^{2+} and calmodulin (Ca^{2+}/CaM) and subsequent autophosphorylation which allows the kinase to

be active even after Ca^{2+} levels decrease. Protein phosphorylation mediated by CaM kinase II has been implicated to play an important role in signaling (McGuinness et al., 1984). CaM kinase also plays an important role in synaptic plasticity such as long-term potentiation (LTP) (Malinow et al., 1988) and in learning and memory.

The CaM kinase II α isoform is neurospecific and is present both pre- and postsynaptically (Burgin et al., 1990; Erondu and Kennedy, 1985). The major postsynaptic density protein was demonstrated to be identical to this subunit (Kennedy et al., 1983; Goldenring et al., 1984). Expression of the α subunit varies during development from barely detectable at 4 days of postnatal life to an increase of 10-fold by day 16 in the frontal cortex (Burgin et al., 1990). CaM kinase II α was indicated in the induction of LTP in the hippocampus (Malenka et al., 1989; Malinow et al., 1989). Mutant mice that are deficient in the α subunit of CaM kinase II (*Camk2a*) were generated (Silva et al., 1992a; 1992b). These mice were deficient in their ability to produce LTP and exhibited spatial learning impairments which confirmed previous studies of the involvement of CaM kinase II α isoform in synaptic plasticity and memory. While plasticity is impaired in these mutants, barrels form normally and their receptive fields properties are similar to wild-type animals which suggests the involvement of CaM kinase II α isoform in subsequent events of neocortex development (Glazewski et al., 1996).

Brain-specific Ca^{2+}/Calmodulin protein kinase II b gene (*Camk2b*) was evaluated as a candidate gene for the *brl* locus. *Camk2b* gene encodes the β subunit of the enzyme and is located on proximal chromosome 11 (Karls et al., 1992; Copeland et al., 1993). In

their study, Karls and his colleagues mapped *Camk2b* locus to chromosome 11 using interspecific backcross analysis. Their results show no recombination between *Camk2b* and Leukemia inhibitory factor (*Lif*) genes suggesting that the two loci are tightly linked. *Camk2b* gene was evaluated as a candidate gene for *brl* for the following reasons: 1) *Camk2b* gene was mapped to the proximal region of chromosome 11, 2) *Camk2b* is highly expressed in the brain, particularly the hippocampus, cortex, amygdala, striatum, lateral septum and cerebellar cortex (Erondu and Kennedy, 1985; Fukunaga et al., 1988; Ouimet et al., 1984; Bennett and Kennedy, 1987; Tobimatsu et al., 1988; Tobimatsu and Fujisawa, 1989; Burgin et al., 1990), 3) *Camk2b* is localized on both sides of the synapse where it is involved in neuronal signaling. Synapsin I, a well known substrate for CaM kinase II, is highly concentrated in the outer surface of presynaptic vesicles and is believed to be involved in the regulation of neurotransmitter release (DeCamilli et al., 1983; Huttner et al., 1983). In addition, CaM kinase II has been suggested to play an important role in long-term potentiation, a cellular model for learning and memory (Bliss and Collingridge, 1993), providing evidence for its role in synaptic activity (Soderling 1993; Lisman 1994; Suzuki 1994), 4) the β subunit is the dominant isozyme at birth and during the first two weeks of postnatal life (Sahyoun et al., 1985; Weinberger and Rostas, 1986; Kelly et al., 1987; Burgin et al., 1990) coinciding with barrel formation (Rice et al., 1985). In their study, Burgin and colleagues reported that the β-mRNA is the major mRNA species in 4-day-old rat forebrains whereas the α-mRNA is barely detectable. During the next two weeks of postnatal life the level of β-mRNA decreases by half while the level of α-mRNA increases by 10-fold. Likewise, barrels are evident in the mouse

somatosensory cortex at 4 days of postnatal life, 5) *Camk2b* is regulated by Ca^{2+} and calmodulin which converts the enzyme from a Ca^{2+}-dependent into a Ca^{2+}-independent state. Autophosphorylation allows the enzyme to maintain its activated state beyond the duration of the Ca^{2+} signal causing a prolonged effect in the cell, and finally, 6) results from the *Camk2a* mutant provided evidence for the involvement of CaM kinase II in cortical activity as well as excluding the involvement of the α subunit in barrel formation.

Camk2b cDNAs were cloned and sequenced in our laboratory by Dr. W. Ourednik from both C57BL/6J and *brl/brl* mice. Sequencing results of the coding region revealed no significant difference in the nucleotide sequence between C57BL/6J inbred mice and *brl/brl* mutant mice partially ruling out *Camk2b* as the *brl* gene. Since expression differences were not ruled out, the 3' untranslated region (3' UTR) was sequenced to find a polymorphism that could be used to map the *Camk2b* locus relative to *brl*.

2.2 Reagents and Solutions

All reagents were autoclaved prior to use for 20 minutes on liquid cycle at 15 lbs/sq. in. unless otherwise stated. All reagents were of molecular grade and purity. Radiolabeled isotopes were purchased from Amersham Life Sciences (USB Cleveland, Ohio; U.S.A). Preparation of reagents and buffers are summarized in appendix A-1.

2.3 Methods

2.3.1 Subjects

Adult C57BL/6J (B6) inbred mice and barrelless (CD-1(ICR)BR, *brl*) mutant mice were used for genotyping animals. The original stock of B6 animals were purchased

from the Jackson Laboratories (Bar Harbor, ME, U.S.A.) while *brl* mutant mice were

obtained from Université de Lausanne (Switzerland). Before the arrival of *brl* mutants to

Halifax, Nova Scotia they were shipped to Charles River Laboratories (Wilmington, MA;

U.S.A.) to eliminate any pathogenic organisms in the colony. Animals were then housed

in the Carlton Animal Care Facility at Sir Charles Tupper Building at Dalhousie

University. Animals were maintained on a regular laboratory diet and water. Protocols for

animal use have been approved by the Dalhousie committee on animal care and usage.

2.3.2. Extraction of DNA from Cerebellum

Mice were killed with an overdose of ether and then decapitated. Brains were

immediately removed and placed in 3.7% formaldehyde solution (BDH, Toronto, ON;

Canada). The right cerebellar hemisphere was excised and transferred to a tube which

was immersed quickly in liquid nitrogen. For DNA preparation, a portion of the

cerebellum was divided into small pieces with a sterile razor followed by the addition of

0.5 ml of freshly prepared extraction buffer. Tubes were incubated overnight, in a

horizontal position, with moderate shaking in a 55°C shaker (G24 Environmental

Incubator Shaker, New Brunswick Scientific Co. Inc. Edison, NJ; U.S.A). The tubes were

then centrifuged in a microcentrifuge (BHG Hermle Z230 M, Mandel Scientific Co.

LTEE/LTD) for 10 minutes. The supernatant was transferred to another tube containing

450 µl of ice-cold isopropyl alcohol (BDH). At this point threads of DNA were visible

where they were transferred with a sterile micropipette tip to another set of tubes each

containing 300 µl of deionized distilled water. Tubes were incubated overnight, in a

vertical position, in a 60°C shaker. DNA concentration was estimated using Beckman,

DU-64 Spectrophotometer (Beckman Instruments, Inc. Harbor Blvd. Fullerton, CA; U.S.A). Samples were prepared at a final concentration of 50 ng/µl of DNA.

2.3.3 Polymerase Chain Reaction (PCR)

All PCR reactions were performed in a total volume of 10 µl unless otherwise stated. The PCR reactions contained 4.5 µl of autoclaved deionized distilled water, 1.0 µl of 10x PCR buffer (100 mM Tris-HCl, 500 mM KCl, 15 mM $MgCl_2$, and .01% gelatin), 0.40 µl of 5 mM dNTP (Pharmacia, Biotech), 0.50 µl of 10 µM of each forward and reverse primer (Beckman Oligo 1000 DNA Synthesizer), 0.10 µl of *Taq* and a final concentration of 150 ng of genomic DNA. PCRs were performed using an automated thermal cycler (PTC-100 Programmable Thermal Controller, MJ Research Inc.), for 35 cycles of 94°C denaturation (1 minute), calculated annealing temperature (1 minute), 72°C extension (2 minute), and 72°C final extension (15 minutes) with an initial denaturation step at 94°C for 2 minutes.

2.3.4 Primer Preparation, Cleavage and Deprotection

Table 2.1 summarizes primer pair sequences used in PCR reactions based on *Camk2b* complementary DNA (cDNA) sequence (Genebank accession number: U63615). Primers were synthesized on a Beckman Oligo 1000 DNA synthesizer and were used in reactions after cleavage and deprotection using Beckman's Ultra Fast Cleavage and Deprotection Kit. Primers were cleaved and deprotected from their synthesized columns according to manufacturer's instructions.

2.3.5 Agarose Gel Electrophoresis

Agarose gels (FMC Bioproducts, Rokland, ME; U.S.A.) were prepared at

Primer	Sequence	Anneal. temp.	Size (b.p.)
F1	GAC AGA GTT GGT GTT TGG AG	60	984
R1	GTG TTT GTC CAC TCA GCT TG		
F2	ACA AAA TTT TGG CAT CGG ATG AAC T	63	807
R2	GTG TTT GTC CAC TCA GCT TG		
F3	AAG GAA AAA GCT GTA AAA ATC TAG C	60	749
R3	GTG TTT GTC CAC TCA GCT TG		
F4	GTG TTT GTC CAC TCA GCT TG	60	260
R4	AGC CTG CCT TCT CTC TAA GC		
F5	AAG GCC AAA ATT GGT TAG GG	58	270
R5	CCT AGC CTG ACT TTG TAA CA		
F6	TGT GGG TGG CCC TGG CCC TT	64	280
R6	AGG TGG ACA GTC CCC TTG GA		
F7	CTA CAA ATC AAG CCA AGG GA	58	290
R7	TTG TGG AGA TAA CAA GGT GG		
F8	TTG CCA TGG ACA GTG TGA GG	58	360
R8	GCA GTT TCC CGA GAC AGA AC		

Table 2.1 List of primer pairs used in genomic DNA amplification of the 3' untranslated region of the *Camk2b* gene as predicted from the published cDNA sequence (Genebank accession number: U63615). Abbreviations: Anneal. temp., annealing temperature; b.p., base pair; F1-F8, forward primers; R1-R8, reverse primers.

concentrations ranging from 1.0 - 2.5 % depending on amplicon size. Ethidium bromide was used (Molecular Sigma Biology, Sigma Chemical Co. St. Louis, MO; U.S.A) at a final concentration of 0.5 µg/ml. DNA samples were mixed with the desired amount of gel-loading buffer, at a final concentration of 1x, and were loaded into the gel slots. Gels were run until a complete separation of DNA was achieved. At the end of the run, electrical current was turned off and the gel was visualized after staining with ethidium bromide and then photographed (Polaroid Land Camera, model MP-4).

2.3.6 Purification of DNA Fragments Using Gene Clean Kit

Purification of DNA fragments from agarose was performed according to manufacturer's instructions (Gene Clean Kit, BIO 101 Inc., Mississauga, ON; Canada). DNA fragments were separated using the appropriate percentage agarose gel. The desired DNA fragment was excised using a sterile razor blade and divided into small pieces after which it was transferred to a pre-weighed 1.5 ml microcentrifuge tube. The tube with the DNA slice was weighed and the weight of the slice was determined. Purification of DNA was performed according to manufacturer's instructions. The DNA pellet was dissolved in a total volume of 10 µl of deionized distilled water. The final yield of DNA was estimated by using 2 µl of the sample to run it against a standard using agarose gel electrophoresis.

2.3.7 Restriction Digestion of DNA

PCR products were subjected to restriction digestion with one of the following enzymes: PvuII (Gibco BRL), HindIII (Gibco BRL), BfaI (New England Biolabs, Beverly, MA; U.S.A.) and AluI (Pharmacia Biotech) in a total volume of 40 µl. The

reaction mixture contained 10 µl of the PCR product, 4 µl of the appropriate 10x buffer, 10 units of the restriction enzyme (1-2 µl) and deionized distilled water to a final volume of 40 µl. The mixture was incubated at 37°C overnight. Finally, the reaction was stopped by the addition of 8 µl of 6x loading buffer. Samples were separated using agarose gel electrophoresis and visualized using ethidium bromide under UV light.

2.3.8 TA Cloning of PCR Products

DNA amplification was performed in a total volume of 50 µl. Samples were fractionated using 1% agarose gel electrophoresis. The desired bands were excised and purified using a Gene Clean Kit. Samples were reconstituted with deionized distilled water to a total volume of 20 µl of which 2 µl was run on an agarose minigels against a known standard to estimate DNA concentration. Amplicons were cloned in PCR II vector using the TA Cloning Kit (Invitrogen San Diego, CA; U.S.A.) according to manufacturer's instructions. Briefly, the ligation reaction contained 1 µl of 10x ligation buffer, 1 µl of PCR II vector (25 ng), 1 µl of T4 DNA ligase, the calculated amount of PCR product. The final volume was adjusted to 10 µl with deionized distilled water and the ligation reaction was incubated at 15°C in a thermocycler overnight.

Vector transformation of bacteria was performed according to manufacturer's instructions with a few modifications. 200 µl of DH5 α competent cells were thawed and 100 µl were transferred into glass tubes incubated on ice. Tubes containing ligation mixture were centrifuged for 10 seconds and then incubated on ice. 5 µl of ligation mixture was transferred into each tube of competent cells. Tubes were then incubated on ice for 15-30 minutes. The bacteria were heat shocked at 42°C for exactly 90 seconds and

then incubated on ice for another 2 minutes. 500 μl of prewarmed LB medium was added

to each tube followed by incubation at 37°C for exactly one hour at 225 rpm in a rotary

shaking incubator. Meanwhile, 40 μl of 25 mg/ml X-Gal and 25 μl of 25 mg/ml of

ampicillin were spread using an L-shaped spreader on top of the prepared LB agar plates

and were incubated at 37°C for approximately one hour. Finally, 200 μl of the

transformation reaction was spread on the top of the agar plates, inverted and then were

incubated in a 37°C incubator overnight to allow white/blue color selection of insert

positive clones. A white colony was inoculated using sterile eppindorf tip into a tube

containing 5 ml LB medium and was incubated at 37°C. The DH5α clones were checked

for the presence of the insert by PCR amplification. Amplification was performed using

the same program conditions used for genomic DNA amplification. PCR reactions were

performed as discussed previously in section 3.2.

2.3.9 Plasmid DNA Preparation

Preparation of plasmid DNA was performed on fresh bacterial cultures that were

grown overnight for all positive clones. Preparation was carried on using DNA EasyPrep

Plasmid (Pharmacia Biotech) according to manufacturer's instructions. DNA samples

were dissolved in a total volume of 50 μl deionized distilled water. Samples were

electrophorised in a 1% agarose gels along with a known standard to estimate DNA

concentration.

2.3.10 Sequencing Plasmid DNA

2.3.10.A Preparation of Plasmid DNA for Sequencing

Sequencing of plasmid DNA isolated from miniprep cultures was performed using Sequenase Version 2.0 (Amersham USB). Alkaline denaturation, neutralization and precipitation of double stranded DNA was performed before sequencing. Briefly, 20 µl of 1M sodium hydroxide was added to 30 µl of plasmid DNA followed by incubation for 10 minutes at room temperature. The mixture was then neutralized with 15 µl of 3M sodium acetate, pH 5.0 and the total volume was adjusted to 100 µl with deionized distilled water. DNA precipitation was carried out by the addition of 300 µl of absolute ethanol (BDH) followed by incubation on ice for 30 minutes. Tubes were then centrifuged at room temperature for 15 minutes and the supernatant was discarded. The pellets were washed twice with 70% ethanol followed by centrifugation each time for 5 minutes in a microcentrifuge at room temperature. The supernatant was decanted and the samples were dried in vacuum (Savant Instruments Inc., Farmingdale, NY; U.S.A.) and subsequently reconstituted in 7 µl of deionized distilled water.

2.3.10.B Sequencing Reaction

Sequencing reactions (Sequenase Vervion 2.0, Amersham USB) were performed according to the manufacturer's instructions. The annealing mixture containing 7 µl of denatured DNA, 2 µl of sequencing buffer, 1 µl of 10 µM primer was incubated at 37°C for 30 minutes followed by incubation at room temperature for 10 minutes after which the mixture was kept on ice. Ice-cold Template-Primer mixture (10 µl) was added to labeling reaction containing 1 µl of .01M Dithiothreitol (DTT), 2 µl of Diluted Labeling Mix

(diluted 5 folds), 0.50 µl of [α-^{35}S] dATP (Amersham USB), and 2 µl of diluted

sequenase enzyme (diluted 8 folds). Tubes were mixed thoroughly and then incubated at

room temperature for 5 minutes. 3.5 µl of each labeling reaction was transferred into each

of the prewarmed termination tubes (2.5 µl), mixed thoroughly and were returned to a

37°C water bath for five more minutes. The reaction was stopped by the addition of 4 µl

of Stop Solution. Before loading, the samples were heated to 85°C for 3 minutes and an

aliquot of 3 µl was used in each lane.

2.3.11 Direct Dideoxy Sequence analysis of PCR Products

Direct sequencing was performed on amplicons of 200-300 b.p. DNA

amplification was performed as described previously in a total volume of 50 µl. Samples

were run on 1.5% agarose gels and the desired band was excised and purified using Gene

Clean Kit. Samples were reconstituted with deionized distilled water in a total volume of

10 µl followed by concentration in the Speedvac® for 30 minutes and then reconstituted

in 14 µl of deionized distilled water. Sequencing analysis was performed using Sequenase

Kit Version 2.0 (Amersham USB) according to manufacturer's instructions with a few

modifications. Briefly, the annealing mixture containing 5 µl of PCR product, 2 µl of 5x

annealing buffer supplied with the T7 kit, 2 µl of 10 µM primer and 1 µl of DMSO was

incubated at 95°C for 5 minutes after which it was immediately immersed in liquid

nitrogen and then was thawed to room temperature. While this mixture was cooling, four

tubes were labeled and filled with 2.5 µl of each termination mixture (dGTP, dATP,

dTTP and dCTP). Thawed Template-Primer mixture (10 µl) was added to the labeling

reaction containing 2 µl of diluted labeling mix (diluted 5 folds), 1.0 µl of [α-^{35}S] dATP,

and 2 µl of diluted sequenase enzyme (diluted 8 folds) and 0.5 µl of autoclaved deionized distilled water. Tubes were mixed thoroughly and then were incubated at room temperature for 5 minutes. 3.5 µl of each labeling reaction was transferred into each of the prewarmed termination tubes, mixed thoroughly and were returned to a 37°C water bath for five more minutes. The reaction was stopped by the addition of 4 µl of stop solution. Before loading, samples were heated to 85°C for 3 minutes and an aliquot of 3 µl was used in each lane in the gel.

2.3.12 Nondenaturing Polyacrylamide Gel Electrophoresis (PAGE)

15% polyacrylamide gels were prepared for a Mini-Protean Cell II electrophoresis system (BioRad). DNA amplification was carried out as previously detailed followed by the addition of 5 µl of 6x loading dye to the PCR product of which 4 µl was loaded into each well along with the molecular-standard marker. Gels were run at 80 volts until the first dye front reached the end of the gel (2-3 hours). Gels were first fixed for 20 minutes in 10% acetic acid followed by three rinses in deionized distilled water for 2 minutes each time. The DNA was visualized by incubating the gels for 30 minutes in 500 ml of silver stain solution after which they were rinsed with deionized distilled water for less than 20 seconds and then were transferred to a tray containing 500 ml of the developing solution where they were removed as soon as the bands appear. Finally, gels were fixed for 5 minutes in 10% acetic acid. Gels were stored after they were soaked for 90 minutes in a solution of 3% glycerol, 40% methanol, 10% acetic acid and them dried at 60°C for one hour and 15 minutes.

2.3.13 Genetic Linkage Map

2.3.13.A DNA panel from Backcrosses and Intercrosses

The genetic linkage map was constructed using intercross and backcross populations of *brl* mutant mice and C57BL/6J (B6) inbred mice. Male *brl* mice were crossed to female B6 mice (*brl* females were sterile) to produce B6*brl*F1 hybrids which were then intercrossed to produce B6*brl*F2 hybrids. At the same time, F1 hybrid females were backcrossed to *brl* males to produce a population of B2 animals of which their females were then backcrossed to *brl* males. Their offspring were again backcrossed to *brl* males for one more generation. *Camk2b* gene was mapped using this population of animals.

2.3.13.B Linkage Analysis

As described previously, the *brl* locus was mapped to proximal chromosome 11 tightly linked with the microsatellite *D11Mit226* (Welker et al., 1996). A high resolution genetic map was constructed around the *brl* locus. This was achieved by increasing the sample number and the addition of new marker loci published by other laboratories. New loci were tested for their linkage and their position relative to other known loci was determined using haplotype analysis method. By comparing the data obtained from the new locus, one can place it relative to known loci based on its haplotype. The genetic distance can be determined by calculating the number of animals that have recombinations between both haplotypes and dividing that over the total number of recombinant animals between two anchor loci. The product will then be multiplied by the distance in cM between the two anchor loci.

2.3.13.C Combined Genetic Map

Independent linkage maps for the intercross and backcross population were constructed and then combined by calculating a weighted average. Weighted averages were calculated from the recombination frequencies in the intercross and backcross population using Fisher's theory of statistical information (Green 1981):-

Weighted mean = (w1x1 + w2x2) ÷ (w1 + w2)

where x1 = recombination frequency; w1 = n1i1; i1 = $4\text{-}5c\text{-}8c^2$ ÷ 2c(1-c)(2+c); n1 = total sample size and c = x1(1-x1). The weighted mean was calculated for the proximal and distal regions separately for each of the intercrosse and backcross population.

2.4 Results

Based on the published cDNA sequence (Karls et al., 1992; Genebank: X63615), a total of eight primer pairs were prepared from the 3' UTR of the *Camk2b* gene. Using primer pair F1/R1 (Table 2.1), the 984 b.p. was amplified in order to confirm a restriction fragment polymorphism (RFLP) reported by a colleague in our laboratory. Amplicons from both alleles were subjected to restriction digestion using *HindIII* and *PvuII* enzymes. *PvuII* digestion gave rise to 150 and 834 b.p. fragments in the B6 allele compared to 150, 234 and 600 b.p. in the *brl/brl* allele. On the other hand, digestion with *HindIII* resulted in two fragments of 610 and 374 b.p. in the *brl/brl* allele as compared to 984 b.p. in the B6 allele. Several attempts were not able to confirm this polymorphism (data not shown). Hence, Genomic DNA amplification, cloning and sequencing of the 3' UTR from both B6 and *brl/brl* alleles was initiated to map the gene in relation to the *brl* locus. For this purpose, the above primer pair was used to amplify the first 984 b.p. of the 3' UTR from

both alleles, which were then cloned and sequenced. Sequencing results revealed no differences between the B6 derived-allele and the published cDNA sequence (Karls et al., 1992). Two polymorphisms were detected in the first 250 b.p. of the 3' UTR at b.p. 1874 (G→A) and b.p. 1931 (A→T) of the published cDNA sequence in B6 and *brl* derived alleles, respectively. Both polymorphisms did not change a restriction site that could be easily used in mapping the gene. The potential restriction site was amplified in a fragment generated by primer pairs F2/R3 and F3/R3 (Table 2.1). Restriction digestion of the amplicons failed to reveal any differences between the B6 and *brl*-derived alleles. Therefore, more primers were prepared. Because of the high GC content of the first 1 kb of the 3' UTR five additional primers were prepared from the second 1 kb of the 3' UTR. Both alleles were amplified using primer pair F4/R4 and the amplicons were sequenced. Again, no differences were detected between the published cDNA sequence and the B6-derived allele while two changes were detected in the *brl* derived allele at b.p. 2763 (G→A) and b.p. 2766 (A →T). When Genomic DNA was amplified from both alleles using the last four primer pairs, an amplicon length polymorphism (*D11Dal1*) was detected using primer pair F7/R7 corresponding to nucleotides 3203-3499 in the published cDNA sequence. Direct sequencing revealed that the B6-derived allele was 14 bases longer due to a substitution of 19 base pair (CCCATGGACACAGGGTAAA) for 5 base pair (GGCTC) present in the *brl/brl* allele. This polymorphism was used to map *D11Dal1* using recombinant animals between *D11Mit74* and *D11Mit226*. Figure 2.1 summarizes the genotyping results of recombinant animals in this region. Calculation of

Figure 2.1 Haplotype analysis of intercross and backcross data. Marker loci are shown

on the left hand side and recombinant haplotypes are shown at the bottom. Black boxes

represent homozygous genotypes while white boxes represent heterozygous genotypes.

Backcross

Intercross

D11Mit74
D11Mit, 1,16, 304,106, 72,
D11Mcg1, D11Dal2
D11Dal1
brl
D11Mit226, 62
D11Mit204
D11Mit2

■ Homozygous

□ Heterozygous
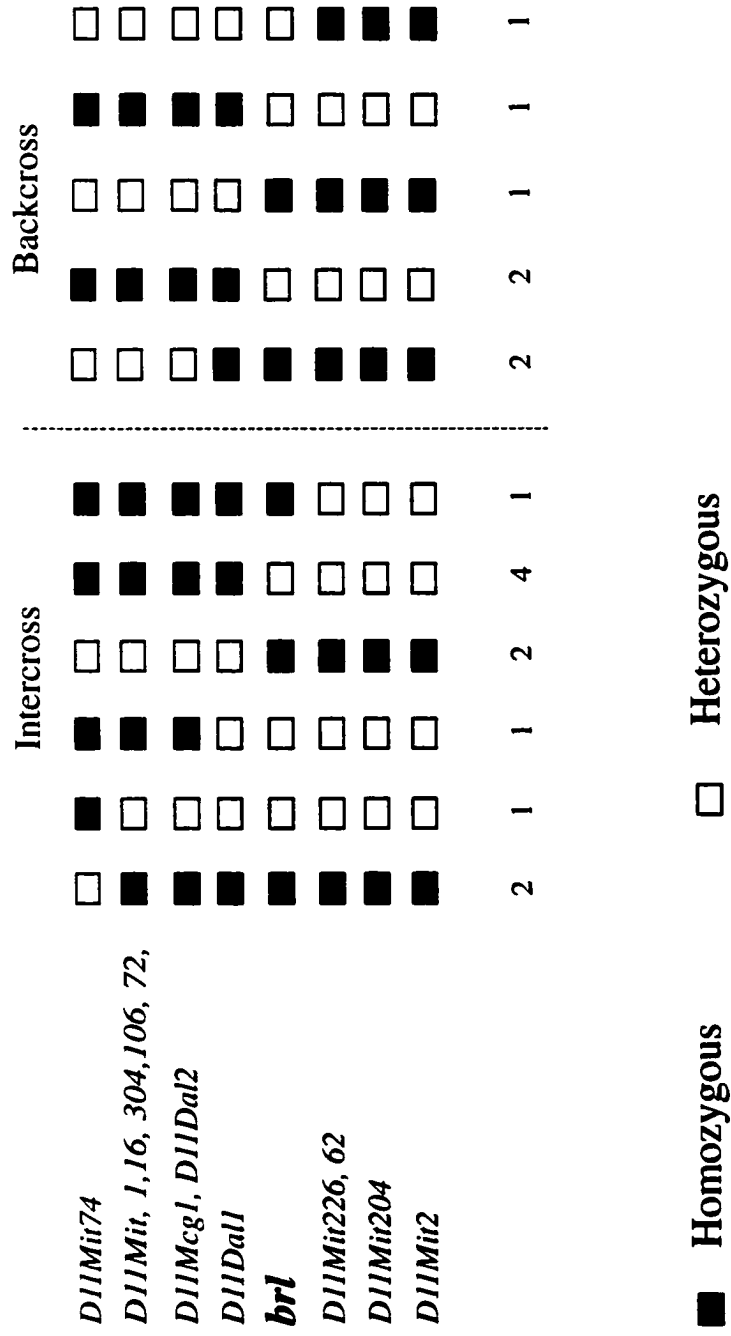
Figure 2.1

recombination frequency using intercross offspring placed the locus at 1.42 cM proximal to *brl*, thus eliminating *Camk2b* as a candidate gene for *brl*, but also shortening the interval containing the *brl* gene (Figure 2.2A). On the other hand, calculation of recombination frequency using backcross offspring mapped *D11Dall* at 0.49 cM proximal to the *brl* locus (Figure 2.2B). The two maps were then combined by calculating the weighted average mean (Figure 2.3) in which the *brl* locus was mapped in an interval of 1 cM, 0.75 proximal to the *brl* locus.

2.5 Discussion

The *Camk2b* gene encodes the β subunit of the CaM kinase II enzyme. It is highly expressed in the forebrain (Erondu and Kennedy, 1985; Bennet et al., 1983). The expression of CaM kinase II subunits is under extensive developmental control (Burgin et al., 1990). The high expression of CaM kinase II in the postsynaptic densities and the autophosphorylation properties makes it a good candidate for involvement in synaptic plasticity, learning and memory. The possible role of this gene in synaptic plasticity led us to evaluate it as a candidate for *brl* since barrel formation involves the appropriate formation of synapses at the right time during development.

Camk2b gene is composed of at least 17 exons of varying lengths, with the longest exon at the 3' end that comprising the whole 3' untranslated region (Karls et al. 1992). Chromosomal localization of the gene to proximal chromosome 11 tightly linked with *Lif* was reported in the above study. *Camk2b* was evaluated as a candidate gene for the *brl* locus. Sequencing of the coding region by Dr. Ourednik revealed no detectable difference in the nucleotide sequence between B6-derived allele and the *brl/brl* allele.

Figure 2.2 A high resolution genetic linkage map in the proximal region of chromosome

11 using intercross (A) and backcross (B) population. A polymorphism *(D11Dal1)* in the

3'UTR region of the *Camk2b* gene was mapped proximal to the *brl* locus (bold). The

distances in cM are shown on the left side of the chromosome with the relative order of

marker loci on the right side.

•
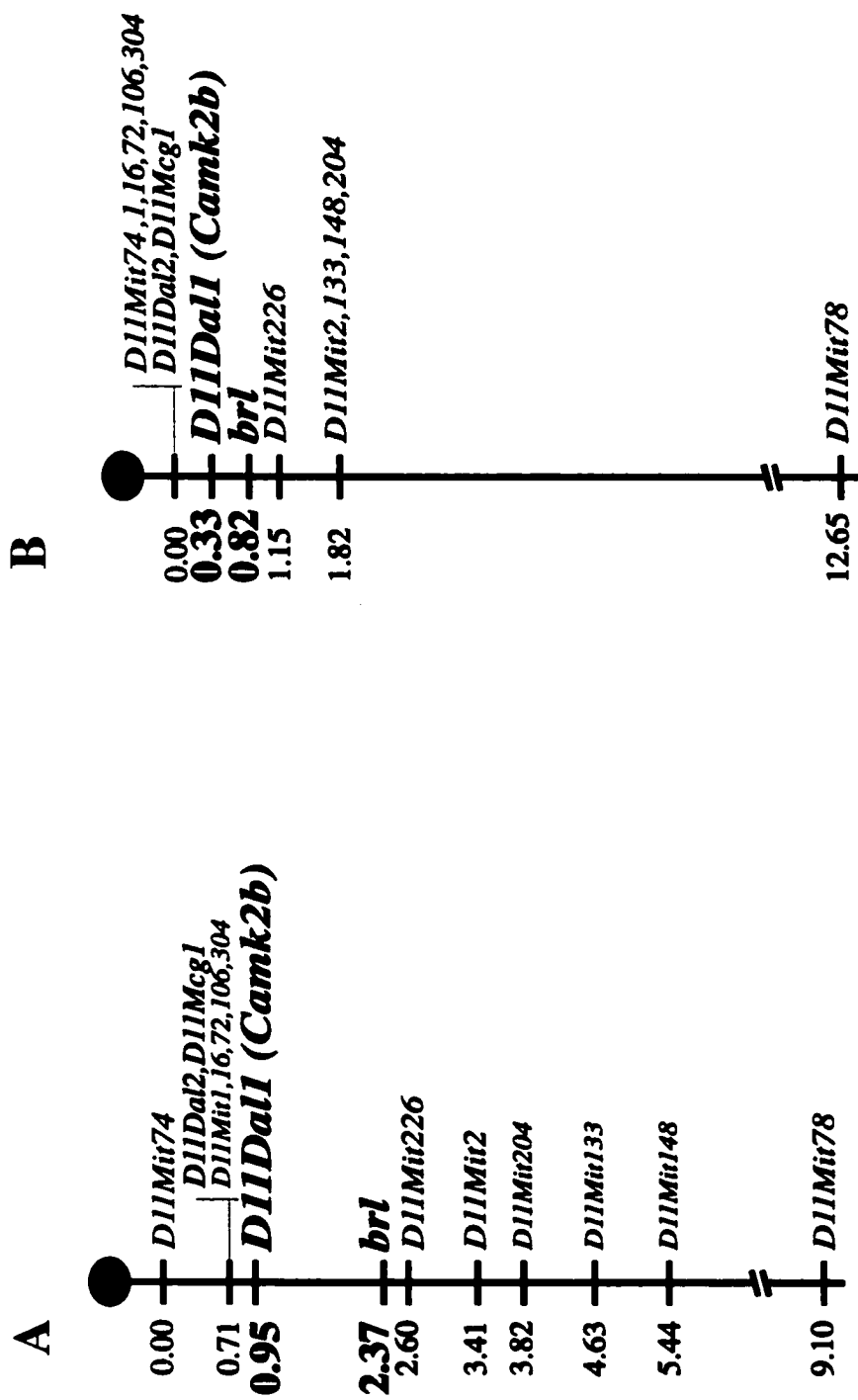
Figure 2.2
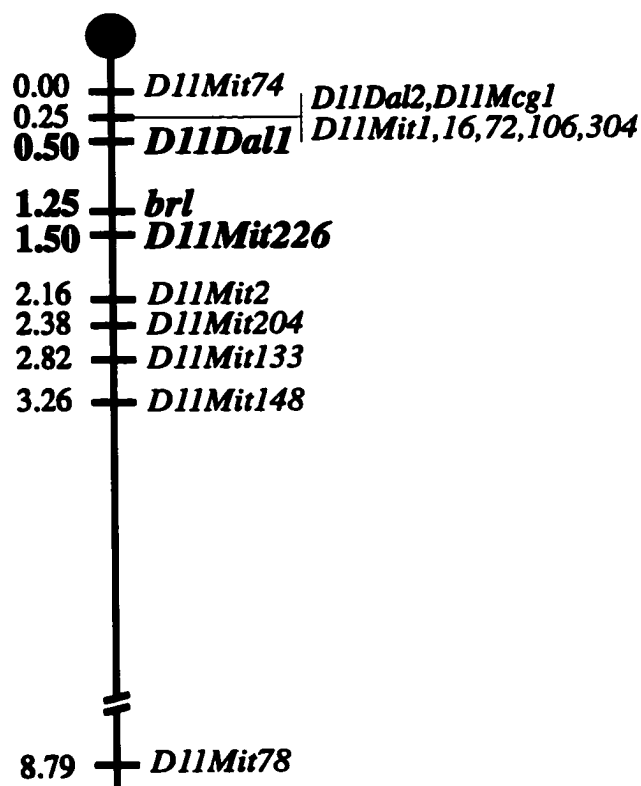
Figure 2.3 A high resolution genetic linkage map of proximal chromosome 11. The weighted averages were calculated from the recombination frequencies in the intercross and backcross maps using Fisher's theory of statistical information. The *brl* locus maps in a 1 cM interval between the markers *D11Dal1* (bold) and *D11Mit226* (bold).

Although this result decreases the potential of the gene as a candidate for *brl*, it was necessary to find a polymorphism in order to map the gene in relation to the *brl* locus and to exclude expression differences between both alleles.

Primer pairs were prepared from the 3' UTR of the published cDNA sequence. Amplicon sizes were the same as calculated from the published cDNA sequence. Moreover, sequencing results revealed no nucleotide differences between B6-derived allele and the published cDNA sequence. Few differences were detected between the B6 and the *brl/brl*-derived alleles, which did not change a restriction digestion site. Polymorphisms were detected in the B6-derived allele at b.p. 1874 of the published cDNA sequence while the *brl* polymorphism was detected at b.p. 1931, 2763 and 2766 of the published cDNA sequence.

Amplification of genomic DNA using primer pair F7/R7 detected an amplicon length polymorphism (*D11Dall*) between B6-derived allele and *brl/brl* allele. Genotyping recombinant animals in the region of interest placed the gene at 0.75 cM proximal to the *brl* locus (Figure 2.3) excluding *Camk2b* gene as a candidate for *brl*, however shortening the *brl* interval to 1 cM. This polymorphism was due to a substitution of 14 base pair in the B6-derived allele.

A high resolution genetic linkage map was constructed around the *brl* locus using a total of 1067 animals. The *brl* locus is in an interval of 1 cM between the markers *D11Dall* and *D11Mit226*. The first step in positional cloning was achieved and we were ready to move to the next step in positional cloning, which was physical mapping.

Physical mapping starts by constructing a contiguous overlap of genomic DNA clones from the region of interest. For this purpose, the flanking markers were used by Dr. L. Schalkwyk (Max-Planck-Institut fuer Molekulare Genetik, abteilung Lehrach, Berlin-Dahlem, Germany) to screen Yeast Artificial Chromosome (YAC) libraries in order to extract genomic DNA fragments that could be aligned in a contig of overlapped clones that completely span the region between the flanking markers.

Chapter 3

Physical Mapping and Identification

of a Candidate Gene for *brl*

3.1 Introduction

Positional cloning strategy was used to isolate the *brl* gene. A high-resolution genetic map was constructed around the *brl* locus (Abdel-Majid et al., 1998) and the flanking markers were used as probes to isolate genomic DNA fragments from established libraries in order to start physical mapping. Physical mapping complements linkage mapping and is based on the direct analysis of DNA rather than on the meiotic chromosomal segregation. Physical maps are divided into "short-range" and "long-range" maps. Short-range maps are generally constructed over a range of 30 kb, while long-range physical maps are usually accomplished over megabase-sized regions using rare-cutting restriction enzymes and pulsed-field gel electrophoresis (PFGE) for separation of large fragments of DNA.

Long-range physical mapping is performed on clones obtained from large insert genomic libraries. The most widely used systems include the phage P1 (Sternberg, 1990; Pierce and Sternberg, 1992) and the yeast artificial chromosomes (YACs) (Burke et al., 1987; Dawson et al., 1986; Hahnenberger et al., 1989). Yeast artificial chromosomes were originally used as a cloning vector by David Burke and Maynard Olson in 1987 at Washington University (Burke et al., 1987). Large fragments of genomic DNA are inserted between two arms of artificial yeast chromosomes, one of which ends with a telomere and a centromere, and in the other a telomere alone, and contain other selectable markers in the yeast host on both arms. The YAC construct is then transfected into the yeast host where it positions alongside host chromosomes and moves into daughter cells at each mitotic division.

The availability of YAC cloning systems, capable of holding large pieces of DNA inserts up to megabase pairs, provided a powerful tool for the construction of physical maps and made it the choice for long-range physical mapping. However, this system has some technical problems. YAC clones are unstable and will give rise to more stable products by deleting parts of their insert. A more prominent problem is chimerism. This is where chimeric clones are formed containing two or more pieces of DNA segments that are not contiguous in the genome. These are found to represent a high fraction of all YAC libraries due to the high efficiency of recombination within the yeast cell. Another problem is that YACs are carried as a single-copy chromosome in a yeast host and yeast cell densities in overnight cultures are lower than *E. coli* cell densities. This leads to longer periods of culture growth with a lower percentage of YAC DNA compared to yeast chromosomal DNA.

A physical map is a hybrid of a "restriction map" and a " contig map". Restriction maps show the order and the distances between cleavage sites of site-specific restriction endonucleases (Nathans, 1979), while contig maps represent the structure of contiguous regions of the genome by specifying the overlap relationship between a set of clones (Olson et al., 1986; Kohara et al., 1987). The approach used in this study was to generate a contig map by adapting the sequence-tagged sites (STS) strategy. An STS is a short single-strand copy of DNA, present once in the genome, that can be detected by PCR amplification. DNA clones are tested for the presence of these STSs and the order of the STSs in the clones is determined. The extent of overlap between adjacent clones can be predicted and clones can be aligned into a contig. STS content mapping is a powerful tool

that aids in the construction of a contig that spans the region of interest of the genome utilizing results obtained from different methods.

In the previous chapter, the evaluation of *Camk2b* gene as a candidate for *brl* and its exclusion based on its position proximal to the *brl* locus was discussed. In addition, a high-resolution genetic map was described in which the *brl* locus was mapped in a 1 cM interval between the markers *D11Dall* and *D11Mit226*. The next step in positional cloning was initiated by using the flanking markers as probes to screen YAC libraries for clones that span the region of interest. This was done in a collaboration with Dr. Leo Schalkwyk (Max-Planck-Institut fuer Molekulare Genetik, Abteilung Lehrach, Berlin-Dahlem, Germany). Figure 3.1 summarizes general protocols used to obtain and analyze YAC clones. Identifying YAC clones from genomic libraries, validation of YAC clones and identifying insert size was performed by Dr. L. Schalkwyk. Analysis of isolated YACs for chimeras using fluorescence *in situ* hybridization (FISH) was performed by Dr. E. Levy (Wellcome Trust Center for Human Genetics, Oxford, England) and obtaining end-clones from YAC clones was performed by my colleague Dr. W. Leong.

3.2 Reagents and Solutions

All reagents were autoclaved for 30 minutes on liquid cycle at 15 lbs/sq. in. prior to use unless otherwise stated. All reagents were of molecular grade and purity. Similarly, all glassware were autoclaved for the same period of time. Preparation of reagents and buffers is presented in Appendix 2.
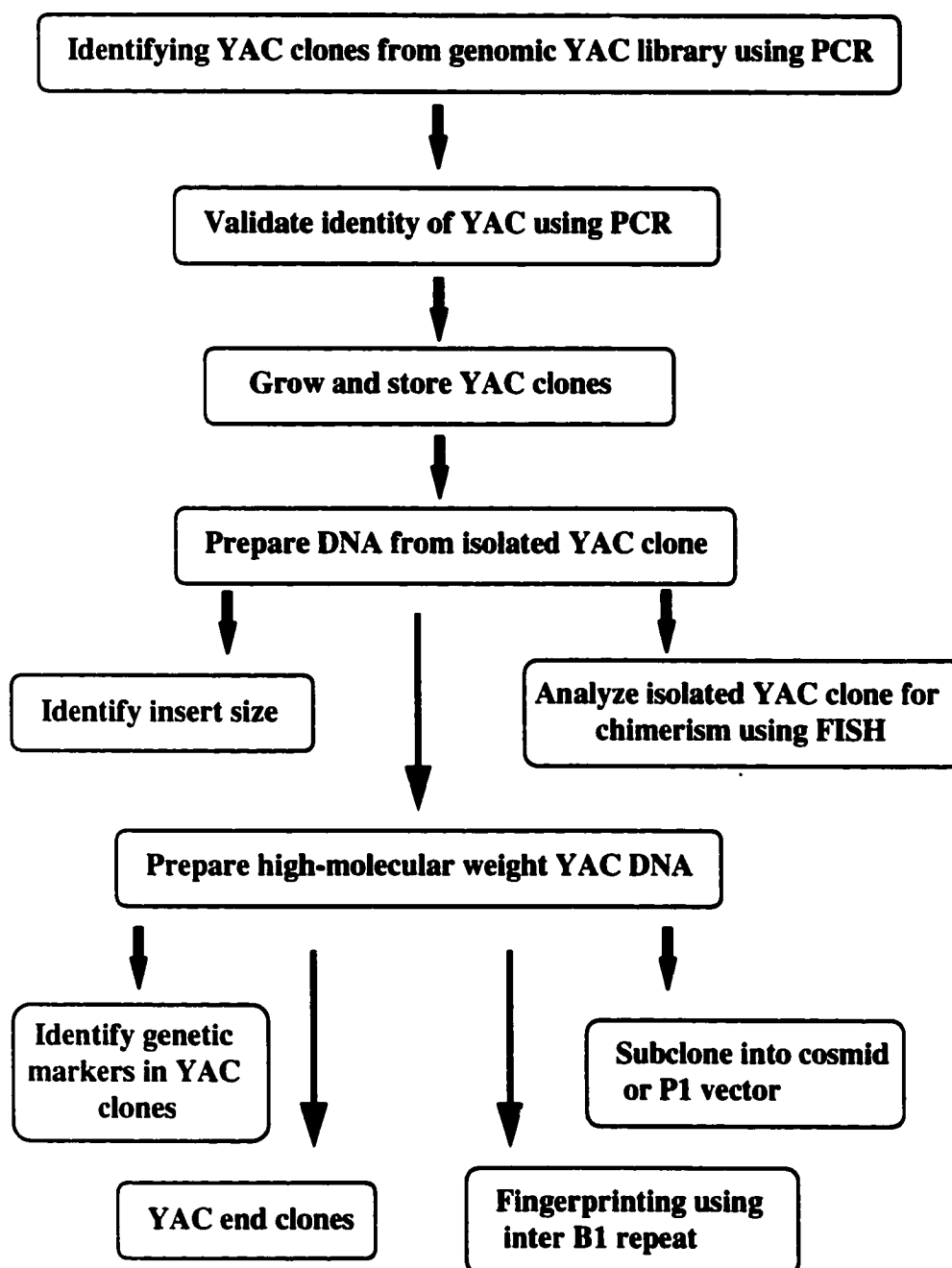
Figure 3.1 Flow chart showing procedures used for identifying and characterization of YAC clones.

3.3 Methods

3.3.1 Storage of YACs and Yeast Strain DNA

All YAC clones were obtained from the Ressourcenzentrum/Primaerdatenbank

des deutschen Humangenomprojektes (RZPD). The host yeast S. cerevisiae AB1380

strain is grown in a YPD (yeast extract-peptone-dextrose) rich media. The vector pYAC4,

which is capable of holding large pieces of inserts of genomic DNA, carries selectable

markers TRP1 and URA3 that when grown in a selective media will allow the selection

of the YAC vector and favors its stability through successive passages. pYAC4 with or

without the insert were always grown in the AHC selective media or on AHC plates.

AB1380 strain containing the pYAC4 with or without the insert were streaked onto AHC

plates (S. cerevisiae AB1380 were streaked onto YPD plates). Plates were inverted and

incubated at 30°C for 48-72 hours. A pink colony was inoculated into AHC media (YPD

media for yeast AB1380) and grown at 30°C for another 48-72 hours. AHC plates were

sealed in paraffin and stored at 4°C up to 4-6 weeks. For long-term storage, a pink colony

was inoculated in 3 mls of the desired media and grown overnight at 30°C. The next

morning, 1 ml of 80% glycerol was added, the tubes were mixed thoroughly and 0.5-1.0

ml aliquots were transferred to cryovials and stored at -70°C until further use.

3.3.2 Preparation of Chromosomal YAC DNA

Several protocols were followed for extraction of YAC DNA from yeast clones

according to standard procedures (Current Protocols in Molecular Biology [6.10.1,

6.10.3]; Current Protocols in Human Genetics [5.1.10]). The following were the most frequently used protocols depending on the purpose and the size of the required DNA.

3.3.2.A Ten-Minute DNA Preparation from Yeast

The following protocol was used to extract DNA from small volume cultures according to Hoffman and Winston (1987) with few modifications. Briefly, a single pink colony was inoculated into 3.0 ml culture of AHC media and grown overnight at 30°C. A 1.5 ml microfuge tube was filled with the culture and cells were collected by centrifugation for 5 seconds using a microcentrifuge. The supernatant was decanted and the cell pellet was vortexed briefly. 0.10 ml of 2% Triton-X-100, 1% SDS, 100 mM NaCl, 10 mM Tris-HCl (pH 8.0), 1 mM Na$_2$EDTA were added to the tube. 0.10 ml of phenol:chloroform:isoamyl alcohol (25:24:1) and 0.20 gm of acid-washed glass beads (BT-5 0.45 mm, Flex-O-lite Ontario, Canada) were added. The tube was vortexed for 5 minutes followed by centrifugation in a microfuge for 5 minutes. 10 µl of 3 M sodium acetate was added to 100 µl of the supernatant. 275 µl of 95% ethanol was added followed by centrifugation for 10 minutes at room temperature. The supernatant was discarded and the pellet was washed twice with 70% ethanol followed by centrifugation for 10 minutes at room temperature. The pellet was air dried and then dissolved in a total of 20 µl of TE buffer. The concentration of DNA was quantitated by electrophorizing 1 µl in a 1% agarose gel electrophoresis against a known standard. 1 ng was used in DNA amplification using PCR.

3.3.2.B Rapid Isolation of Yeast Chromosomal DNA

The following protocol (Currrent Protocols in Molecular Biology, chapter 13.11.2) was used with few modifications for DNA preparation for use in Southern blot hybridization analysis and/or for DNA amplification using PCR. A single pink colony was inoculated into a 10 ml culture of AHC media. The cultures were grown for 48-72 hours at 30°C until stationary phase was reached. The cultures were spun in a table top centrifuge at 1200 x g followed by aspiration of supernatant. Cell pellets were resuspended in 0.5 ml water and centrifuged for 5 seconds. The supernatant was poured off and the pellet vortexed briefly. Cells were resuspended in 200 μl of breaking buffer (2% Triton, 1% SDS, 100 mM NaCl, 10 mM Tris-HCl (pH 8.0), 1 mM EDTA, pH 8.0). 0.3 gm of acid washed glass beads and 200 μl of phenol:chloroform:isoamyl alcohol (25:24:1) were added and vortexed at highest speed for 3 min. 200 μl of TE (10 mM Tris-HCl and 1 mM EDTA, pH 8.0) buffer was added and then the tubes were centrifuged at high speed for 5 minutes and the aqueous layer was transferred to a clean microcentrifuge tube. 1 ml of 100% ethanol was added and tubes were mixed by inversion followed by centrifugation at high speed for 3 min. The supernatant was discarded and 0.4 ml of TE buffer and 30 μl of 1 mg/ml RNase A were added and the tubes were incubated at 37°C for 30 min. 10 μl of 5M ammonium acetate and 1 ml of 100% ethanol were added and the tubes were mixed by inversion. The tubes were centrifuged at high speed for 3 minutes and supernatant was discarded. The pellet was allowed to air dry after which it was resuspended in a total volume of 100 μl TE buffer. Samples were diluted 10 times before use in a PCR reaction.

3.3.3 Preparation of High-Molecular-Weight DNA Size in Agarose Plugs

A single pink yeast colony was inoculated in 5 ml of AHC media. The culture was grown at 30°C for 48-72 hours until it reached saturation. Samples were centrifuged at 2000 rpm using a clinical centrifuge. The supernatant was discarded and cells were resuspended in 250 µl of sorbitol solution (1.2 M Sorbitol [Sigma Co.], 10 mM Tris-HCl (pH 7.5), 20 mM EDTA, 14 mM β-mercaptoethanol and 0.1 mg/ml zymolaze 20-T [ICN Biomedicals]). 250 µl of low melting agarose (Bio-Rad; 1.5% in sorbitol solution containing β-mercaptoethanol) was added to each sample. Samples were quickly mixed and 100 µl was poured into the prepared plug molds. Plugs were pushed out from the molds into 15 ml tubes containing 200 µl of sorbitol solution where they were incubated at 37°C for one hour. The solution was decanted and 5 ml of lysis buffer was added (1% LDS [Sigma Co.], 0.1 M EDTA [Fisher Scientific], 10 mM Tris-HCl, pH 8.0) into each tube. The tubes were then incubated at 37°C for two hours and mixed by swirling every 15 minutes. At the end of the two hours period, the lysis buffer was removed and replaced with 5 ml of fresh lysis buffer, and then incubated overnight at 37°C. The next day lysis buffer was removed and replaced with 5 ml of fresh lysis buffer. Half of a plug was washed three times with 500 µl TE buffer for 45 minutes each. The plug was finally dissolved in 1.0 ml TE buffer and incubated in a 70°C water bath until the plug dissolved completely.

3.3.4 Southern Blot Hybridization

3.3.4.A Southern Blot Hybridization Using YAC End Clones Probes

3.3.4.A.I Restriction digest and Southern blot

0.5-1.0 µg of yeast chromosomal DNA from YACs 110g8, 52d5, yeast and

pYAC4 or 2 µg of mouse genomic DNA were digested with two restriction digestion

enzymes *EcoRI* and *BamHI* (Gibco BRL, Burlington, Ontario) as mentioned previously

(chapter 2). The digested DNA was dried in a speed vacuum, dissolved in a total volume

of 10 µl of tris borate (TBE) buffer and subjected to Southern analysis according to

standard protocols (Sambrook et al., 1982 pp: 383-386). The blots were hybridized

overnight using a 3 kb and 1 kb end fragments (prepared by my colleague Dr. Leong)

obtained from two YAC clones 110g8 and 52d5, respectively. The probes were labeled

using the random primer DNA labeling system as described below.

3.3.4.A.II Radiolabeling of YAC end clones

End clones from the two YACs 110g8 and 52d5 (150 ng each) were labeled using

the random primer DNA labeling system according to manufacturer's instructions (Gibco

BRL, Burlington; Ontario). The radiolabeled probe was separated from the

unincorporated radioisotope using Sepharose G-50 columns (Boehringer Mannheim)

according to manufacturer's instructions.

3.3.4.B. Southern hybridization using oligonucleotide probes

3.3.4.B.I Southern Blots

DNA amplification was performed using mouse genomic DNA, yeast

chromosomal DNA from YAC 110g8 for the microsatellite primer *D11Mit62*. Minigels

were run at 85 volts for 45 minutes. Southern hybridization analysis was performed as

mentioned above with the exception of the deletion of the depurination step since the

expected product was less than 5 kb. The blots were hybridized with the radiolabeled

microsatellite *D11Mit62* probe. Hybridization of the end labeled oligonucleotide was

performed according to standard procedures (Current Protocols in Human Genetics, pp:

2.4.2). The blots were hybridized with the prewarmed hybridization buffer, 7% SDS, 0.25

M NaCl, 0.13 M sodium phosphate (pH 7.0), containing the probe (1 pmole of

oligonucleotide per 1 ml of buffer) at 65°C for one hour after which they were washed

twice with the low stringency wash (6XSSC, 0.1% SDS) at 65°C.

3.3.4.B.II Radiolabeling of Oligonucleotide Probe

The oligonucleotide *D11Mit62* was radiolabeled using the 5' end labeling

according to standard procedures (Sambrook et al., 1982, pp: 122-123) with few

modifications. 20 pmoles of *D11Mit62* or $(CA)_n$ repeat, 20 units of T4 polynucleotide

kinase, and 3 µl of 10x kinase buffer (500 mM Tris-HCl (pH 7.4), 100 mM $MgCl_2$, 50

mM DTT, 1 mM spermidine, and 1 mM EDTA (pH 8.0) and 0.3 µl of $[\gamma^{32}P]dATP$ in a

total volume of 30 µl were mixed and incubated at 37°C for one hour. 20 µl of TE buffer

was added and the labeled DNA was separated from the unincorporated $[\gamma^{32}P]dATP$ by

centrifugation through small columns of Sephadex G-50.

3.3.5 Preparation of STSs for Physical Mapping

A composite map was prepared from available genetic information from different

web sites including the Whitehead Institute (http://www-genome.wi.mit), the Jackson

laboratory (http://www.jax.org), the European Collaborative Interspecific Mouse

BackCross (EUCIB; http://www.hgmp.mrc.ac.uk/MBx), genome database (GDB; http://www.gdb.org), Oxford MRC (http://www.mgu.har.mrc.ac.uk), and Copeland maps (Appendix 3). Once this was accomplished, several STSs were chosen based on their position from the composite map. An STS consists of a short, single-copy DNA sequence that can be detected using PCR. A total of 20 microsatellite markers were prepared as described previously in chapter 2 and used to screen the YAC clones (http://www-genome.wi.mit; Appendix 4). These markers included: *D11Mit1, 16, 129, 228, 106, 73, 304, 72, 305, 71, 148, 150, 162, 259, 74, 204, 2, 226, 62, 149*. In addition, STSs from seven different genes were prepared from published sequences including insulin-like growth binding protein 1 (*Igfbp1*), insulin-like growth binding protein 3 (*Igfbp3*), zinc finger protein, subfamily 1A, 1 (*Ikaros*, currently *Znfn1a1*), transcobalamin 2 *(Tcn-2*, currently *Tcn2)*, Ewing sarcoma homologue (*Ewsh*), neurofilament, heavy polypeptide (*Nfh*) and glucokinase activity (*Gk*), and two were developed in our laboratory *D11Dal1* (a polymorphism in the *Camk2b* gene) and *D11Dal2* (a polymorphism in the *Lif* gene).

3.3.6 PCR Amplification from Chromosomal and Plug YAC DNA for STS content

PCR amplification from both chromosomal and plug YAC DNA was performed in a total volume of 25 µl. 1-2 ng of YAC DNA was used in a solution containing 1x PCR buffer (0.01 M Tris-HCl (pH 8.8), 200 µM each dNTP, 0.5 µM each forward and reverse primers and 5 U/ml Taq polymerase). Amplification of microsatellites was performed in a thermal cycler for a total of 35 cycles with 94°C denaturation for 45 seconds, annealing temperature at 57°C for 45 seconds with an extension time of 1 minute at 72°C and an initial denaturation at 94°C for 3 minutes. Amplification of YAC

DNA for different genes was carried at different conditions depending upon the size of the product and the annealing temperature. Each PCR amplification was performed three times to confirm the presence of the STS marker, using the yeast AB1380 strain and the pYAC4 vector without insert as negative controls, and the mouse genomic DNA as a positive control.

3.3.7 B1-PCR Fingerprinting of YAC Clones

B1-PCR fingerprinting is another strategy for constructing a contig of YAC clones for a particular genomic region. This method involves PCR amplification of mouse-specific B1 repeat sequences. The unique pattern of B1-PCR products generated from YAC clones determines the extent of overlap shared by the clones that are tested positive for a given locus. Since B1 sequences are specific for the mouse genome, this method is also used to confirm the presence of mouse genomic inserts in YAC clones. B1-PCR finger printing was performed in a total volume of 20 µl. 1 µl of YAC DNA was used in a solution containing 1x PCR buffer, 0.01 M Tris-HCl (pH 8.8), 200 µM each dNTP, 1.0 µM of either B1 R (AGT TCC AGG ACA GCC AGG GCT AYA CAG A, with Y = C or T), B1 L (ACT CAG AAA TCY RCC TGC CTC TGC CTC with Y = C or T and R = A or G) or B1 A (GTC CGG CCG CCT GGA ACT CAC TCT GAA GAC) and 20 U of Taq polymerase. PCR amplification carried out for 30 cycles at 95°C (30 seconds), 60°C (1 minute), 72°C (5 minutes) with initial denaturation at 95°C for 150 seconds and final extension of 15 minutes at 72°C.

3.4 Results

The construction of a physical map around the region of the barrelless locus was initiated by screening YAC libraries for genomic clones using the flanking markers *D11Mit226* and *D11Dal1*, in addition to the marker *D11Mit149*. Subsequently, more clones from the Whitehead YAC library (WC 11.0 and WC 11.1; as of summer 1996) and YAC clones probed with end fragments obtained from YAC clones 110g8 and 52d5 were used. All PCR amplifications of YAC clones were repeated three times before a YAC clone was considered positive for a given marker. Table 3.1 summarizes data obtained from DNA amplification using PCR for all 29 STSs and screening a total of 68 YAC clones.

Amplicon sizes for all the STSs were of the expected size except for the YAC clone 110g8. When this clone was amplified using the microsatellite *D11Mit62*, a smaller amplicon was obtained compared to the B6 wild-type mouse genomic DNA. In order to verify that this was the correct amplicon, southern blot hybridization analysis was performed using two different probes, the microsatellite *D11Mit62* and a $(CA)_n$ repeat probe. Both probes hybridized to the amplicon from YAC clone 110g8 confirming the presence of this STS in the clone.

Southern blot analysis was also performed in order to check for the presence of an overlap between YAC clones 110g8 and 52d5. End fragments from both YAC clones prepared by my colleague Dr. Leong (3 kb and 1 kb for YAC clones 110g8 and 52d5, respectively) were used as probes for hybridization. Results using two different restriction endonucleases, revealed that the 1 kb fragment obtained from YAC 52d5 hybridized to

Table 3.1 Characterization of YAC clones from the *brl* region. The 68 isolated YAC clones are listed along with the results of testing for the presence (+ve) or absence (blank) of a specific marker. Screening of YACs, using the 29 STSs, was repeated three times before a YAC clone was considered positive for the presence of a specific STS. Abbreviations: *D11Dal6*, a polymorphism in the *Igfbp1* gene; *D11Dal7*, a polymorphism in the *Igfbp3* gene; *D11Dal8*, a polymorphism in the *Gk* gene; *D11Dal9*, a polymorphism in the *Ewsh* gene; *D11Dal10*, a polymorphism in the *Nfh* gene; *D11Mit#*, Whitehead Institute markers.

No.	Library Name	Short name	Probe	D11Mit74	D11Dal9	D11Dal10	D11Mit72	D11Mit304	D11Mit106	D11Mit16
1	ICRFy902 10b11	10b11	D11Mit226							
2	ICRFy902 10b11	10b11	D11Mit226							
3	ICRFy902 110g8	110g8	D11Mit226							
4	ICRFy902 110g8	110g8	D11Mit226							
5	ICRFy902 117b1	117b1	D11Mit226							
6	ICRFy902 117b1	117b1	D11Mit226							
7	ICRFy902 23d6	23d6	D11Mit149							
8	ICRFy902 23d6	23d6	D11Mit149							
9	ICRFy902 44d5	44d5	D11Mit226							
10	ICRFy902 44d5	44d5	D11Mit226							
11	ICRFy902 44d6	44d6	D11Mit226							
12	ICRFy902 44d7	44d7	D11Mit226							
13	ICRFy902 46a10	46a10	Camk2b							
14	ICRFy902 46a10	46a10	Camk2b							
15	ICRFy902 76f8	76f8	D11Mit149							
16	ICRFy902 88e2	88e2	D11Mit226							
17	ICRFy902 88e3	88e3	D11Mit226							
18	ICRFy903 26f11	26f11	D11Mit226							
19	ICRFy903 26f11	26f11	D11Mit226							
20	ICRFy903 26f12	26f12	D11Mit226							
21	ICRFy903 26f12	26f12	D11Mit226							
22	ICRFy903 26f5	26f5	D11Mit226							
23	ICRFy903 26f5	26f5	D11Mit226							
24	ICRFy903 26f6	26f6	D11Mit226							
25	WIBRy910 127f3	127f3	D11Mit149							
26	WIBRy910 127f3	127f3	D11Mit149							
27	WIBRy910 159c8	159c8	D11Mit149							
28	WIBRy910 159c8	159c8	D11Mit149							
29	WIBRy910 171c9	171c9	Camk2b							
30	WIBRy910 189e4	189e4	D11Mit226							
31	WIBRy910 189e4	189e4	D11Mit226							
32	WIBRy910 52d5	52d5	D11Mit226							
33	WIBRy910 52d5	52d5	D11Mit226							
34	WIBRy910 89a7	89a7	Camk2b							

No.	Library Name	Short name	Probe	D11Mit74	D11Dal9	D11Dal10	D11Mit72	D11Mit304	D11Mit106	D11Mit16
35	WIBRy910 89a7	89a7	Camk2b							
36	WIBRy910 96a7	96a7	Camk2b							
37	WIBRy910 96a7	96a7	Camk2b							
38	WIBRy903 26f6	26f6	D11Mit226							
39	WIBRy910 179c9	179c9	Camk2b							
40	WIBRy917 281e2	281e2	D11Mit72,304				+ve	+ve	+ve	+ve
41	WIBRy917 281d12	281d12	D11Mit304					+ve	+ve	+ve
42	WIBRy917 323e8	323e8	D11Mit72,304					+ve	+ve	+ve
43	WIBRy917 274f12	274f12	D11Mit304					+ve	+ve	+ve
44	WIBRy917 188c2	188c2	D11Mit304							
45	WIBRy917 87e12	87e12	D11Mit72,304				+ve	+ve	+ve	+ve
46	WIBRy917 416g5	416g5	D11Mit304					+ve	+ve	+ve
47	WIBRy917 397c2	397c2	D11Mit72,304			+ve	+ve	+ve	+ve	+ve
48	WIBRy917 415g9	415g9	D11Mit72,304				+ve		+ve	+ve
49	WIBRy917 153e1	153e1	D11Mit72				+ve		+ve	+ve
50	WIBRy917 380f6	380f6	D11Mit71							
51	WIBRy917 121c10	121c10	D11Mit71							
52	WIBRy917 132d12	132d12	D11Mit71							
53	WIBRy917 395c10	395c10	D11Mit129							
54	WIBRy917 350e9	350e9	D11Mit129							
55	WIBRy917 136g12	136g12	129,62,226							
56	WIBRy917 138b3	138b3	D11Mit129							
57	WIBRy917 357d10	357d10	D11Mit62,226							
58	WIBRy917 458f1	458f1	D11Mit62							
59	WIBRy917 144e1	144e1	D11Mit62,226							
60	WIBRy917 114b9	114b9	D11Mit62							
61	WIBRy917 125b12	125b12	D11Mit226							
62	ICRFy902 102g8	102g8	D11Dal3							
63	ICRFy902 103h9	103h9	D11Dal3							
64	ICRFy903 36b6	36b6	D11Dal3							
65	WIBRy910 72d4	72d4	D11Dal3							
66	WIBRy910 82d4	82d4	D11Dal3							
67	WIBRy910 120d12	120d12	D11Dal3							
68	WIBRy910 18g10	18g10	D11Dal5							

No.	D11Dal2	D11Mit1	D11Mit73	D11Dal1	D11Dal6	D11Dal7	D11Dal8	D11Mit71	D11Mit129	D11Mit62	D11Mit226	D11Mit259
1												
2												
3								+ve		+ve	+ve	
4												
5												
6												
7												
8												
9												
10												
11												
12												
13												
14												
15												
16												
17												
18												
19												
20												
21												
22												
23												
24												
25												
26												
27												
28												
29												
30												
31												
32											+ve	
33												
34												

No.	D11Dal2	D11Mit1	D11Mit73	D11Dal1	D11Dal7	D11Dal6	D11Dal8	D11Mit71	D11Mit129	D11Mit62	D11Mit226	D11Mit259
35												
36												
37												
38												
39				+ve								
40	+ve											
41	+ve	+ve										
42	+ve											
43	+ve											
44												
45	+ve											
46	+ve											
47	+ve											
48	+ve											
49	+ve											
50					+ve	+ve	+ve					
51						+ve	+ve	+ve				
52							+ve					
53					+ve	+ve	+ve		+ve			
54									+ve			
55									+ve	+ve	+ve	
56									+ve			
57												
58										+ve		
59										+ve	+ve	
60										+ve		
61											+ve	
62											+ve	
63												
64												
65												
66												
67					+ve							
68						+ve						

No.	D11Mit150	D11Mit204	D11Mit305	D11Mit2	D11Mit148	D11Mit162	D11Mit228	D11Mit149
1								
2								
3								
4								
5								
6								
7							+ve	
8							+ve	
9								
10								
11								
12								
13								
14								
15								
16								
17								
18								
19								
20								
21								
22								
23								
24								
25								
26								
27							+ve	
28							+ve	
29								
30								
31								
32								
33								
34								

No.

D11Mit150 D11Mit204 D11Mit305 D11Mit2 D11Mit148 D11Mit162 D11Mit228 D11Mit149

35
36
37
38
39
40
41
42
43
44
45
46
47
48
49
50
51
52
53
54
55
56
57
58
59
60
61
62
63
64
65
66
67
68

both YAC clones, while the 3 kb fragment hybridized only to YAC clone 110g8. These results suggest that there is an overlap between both clones; moreover, it provided us with the order of the STSs on both clones.

Screening the first batch of 39 YAC clones revealed that the three STSs, *D11Mit226*, *D11Mit62* and *D11Mit149*, were present on only three YAC clones. Results from our genetic linkage map revealed that the marker *D11Mit149* did not map to the right region on proximal chromosome 11 as reported by the Whitehead Institute; hence, this marker was not used for subsequent screening of any other YAC clone.

3.5 Discussion

Positional cloning strategy was followed in order to isolate the gene responsible for the barrelless phenotype. The first stage of positional cloning was initiated by construction of a high-resolution genetic linkage map to get as close as possible to *brl* as detailed in the previous chapter. The second stage started by obtaining genomic clones in YACs using the flanking markers *D11Mit226* and *D11Dall* as probes in order to develop a contig of overlapped clones that completely spans the region. The generation of a contig was accomplished by the characterization of YAC clones for specific markers or landmarks and the identification of genes that are physically present on these clones.

A total of 68 YACs were received from Dr. Schalkwyk that were pulled out from screening YAC genomic libraries using *brl* flanking markers, YAC end clones, and Whitehead Institute markers. The YAC contig was: 1) initiated by screening two YAC libraries, "ICRFy902" (Larin et al., 1993) and "WIBRy910" (Kusumi et al., 1993), with *D11Dall* and *D11Mit226*; 2) extended by screening these libraries and the "WIBRy917"

library (Haldi et al., 1996) with STSs from YAC end-clones (*D11Dal3* and *D11Dal4*); and 3) completed after the addition of Whitehead Institute contig WC11.0. and WC11.1. A total of 29 STSs were used for screening and characterization of these YAC clones using PCR based analysis and/or Southern blot hybridization analysis. Proper positive (B6 mouse genomic DNA) and negative (yeast strain AB1380 and pYAC4 vector without the insert) controls were used in all experiments. YAC clones were also amplified using inter B1-PCR fingerprinting to verify the presence of mouse genomic inserts in the clones. Based on the results summarized in Table 3.1, a partially complete contig of overlapped clones was generated (Figure 3.2; YAC clone characterization using STSs *D11Dal3, 4, 5* was performed by my colleague Dr. Leong). The order of the STSs was predicted from information obtained from characterization of the YAC clones, our genetic linkage and finally from the composite map.

STS-content mapping placed four genes, adenylyl type I gene (*Adcy1*), *Gk*, *Igfbp1*, and *Igfbp3* from the region of conserved synteny with human chromosome 7 (Copeland et al., 1993; Edelhoff 1995) and one gene (*Nfh*) from the region of conserved synteny with human chromosome 22. The physical map demonstrated that the distance of the barrelless interval is larger than the distance the genetic linkage map has predicted. More YAC clones had to be added in order to construct a complete contig that spans the region. Finally, deletions of insert were detected in this contig as indicated by open circles in Figure 3.2.

The physical map identified adenylyl cyclase type I (*Adcy1*) as a candidate gene for *brl*. Using primer pairs prepared from the calmodulin binding site (*D11Dal5*), *Adcy1*
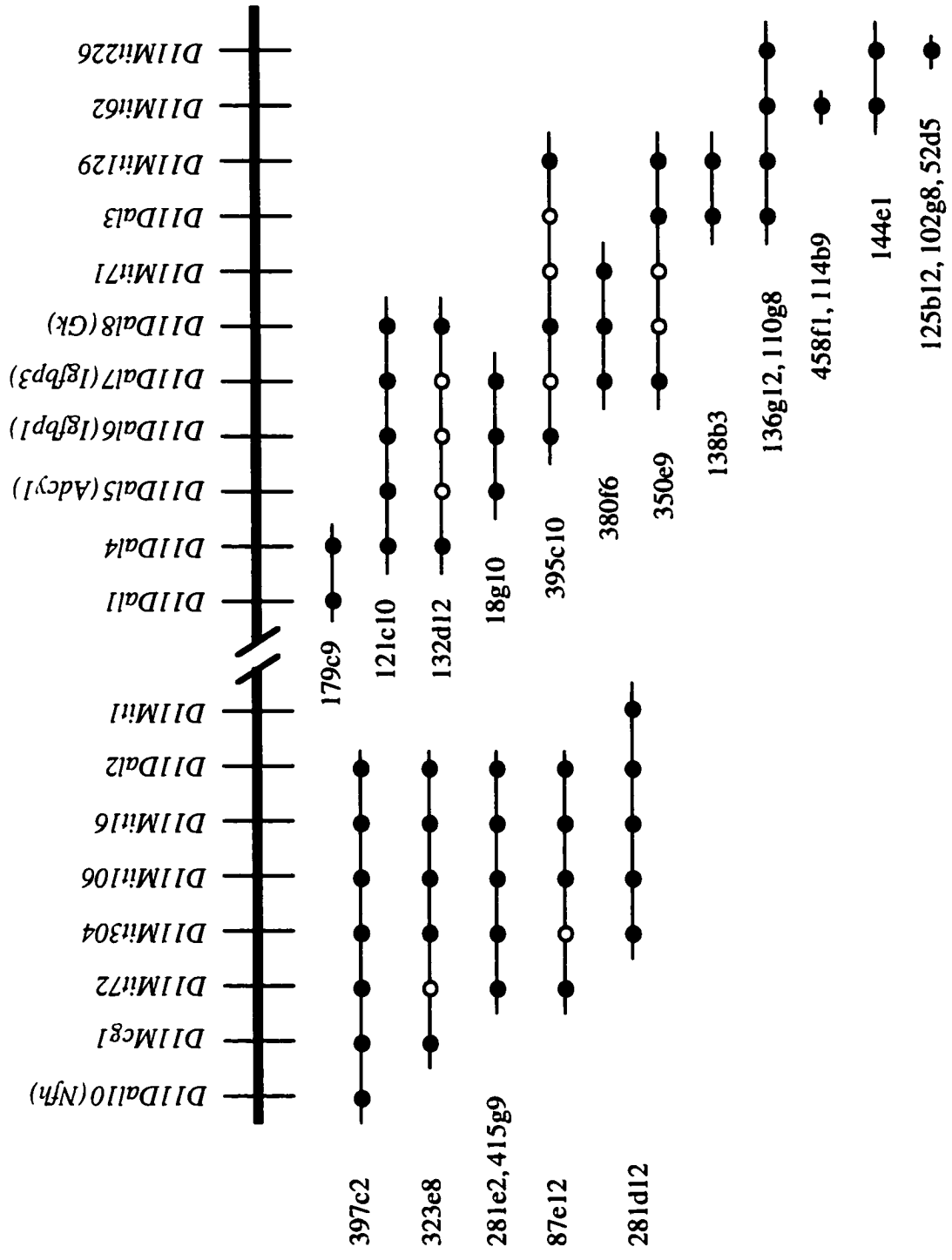
Figure 3.2 STS-content mapping of YAC clones in the region around the *bl* locus. The indicated order was deduced from Table 3.2 with the exception of markers *D11Dal3,4,5*. Deletions in YAC clones are represented by empty circles, while filled black circles represent STS's present in YAC clones.

was placed by my colleague Dr. Leong only on one YAC clone, 121c10. The adenylyl

cyclase family are membrane bound enzymes that catalyze the formation of cAMP, an

important second messenger that is involved in many signaling pathways. Adenylyl

cyclase type I is neurospecific (Xia et al., 1993) and is expressed in areas of the brain that

play an important role in neuroplasticity and learning and memory (Xia et al., 1991).

Hence, evaluation of adenylyl cyclase type I gene was performed at the biochemical and

the molecular level to determine whether it was the gene responsible for the barrelless

phenotype.

Chapter 4

Evaluation of Adenylyl Cyclase Type I

as a Candidate Gene for *brl*

4.1 Introduction

A physical map that spans the *brl* locus was constructed in order to isolate and identify the *brl* gene. Additionally, the physical map identified several candidate genes from the region of conserved synteny with human chromosome 22 and 7. One of these genes, adenylyl cyclase type I (*Adcy1*) gene was evaluated as a candidate for the following reasons: 1) *Adcy1* mapped physically to the *brl* region, 2) adenylyl cyclase type I (AC1) is neurospecific (detected only in the brain, retina and adrenal medulla based on northern blot analysis [Xia et al., 1993]), 3) AC1 is expressed in areas of brain that are normally associated with neuroplasticity including the CA1-CA3 region of the hippocampus and dentate gyrus (Xia et al., 1991), 4) AC1 expression increases in rats and mice during the first two weeks of postnatal life, coincident with barrel formation (Villacres et al., 1995). These characteristics of AC1 are consistent with the hypothesis that this enzyme is important for neuroplasticity and spatial memory in vertebrates.

Adenylyl cyclase (ATP pyrophosphate-lyase [cycling] E.C. 4.6.1.1) is a membrane bound enzyme that catalyzes the conversion of adenosine triphosphate (ATP) to 3'5'-cyclic adenosine monophosphate (cAMP) and pyrophosphate in the presence of guanosine triphosphate (GTP) and magnesium ions as shown below:

$$\text{Adenosine 5'- *P-P-P} \xrightarrow[\text{ATP, Mg}^{2+}]{\text{Adenylyl cyclase}} \text{Adenosine3'5'- *P + P-P}$$
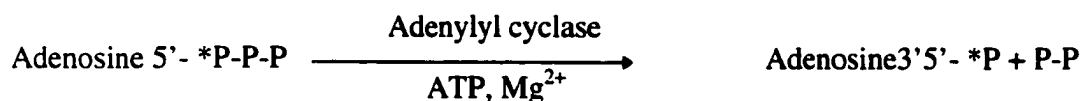
Mammalian adenylyl cyclase (AC) is regulated by different hormones and neurotransmitters through guanosine triphosphate heterotrimeric binding protein (G protein) coupled receptors (reviewed by Ross and Gilman 1980; Gilman, 1989; 1995).

The adenylyl cyclase system consists of three main components: a heptahelical receptor, a heterotrimeric G protein and adenylyl cyclase enzyme. Binding of a hormone or neurotransmitter to a stimulatory receptor causes activation of a G protein, G_s, promoting the dissociation of the α subunit from the $\beta\gamma$ subunit which will in turn stimulate adenylyl cyclase enzyme. The enzyme system is inhibited by a similar mechanism where binding of an inhibitory ligand to an inhibitory receptor will activate another G protein coupled receptor, G_i. Activation of G_i will result in the dissociation of the α_i from the $\beta\gamma$ subunits. Both subunits can inhibit adenylyl cyclase activity.

Adenylyl cyclase type I gene was evaluated at the biochemical level by assaying the enzyme activity in both wild-type and *brl* mutant mice, and at the molecular level by mapping the gene to the genetic linkage map and searching for the mutation in the gene. In addition, mice homozygous for a null mutation (knockout) in the adenylyl cyclase type I gene (*Adcy1*) were examined for the presence of barrels in their somatosensory cortex.

4.2 Reagents and Solutions

All reagents were of molecular grade and purity. Preparation of reagents are described in Appendix 5. cAMP formation was assayed using Amersham's (Life Sciences) enzymeimmunoassay (EIA) kit.

4.3 Methods

Figure 4.1 summarizes various steps used to assay adenylyl cyclase activity in membrane brain preparations from wild-type and *brl/brl* mutant mice.
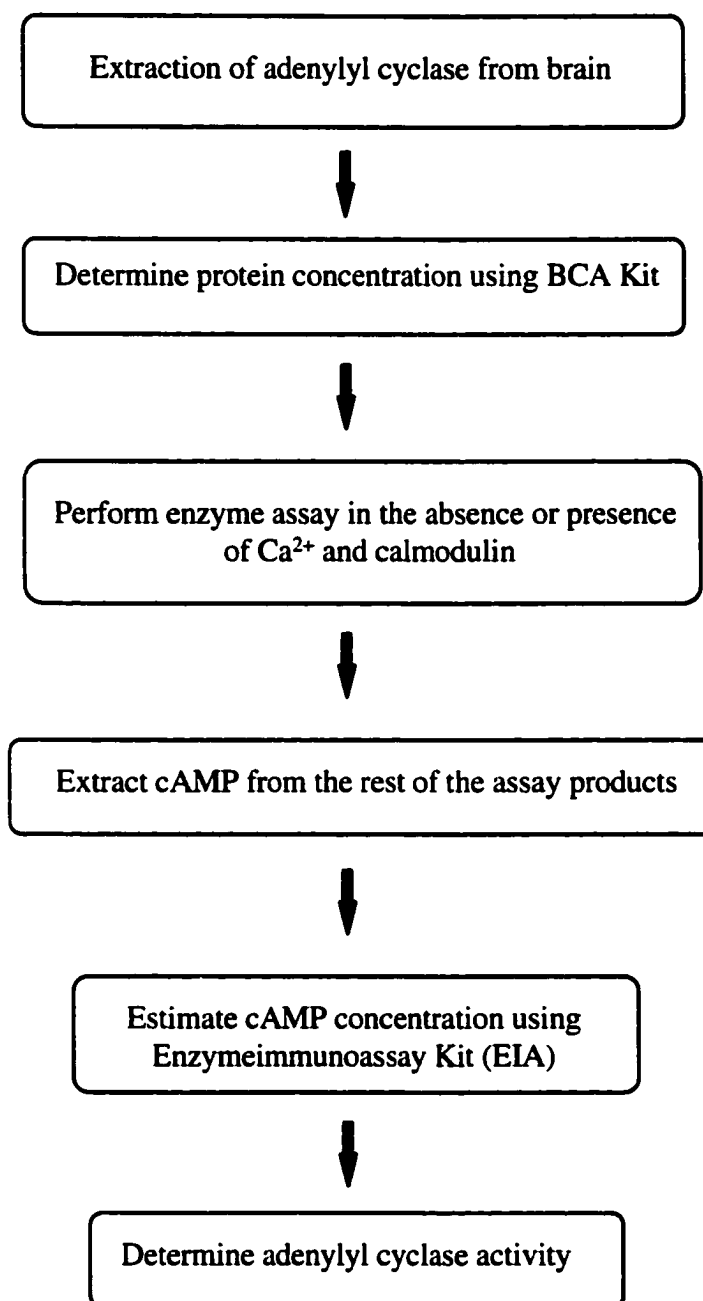
Figure 4.1 A flow chart representing the steps involved in determining adenylyl cyclase activity from brain homogenate preparations from wild-type and barrelless mutant mice.

4.3.1 Preparation of Detergent-dispersed Adenylyl cyclase

Two-week-old wild-type (B6) and *brl* mutant mice were sacrificed using carbon dioxide. Brains were removed immediately and immersed in cold phosphate- buffered saline solution. Membrane protein fractions were prepared according to Johnson and Sutherland (1973). Briefly, brains were weighed and nine volumes of ice-cold homogenization buffer (0.25 M sucrose [Fisher Scientific], 0.1 M glycylglycine (pH 7.5) [Sigma Co.], 2 mM $MgCl_2$ [Fisher Scientific], 1 mM EDTA [Fisher Scientific], and 3 mM dithiothreitol [Sigma Co.]) were added followed by homogenization on ice with three passes of a glass-teflon motor driven homogenizer. The homogenate was centrifuged at 5,000 rpm (3,000 x g) using a Beckman JA-20 centrifuge for 10 minutes after which the supernatant was discarded. The pellet was resuspended in nine volumes of homogenization buffer followed by centrifugation. The process of homogenization and centrifugation was repeated for a total of three times. The fourth homogenate was resuspended in ice-cold homogenizing buffer containing 1% Lubrol (ICN Biomedicals) followed by centrifugation at 15,000 rpm (27,000 x g) for 20 minutes. The supernatant was collected and aliquoted into small volumes and stored at -70°C until use.

4.3.2 Estimation of Protein Concentration

Protein concentration was determined using the BCA Protein Assay Reagent (Pierce, Rockford, Illinois, U.S.A.) according to manufacturer's instructions with few modifications. Briefly, bovine serum albumin (BSA) standards were prepared at a final concentration of 25-2000 µg/ml using the homogenized buffer containing 1% Lubrol as a diluent (diluted 20 times). 0.1 ml of the sample (diluted 20 times), standard or the diluted

homogenized buffer was added into each tube. 2 ml of working reagent (50 parts of reagent A + 1 part of reagent B) was added followed by incubation at 37°C for 30 minutes. The tubes were cooled to room temperature and the absorbance was measured at 562 nm against water as a reference within the next 10 minutes. The standard or sample results were subtracted from the blank results and a curve was drawn showing the correlation between the net A_{562} and the concentration in $\mu g/ml$. The concentration of the sample was predicted from the standard curve (Figure 4.2) and the total concentration was calculated after multiplying by the dilution factor.

4.3.3 Adenylyl Cyclase Enzyme Assay

Assaying adenylyl cyclase activity *in vitro* presents a number of problems: 1) the enzyme is present in extremely small amounts in membrane preparations, 2) since other kinases are present at higher concentrations, the adenylyl cyclase enzyme has to compete with them for ATP, 3) cAMP is quickly hydrolyzed to 5' adenosine monophosphate (5'-AMP) especially in the presence of high activity enzymes in these membrane preparations, and lastly, and lastly, 4) the enzyme is inactivated by the presence of cyclic nucleotide phosphodiesterases, hence these enzymes should be inhibited in order to accurately measure the rate of cAMP formation.

The enzyme assay was performed, with and without free Ca^{2+} (estimated to be 300-500 nM) and 2.4 μM calmodulin (CaM; Sigma Co., 55,000 U/mg solid), in a 250 μl volume containing 30 μg of membrane preparation, 20 mM Tris-HCl (pH 7.4), 1 mM ATP (Sigma Co.), 5 mM $MgCl_2$, 1 mM 3-isobutyl-1-methyl-xanthine (IBMX, Sigma Co.), 1 mM EDTA, 0.1% BSA (Boehringer Mannaheim), 20 mM creatine phosphate
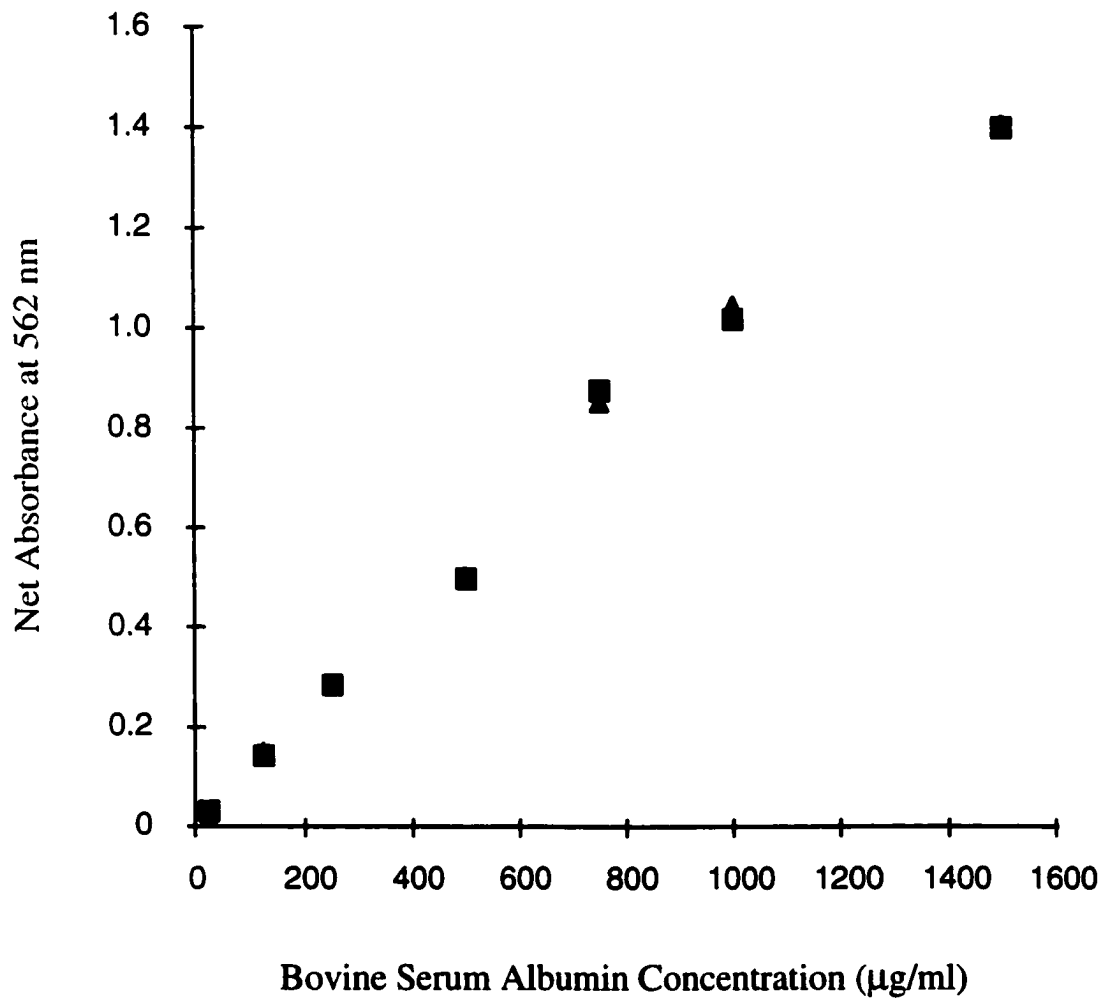
Figure 4.2 A standard curve representing the correlation of the net absorbance at 562 nm with the bovine serum albumin concentration measured by the BCA kit. Points represent duplicate measurements. Stock solution was prepared at 2 mg/ml.

(Sigma Co.), 60 U/ml creatine phosphokinase (CPK, from rabbit muscle, Boehringer Mannaheim), 20 U/ml myokinase (from rabbit muscle, Boehrengir Mannaheim) and 8 U/ml adenosine deaminase (Sigma Co., 400U/0.4 ml). Free Ca^{2+} concentration was estimated using the Bound and Determined computer program (Brooks and Storey, 1992). The assay was incubated at 30°C for 20 minutes, and the reaction was stopped by the addition of 250 µl of 2% SDS followed by boiling for 2 minutes.

4.3.4 Extraction of cAMP

cAMP was extracted using the liquid phase method according to manufacturer's instructions. Briefly, 975 µl of absolute ethanol was added to the enzyme assay product and the tubes were incubated at -70°C for 5 minutes. The supernatant was discarded and the resultant precipitate was washed with ice-cold ethanol at a final concentration of 65% followed by centrifugation at 2000 x g for 15 minutes at 4°C. Finally, the extract was dried using centrifugation in a vacuum and then dissolved in a final volume of 500 µl of assay buffer (Amersham kit). The extracts were diluted 75 times before cAMP measurement was performed.

4.3.5 Measurement of cAMP formation

Measurement of cAMP formation was performed using Amersham's cAMP enzymeimmunoassay (EIA) system (Amersham, Oakville, Ontario, Canada) according to manufacturer's instructions. The assay is based on a competition between unlabeled cAMP and peroxidase-labeled cAMP for a limited number of binding sites on a cAMP specific antibody. The amount of the peroxidase-labeled cAMP will be inversely proportional to the concentration of the added unlabeled cAMP.

All reagents were equilibrated to room temperature. Assay buffer, standard solutions, antiserum, cAMP peroxidase conjugate and wash buffer were prepared according to manufacturer's instructions. The assay protocol was performed using the non-acetylation method as described in Table 4.1.

4.3.6 Calculation of Adenylyl Cyclase Specific Activity

Adenylyl cyclase activity is determined by measuring cAMP concentrations generated by the enzyme *in vitro*. cAMP concentrations were calculated as follows. The average optical density was calculated for each set of replicate wells. The percentage of bound cAMP for each of the samples and the standards was calculated as described by the manufacturer according to the following equation :

$\%B/B_0$ = [(Sample or Standard OD - NSB OD) ÷ (B_0 OD - NSB OD)] x 100 where NSB is non specific binding and B_0 is the binding in the absence of a standard. A standard curve was generated by plotting the percentage B/B_0 against the log cAMP concentration (Figure 4.3).The amount of cAMP in sample was read directly from the curve and then was subtracted from its control. The specific enzyme activity was calculated according to the following equation:

Adenylyl cyclase activity = (Net cAMP conc. x .01875)/ protein conc. (mg)

  (pmole/minute/mg)

4.3.7 Histology of Adenylyl cyclase Knockout Mice

Seven-month-old mice homozygous for a targeted disruption of either *Adcy1* and *Adcy8* genes were obtained from U. Washington (Seattle; U.S.A.). 50 μm thick sections

Table 4.1 Adenylyl cyclase enzymeimmunoassay protocol using the non-acetylation

method. The substrate blank was omitted since the non-specific binding in the assay is so

low and the non-specific binding (NSB) wells were used to blank the microtiter plate.

Reagent	Non-specific binding (NSB) µl	Zero standard (B_0) µl	Standards (µl)	Sample (µl)	Substrate blank (µl)
Buffer	200	100	-	-	-
Standard	-	-	100	-	-
Sample	-	-	-	100	-
Antiserum	-	100	100	100	-
	Microtiter plate was covered and incubated at 3-5°C for 2 hours				
Peroxidase conjugate	50	50	50	50	-
	Microtiter plate was covered and incubated at room temperature for exactly 60 minutes while shaking				
	Solution was aspirated and wells were washed four times with 400 µl wash buffer				
Substrate	150	150	150	150	150
	Microtiter plate was covered and incubated at room temperature for exactly 60 minutes while shaking				
1.0 M Sulphuric acid	100	100	100	100	100
	Contents were shaken and the optical density was measured at 450 nm				

Table 4.1
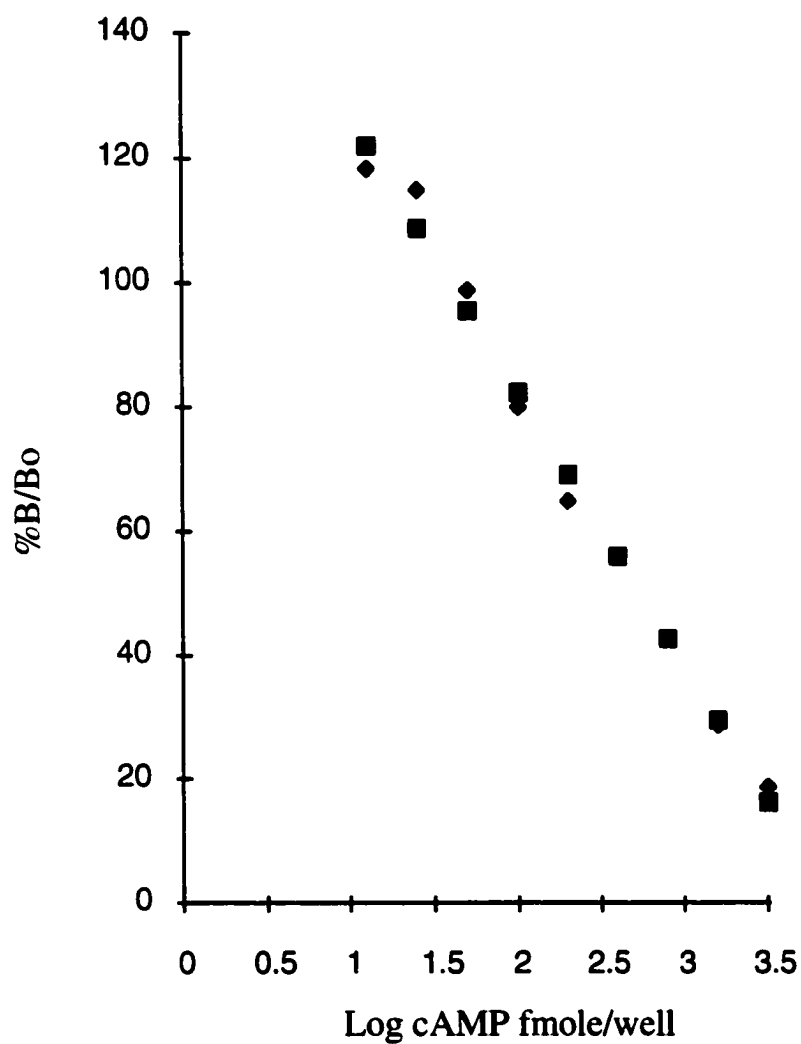
Figure 4.3 Standard curve representing the percent B/B_0 as a function of the log cAMP concentration in fmole/well using the non-acetylation protocol. Standard curve solutions were prepared at 12.5-3200 fmole. Abbreviations: $\%B/B_0$, percent of bound cAMP; log, logarithm; fmole, concentration of cAMP in femtomole ($= 10^{-12}$ mole).

were cut parallel to the pial surface overlying the primary somatosensory cortex, and stained with cresyl violet (Nissl).

4.3.8 Mapping of D11Dal11

Sequencing of *Adcy1* cDNA from B6 (Genbank AF053980) and *brl* mutant mice (by my colleague Dr. Leong) revealed a polymorphism in the 5' end of the coding region (*D11Dal11*). Genomic DNA amplification of the 5' end of the *Adcy1* gene was performed using half nested PCR for all animals that were recombinant between *D11Mit74* and *D11Mit226*. The first step of amplification was performed in a total volume of 25 µl containing 1x PCR buffer (0.01 M Tris-HCl, pH 8.8), 200 µM dNTP, 0.4 pmole of degenerate primer **A93** 5'-GCT AAG GGC TCG CAC CCC GTN CAY TGY GT-3' (where N=A/C/G/T and Y=C/T), 0.2 pmole of **R1** 5'-CTC AAT GCA GTT CCG GGC CT-3' specific primer, and 250 ng of mouse genomic DNA. The second step of amplification was performed using 1 µl of the amplified PCR product (diluted 100 times) in a total volume of 25 µl containing 1x PCR (0.01 M Tris-HCl (pH 8.8), 200 µM dNTP, 0.2 pmole of both forward **F1** 5'-GCT GCT CTT CAG CCT CAC CTT-3' and reverse **R1** specific primers). Cycling parameters were: 94°C (3 minutes) - [94°C (45 seconds)- 58°C (45 seconds) - 72°C (1 minute)] 35x - 72°C (10 minutes) - 15°C. Amplified products were analyzed by electrophoresis in 1.5% agarose gels. Amplicon sizes were 482 b.p. from the first PCR amplification and 375 b.p. from the second amplification. The second PCR product was digested using *BanI* (20,000 U/ml, New England Biolabs) restriction endonuclease (as described previously in chapter 2) to give rise to two bands of 262 b.p. and 113 b.p. in the B6-derived allele and 375 b.p. in the *brl/brl* derived allele.

4.4 Results

Adenylyl cyclase activity in brain membrane preparations from both wild-type and

brl/brl mutant mice was measured in the absence (Table 4.2) or presence (Table 4.3) of

Ca^{2+} and calmodulin. Basal adenylyl cyclase activity (without Ca^{2+}/CaM) in *brl/brl* mice

was half of wild-type mice, yet this difference was not statistically significant (Figure

4.4). However, there was a significant difference in enzyme activity in the presence of

Ca^{2+} and calmodulin ($t = 5.7$, df = 3.0, $p = 0.01$). This was the result of a six-fold increase

in adenylyl cyclase activity in wild-type mice, whereas no increase in enzyme activity was

observed in *brl* mutants.

Sections through layer IV of the somatosensory cortex of *Adcy1* knockout mice

revealed the absence of barrels (Figure 4.5A) compared to *Adcy8* knockout mice (Figure

4.5B) that displayed the presence of a normal pattern of barrels.

A polymorphism that was found in the 5' end of the coding region of the *Adcy1*

gene (*D11Dal11*) was detected in all ICR-derived lines. Genotyping recombinant animals

(Figure 4.6) in the *brl* interval mapped *D11Dal11* to be 0.17 cM proximal to the *brl* locus

(Figure 4.7).

4.5 Discussion

The mammalian adenylyl cyclase family is composed of at least nine isoforms

encoded by at least nine genes and additional variants that differ in their regulatory

properties and tissue distributions (Krupinski et al., 1989; Feinstein et al., 1991; Gao and

Sample	Average O.D.	Average B/B$_0$	Conc.(fmol/well)	Net conc.	Specific Activity
B$_0$	1.365				
Control	1.182	86.593	80.362		
B6 #1	1.064	77.949	126.257	45.895	20.49
B6 #2	1.054	77.216	131.184	50.822	31.76
brl #1	1.150	84.25	90.836	10.474	5.46
brl #2	1.156	84.689	88.773	8.412	5.26
B$_0$	1.634				
Control	1.321	80.870	58.333		
B6 #3	1.042	63.772	171.229	112.896	70.56
B6 #4	1.094	66.978	139.773	81.440	50.90
brl #3	1.084	66.331	145.579	87.246	58.42
brl #4	1.211	74.140	89.069	30.736	19.21

Table 4.2 Basal adenylyl cyclase activity (pmole/min/mg protein) in brain membrane preparations of wild-type (B6) and *brl* mutant (n=4).

Sample	Average O.D.	Average B/B₀	Conc.(fmol/well)	Net conc.	Specific Activity
B₀	1.365				
B6 #1	0.607	44.444	727.241	669.424	298.85
B6 #2	0.634	46.446	654.984	597.167	373.23
brl #1	1.127	82.539	99.325	41.508	21.62
brl #2	1.150	84.249	90.836	33.019	20.64
B₀	1.365				
Control	1.257	76.912	74.883		
B6 #3	0.867	53.048	335.811	260.928	163.08
B6 #4	0.767	46.936	493.251	418.368	261.48
brl #3	1.116	68.274	128.930	54.047	36.19
brl #4	1.162	71.129	107.747	32.864	20.54

Table 4.3 Adenylyl cyclase activity (pmol/min/mg protein) in the presence of Ca^{2+} (estimated to be 300-500 nM) and CaM (2.4 µM) in brain membrane preparations of wild-type (B6) and *brl* mutant.
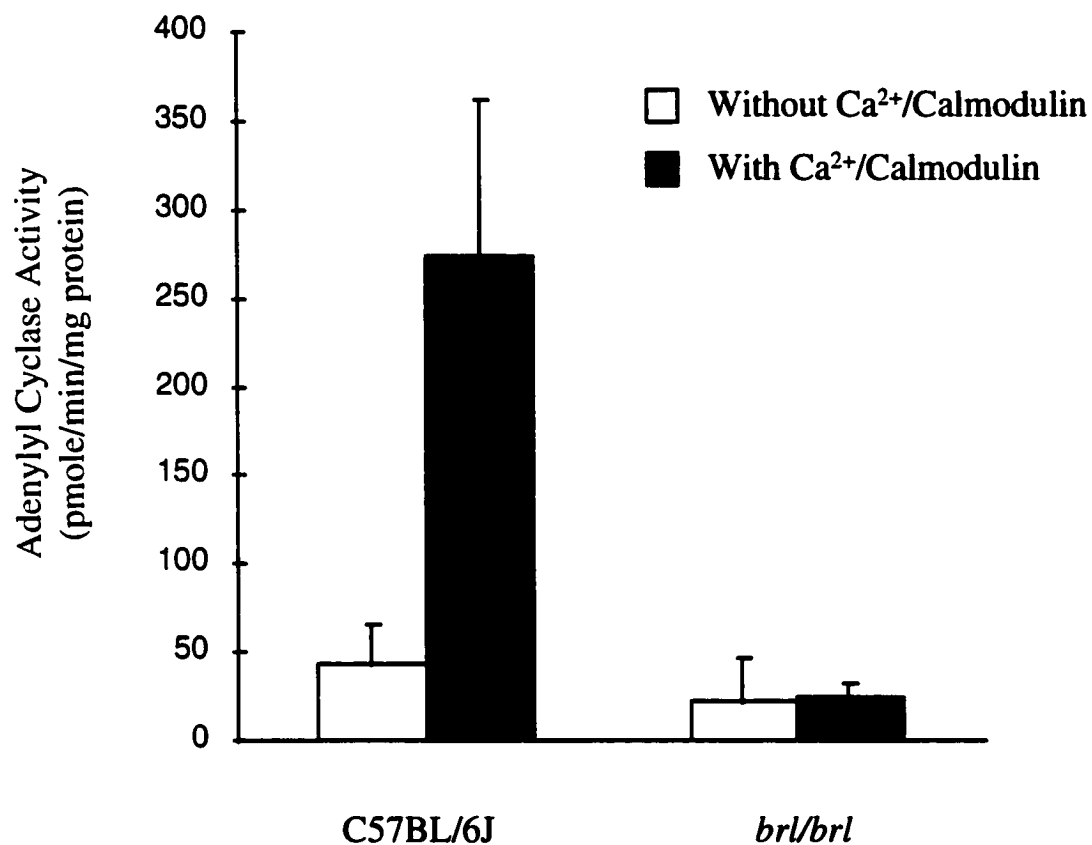
Figure 4.4 Adenylyl cyclase activity in two-week-old wild-type and *brl/brl* mutant mice. Enzyme activity in brain membrane protein fractions was measured in the absence (white bars) or presence (black bars) of free Ca^{2+} (estimated to be 300-500 nM) and calmodulin.

Figure 4.5 Digitized images of layer IV of SI cortex from seven-month-old *Adcy1* (A)

and *Adcy8* (B) knockout mice. *Adcy1* knockout mice display a barrelless phenotype,

whereas *Adcy8* knockout mice have the normal pattern of barrels separated by cell-sparse

septa.
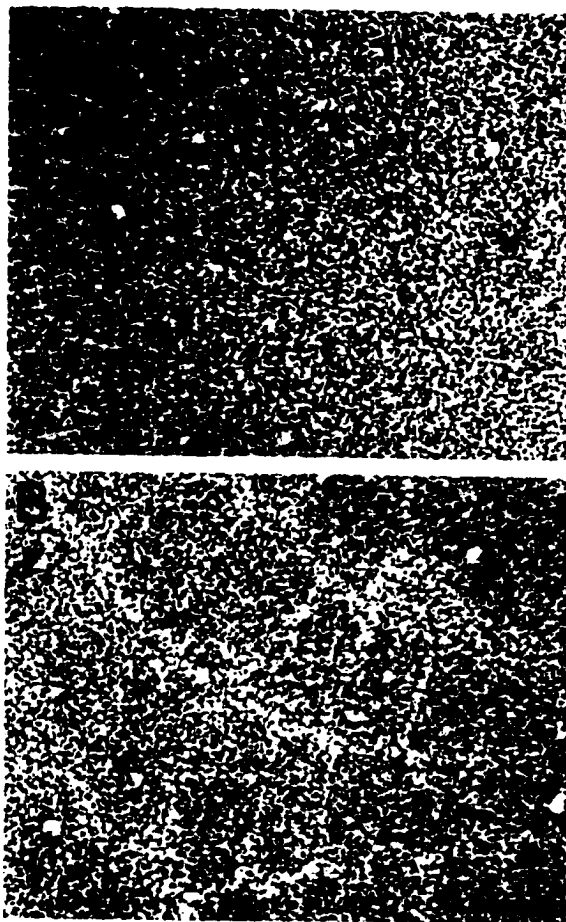
Figure 4.5

Figure 4.6 Haplotype analysis of intercross and backcross data. Marker loci are shown on the left hand side with recombinant haplotypes shown at the bottom. The black boxes represent homozygous genotypes while the white boxes represent heterozygous genotypes.
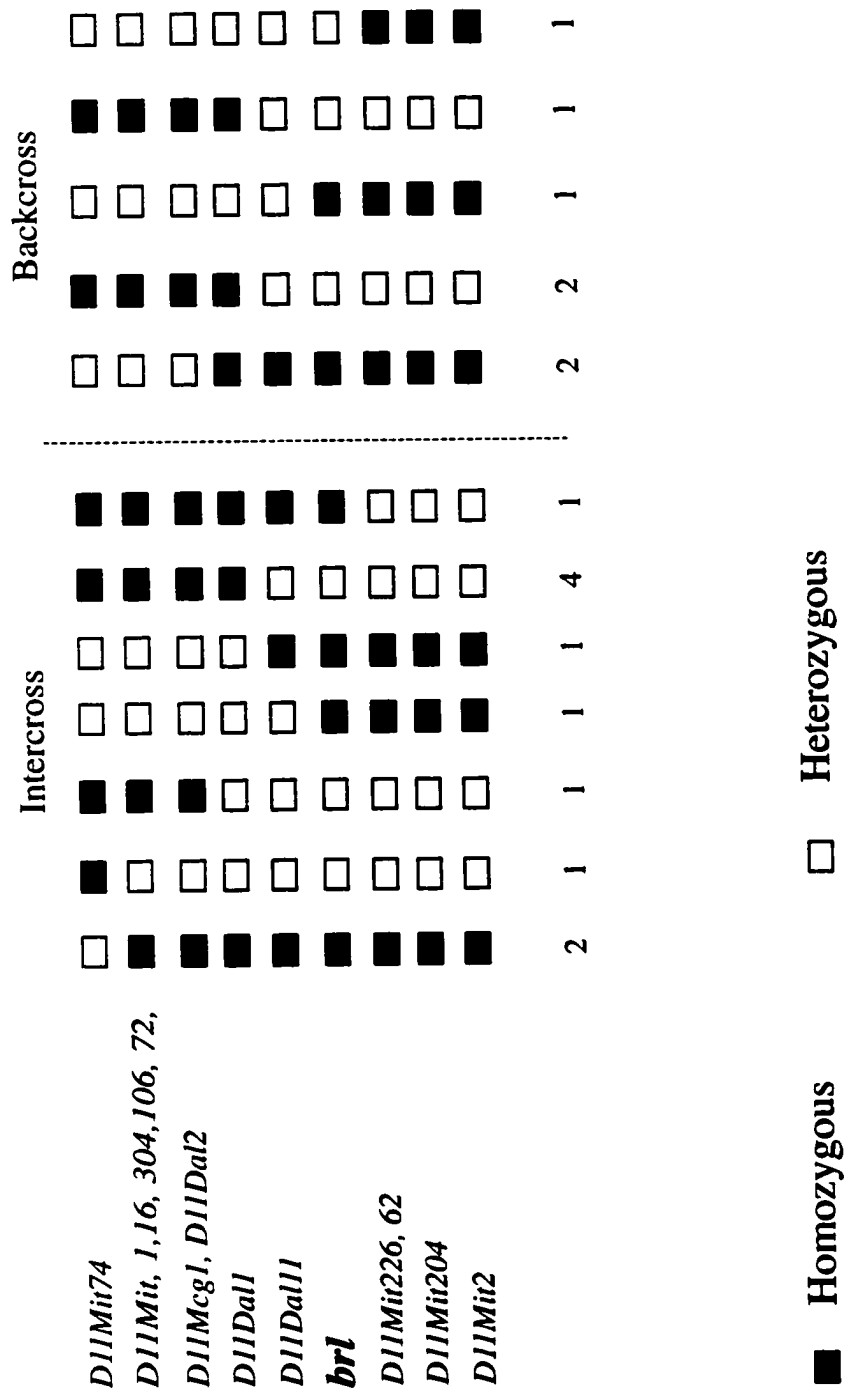
Figure 4.6
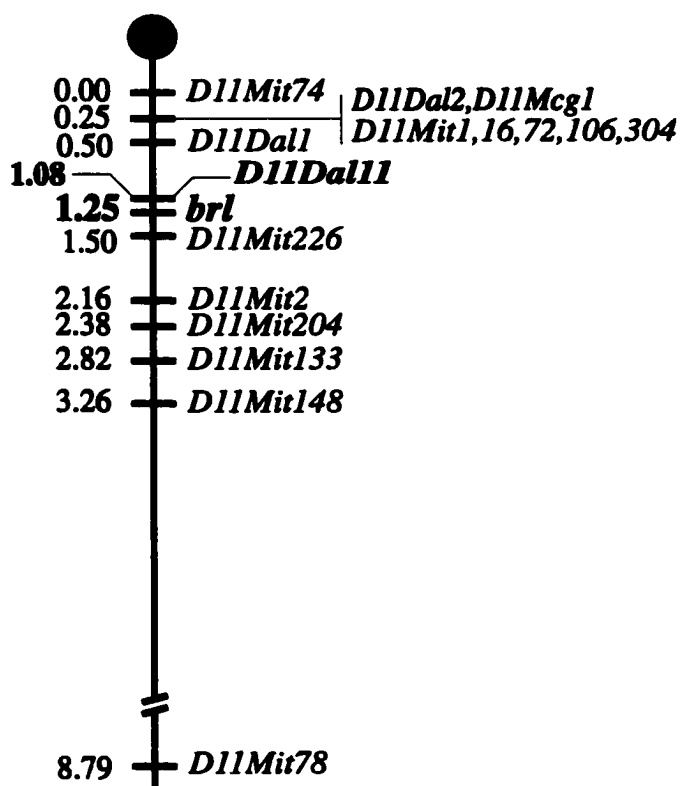
Figure 4.7 A high resolution genetic linkage map in the proximal region of mouse chromosome 11. The marker *D11Dal11* (bold) is a polymorphism in the 5' end of the adenylyl cyclase type I gene and mapped 0.17 cM proximal to the *brl* locus (bold). The *brl* locus now lies in an interval of 0.42 cM.

Gilman 1991; Bakalyar and Reed 1990; Ishikawa et al., 1992; Yoshimura and Cooper 1992; Katsushika et al., 1992; Premont et al., 1992; Wallach et al., 1994; Glatt and Snyder, 1993; Cali et al., 1994; Watson et al., 1994; Hellevuo et al., 1995; Defer et al., 1994; Premont et al., 1996; Paterson et al., 1995; reviewed in Iyengar 1993; Taussig and Gilman, 1995; Cooper et al., 1995; Krupinski et al., 1992). Based on their sequences and functional similarities, they have been divided into four distinct subfamilies which reflect their distinct pattern of regulation: 1) Ca^{2+}/calmodulin sensitive ACs (AC1, AC3, AC8); 2) Ca^{2+}/calmodulin insensitive ACs (AC2, AC4, AC7); 3) Ca^{2+}- inhibitable ACs (AC5, AC6); 4) AC9 which is sensitive to indirect effects of Ca^{2+}. While ACs differ in their response to modulatory factors such as Ca^{2+}, $\beta\gamma$ subunits of the G protein, cAMP-dependent protein kinase (PKA) and protein kinase C (PKC), all of them are activated by the $G_{s\alpha}$ subunit of the G protein and forskolin. In a more recent study (Buck et al., 1999), a distinct class of mammalian adenylyl cyclase was described. This adenylyl cyclase is soluble and insensitive to G protein or forskolin regulation. The varied pattern of regulation allows the cell to change its cAMP levels in response to a variety of signals, therefore, varying its physiological functions.

All ACs share a common topology based on secondary structure analysis and sequence similarity. The proteins are predicted to have a short amino-terminal cytoplasmic tail, two alternating sets of six transmembrane hydrophobic domains (M_1 and M_2), two sets of large hydrophilic cytoplasmic domains (C_1 and C_2) followed by a long carboxy-terminal cytoplasmic tail. No catalytic activity is detected when each half of the cytoplasmic domains is expressed separately; however, coexpression of the two halves

results in retrieval of enzymatic activity (Tang et al., 1991). Recently, the crystal structure

of the adenylyl cyclase catalytic core has been determined (Zhang et al., 1997). The

cytoplasmic tail exists as a dimer that has a wreathlike structure with the ATP binding

site in the ventral cavity.

Adenylyl cyclase type I, AC1 (EC 4.6.1.1), is a membrane bound enzyme that

catalyzes the formation of cAMP, an important second messenger. It was mapped to

mouse chromosome 11 (conserved synteny with human chromosome 7 [Villacres et al.,

1993]) using fluoroscence in situ hybridization (FISH) (Edelhoff et al., 1995). AC1 is

neurospecific (Xia et al., 1993; Drescher et al., 1997; Matsouka et al., 1997) and is

expressed in areas of the brain that play important roles in neuroplasticity (Xia et al.,

1991). The enzyme is not stimulated by activation of Gs-coupled receptors alone in vivo,

nonetheless it is stimulated when receptor activation is coupled with Ca^{2+} (Wayman et al.,

1994). AC1 activity is directly stimulated by Ca^{2+} and calmodulin in vivo (Tang et al.,

1991; Wu et al., 1993; Wu et al., 1995). Point mutagenesis in the CaM-binding domain

diminishes the ability of Ca^{2+}/CaM to stimulate enzyme activity (Wu et al., 1993). The

physiological role of AC1 is not known; however, it is believed that it may link changes

in intracellular free Ca^{2+} to increases of cAMP and thus couple the calcium and cAMP

systems (Choi et al., 1992).

Evaluation of Adcy1 as a candidate for brl gene was performed by measuring the

biological activity of its product in brain membrane preparations of wild-type and brl/brl

mutant mice. There is no direct assay to measure the enzyme activity in vitro, hence the

enzyme activity is assayed indirectly by measuring the amount of enzyme-generated

cAMP. Most protocols measure the ^{32}P cyclic AMP formation from [α-^{32}P] ATP (Salomon et al., 1974; Salomon, 1979; Krishna et al., 1968). A new methodology was developed using an enzymeimmunoassay for the measurement of cAMP. Assaying the enzyme activity *in vitro* is very difficult due to its presence in extremely small amounts in membrane preparations (0.01-0.001%), and due to the instability of the enzyme in the presence of other kinases and inhibitors. Accordingly, phosphodiesterase activity inhibitors, ATP-regenerating systems, divalent ions, chelating systems, and adenosine and adenosine monophosphate degenerating enzymes were important factors that were added to the enzyme assay reaction to enable the measurement of adenylyl cyclase activity more accurately. Cyclic AMP derived from adenylyl cyclase was extracted from the rest of the enzyme assay products before measurement using an enzymeimmunoassay approach.

Basal adenylyl cyclase activity in *brl/brl* mutant mice was half of that measured in wild-type mice (Abdel-Majid et al., 1998; Figure 4.4), however this decrease was not statistically significant. However, measurements of the enzyme activity in the presence of Ca^{2+} and calmodulin as stimulators revealed a significant difference in enzyme activity in *brl/brl* mutant mice compared to wild-type. While adenylyl cyclase activity increased by six-fold in wild-type mice, there was no increase in enzyme activity in *brl* mutants. These results are comparable with previous published results reported in *Adcy1* knockout mice (Villacres et al., 1995). The finding that a non-functional AC protein was detected in the *brl* mutant mouse suggested further evaluation of *Adcy1* at the molecular level.

Sequencing of the AC1 cDNA from both wild-type and *brl/brl* alleles (by Dr. Leong; Abdel-Majid et al., 1998) revealed the presence of two differences, a

polymorphism at the 5' end of the coding region (*D11Dal11*) and an early retrotransposon (ETn) insertion (Genbank AF053979). The first difference was a polymorphism that mapped 0.17 cM proximal to the *brl* locus (Figure 4.7), while the second was the mutation which co-segregated with the *brl* phenotype (Figure 4.8). A loss-of-function mutation due to an insertion of an ETn in various genes has been previously reported (Steinmeyer et al., 1991; Mitreiter et al., 1994). In these reports, the ETn insertion lead to alternative splicing and premature termination of transcripts. Furthermore, Northern blot analysis has confirmed the presence of two aberrant transcripts in the *brl* mutant instead of the normal transcript present in wild-type mice (Leong et al., 1999). Finally, the causal relationship between *Adcy1* and *brl* was confirmed when *Adcy1* knockout mice displayed the barrelless phenotype (Figure 4.5A; Abdel-Majid et al., 1998) in contrast to mice homozygous for targeted disruption of *Adcy8* which displayed the normal pattern of barrels with the cell sparse centers and septa (Figure 4.5B).

cAMP plays a vital role in signaling pathways and in neuroplasticity in both vertebrates and invertebrates. Biochemical, behavioral and genetic studies in the fruit fly, *Drosophila melanogaster*, have provided evidence for the involvement of cAMP pathway in learning and memory. Four *Drosophila* mutants (*dunce*, *rutabaga*, *Ddc*, and *turnip*), which lack genes involved in cAMP pathway, had varied degrees of learning deficits, thus providing evidence for the importance of cAMP in acquisition and memory. The role of cAMP in learning and memory extends to *Aplysia* and mice. In *Aplysia*, cAMP is
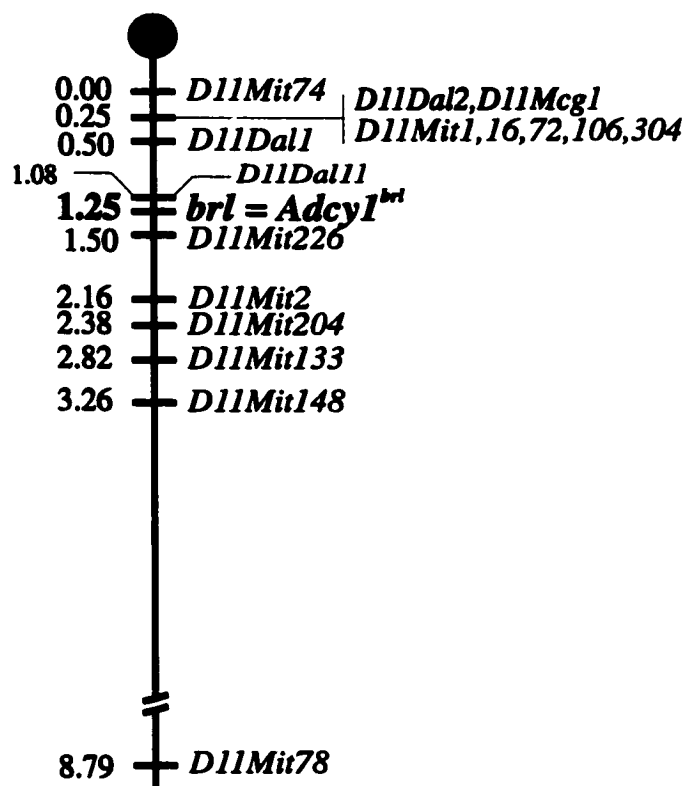
Figure 4.8 Final genetic linkage map in the region of the *brl* locus in proximal mouse chromosome 11. A mutation in the Adenylyl cyclase type I gene (*Adcy1*) co-segregated with the barrelless phenotype in all animals that were recombinant between *D11Mit74* and *D11Mit226*. A polymorphism (*D11Dal11*) in the 5' end of the adenylyl cyclase type I gene lies at 0.17 cM proximal to the mutation.

required for short-term (Brunelli et al., 1976; Walters et al., 1983) and long-term (Montarolo et al., 1986; Dash et al., 1990) facilitation in the synaptic connections between sensory and motor neurons of the gill- and tail-withdrawal reflexes. It is believed that short- and long-term facilitation occurs through the release of serotonin (5-HT), which will activate adenylyl cyclase and hence strengthen synaptic connections in the reflex pathway (Castelluci et al., 1980; Hawkins et al., 1993). In mice, targeted disruption of genes involved in cAMP pathways produced mice that are deficient in long-term memory (Bourtchuladze et al., 1994). The role of AC1 in synaptic plasticity was confirmed when mice homozygous for a targeted disruption of *Adcy1* were deficient in spatial memory and showed depression of long-term potentiation (LTP) in the hippocampus (Wu et al., 1995) and a nearly complete blockade of LTP in the cerebellum (Storm et al., 1998). Finally, it has recently been reported that an impairment of Ca^{2+}/calmodulin AC1 is involved in the pathogenesis of dementia type of Alzheimer disease (Yamamoto, 1997), and in the pathophysiology of alcoholism (Hashimoto et al., 1998) in humans.

A similar barrelless phenotype to that observed in *Adcy1* mutants was found in mice homozygous for a targeted disruption of monoamine oxidase A (*Maoa*) (Cases et al., 1995; 1996). In these knockout mice, excess brain 5-HT during early postnatal development is responsible for the absence of barrels. Available data support a role for glutamatergic neurotransmission in the refinement of the thalamocortical projections since whisker-related patterns fail to develop in the brainstem, thalamus, and cortex of mice deficient of the NMDA receptors (Li et al., 1994; Iwasato et al., 1996; 1997), and

pharmacological blockade of NMDA receptors in normal somatosensory cortex disrupts thalamocortical projections and columnar organization of barrels (Fox et al., 1996) and produces a barrelless phenocopy in rats (Mitrovic et al., 1996).

The barrelless phenotype may result from loss of AC1 in cortical dendrites or from thalamocortical afferents (TCAs). cAMP has been reported to stimulate neurite outgrowth *in vitro* (Zheng et al., 1994; Song et al., 1997; Lotto et al., 1999), hence its absence from cortical dendrites will impair their contribution to barrel formation. On the other hand, if the site of gene action is in the TCAs then cAMP absence will lead to a reduced glutamate release and a reduced neurotransmission causing thalamic afferents to grow beyond barrel domains. Accordingly, we propose the following: The shared phenotypic features of the *Maoa* knockout mice and *Adcy1* mutants, and the NMDA receptor blockade suggest the involvement of serotonin, cAMP pathway and glutamate neurotransmission in barrel formation (Figure 4.9). A nine-fold increase in 5-HT concentration in these knockout brains was found during the critical period of barrel development (Cases et al., 1995). Conversely, early depletion of 5-HT delayed barrel development and reduced their size due to a decrease in the growth of the TCAs (Bennett-Clarke et al., 1994). In the first two weeks of prenatal life, thalamic axons express genes encoding the serotonin transporter (Bennett-Clarke, 1996; Lebrand et al., 1996; Bruning and Liangos, 1997) and the vesicular monoamine transporter (Lebrand et al., 1996; 1998) as well as the serotonin receptor 5-HT$_{1B}$ (Bennett-Clarke et al., 1993) which decreases adenylyl cyclase activity (Bouhelal et al., 1988). This reduced PKA activity in VB thalamic terminals inhibits presynaptically the excitatory thalamocortical transmission

Figure 4.9 A schematic representing three neuronal processes in the barrel hollow. Only

cortical dendrites (cortex), thalamocortical afferents (TCAs), and serotonergic afferents

(5-HT) are represented. High levels of 5-HT in the first two weeks of perinatal life will

inhibit adenylyl cyclase activity (AC) through serotonin receptor 1B subtype (5-HT$_{1B}$)

that will result in reduced levels of cAMP. The decrease in cAMP concentration will

result in a reduction in cAMP-dependent protein kinase (PKA) activity, which, in turn,

will reduce the activity of Ca^{2+} ion channels and hence reduce Ca^{2+} influx (solid arrows).

These events will lead to a reduced glutamate release and reduced neurotransmission in

the TCAs.
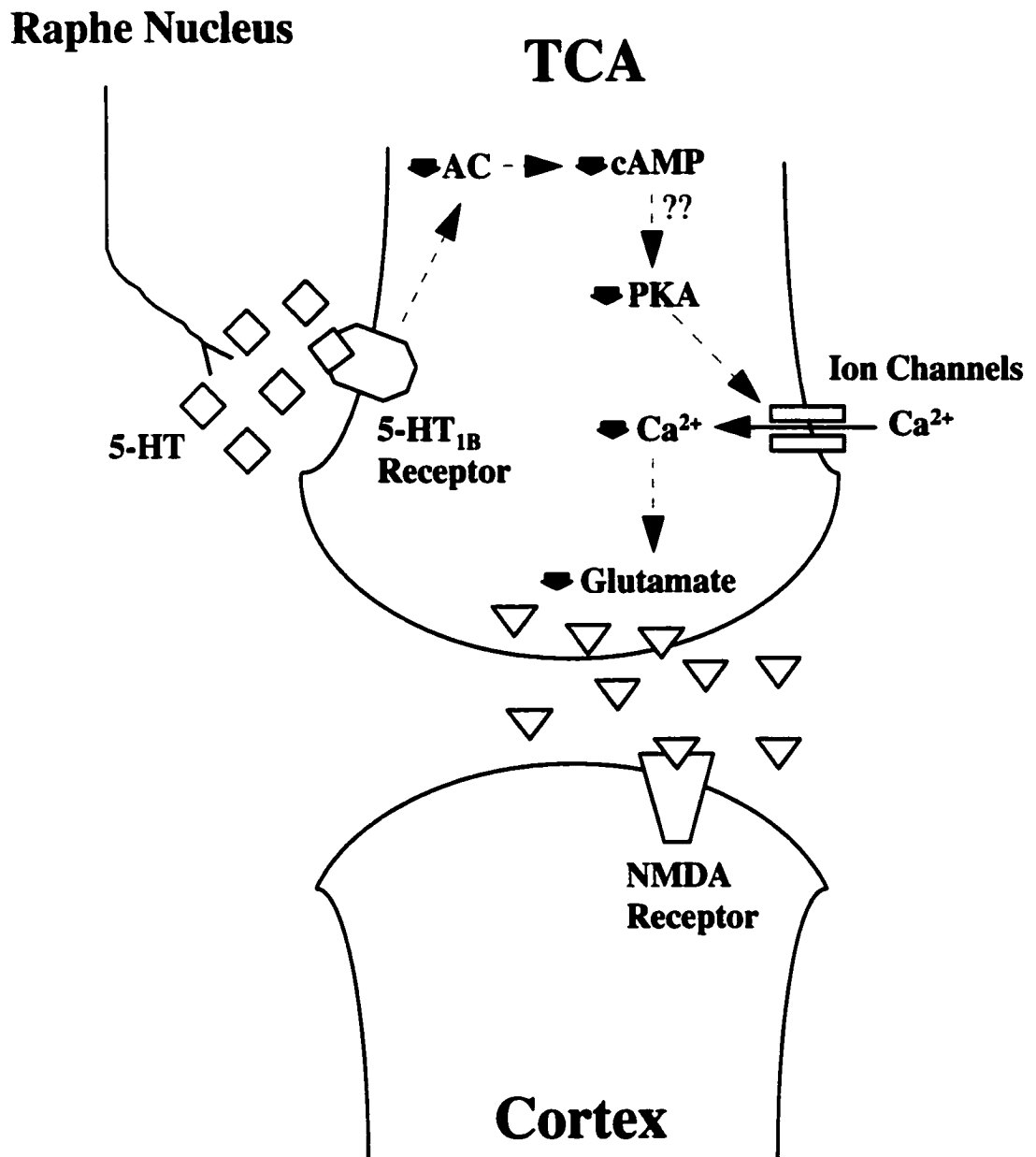
Figure 4.9

(Rhoades et al., 1994). Reduction of neurotransmission due to a loss-of-function mutation in the *Adcy1* gene will therefore lead to disruption of the topographic refinement of thalamocortical projections and accordingly abolishes barrel formation in the somatosensory cortex.

Alternatively, a barrelless phenotype may result from loss of *Adcy1* in the posterior medial (POm) thalamic projections to the cortex, which terminate in the septa between barrels in layer IV (Koralek et al., 1988; Chmielowska et al., 1989; Lu and Lin, 1993). The presence of septa between barrels defines prominent barrels in rodents, and their absence in certain species give rise to indistinct barrels (Rice and Van der Loos, 1977). However, it is highly unlikely that a barrelless phenotype results from loss of adenylyl cyclase in the POm nucleus due to the following reasons: 1) it has been reported that sensory thalamic nuclei express AC1 during development (Matsouka et al., 1997); however, it is not clear whether POm nucleus expresses this enzyme, and 2) the developmental time course of the POm projections has not been examined yet (Rice, 1995).

Finally, these results provide the first evidence for the involvement of cyclic nucleotide signal transduction systems in barrel formation. Since pattern formation is not specific for the barrel cortex, or for that matter for rodents, cAMP may play a more general role in cortical specification. In the next few chapters, we will try to discover molecular mechanisms that play important roles in barrel formation in particular and in pattern formation in general. As summarized in figure 4.9, the main target of cAMP is cAMP-dependent protein kinase (PKA), which almost accounts for all cAMP biological effects. In order to determine whether PKA is the cAMP downstream target that is

disrupted in the barrelless mutant in the thalamocortical afferents, various PKA null

mutant mice were examined for the presence of barrels in their SI cortex.

Chapter 5

Involvement of Protein Kinase A

in Barrel Formation

5.1 Introduction

We hypothesized earlier (chapter 4) that loss-of-function mutation in *Adcy1* in the thalamocortical afferents results in a *brl* phenotype. Since this gene was well characterized, the initial goals were modified. The main goal at this stage was to identify signaling pathways involved in barrel formation. Thus, it was logical to investigate the involvement of cAMP downstream targets.

cAMP transduction pathways play a pivotal role in cell signaling where it is involved in various cellular responses through the activation of target proteins. It exerts its effect mainly through the activation of cAMP-dependent protein kinase (PKA), which controls many biochemical events through the phosphorylation of target proteins. PKA is a heterotetramer composed of two regulatory (R) and two catalytic (C) subunits that exist in different isoforms. Four regulatory (*Prkar1a, Prkar1b, Prkar2a, and Prkar2b*) and two catalytic subunit genes (*Pkaca* and *Pkacb*) have been identified. Each subunit has been disrupted by homologous recombination in embryonic stem cells (Qi et al., 1996; Amieux et al., 1997; Brandon et al., 1997; Burton et al., 1997). Loss of the RIα isoform in *Prkar1a* knockout mice is an embryonic lethal condition (Burton et al., 1997). Some cAMP signaling pathways involve activation of cyclic nucleotide gated channels (Zimmerman et al., 1995; Kaupp et al., 1995) or cAMP-regulated guanine nucleotide exchange factors (Kawasaki et al., 1998). In order to determine whether PKA is the downstream target of the cAMP pathway that is disrupted in *Adcy1* mutant mice, we examined the barrel field morphology in the five viable PKA null mutant mice using cresyl violet (Nissl) staining and cytochrome oxidase (CO) histochemistry.

5.2 Reagents and Solutions

All reagents were of molecular grade. Cytochrome oxidase reagents were purchased from Sigma Co. Phosphate buffer, paraformaldehyde and alcohol were from BDH.

5.3 Methods

5.3.1 Animals

Targeting of embryonic stem cells, establishment of chimeras and mouse lines carrying mutations in the RIβ, RIIα, RIIβ, and Cβ PKA subunit genes have been described (Brandon et al., 1995a; 1995b; Qi et al., 1996; Burton et al., 1997; Brandon et al., 1998). Ten-week-old mice homozygous for targeted disruption of the PKA subunit genes RIβ (n=3), RIIα (n=3), RIIβ (n=8), Cα (n=3), and Cβ (n=3) (University of Washington, Seattle, U.S.A.) were given a lethal dose of sodium pentobarbital, and then were transcardially perfused first with 0.1 M phosphate-buffered saline (PBS; pH 7.4) then with chilled 4% paraformaldehyde in 0.1 M PBS. Brains were removed from the skull and were postfixed for 24 hours in the same fixative.

5.3.2 Histology of the Barrel Field

Due to the position of the barrel field at the arcing dorsal surface of the hemisphere, it is of great importance to optimize the orientation of brains for proper demonstration of barrels. The barrel field was approached using sections parallel to the pial surface overlying the somatosensory cortex (figure 7 in Woolsey and Van der Loos, 1970). Brains were cut at the midline, and each hemisphere was mounted in a 10°

anterior-posterior tilt on a wedge that was glued to a metal cube and inclined 30°

medially. Hemispheres were sectioned serially at a thickness of 50 μm using a vibratome.

Sections were mounted on gelatin-coated slides, dried overnight and then stained either

with cresyl violet (Nissl) stain or CO histochemistry.

5.3.2.A Cresyl violet (Nissl) stain

Slides were dehydrated in a series of ethanol dilutions (50, 70, 95 and 100%) for

two minutes and then were dipped in two changes of 100% xylene for two minutes each

time. Slides were then rehydrated in the same manner in decreasing dilutions of ethanol

after which they were rinsed with running tap water and then were immersed in cresyl

violet stain (0.1%) for 5-8 minutes. Slides were rinsed again under running tap water and

then were immersed in acid alcohol (10% acetic acid) for blue differentiation. Finally,

slides were dehydrated in increasing dilutions of alcohol (50, 70, 95 and 100%) followed

by dipping in two changes of 100% xylene and then were coverslipped using a synthetic

resin (Entellan; Merck, Germany).

5.3.2.B Cytochrome Oxidase (CO) Histochemistry

In the barrel field, cytochrome oxidase histochemistry gives rise to darkly stained

patches coincident with thalamocortical afferents termination. Regions of high enzymatic

activity are present in the barrel hollow with the barrel sides and septa being less reactive.

This pattern of staining arises mainly from reactive mitochondria present on dendrites and

axonal terminals of the barrel neuropil and to a lesser degree from neuronal perikarya

(Wong-Riley and Welt, 1980; Wong-Riley, 1989). CO staining pattern in the barrelless

mutant displays diffuse staining, a pattern that contrasts the wild-type pattern. Therefore, CO histochemistry was used as a marker for thalamic afferents termination.

Sections were collected in 0.1 M phosphate buffer (PB; pH 7.4) and then were mounted on gelatin double subbed slides. Slides were allowed to dry overnight and the next morning they were dipped in 4% paraformaldehyde in 0.1 M phosphate buffer (pH 7.4) for one hour followed by a few rinses with distilled water. Sections were reacted for CO as described by Wong-Riley (1979). Briefly, slides were incubated for 6-8 hours at 37°C in 0.1 M phosphate buffer containing 4 g sucrose (BDH), 50 mg diaminobenzidine (DAB; Sigma Co.) and 30 mg cytochrome C (from horse heart, Sigma Co.) in a total volume of 100 ml 0.1 M PB buffer. At the end of the incubation period slides were rinsed in three changes of 0.1 M phosphate buffer (pH 7.4), dehydrated and coverslipped.

5.4 Results

Examination of the barrel field using Nissl-stained sections revealed the presence of barrels in PKA knockout mice; however, one of the five PKA knockout mouse lines displayed defects in barrel morphology (Figure 5.1). Barrels in mice lacking the RIIβ subunit were hard to discern because the septa and barrel hollows displayed less reduction in cellularity relative to the barrel sides (Figure 5.1D) than in wild-type animals (Figure 5.1A).

Examination of barrels in all five PKA knockout mouse lines using CO-stained sections revealed the presence of a multifocal pattern as is observed in wild-type animals (Figure 5.2). This multifocal pattern contrasts with CO-stained sections of barrelless (*Adcyl^{brl}*) mutant mice in which CO-reactivity displays a diffuse staining pattern in layer

Figure 5.1 Digitized images of cresyl violet (Nissl) stained sections of layer IV of the somatosensory cortex of adult wild-type mice (A), RIβ (B), RIIα (C), RIIβ (D), Cα (E), and Cβ1 (F) null mutant mice. 50μm-thick sections were cut parallel to the pial surface overlying the primary somatosensory cortex. Scale bar = 200 μm.
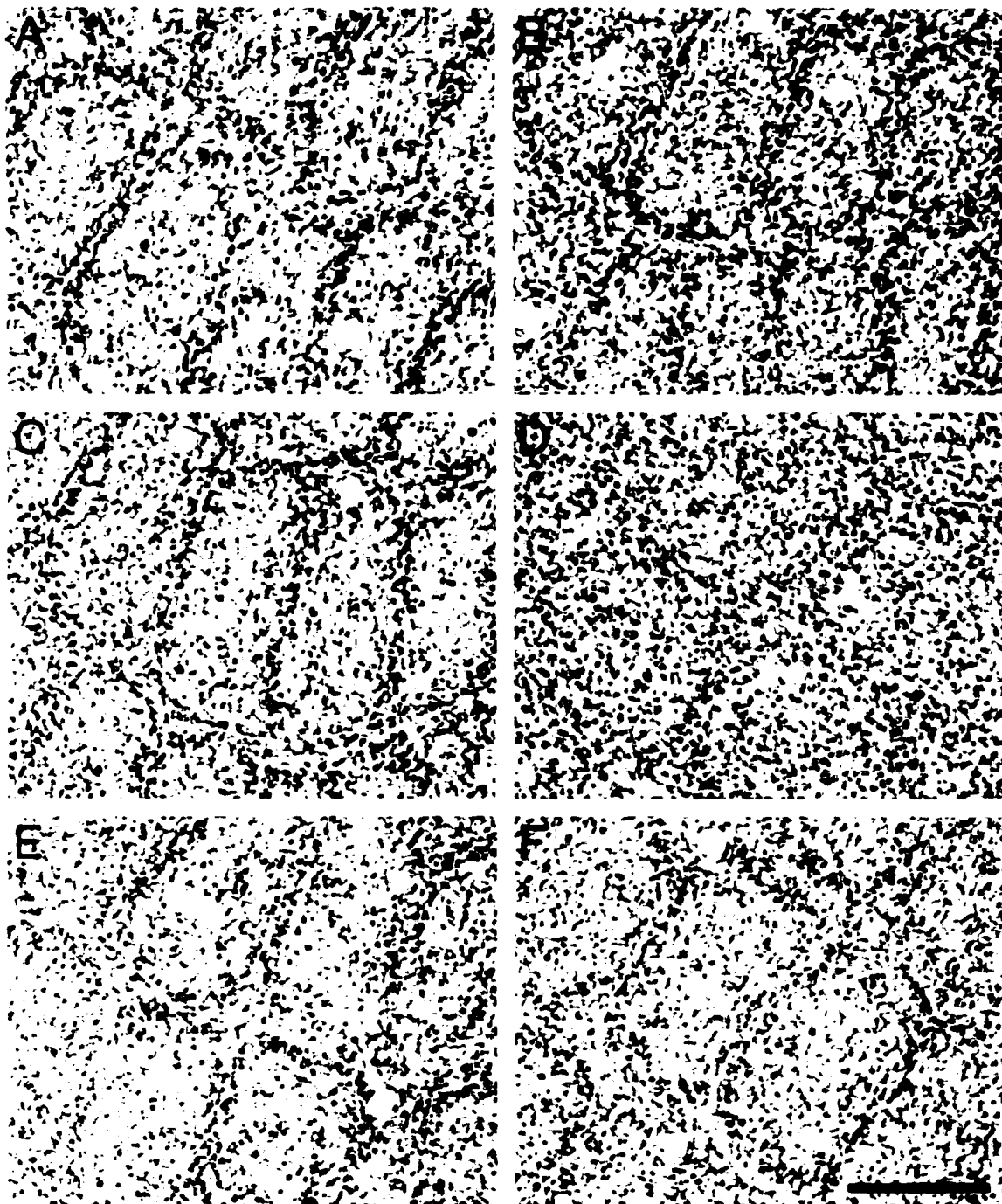
Figure 5.1

Figure 5.2 Digitized images of cytochrome oxidase stained sections of layer IV of the somatosensory cortex of adult wild-type mice (A), RIIβ (B), and barrelless mutant mice (C). Examination of barrel morphology in the five PKA mutant mice revealed the presence of darkly stained patches coincident with thalamocortical afferent terminations, a pattern that was indistinguishable from that of wild-type. In contrast to the darkly stained clusters observed in wild-type, in barrelless mutant mice, the CO staining pattern was uniform. Scale bar = 200 μm.
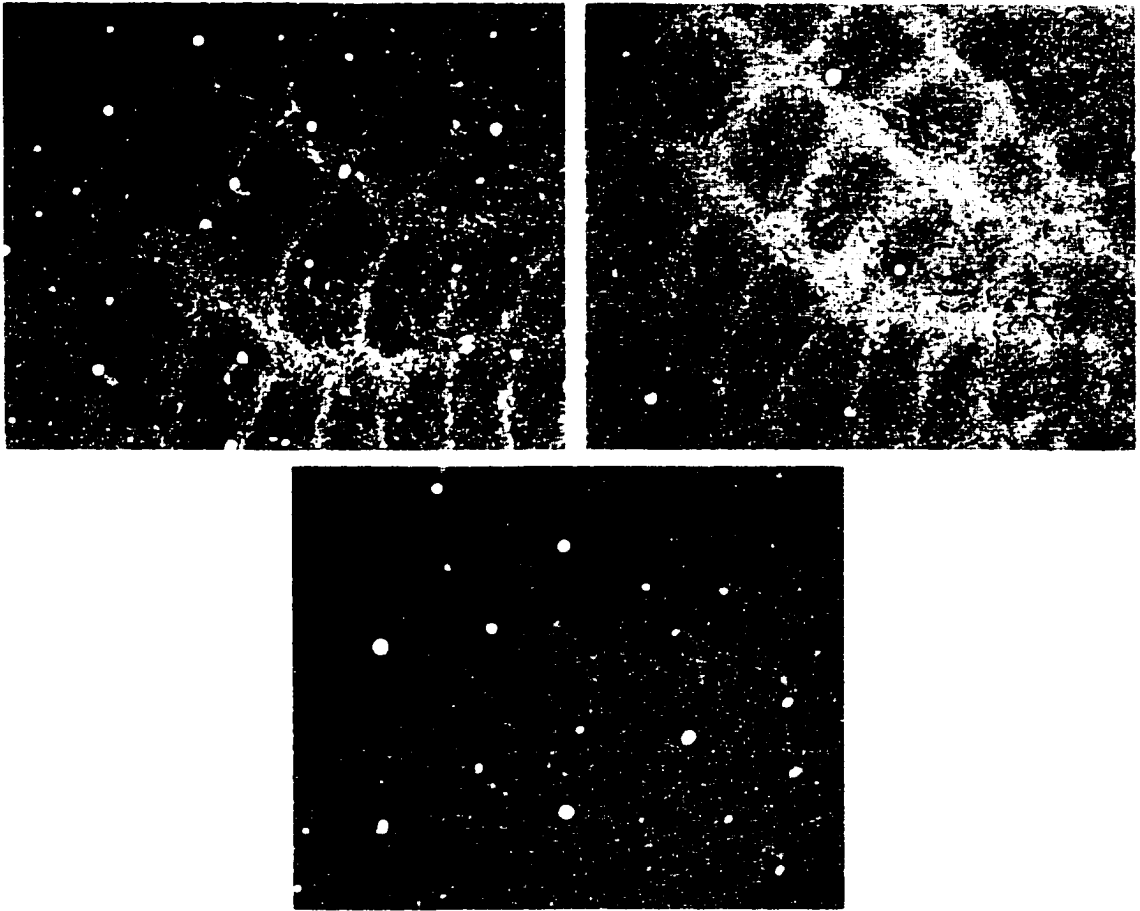
Figure 5.2

IV of the somatosensory cortex (Figure 5.2C). CO staining was observed in the barrel hollows, giving rise to the pattern of darkly stained patches coincident with the thalamocortical afferent terminations. The contrast between staining of the barrel-like domains and the surrounding tissue was reduced in RIIβ mutants relative to wild-type controls and the other PKA subunit knockouts. In addition, the anterolateral barrel subfield of RIIβ knockouts is uniformly stained with little evidence of barrel-like domains (data not shown).

5.5 Discussion

The five PKA knockouts examined here had barrels in their somatosensory cortices and barrel-like domains in cytochrome oxidase histochemistry, suggesting normal segregation of thalamocortical afferents within the barrel hollows. The barrels in mice lacking the RIIβ subunit were less well defined. The finding that RIIβ mutant mice had the poorest barrel morphology may not be surprising as they have the largest reported decrease in PKA activity and other signs of neurological disorder (Brandon et al., 1998). Total PKA activity is reduced by 75% in striatum and 50% in hippocampus (Brandon et al., 1997; 1998). In the primary somatosensory cortex of one-week-old RIIβ knockout mice, PKA activity was reduced by 40% (Abdel-Majid et al., 1999). Moreover, immunohistochemistry with monoclonal antibody to RIIβ subunit revealed immunoreactive cell bodies through layer IV and the supragranular layers (II and III). In layer IV, low contrast patches of immunoreactive somata appear to be imbedded in a diffuse immunoreactive neuropil (Abdel-Majid et al., 1999).

As hypothesized previously, a loss-of-function mutation in the *Adcyl* gene should reduce cAMP levels and PKA activity in TCAs and therefore may lead to a barrelless phenotype through reduced glutamate release (Abdel-Majid et al., 1998). Since the *Adcyl*^{brl} and monoamine oxidase A (*Maoa*) mutant mice have a barrelless phenotype with an overgrowth of thalamocortical afferents in layer IV (Welker et al., 1996; Cases et al., 1995; 1996), this suggests that the site of action of *Adcyl* might be in the TCAs without ruling out the possibility that it may also act in cortical neurons. On the other hand, the presence of barrels in PKA knockout mouse lines suggests that PKA is not the downstream target of cAMP signaling pathway in the thalamocortical afferents disrupted in the *Adcyl* (barrelless) mutant mice.

The presence of barrels in PKA mutant mice can be explained by several possibilities. One is that redundancy in PKA subunits in the TCAs protects against a barrelless phenotype. Compensatory mechanisms have been reported in mice with targeted disruption of R subunits genes. For example, there was an increase in the RIα subunit in mice lacking the RIβ (Brandon et al., 1995b), RIIα (Burton et al., 1997), and RIIβ (Cummings et al. 1996) subunits. Thus, it is possible that the site of gene action of the RIIβ subunit might be the same as that in the *Adcyl* mutant mice, but the mutant phenotype is less severe because of compensation of other PKA subunits.

Alternatively, the site of action of RIIβ and AC1 may be different, suggesting that PKA is not the downstream target of cAMP in the TCAs. It is possible that AC1 acts in both TCAs and cortical neurons whereas PKA acts only in cortical neurons. Other possible downstream targets for cAMP signaling are cyclic-nucleotide-gated (CNG)

channels (reviewed in Zimmerman, 1995; Kaupp, 1995) and cAMP-regulated guanine nucleotide exchange factors (Kawasaki et al., 1998).

CNG channels have been reported to be involved in sensory axonal guidance (Coburn and Bargmann 1997). In *C. elegans*, sensory axons of *tax-2* and *tax-4* mutants terminate in inappropriate regions, bypassing their normal site of termination suggesting that CNG channel activity limits axonal outgrowth of sensory neurons. If CNG channels are the downstream target of the TCAs, then their inactivation due to low levels of cAMP can result in a barrelless phenotype.

Another possibility is that the cAMP-mediated pathway in the TCAs exerts its effect through direct coupling to Ras superfamily signaling pathway (Kawasaki et al., 1998). In this recent study, the authors report the presence of a family of proteins that contain domains for both cAMP and guanine nucleotide exchange factor that selectively activate Rap1 in a cAMP dependent manner.

The above results suggest that the site of action of the RIIβ subunit is in layer IV cortical neurons. The mutant phenotype is distinct from that in *Adcy1* mutants. In addition, the RIIβ mutant phenotype resembles that of phospholipase C beta-1 (PLC-β-1) mutants. As in the RIIβ knockout, there is an absence of clearly-defined barrel walls and hollows, and cytochrome oxidase histochemistry reveals barrel-like domains (Hannan et al., 1998a). Thus we believe that protein kinase A plays a role in barrel formation by influencing cortical neuron dendrite growth in response to thalamocortical afferent activity.

Chapter 6

Neurotrophins Alter

Somatosensory Patterning

.

6.1 Introduction

In order to identify molecules that play a role in barrel formation, it was necessary to identify the signal that cortical neurons release in response to thalamocortical innervation. In doing so, several criteria were taken into consideration: 1) this signal(s) is expressed during the first week of development in the cortex and/or thalamus (when barrels are formed), 2) it plays a role in synaptic plasticity, 3) activity-dependent mechanisms regulate its expression or release, and lastly, 4) this signal modulates axonal and/or dendritic growth. Indeed, neurotrophins were attractive candidates that meet the above criteria.

Neurotrophins are a group of structurally related proteins that are required for the survival, differentiation, and maintenance of connections of specific neuronal populations during development and in adulthood (Levi-Montalcini, 1987a; 1987b; Thoenen et al., 1987, Barde, 1989; Thoenen, 1991; Davies, 1994). They are widely expressed in the peripheral and central nervous systems (Ernfors et al., 1990; Maisonpierre et al., 1990; Korsching, 1993; Zhou and Rush, 1994; Pitts and Miller, 1995; Friedman et al., 1998;) where they promote the survival of a specific population of neurons (Chun and Patterson, 1977; Hartikka and Hefti, 1988; Barbacid, 1994; Snider, 1994; Lewin and Barde, 1996). The neurotrophin family includes nerve growth factor (NGF), brain-derived neurotrophic factor (BDNF), neurotrophin-3 (NT-3), neurotrophin-4/5 (NT-4/5) (for reviews see Davies, 1994; Lindsay, 1994; Bothwell, 1995; Lewin and Bard, 1996), neurotrophin-6 (NT-6) which was discovered in fish (Götz et al., 1994), and neurotrophin-7 (NT-7),

which is the most recent addition to the neurotrophin family that was discovered in zebrafish (Nilsson et al., 1998).

The biological effects of neurotrophins are mediated through binding to the low-affinity p75 receptor (for reviews, see Carter et al., 1996; Dechant and Barde, 1997) and to the high-affinity Trk family of the tyrosine kinase receptors (for reviews, see Glass and Yancopoulos, 1993; Dechant et al., 1994; Barbacid, 1995a; 1995b). TrkA is the NGF receptor, TrkB is the receptor for both BDNF and NT-4, and TrkC is the primary receptor for NT-3, although NT-3 binds at high concentrations to TrkA and TrkB receptors as well. TrkB and TrkC are also present in a truncated noncatalytic form (Barbacid, 1995b). Null mutant mice were generated for all the neurotrophins and their receptors (Klein et al., 1993; Smeyne et al., 1994; Jones et al., 1994; Crowley et al., 1994; Klein et al., 1994; Ernfors et al., 1994a; 1994b; Fariñas et al., 1994, Snider, 1994). Examination of the SI cortex in BDNF (Jones et al., 1994), TrkA, TrkB and TrkC (Henderson et al., 1995) null mutant mice revealed the presence of barrels; however, these results can be explained by the presence of compensatory mechanisms that compensate for the loss of the neurotrophin.

More recently, it has been demonstrated that neurotrophins have a more complex function than merely enhancing survival and growth of neurons. Numerous lines of evidence implicate neurotrophins involvement in: 1) long-term potentiation (LTP) (Patterson et al., 1996; Figurov et al., 1996; Kang et al., 1997; Akaneya et al., 1997), 2) modulating synaptic plasticity in activity-dependent manner (Zafra et al., 1991; Lohof et al., 1993; Kim et al., 1994; Kang and Schuman, 1995; Cabelli et al., 1995; Levine et al.,

1995; Lo, 1995; Thoenen, 1995; Berninger and Poo, 1996; Bonehoeffer, 1996; Cellerino and Maffei, 1996; Cabelli et al., 1997; Levine et al., 1998; McAllister et al., 1998; Sherwood and Lo, 1999), 3) remodeling of axonal and dendritic growth (Valverde, 1968; Volkmar and Greenough, 1972; Wiesel, 1982; Katz et al., 1989; Cohen-Corey et al., 1991; Goodman and Shatz, 1993; Bailey and Kandel, 1993; Cohen-Cory and Fraser, 1995; McAllister et al., 1995; 1997; Lentz et al., 1999), and 4) providing guidance cues for developing neurons (Ming et al., 1997; Song et al., 1997; 1999).

Previously, it was hypothesized that an excessive reduction in the thalamocortical activity, and a reduction in glutamate neurotransmission resulted in overgrowth of the thalamocortical afferents and hence a barrelless phenotype (Chapter 4; Abdel-Majid et al., 1998). A corollary to this hypothesis proposes that, in wild-type mice, increasing glutamatergic activity at TCA terminals during barrel development leads to synapse stabilization and TCA growth arrest. Thus, the role of neurotrophins in barrel formation was examined.

6.2 Materials

Neurotrophins BDNF, NT-3 and NT-4/5 were a generous gift from Regeneron Pharmaceuticals, Inc., (Tarrytown, NY; U.S.A.). NGF was purchased from AUSTRAL Biologicals (San Ramon, CA; U.S.A). Sheep anti-neurotrophin 3 (IgG fraction) polyclonal antibody was purchased from CHEMICON International, Inc. (Temecula, CA; U.S.A).

6.3 Methods

All surgeries were performed in strict compliance with the policies and guidelines of the Canadian Counsel on Animal Care, and were approved by the Animal Care Committee at Dalhousie University. Intracortical injections were performed under sterile conditions at two days (P2) and at two and half (P2.5) days of postnatal life (P0 is the first 24 hours after birth). Pups were anesthetized by hypothermia, taped to a stage and then were injected stereotaxically (2.5 mm anterior to Bregma, 1.2 mm from the midline, and 1 mm ventral to the skull) with 300 nl of physiological saline or an equal volume of one of the following: NGF (1 mg/ml), NT-4/5 (0.58 mg/ml), BDNF or NT-3 at a high concentration of 10 mg/ml or at a low concentration of 0.58 mg/ml. After surgery, the pups were warmed on an electrical heating pad and then returned to their mother. At three weeks of age the animals were weighed, deeply anesthetized with an overdose of pentobarbital, perfused through the ascending aorta first with 0.1 M phosphate buffered saline (pH 7.4) and then with chilled 4% paraformaldehyde. Brains were removed from the skull, weighed and then postfixed in the same fixative for 24-36 hours. The contralateral hemisphere was used as an internal control for each intracortical injection, while saline injected animals were used as a control between groups. Brain sectioning and histology were performed as described in section 5.3.2.

6.4 Results

Mice homozygous for targeted disruption of the neurotrophin-4/5 (*Ntf5*) gene (Conover et al., 1995) have barrels (Figure 6.1C); however, the barrel walls appear to be

Figure 6.1 Digitized images of layer IV of the somatosensory (SI) cortex of adult wild-

type mice (A, B), NT-4/5 null mutant mice (C, D) and $Adcyl^{brl}$ mutant mice (E, F).

Sections (50 mm thick) were cut parallel to the pial surface overlying the SI cortex and

were then processed for either cresyl violet (Nissl) staining (A, C, E) or for cytochrome

oxidase histochemistry (B, D, F). Scale bar = 200 µm.
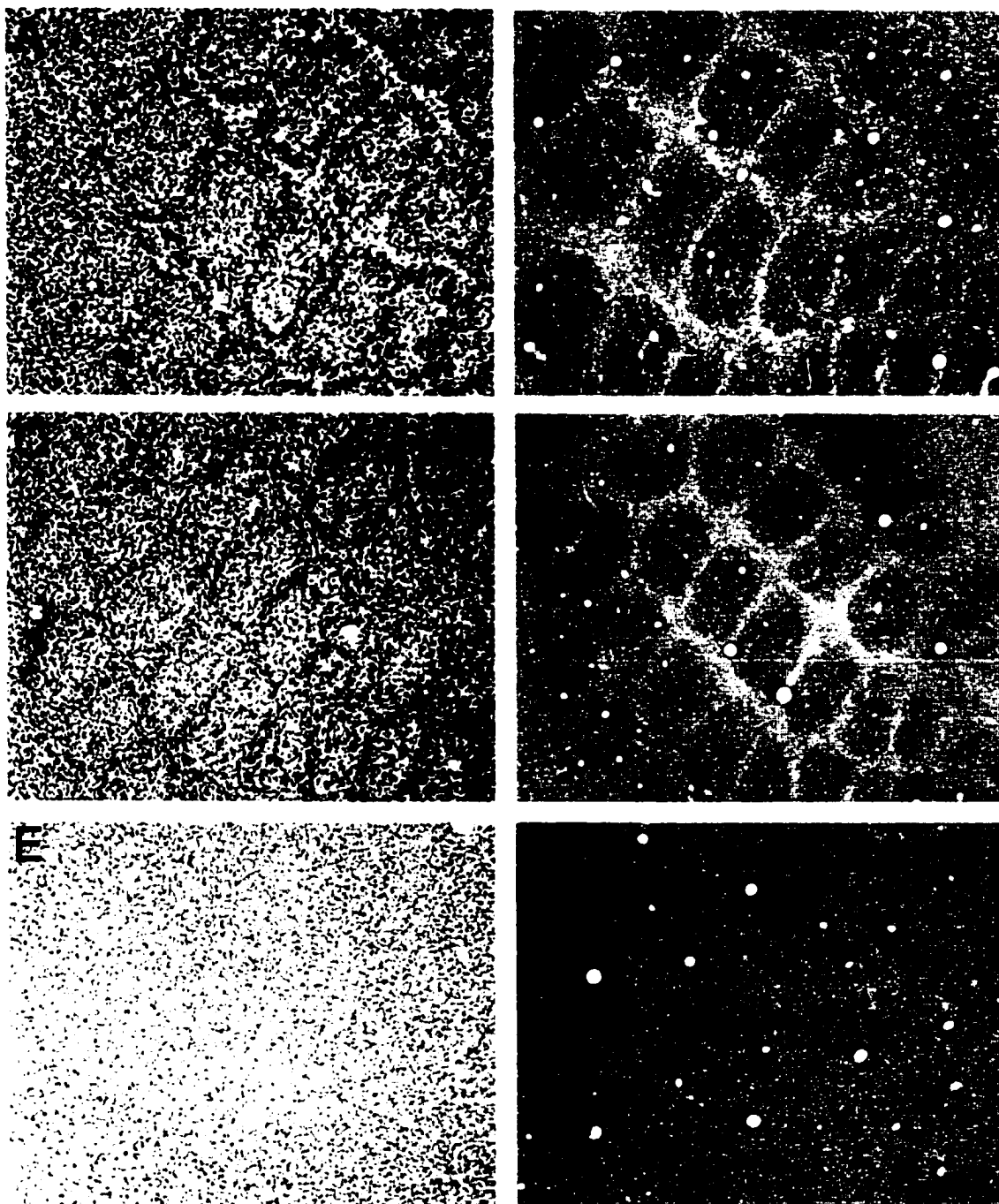
Figure 6.1

less cellular than normal (Figure 6.1A). CO histochemistry reveals normal segregation of TCAs into barrel-like domains (Figure 6.1D), a pattern indistinguishable from wild type (Figure 6.1B).

Intracortical injections of BDNF and NT-3 at the high concentration, but not of saline, NGF or NT-4/5, disrupted barrel formation in 80% of the wild type mice injected at two days of age (P2) and 20% of those injected at 2.5 days of age (Figure 6.2 and Table 6.1). The extent of loss of barrels varied from loss of two rows of posteromedial barrels closest to the injection site to the loss of all five posteromedial barrel rows. The smaller anterolateral barrels were similarly affected. No effects were observed in the contralateral cortex (data not shown). None of the above treatments had an effect on body or brain weight (data not shown), suggesting that neurotrophin injections did not generally affect brain development.

Intracortical injections of BDNF (n = 9) and NT-3 (n = 12) at low concentrations resulted in a barrelless phenocopy in a small percentage of animals (Table 6.1). Intracerebral injections of the four neurotrophins singly (n = 16) or an antibody specific for NT-3 (n = 11) at two days of age failed to correct the barrelless phenotype in $Adcyl^{brl}$ mutant mice (data not shown).

6.5 Discussion

The current study investigated the role of neurotrophins in the development of patterning in the primary somatosensory cortex. Present results demonstrate that loss of NT-4/5 in knockout mice and exogenous application of BDNF and NT-3 in wild-type animals disrupted the formation of cortical barrels in the SI cortex of mice.

Figure 6.2 Digitized images of layer IV of the somatosensory cortex of three-week-old wild-type mice that had been injected with one of the following neurotrophins at two days of age (P2): Saline (A and B), NGF (C and D), BDNF (E and F), NT-3 (G and H), or NT-4/5 (I and J). Nissl-stained sections (A, C, E, G and I) are represented on the left side, while CO-stained sections (B, D, F, H and J) are presented on the right hand side. Scale bar = 200 μm.
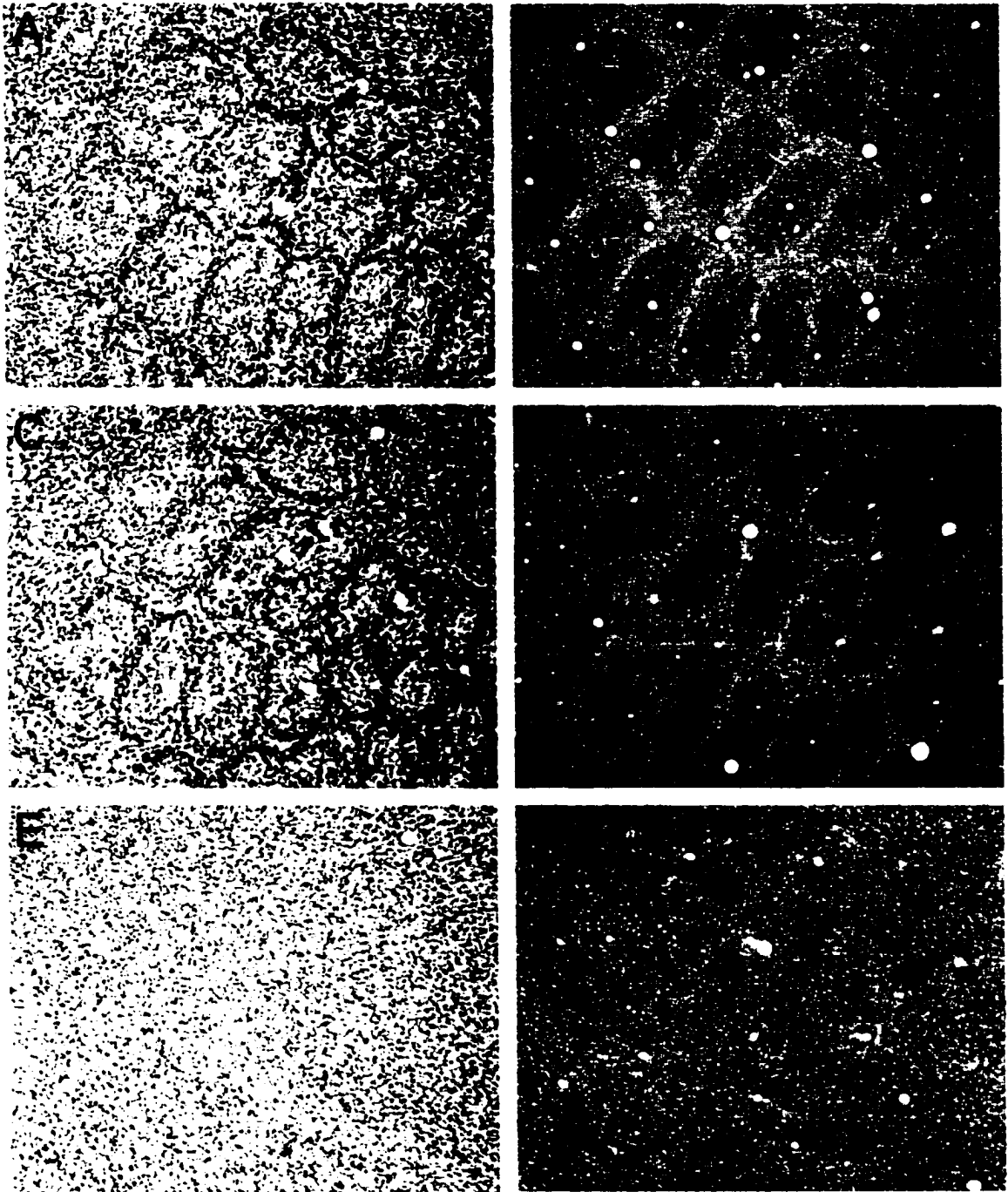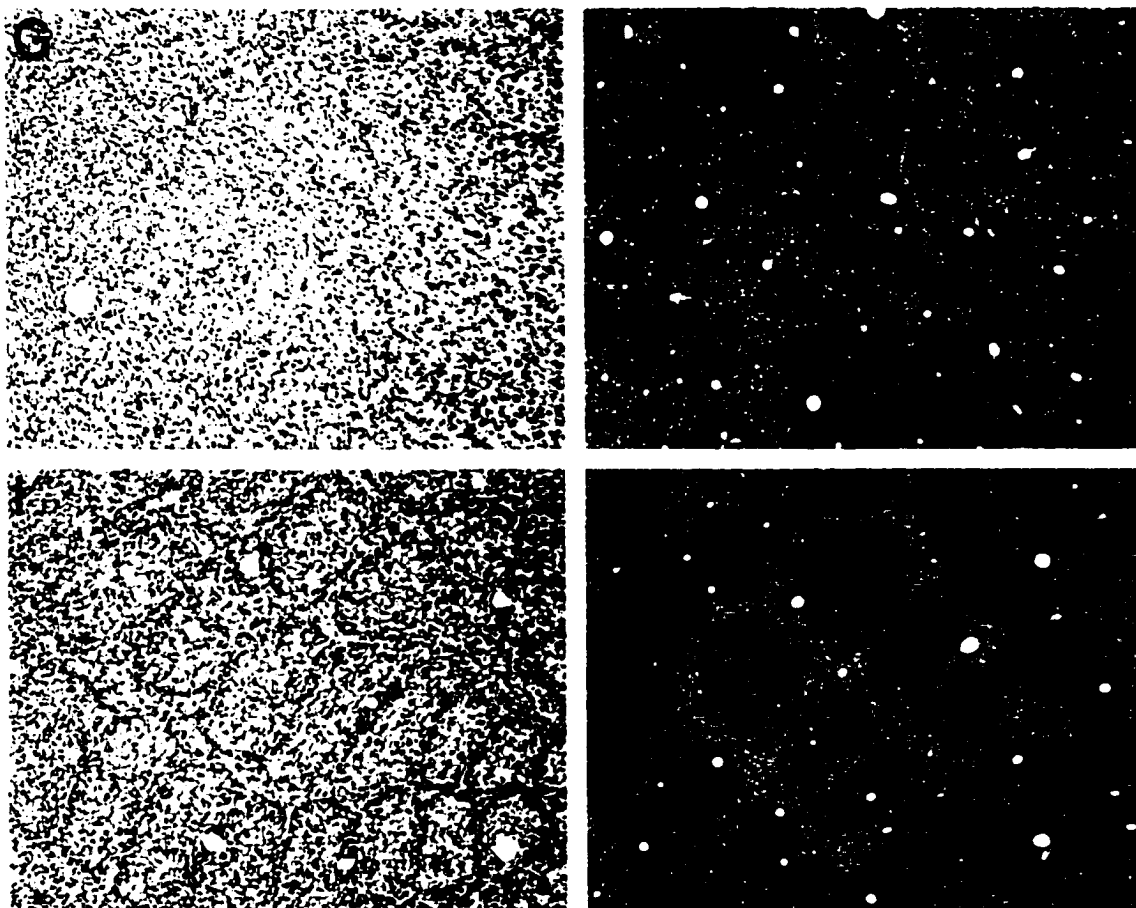
Figure 6.2

Figure 6.2

	P2		P2.5	
	Wild-type	**Barrelless**	**Wild-type**	**Barrelless**
Saline	5	0	6	0
NGF (1 mg/ml)	7	0	6	0
BDNF (10 mg/ml)	2	12	4	0
BDNF (0.58 mg/ml)	6	3		
NT-3 (10 mg/ml)	3	8	5	2
NT-3 (0.58 mg/ml)	10	2		
NT-4/5 (0.58 mg/ml)	7	0	6	0

Table 6.1 Results of intracortical injections of saline or a neurotrophin into wild-type C57BL/6J inbred mice at 48 hours after birth (P2) or between 48 and 60 hours after birth (P2.5). A total of 123 animals were injected, of which twenty-nine were discarded because the injections were not near the barrel field or caused cavitated lesions. Some of the excluded animals were later found to display a barrelless phenotype.

Loss of NT-4/5 in null mutant mice resulted in poorly-formed barrels. These deficits are similar to those observed in mice lacking the phospholipase C-beta-1 (PLC-β-1) (Hannan et al., 1998a), which has been localized by immunohistochemistry to cortical neurons in the rat developing SI cortex (Hannan et al., 1998b). Thus, the site of NT-4/5 action may be in cortical neurons rather than on TCAs and suggests that it has only minor effects on barrel formation.

The biological effects of BDNF and NT-3, the two neurotrophins that disrupted barrel formation, are chiefly mediated through the activation of TrkB and TrkC receptors, respectively (Chao, 1992; Ip and Yancopoulos, 1996; Lewin and Barde, 1996). TrkB and TrkC mRNA expression are developmentally regulated in the cortex and thalamus, with highest levels of expression during the first week of postnatal life (Ringstedt et al., 1993; Dugich-Djordjevic et al., 1993). Moreover, NT-3 is the most abundant neurotrophin in the neocortex during embryonic development with high expression in newborns (Maisonpierre et al., 1990). BDNF mRNA in the cortex is upregulated during development (Maisonpierre et al., 1990) and after sensory stimulation (Castrén et al., 1992; Schoups et al., 1995; Rocamora et al., 1996), implying that they play a role in cortical development. Neurons in the barrel wall express BDNF and TrkB in neonatal mice, and cauterization of whisker follicles at birth results in a down regulation of BDNF and TrkB mRNA levels in the corresponding barrels (Singh et al., 1997). Thus, it is possible that injections of exogenous BDNF disrupts the normal interaction between cortical derived BDNF and the growing TCAs. The observation that BDNF and NT-3 have similar effects on barrel formation during development is in contrast with a previous

report that these neurotrophins have opposing effects on dendritic growth in layer IV cortical neurons, with BDNF enhancing dendritic growth of layer IV pyramidal cells, and NT-4/5 enhancing dendritic growth of layer VI pyramidal neurons (McAllister et al., 1997).

Differences in effects of exogenous BDNF and NT-4/5 or loss of these neurotrophins are not completely surprising. Although they activate the same receptor, they show different affinities, which would result in distinct biological functions (Ibáñez, 1994; Conover et al., 1995; Windisch et al., 1995). In vitro, neurons in cortical layers V and VI respond to NT-4/5 but not BDNF, whereas the reverse is true for neurons in layer IV (McAllister et al., 1995). Moreover, NT-4/5 had a significant effect on striatal neuronal survival in organotypic slices, while BDNF and NT-3 increased glutamic acid decarboxylase activity in cultures from rat ventral mesencephalon (Ardelt et al., 1994; Hyman et al., 1994).

The simplest explanation for the disruption of cortical barrels by exogenous application of BDNF and NT-3 is that these neurotrophins stimulate TCA growth, preventing their segregation into barrel-like domains. This hypothesis is supported by the absence of barrel-like CO-positive patches similar to what is seen in $Adcyl^{brl}$ mutants, and further is consistent with the classical roles of neurotrophic factors, which include neurite outgrowth (Levi-Montalcini, 1987; Snider and Johnson, 1989; Kuffler, 1994; Lundborg et al., 1994) and chemoattraction (Letourneau, 1978; Menesini-Chen et al., 1978; Gundersen and Barrett, 1980). In addition, gradients of BDNF and NT-3 can guide

turning of the growth cones of isolated *Xenopus* spinal neurons (Ming et al., 1997; Song et al., 1997; Song et al., 1999).

Alternatively, the effects of exogenous BDNF and/or NT-3 may be mediated by serotonergic or cortical neuronal activity. High serotonergic activity in the first few days of postnatal life has been implicated in the pathogenesis of the barrelless phenotype of *Maoa* knockout mice (Cases et al., 1995; 1996). In addition, infusion of BDNF into the neocortex of adult rats causes sprouting of serotonergic nerve terminals and augments serotonergic activity (Mamounas et al., 1995; Siuciak et al., 1996). These effects of BDNF may be ascribed to the expression of the TrkB receptor by serotonin neurons of the raphe nuclei (Yan et al., 1997).

Several lines of evidence implicate neuronal activity in the regulation of the production and release of neurotrophins (Castrén et al., 1992; Lindholm et al., 1994; Blöchl and Thoenen, 1995; 1996). It has been demonstrated that neurotrophins modulate synaptic efficacy through changes in NMDA receptor function (Levine et al., 1998; Lin et al., 1998). Moreover, NMDA-dependent processes such as long-term potentiation (LTP) and long-term depression (LTD) are involved in synaptic elimination of inappropriate synapses or consolidation of appropriate synapses during development. Both of these processes were reported to be present during the first week of postnatal life of the rat SI cortex at the thalamocortical synapses (Crair and Malenka, 1995; Feldman et al., 1998; Isaac et al., 1997). Many of these synapses are silent at birth, because they either contain non-functional alpha-amino-3-hydroxy-5-methyl-4-isoxazolepropionic acid (AMPA) glutamate receptors or do not have them at all (Isaac et al., 1995; Liao et al., 1995;

Durand et al., 1996; Isaac et al., 1997; Rumpel et al., 1998; Liao et al., 1999). During the first week of postnatal life silent synapses are converted into functional ones by acquiring AMPA receptors (Gomperts et al., 1998; Liao et al., 1999; Petralia et al., 1999). BDNF was reported to modulate the expression of AMPA receptors (Narisawa-Saito et al., 1999) and BDNF, NT-4/5 and NT-3 can increase glutamate transmission in the hippocampus (Lessmann et al., 1994; Lessmann and Heumann, 1998; Scharfman, 1997; Kang and Schuman, 1995), while NT-3 can inhibit GABAergic transmission in embryonic cortical neurons (Kim et al., 1994). Thus, exogenous application of BDNF and NT-3 in the developing somatosensory cortex may increase neuronal activity, thereby disrupting the pattern and level of activity at thalamocortical synapses, and ultimately barrel formation.

Neurotrophins play an important role in other regions in the brain. Recently, it has been reported that the TrkB receptor and its ligands (BDNF and NT-4/5) play an important role in the development of ocular dominance columns (Cabelli et al., 1995; 1997). Neutralizing endogenous neurotrophin receptors with Trk receptor antibodies (Trk-IgG) or the local infusion of BDNF and NT-4/5, but not NGF or NT-3, during the critical period in kittens inhibits the formation of ocular dominance columns and activity-dependent pruning of the lateral geniculate nucleus terminals in visual cortex. The involvement of BDNF and NT-3 in patterning has also been shown by alteration of cerebellar foliation in BDNF and NT-3 null mutant mice (Schwartz et al., 1997; Bates et al., 1999).

Chapter 7

General Discussion

The main goal of this dissertation was to determine some of the molecular and cellular mechanisms that underlie pattern formation in the mouse somatosensory cortex. In order to accomplish this goal, several approaches were used including the isolation of a gene responsible for patterning and the identification of molecules that play important role in pattern formation in the SI cortex. Results from studies presented in this dissertation can be summarized in the following points: 1) A mutation in the adenylyl cyclase type I gene (*Adcy1*) caused the *brl* phenotype. 2) The effect of *Adcy1* was not through its downstream target cAMP-dependent protein kinase (PKA) in thalamocortical afferents. 3) PKA plays a role in barrel formation through its effect on layer IV cortical neurons. 4) Loss of neurotrophin-4/5 (NT-4/5) results in a phenotype that is similar to PKA null mutant mice. 5) Intracortical injections of exogenous BDNF and NT-3 disrupts patterning in the SI cortex of mice. Taken together, the above results provide strong evidence for the involvement of the cAMP signaling pathway as well as neurotrophic growth factors in pattern formation of the somatosensory cortex, thus indicating new mechanisms for patterning in the cerebral cortex.

7.1 Role of Second Messenger Systems in the SI Cortex

In multicellular organisms, cells communicate with each other by secreting signaling molecules that bind to specific protein receptors of target cells. Binding of an extracellular signaling molecule (a ligand) to a receptor is the first step in signal transduction pathways that will initiate a cascade of molecular and biochemical events, thereby influencing the behavior of target cells (Hardie, 1990; Snyder, 1985). Ligands

bind with a high affinity to their receptors and some of them initiate the production of intracellular messengers, also called second messengers (Kahn, 1976). There are three main types of second messenger signaling pathway: adenosine 3',5'-cyclic monophosphate (cAMP), Ca^{2+}, and inositol phospholipid. Second messenger molecules mediate their effects mainly through the phosphorylation of protein kinases which, in turn, will activate their target proteins.

cAMP is a ubiquitous second messenger that was discovered over 40 years ago (Rall et al., 1957; Sutherland and Rall, 1958a; 1958b). It is synthesized from adenosine triphosphate by a plasma-membrane-bound enzyme adenylyl cyclase in response to binding of an extracellular signal to a stimulatory receptor (Pastan, 1972; Schramm and Selinger, 1984). A variety of extracellular signals control cAMP levels by modulating the activity of adenylyl cyclase (for reviews see Gilman, 1987; Sutherland, 1972). cAMP mediates its effects mainly through the activation of PKA, which controls many biochemical events through the phosphorylation of target proteins.

Ca^{2+} is another widely used intracellular messenger that is responsible for a variety of cellular responses. It plays a role in all eukaryotic cells and more importantly in nerve cells. In nerve cells, depolarization of the plasma membrane causes a Ca^{2+} influx into the nerve terminal via voltage-gated Ca^{2+} channels which will initiate the release of a neurotransmitter (for review see Augustine et al., 1987). Ca^{2+} binds to the intracellular receptor calmodulin, after which the complex binds to various target proteins and thereby alters their activity. Most of Ca^{2+} effects are mediated by a family of Ca^{2+}/calmodulin-dependent protein kinase which, in turn, will phosphorylate target proteins.

While some extracellular signals induce cAMP or Ca^{2+} signaling pathways, others induce inositol phospholipid transduction pathways through the activation of phospholipase C-β (PLC-β). PLC-β will hydrolyzed phosphatidylinositol biphosphate to produce two second messengers: inositol triphosphate, which releases calcium from internal stores, and diacylglycerol, which activates protein kinase C (for review see Bansal and Majerus, 1990).

The three signaling pathways work in concert to exert cellular responses (for review see Cohen, 1988). Ca^{2+} influences enzymes that breakdown or produce cAMP. PKA phosphorylates Ca^{2+} channels and inositol triphosphate receptors in the endoplasmic reticulum. Additionally, PKA and Ca^{2+}/CaM kinases can phosphorylate different sites on the same protein, thus allowing these proteins to be regulated by both Ca^{2+} and cAMP. Moreover, Ca^{2+} directly modulates the activity of certain types of adenylyl cyclase, e.g., Type I (Tang et al., 1991), thus coupling the Ca^{2+} and cAMP systems (Choi et al., 1992).

Several studies have demonstrated the importance of cAMP transduction pathway in learning and memory and in regulation of gene transcription both in invertebrates and vertebrates (Brunelli et al., 1976; Walters et al., 1983; Livingstone et al., 1984; 1985; Levin et al., 1992; Bourtchuladze et al., 1994; Blitzer et al., 1995; Sassone-Corsi, 1995; Wu et al., 1995; Feany and Quinn, 1995; Xia and Storm, 1997; Wong et al., 1999). In fact, results presented in this dissertation provide the first evidence for the involvement of cAMP signaling pathway in pattern formation in the SI cortex of vertebrates (chapter 4; Abdel-Majid et al., 1998), thus revealing a new role for this signaling pathway in the development of the central nervous system.

As described above, cAMP mediates its effects mainly through PKA. Therefore, it was logical to hypothesize that loss-of-function mutation of *Adcyl* gene in the thalamocortical afferents will decrease cAMP levels which, in turn, will cause a reduction in PKA activity and that will result in a barrelless phenotype (chapter 4; Abdel-Majid et al., 1998). Results presented in this dissertation (chapter 5) suggest that this is not the case, since PKA null mutant mice have barrels. Few possibilities can explain the presence of barrels in PKA knockout mice. Redundancy in PKA subunits in the thalamocortical afferents protects against a barrelless phenotype. Alternatively, cAMP in the thalamocortical afferents may exert its effects through downstream targets other than PKA (for example, cyclic nucleotide gated channels) and that the site of gene action of PKA is on layer IV cortical neurons rather than in the thalamocortical afferents. In support of the second proposal, PLC-β-1 mutant mice displayed a phenotype similar to PKA mutant mouse lines (Hannan et al., 1998a) and that PKA was localized into layer IV cortical neurons during development (Abdel-Majid et al., 1999).

Ca^{2+} plays a role in glutamate release in the thalamocortical afferents. In the first two weeks postnatally, serotonin inhibits adenylyl cyclase activity through $5-HT_{1B}$ receptor (Bouhelal et al., 1988), which reduces cAMP and PKA levels thus reducing Ca^{2+} influx and hence glutamate release and neurotransmission (Rhoades et al., 1990). Furthermore, Ca^{2+} directly activates adenylyl cyclase type I, which is non-functional in *brl* mutant mice. Ca^{2+} also plays a role in postsynaptic cortical neurons via the activation of NMDA receptors. Pharmacological blockade of NMDA receptors in rats at birth affects the topographic refinement of thalamocortical afferents (Mitrovic et al., 1996; Fox

et al., 1996). Thus, it is apparent that the three second messenger signaling pathways are involved in pattern formation in the SI cortex of rodents, hence providing evidence for a new role of these transduction systems during development.

7.2 Role of Activity in the SI cortex

As discussed earlier (chapter 1), there is a great deal of controversy around the role of activity in the formation of somatotopic maps in the trigeminal system. Available information from studies performed in the visual system provide compelling evidence for the involvement of activity and in particular NMDA receptor mediated-activity in the refinement of topographic maps (for reviews see Constantine-Paton, 1990; Shatz, 1990; Goodman and Shatz, 1993; Katz and Shatz, 1996); however, most scientists will argue differently around the role of activity in the trigeminal system (for reviews see O'Leary et al., 1994; Purves et al., 1994). In the visual system, activity-dependent competition between inputs from one eye and the other is important for the formation of eye-specific laminae in the lateral geniculate nucleus (Shatz and Stryker, 1988) and forms the basis of ocular dominance columns in the visual cortex (Stryker and Harris, 1986). In contrast, blocking activity in the trigeminal system, either by the application of tetrodotoxin or the pharmacological blockade of NMDA receptors, did not have an effect on the formation of somatotopic maps (Henderson et al., 1992; Chiaia et al., 1992d; Schlaggar et al., 1993).

Results presented in this dissertation provide clear evidence for the involvement of activity-dependent mechanisms in establishment of cortical maps. A loss-of-function mutation in *Adcy1* might cause a reduction in glutamatergic neurotransmission and

subsequently disrupt barrel formation (chapter 4; Abdel-Majid et al., 1998). In support of this hypothesis, cytoarchitectonic barrels were absent in Nissl-stained sections in rats treated systemically or locally with an antagonist to NMDA receptors (Mitrovic et al., 1996), or when monoamine oxidase A was disrupted by targeted mutation in mice (Cases et al., 1995; 1996). More recently, it was shown that 5-HT$_{1B}$ agonists enhance neurite outgrowth from thalamic neurons in culture, an effect that is prevented by blockade of activity through the application of TTX (Lotto et al., 1999). Such a result can explain the presence of barrels in TTX-treated animals (Chiaia et al., 1992d).

A crucial role for NMDA receptors in activity-dependent mechanisms has been reported recently (Iwasato et al., 1997). NMDA receptor is formed of the subunit NR1 (ξ) and at least one of four of the NR2 (ϵ) subunits (Nakanishi 1992). NR1 and NR2 were disrupted by targeted mutation but unfortunately these mutants die shortly after birth which prevents the examination of whisker-related patterns in the thalamus and the cortex (Li et al., 1994; Kutsuwada et al., 1996). For this purpose, Tonegawa and colleagues (Iwasato et al., 1996; 1997) tried to change the level of ectopic expression of the NR1 subunit in the knockout mouse. Their results indicate that low expression of NR1 transgene had no effect on whisker-related patterns in the trigeminal pathway. However, when the NR1 transgene was expressed at high levels, whisker-related patterns were absent in brainstem, thalamus and SI cortex providing evidence for the importance of NMDA receptor mediated-activity in the formation of whisker-related patterns at all levels of the trigeminal pathway.

In recent years, it has been proposed that activity-dependent mechanisms such as long-term potentiation and long-term depression play an important role in the refinement of thalamocortical inputs in the barrel cortex (Crair and Malenka, 1995; Isaac et al., 1997; Feldman et al., 1998). Both processes can be induced only in the first week of postnatal life, which matches closely with critical period of barrel formation.

The above findings, including results presented in this dissertation, provide compelling evidence for the involvement of activity-dependent mechanisms in establishing of topographic maps in the trigeminal system of rodents. These results are in contrast with previous reports suggesting that neural activity does not play a role in formation of patterns in the whisker-to-barrel pathway (Henderson et al., 1992; Chiaia et al., 1992d; Schlaggar et al., 1993). However, it is plausible that in these studies pharmacological treatment was applied too late during development to disturb patterns that have already been established. For example, blocking the infraorbital nerve at birth (Henderson et al., 1992) will not have an effect on the emergence of barrelettes in the brainstem since these patterns are already in place by E20 (Chiaia et al., 1992b; 1992c).

7.3 Role of Neurotrophic Factors in the SI Cortex

Hamburger and Levi-Montalcini in 1949 demonstrated that peripheral targets regulate the survival of sensory ganglion neurons in the chick embryo. They also drew attention to the process of "normal" or "naturally occurring cell death" in sensory ganglia. Additionally, they proposed that both natural cell death and neuronal death in sensory ganglia following limb removal result from lack of target-derived substances necessary

for growth and survival, which they termed "trophic" or "neurotrophic" factors (Hamburger and Levi-Montalcini, 1949; Levi-Montalcini and Hamburger, 1951). From these observations the neurotrophic hypothesis emerged. The central tenet of the neurotrophic hypothesis was that during development neurons compete for a limited supply of target-derived trophic factors for their survival. The neurotrophic hypothesis was modified later on to include new observations (Purves and Lichtman, 1985; Purves, 1986; Purves, 1988). It was proposed that active postsynaptic cells will release these factors, and presynaptic terminals that are active at the time of release would be able to compete more successfully for these factors rather than terminals that were inactive at the time of release.

Nerve growth factor (NGF) was the first member of the neurotrophic factor family to be identified (Levi-Montalcini and Hamburger, 1953; Levi-Montalcini and Cohen, 1956). NGF supports the survival of a subpopulation of embryonic dorsal root ganglia and sympathetic neurons, but not parasympathetic or motor neurons (Arakawa et al., 1990; Deckwerth and Johnson, 1993; Henderson et al., 1993; Braun et al., 1996). NGF acts directly on these neurons increasing their size, number, and dendritic and axonal outgrowth (Levi-Montalcini, 1964; 1987a; 1987b; Hamburger et al., 1981). Other members of this family have been discovered (BDNF, NT-3, NT-4/5, NT-6, and NT-7). In recent years, a new role for neurotrophins in the central nervous system has emerged. In addition to their long-lasting effects on neurons (Levi-Montalcini, 1987a), they also play an important role in activity-dependent synaptic plasticity (Zafra et al., 1991; Lohof et al., 1993; Kim et al., 1994; Kang and Schuman, 1995; Levine et al., 1995; Cellerino

and Maffei, 1996; Figurov et al., 1996, Lu and Figurov, 1997; Lessman, 1998; Levine et al., 1998a; 1998b).

In the trigeminal system, neurotrophins play a role in whisker pad innervation, and in the formation of whisker-related patterns in the brainstem complex, and the SI cortex.

7.3.1 Neurotrophins in the Whisker Pad

Members of the nerve growth factor family are differentially expressed in the rodent whisker pad. BDNF and NT-3 are localized to the dermal mesenchyme of the whisker follicle and their expression is high at E11.5 and at E11, respectively (Schecterson and Bothwell, 1992). NGF, on the other hand, is predominantly localized to the epithelial mesenchyme and its expression peaks at E14.5 (Davies et al., 1987; Schecterson and Bothwell, 1992). NT-4 is also expressed in the whisker follicles and levels decrease between E13 and E20. The generation of mutant mice that are deficient in neurotrophins or their receptors has offered valuable information in understanding the role of these factors in the development of the whisker pad. Examination of the whisker pad in these knockout mice revealed that innervation is dependent on a balance between neurotrophins, and some innervation is dependent on one neurotrophin and at least one neurotrophin receptor, while others are dependent upon multiple neurotrophins and multiple receptors (Arvidsson et al., 1995; Wilkinson et al., 1995; Fundin et al., 1997; Rice et al., 1998). Overexpression of NGF in transgenic mice increased the number and branches of small unmyelinated fibers to the intervibrissal fur of the mystacial pad confirming that NGF modulates sensory innervation density (Davies et al., 1997).

7.3.2 Neurotrophins and Whisker-related Patterns in the V Brainstem

A combination of different neurotrophic factors regulates the survival rate of V ganglion cells during embryonic development. Before E11, V ganglion cells are dependent on BDNF or NT-3 for their survival and after E11 they switch to be solely dependent on NGF (for review see Davies, 1997). The expression of NGF is downregulated after E14, which is coincident with the period of naturally occurring cell death in the V ganglion. Several groups have investigated the role of neurotrophins on naturally occurring cell death in the V ganglion, and their effects on formation of whisker-related patterns in the brainstem trigeminal complex. Henderson et al. (1994) injected NGF, NGF antibody or NGF receptor antibody (IgG-192) systematically into rat fetuses (at E15, E16, E18 or at E15 and again at E18) at the time when natural cell death occurs (E14 - E19) in the V ganglion cells. Their results indicate that NGF injections at E15 and again at E18 has resulted in a 36% increase in V ganglion cell survival rate. Moreover, somatotopic patterns in the trigeminal brainstem complex were disrupted in newborn rats. On the other hand, a decrease in V ganglion cell survival rate, due to injections of either NGF antibody or IgG-192 at E15 and again at E18, did not have an effect on patterning in the brainstem. In support of the above findings, it was reported that loss of 83% of V ganglion cells in guinea pig, due to fetal injection of NGF antibody, did not alter whisker-related patterns in the brainstem, thalamus, and cortex (Sikich et al., 1986). The above results indicate that naturally occurring cell death in the V ganglia as a consequence of neurotrophin regulation is important in the formation of somatotopic patterns in the trigeminal brainstem complex.

In marked contrast to the above findings, Jhaveri et al. (1996) reported that naturally occurring cell death in V ganglion cells does not play a role in the formation of whisker-related patterns in the brainstem, and that other mechanisms control the development of whisker-related patterns. In these experiments, the authors used transgenic mice that overexpress NGF in the skin of the whisker pad (Albers et al., 1994). Although NGF overexpression rescued V ganglion cells from naturally occurring cell death, and their survival rate was doubled as compared to wild-type littermates, whisker-related patterns developed normally in their brainstem. It is surprising that a 36% increase in the survival rate of V ganglion cells in rats has disrupted whisker-related patterns in the V brainstem complex, whereas a 100% increase in the survival rate of V ganglion cells in mice did not have the same effect. The discrepancy between results from both studies could be explained by species-differences or most likely by the expression of NGF in the right place at the right time during development of the whisker pad in transgenic mice, in contrast to systemic injections that might have an effect on the peripheral as well as on central patterns in the trigeminal system. Moreover, differences between innervation densities of the whisker follicles and the interwhisker skin were also noted between transgenic mice and systemic injected rats (Rice et al., 1994; 1995).

7.3.3 Neurotrophins and Barrels in the SI Cortex

Information available on the role of neurotrophins in activity-dependent plasticity in the somatosensory cortex is very limited. In these earlier studies, a role for BDNF, NT-3 and NGF in the SI cortex was reported. While BDNF and NGF play a role in

modulation of functional representation of whiskers in adults (Prakash et al., 1996), systemic NGF application failed to rescue barrel formation after transection of the infraorbital nerve at birth (Henderson et al., 1993), and application of BDNF and NT-3 in the whisker pad rescued barrels from effects that usually occur in the cortex after denervation at birth (Calia et al., 1998).

Results presented in this dissertation provide new evidence for a role for neurotrophins in the development of somatotopic maps in the SI cortex. Present results indicate that intracortical injections of BDNF and NT-3 can produce a barrelless phenocopy, and that loss of NT-4/5 in knockout mice results in poorly-formed barrels. Additionally, these results argue for the critical presence of neurotrophins at a certain level at a specific time during development.

Neurotrophins have been implicated in axonal growth and elongation (Snider and Johnson, 1989; Kuffler, 1994; Lundborg et al., 1994), and in axonal guidance as chemoattractants (Gundersen and Barrett, 1979; Letourneau, 1978; Wang and Zheng, 1998; Song et al., 1997, Ming et al., 1997). The response of the axonal growth cones to cues in the environment, whether repulsion or attraction, depends on the level of cyclic nucleotides in their growth cone (Song et al., 1997; 1998; 1999). For example, BDNF triggers an increase in cytosolic Ca^{2+}, which leads to increased levels of cAMP in the growth cone and hence results in an attractive turning response (Lohof et al., 1992). Thus it is conceivable that neurotrophin effects observed here could be due to their effect on the turning response of the thalamocortical afferent growth cones.

In the past few years, several studies have reported the involvement of TrkB and its ligands in activity-dependent mechanisms during development of the visual system (Cabelli et al., 1995; Riddle et al., 1995; McAllister et al., 1995; 1996; Cabelli et al., 1997; McAllister et al., 1997; 1999). However, results presented in this dissertation provide the first evidence for the involvement of neurotrophins in the development of the SI cortex, therefore, revealing new cellular mechanisms for the formation of somatotopic maps.

7.4 Other Factors Related to Formation of Somatotopic Maps

Various factors play important roles in the formation of whisker-related patterns in the trigeminal system. Table 7.1 summarizes these factors listed according to their effects in the pathway starting peripherally with the whisker pad and ending with the SI cortex. Only factors that influenced barrels in the posteromedial barrel subfield were listed in the table, others that had an effect on brain weight and cortical size, and indirectly affected the size of the barrel field, such as insulin-like growth factor (Beck et al., 1995; Gutierrez-Ospina et al., 1996) were excluded.

Factors that affect the whisker pad include: activin and follistatin (Jhaveri et al., 1998). Activin is a member of the transforming growth factor-β superfamily and follistatin is an activin binding protein. Mice lacking follistatin die within a few hours after birth, while activin mutant mice die within 24 hours of birth because of suckling impaired responses. Activin deficient mice do not have whiskers, whisker follicles are malformed and whisker-related patterns are absent in the brainstem trigeminal complex.

Table 7.1 List of factors playing a role in the formation of whisker-related patterns in the whisker-to-barrel pathway. Various factors affect somatotopic representation at different levels of the neuraxis and with varying degrees. Abbreviations: KO, knockout mouse; Tg, transgenic mice; CamkIIα, Ca^{2+}/calmodulin protein kinase II α subunit; Trk, tyrosine kinase receptor; FGF2, fibroblast growth factor 2; MAOA inhibitor, monoamine oxidase A inhibitor; GAP-43, growth associated protein-43; TTX, tetrodotoxin; *Adcy1*, adenylyl cyclase type I; NGF, nerve growth factor; PLC-β-1, phospholipase C-β-1; BDNF, brain-derived neurotrophic factor; NT-3, neurotrophin-3; NT-4/5, neurotrophin-4/5; 5,7-DHT, 5,7-dihydroxytryptamine; APV and MK801, antagonists for NMDA receptors; PKA, cAMP-dependent protein kinase; 5-HT, serotonin; TCAs, thalamocortical afferents; NMDA ε4, NMDA regulatory subunit 2 ε isoform; NR1* transgenic mice for the NMDA regulatory subunit 1 with high expression of the transgene. NR1** transgenic mice with low expression of the transgene.

Factor	Treatment	Effect	Reference
A- Whisker Pad			
Activin βA	KO	whiskers are absent barrelettes are absent	Jhaveri et al., 1998
Follistatin	KO	whiskers are thin and curled, barrelettes are poorly formed	Jhaveri et al., 1998
B- Trigeminal Sensory Neurons			
NR2 ε2	KO	barrelettes are absent	Kutsuwada et al., 1996
NR1	KO	barrelettes are absent	Li et al., 1994
NR1*	Tg	barrelettes, barreloids, and barrels are absent	Iwasato et al., 1996; 1997
NR1**	Tg	barrelettes, barreloids, and barrels are normal	Iwasato et al., 1996; 1997
NMDA ε4	KO	barrelettes, barreloids, and barrels are normal	Ikeda et al., 1995
NGF	exogenous	barrelettes are absent	Henderson et al., 1994
Infraorbital nerve	TTX	barrelettes, barreloids, and barrels are normal	Henderson et al., 1992
	Blocking axonal transport	whisker-related patterns are absent	Chiaia et al., 1996
C- Primary Somatosensory Cortex			
1. Barrelless			
Adcy1	*Adcy1^{brl}*	barrels are absent	Welker et al., 1996; Abdel-Majid et al., 1998

Factor	Treatment	Effect	Reference
Adcy1	KO	barrels are absent	This thesis; Abdel-Majid et al., 1998
BDNF	exogenous	barrels are absent	This thesis
NT-3	exogenous	barrels are absent	This thesis
GAP-43	KO	barrels are absent	Maier et al., 1998; 1999
MAOA	KO	barrels are absent	Cases et al., 1995; 1996
MAOA inhibitor	clorgyline	barrels are absent	Vitalis et al., 1998
NMDA	APV MK801	barrels are absent	Mitrovic et al., 1996
Ablation of TCAs	thalamotomy	barrels are absent	Wise and Jones, 1978

2. Abnormal Barrels

Factor	Treatment	Effect	Reference
NT-4/5	KO	poorly-formed barrels	This thesis
PLC-β-1	KO	poorly-formed barrels	Hannan et al., 1998a
PKA	RIIβ KO	poorly-formed barrels	This thesis
Ablation of layer IV cortical neurons	X-irradiation	aggregates of neurons	Ito, 1995
Reeler	mutant	barrels are small and irregular in shape	Cragg, 1975 Welt and Steindler, 1977 O'Brien et al., 1987

3. Delayed or Changed Barrel Size

Factor	Treatment	Effect	Reference
Hypothyroidism	Congenital	barrel formation is delayed by three days	Calikoglu et al., 1996

Factor	Treatment	Effect	Reference
Malnutrition	Protein	barrel formation is delayed by two days	Vongdokmai, 1980
5-HT depletion	5,7-DHT Fenfluramine	barrel formation is delayed	Blue et al., 1991; Bennett-Clarke et al., 1994; 1995; Rhoades et al., 1998
FGF2	KO	barrels are reduced in size	Ortega et al., 1998
BDNF	exogenous	barrels are smaller by 16%	Penschuck et al., 1999
NMDA	APV	barrels are larger by 16%	Penschuck et al., 1999

4. Normal Barrels

Factor	Treatment	Effect	Reference
BDNF	KO	barrels are normal	Jones et al., 1994
CamkII α	KO	barrels are normal	Glazewski et al., 1996
NGF	exogenous	barrels are normal	This thesis
NT-4/5	exogenous	barrels are normal	This thesis
PKA	RIIα KO	barrels are normal	This thesis
PKA	RIβ KO	barrels are normal	This thesis
PKA	Cα KO	barrels are normal	This thesis
PKA	Cβ KO	barrels are normal	This thesis
Semaphorin III	KO	barrels are normal	Ulupinar et al., 1999
Tenascin	KO	barrels are normal	Steindler et al., 1995

Factor	Treatment	Effect	Reference
Tenascin	KO	barrels are normal	Mitrovic and Schachner, 1995
TrkA receptor	KO	barrels are normal	Henderson et al., 1995
TrkB receptor	KO	barrels are normal	Henderson et al., 1995
TrkC receptor	KO	barrels are normal	Henderson et al., 1995

Follistatin deficient mice have thin and curled whiskers, follicles were misoriented and whisker-related patterns in the brainstem were not well developed as in wild-type controls. It is noteworthy to mention that higher order trigeminal patterns develop sequentially and that pattern formation in the thalamus and the cortex will not form if whisker-related patterns were absent from the brainstem trigeminal complex (Killackey and Fleming, 1985; Killackey et al., 1990; Rhoades et al., 1990; Woolsey et al., 1990).

A role for NMDA activity, neurotrophins and intact periphery in formation of trigeminal brainstem complex patterns has been demonstrated. Whisker-related patterns in the trigeminal brainstem complex were disrupted in knockout and transgenic mice for the NMDA receptor regulatory subunits (Li et al., 1994; Kutsuwada et al., 1996; Iwasato et al., 1996; 1997). These mutants provide evidence for the importance of NMDA receptor mediated-activity in formation of somatotopic maps in the trigeminal system. In contrast to the above findings, blockade of activity by tetrodotoxin at birth did not alter the representation of whisker-related patterns in the brainstem trigeminal complex (Henderson et al., 1992). On the other hand, neonatal blockade of axonal transport in the infraorbital nerve (Chiaia et al., 1996) and systemic application of NGF in rat fetuses (Henderson et al., 1994) prevented the formation of whisker-related patterns in the trigeminal system.

A variety of factors can influence the formation of cytoarchitectonic barrels. Variations in barrel morphology ranged from the complete absence of barrels, delayed barrel formation, and change in their size, to the formation of abnormal barrels. Factors that abolish barrels from the SI cortex include molecules that play a role in activity-

dependent mechanisms such as NMDA receptors (Iwasato et al., 1996; 1997), serotonin (Cases et al., 1995; 1996; Vitalis et al., 1998), cAMP (Welker et al., 1996; Abdel-Majid et al., 1998), exogenous BDNF (chapter 6), and exogenous NT-3 (chapter 6) or molecules involved in axonal guidance such as GAP-43 (Maier et al., 1998; 1999). All the above manipulations had an affect on the topography of the thalamocortical afferents with no effects on somatotopy in the SI cortex, with the exception of the GAP-43 mutant mice. Loss of barrels by pharmacological treatment or by genetic targeting in the above studies was attributed to an overgrowth of the thalamocortical afferents terminating in layer IV, while in GAP-43 knockout mice thalamocortical afferents are misrouted and fail to extend to their targets in layer IV of the cortex, hence resulting in loss of somatotopy in the SI cortex. Furthermore, exogenous application of BDNF and NT-3 by intracortical injections abolishes barrel formation (chapter 6).

While the above mentioned factors abolished barrels, others resulted in abnormal barrels. These factors included loss of PKA (chapter 5), NT-4/5 (chapter 6) and PLC-β-1 (Hannan et al., 1998b) in knockout mice. All these mutant mice displayed a varied degree of abnormalities in the distribution of cortical neurons in layer IV of the SI cortex without an effect on the segregation of thalamocortical afferents, as observed in cytochrome oxidase histochemistry. The reeler mutant, on the other hand, had few normal barrels but the majority of barrels were small and irregular in shape (Cragg, 1975; Welt and Steindler, 1977; O'Brien et al., 1987). Irradiation of the cortex at the time when layer IV neurons are generated (E17) also has an effect on barrel formation (Ito, 1995). The author reported that barrels were absent from the cortex. However, since patches of

thalamocortical afferents, albeit smaller, were present in cytochrome oxidase stained-sections along with the presence of some sort of barrel arrangement, these types of barrels were categorized with this group rather than with the barrelless group.

The last group of factors that influenced barrel formation include factors that delayed barrel formation for few days; however, they developed normally afterwards. These factors include congenital hypothyroidism (Calikoglu et al., 1996), malnutrition (Vongdokmai, 1980) and serotonin depletion by systemic injection of a neurotoxin (Bennett-Clarke et al., 1994; 1995; Rhoades et al., 1998). Loss of fibroblast growth factor 2 in knockout mice reduced the cortex thickness and the size of barrels. Modulation of cortical activity by infusion of BDNF or NMDA receptor antagonist in newborn rats resulted in equal and opposite effects on barrels size (Penschuck et al., 1999).

Lastly, it appears that a certain level of activity must be maintained at the thalamocortical synapses for normal barrel formation, modulating the pattern and level by increasing (e.g. exogenous BDNF or NT-3) or decreasing (e.g. decrease cAMP levels, or high serotonin levels) activity will disrupt patterning in the SI cortex. Figure 7.1 summarizes results presented in this dissertation. In wild-type animals, high levels of serotonin during the first two weeks of postnatal life decreases glutamate neurotransmission as synapses are established, thalamocortical afferents are segregated, and cortical barrels are formed. A mutation in adenylyl cyclase type I gene might cause a successive reduction in activity which results in overgrowth of thalamocortical afferents and loss of cortical barrels. On the other hand, increasing activity levels by exogenous BDNF or NT-3 will result in a barrelless phenocopy. Other factors that seem to have their

Figure 7.1 A schematic drawing summarizing results presented in this dissertation. At birth, TCAs are present in layer IV; however, their terminals are not arborized yet (top). During the first week postnatally, TCA terminals arborize forming a dense plexus of clusters that terminate into the barrel boundaries (wild-type, bottom). A variety of factors can affect cytoarchitectonic barrels in two different directions. Loss-of-function mutation in adenylyl cyclase type I (*Adcy1*), or exogenous application of BDNF or NT-3 causes a barrelless phenotype and overgrowth of thalamocortical afferents in layer IV (barrelless, bottom), whereas loss of NT-4/5 (*Ntf5*) and PKA subunit (*Prkar2b*) by gene targeting results in poorly-formed barrels without an effect on the segregation of the thalamocortical afferents (poorly-formed barrels, bottom).

CTX

TCA

- Ntf5

- Prkar2b

Normal
Development

+ BDNF

+ NT-3

- Adcy1

**Poorly-formed
Barrels**

Wild-type

Barrelless
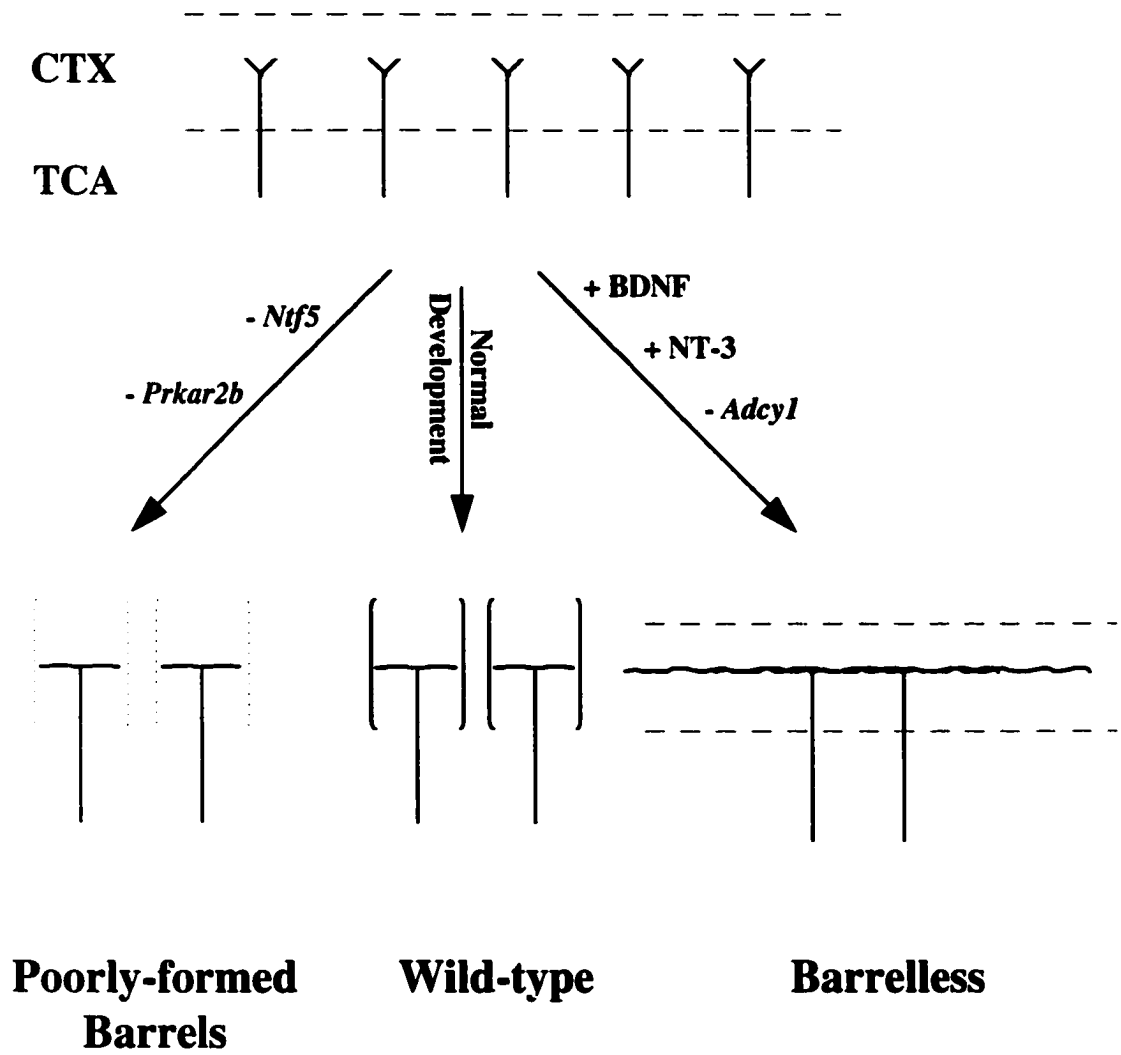
Figure 7.1

site of action on layer IV cortical neurons do not abolish barrels completely. Instead they affect the distribution of layer IV cortical neurons without affecting the segregation of the thalamocortical afferents, giving rise to poorly-formed barrels.

7.5 Future Perspectives

The main objective of the studies presented in this dissertation was to discover molecular mechanisms that underlie patterning in the cerebral cortex. In order to achieve this goal, we started to construct a pathway for molecules that play a role in pattern formation of the murine SI cortex. Present results provide new evidence for the involvement of second messenger system signaling pathways and neurotrophins in pattern formation. However, certain caveats are still present in this pathway that have not been solved yet: 1) What are the downstream targets of cAMP in the thalamocortical afferents? 2) What is the role of upstream effectors such as the 5-HT_{1B} receptor in the thalamocortical afferents? 3) If BDNF and NT-4 exert their effects through the activation of the same receptor, how come they resulted in different effects. 4) How do neurotrophins exert their effects in the cortex?

Since I am more interested in cAMP signaling pathways, the following discussion will only deal with this issue. As mentioned previously, cAMP exerts its effects mainly through PKA; however, in recent years new lines of evidence started to emerge. It has been reported that cyclic nucleotides can directly activate cyclic nucleotide gated (CNG) channels in the photoreceptors of the retina. Since then, it has been shown that they are present in neuronal and non-neuronal tissues (for reviews see Kaupp, 1991; Barnstable,

1993; Firestein and Zufall, 1994; Yau, 1994; Zufall et al., 1994). Evidence from *C. elegans* mutants argues for a role of CNG channels activity in axonal outgrowth where axons of sensory neurons terminate in inappropriate positions (Coburn and Bargmann 1997).

It is not known, yet, whether the ventrobasal complex of the thalamus or the somatosensory cortex express these channels during the first week when barrels are formed. In order to answer this question, we tried to determine whether CNGs are expressed in one-week-old wild-type and barrelless mutant mice, using reverse transcriptase polymerase chain reaction. Preliminary attempts to amplify olfactory and retina CNG channels were unsuccessful (R. Abdel-Majid, unpublished results); however, it may be worth using other molecular methods such as northern blot analysis or *in situ* hybridization to determine whether they are expressed in the thalamus and/or cortex during the critical period of barrel formation.

cAMP activates CNG channels causing an increase in Ca^{2+} influx into the cytosol. A mutation in the *Adcy1* gene will decrease cAMP levels which, in turn, will decrease the activity of these channels and will result in an overgrowth of the TCAs. This hypothesis is supported by evidence from *C. elegans* mutants. Loss of CNG channel activity causes an overgrowth of their sensory axons and their termination in inappropriate positions (Coburn and Bargmann, 1997). If the downstream target of cAMP in the thalamocortical afferents is cyclic nucleotide gated channel, then according to our hypothesis these mutants should be barrelless. Finally, the olfactory cyclic nucleotide gated channel has

been targeted by gene disruption (Brunete et al., 1996). Thus, it is worth examining these

mutants for the presence of barrels in their somatosensory cortex.

Appendix 1

40% Acrylamide/bisacrylamide solution

acrylamide	380 gm
N,N' methyenebisacrylamide	20 gm

Adjust the final volume to one liter with deionized distilled water. Filter solution and store in dark bottles at room temperature.

30% Acrylamide/bisacrylamide solution

acrylamide	43.50 gm
N,N' methylenebis-Acrylamide	1.52 gm

Adjust the final volume to 150 ml with deionized distilled water. Filter solution and store in dark bottles at room temperature.

15% Acrylamide/bisacrylamide solution

30% acrylamide/bisacrylamide	10 ml
1.5 M Tris-HCl (pH 8.8)	5 ml
deionized distilled water	5 ml
10% APS	113 µl
TEMED	10 µl

Adjust the final volume to 150 ml with deionized distilled water. Filter solution and store in dark bottles at room temperature.

10% Acetic acid

glacial acetic acid	10 ml
deionized distilled water	90 ml

Agarose gels

Agarose gels are prepared at different concentration depending upon the size of the DNA to be separated. Agarose gels are prepared in 1x TAE buffer by dissolving the required amount in the buffer and autoclaving until all the powder is dissolved completely (2 - 5 minutes). Ethidium bromide is added at a final concentration of 5 µg/ml and finally gels

are poured when the temperature of the solution reaches 60 °C allowing 30 - 45 minutes for polymerization.

Buffer gradient gel solution

Top mix

urea	115 gm
10x TBE	12.5 ml

Add:

40% acrylamide/bisacrylamide	37.5 ml

Adjust the final volume to 250 ml with deionized distilled water.

Bottom mix

urea	46 gm
10x TBE	25 ml

Add:

40% acrylamide/bisacrylamide	15 ml

Adjust the final volume to 100 ml with deionized distilled water.

Add:

sucrose	10 gm
bromophenol blue	5 mg

Developing reagent for polyacrylamide gel electrophoresis (3% Na_2CO_3, 5.5% formaldehyde, .002% sodium thiosulfate)

sodium carbonate	15 gm
37% formaldehyde	0.75 ml
sodium thiosulfate	0.50 ml

5 mM dNTP solution

Dilute 5 µl of 100 mM stock solution of each GTP, ATP, CTP and TTP into a total volume of 100 µl with deionized distilled water. Store at -20 °C.

DNA Extraction buffer

To prepare 25 ml of extraction buffer:

1 M Tris-HCl (pH 8.5)	2.5 ml

0.50 M EDTA (pH 8.0)	0.25 ml
20% SDS	0.25 ml
3M NaCl	1.67 ml
proteinase K (100 mg/ml)	25 μl

Adjust the final volume to 25 ml with deionized distilled water.

DNA markers

Dilute stock solution of 1 kb and 100 b.p. to a final concentration of 100 ng/μl.

0.50 M EDTA solution, pH 8.0

| Na$_2$EDTA.2H$_2$O | 186.1 gm |
| deionized distilled water | 700 ml |

Adjust pH with concentrated hydrochloric acid. Adjust the final volume to 1 L with deionized distilled water. Autoclave solution.

Ethidium bromide

Dissolve 10 mg of ethidium bromide into 1 ml of deionized distilled water. Store solution in a dark bottle. Ethidium bromide is used at a final concentration of 0.50 μg/ml.

LB medium

tryptone	10 gm
yeast extract	5 gm
NaCl	5 gm
1 N NaOH	1 ml

Complete to 1 L with deionized distilled water. Autoclave solution.

LB plates

tryptone	10 gm
yeast extract	5 gm
NaCl	5 gm
1 N NaOH	1 ml
agar	15 gm

Complete to 1 L with deionized distilled water. Autoclave solution. When solution is warm enough add ampicillin to a concentration of 50 μg/ml.

10x PCR buffer

1.0 M Tris-HCl (pH 9.3)	1.25 ml
2.5 M KCl	1.0 ml
5 M MgCl$_2$	20 µl
1 M DTT	50 µl
ddH$_2$O	2.68 ml

Divide into 500 µl aliquots and store at -20°C.

Proteinase K

Stock solution is prepared at a concentration of 100 mg/ml. Store solution at -70°C.

Running buffer for polyacrylamide gel electrophoresis (50 mM Tris-HCl, 380 mM glycogen)

1 M Tris-HCl (pH 8.3)	50 ml
glycogen	28 gm

Adjust final volume to 1 L with deionized distilled water.

3 M Sodium acetate, pH 4.5 - 5.2

sodium acetate	61.52 gm
deionized distilled water	150 ml

Adjust pH between 4.5 - 5.2 with glacial acetic acid. Adjust the final volume to 250 ml with deionized distilled water. Autoclave solution.

3 M Sodium chloride

Dissolve 12 gm of sodium hydroxide in 100 ml of deionized distilled water. Autoclave solution.

20% Sodium dodecyl sulfate (SDS)

Dissolve 20 gm of SDS in 100 ml of autoclaved distilled water.

2 M Sodium hydroxide

Dissolve 80 gm of sodium hydroxide in 1 L of deionized distilled water.

3 M Sodium hydroxide

Dissolve 120 gm of sodium hydroxide in 1 L of deionized distilled water.

Silver stain solution for polyacrylamide gel electrophoresis (0.1% AgNO3, 5.5% formaldehyde)

silver nitrate	0.5 gm
37% formaldehyde	0.75 ml

Adjust volume to 500 ml with deionized distilled water.

1.0 M Tris-HCl, pH 8.5

Tris-(hydroxymethyl)-methylamine	121 gm
deionized distilled water	800 ml

Adjust pH to 8.5 with concentrated hydrochloric acid. Adjust the final volume to 1 L with deionized distilled water. Autoclave solution.

TE buffer, pH 7.5 (10 mM Tris, 1 mM EDTA)

Tris-HCl	0.6055 gm
Na$_2$EDTA.2H$_2$O	0.186 gm
deionized distilled water	300 ml

Adjust pH to 7.5 with concentrated hydrochloric acid. Adjust the final volume to 500 ml with deionized distilled water.

50x Tris-acetic-EDTA buffer (TAE)

Tris-HCl	242 gm
glacial acetic acid	57 gm
Na$_2$EDTA.2H$_2$O	37.2 gm

Adjust the final volume to 1 L with deionized distilled water. Autoclave solution.

10x Tris-boric-EDTA buffer (TBE)

Tris-HCl	108 gm
boric acid	55 gm
Na$_2$EDTA.2H$_2$O	9.3 gm

Adjust the final volume to 1 L with deionized distilled water. Autoclave solution.

Appendix 2

Adenine hemisulfate (2 mg/ml (0.2%)

Dissolve 0.05 gm in 250 ml of double distilled water (ddH$_2$O). Autoclave solution.

AHC medium (selective media for growing YACs)

95 ml of 2% glucose & 1% casamino acids.

5 ml of 20x YNB w/o amino acids

1 ml of 0.2% adenine hemisulfate

AHC plates

YNB w/o amino acids   1.7 gm

casamino acids   10 gm

Add 900 ml of water and adjust pH to 5.8, then add 20 gm of agar. Autoclave solution. When solution is warm to the touch add:

0.2% adenine hemisulfate   10 ml

20% glucose   100 ml

Pour in petri dishes and allow them to cool in a laminar flow hood.

Breaking buffer (2% Triton, 1% SDS, 100 mM NaCl, 10 mM Tris-HCl (pH 8.0), 1 mM EDTA)

Triton X-100   2 ml

20% SDS   5 ml

5 M NaCl   2 ml

1 M Tris-HCl (pH 8.0)   1 ml

0.5 M EDTA (pH 8.0)   0.2 ml

Adjust final volume to 100 ml with deionized distilled water.

0.5 M EDTA, pH 8.0

Dissolve 186.10 gm of disodium ethylene diamine tetracetate.2H$_2$O in 800 ml of deionized distilled water. Adjust pH to 8.0 with NaOH and complete final volume to 1 L. Autoclave solution.

194

glucose & casamino acid (2% glucose & 1% casamino acids)

| glucose | 20 gm |
| casamino Acid | 10 gm |

Adjust the volume to one liter with deionized distilled water. Autoclave solution.

1.5% Low gelling agarose

Dissolve 1.5 gm of low gelling agarose in 100 ml of sorbitol solution at 70°C water bath. This process will take 15-20 minutes. Keep in water bath until use.

Lysis solution (1% LDS, 0.1 M EDTA, and 10 mM Tris-HCl, pH 8.0)

lauryl dodecyl sulfate (LDS)	5 gm
0.5 M EDTA (pH 8.0)	100 ml
1 M Tris-HCl (pH 8.0)	5 ml

Adjust the final volume to 500 ml with deionized distilled water.

5 M Potassium acetate, pH 4.8

| glacial acetic acid | 29.5 ml |

Add KOH pellets to adjust pH to 4.8. Adjust volume to 100 ml with deionized distilled water and store at room temperature.

20XSSC

sodium chloride	175.30 gm
sodium citrate	88.2 gm
ddH$_2$O	800 ml

Adjust pH to 7.0 with few drops of 10 N NaOH. Adjust the final volume to 1 L with deionized distilled water. Autoclave solution.

Sorbitol solution (1.2 M Sorbitol, 10 mM Tris-HCl (pH 7.5), 20 mM EDTA)

sorbitol	43.73 gm
1 M Tris-HCl (pH 7.5)	2 ml
0.5 M EDTA (pH 8.0)	8 ml

Adjust final volume to 200 ml with deionized distilled water. Before use 1 µl of β-mercaptoethanol solution and 10 µl of zymolaze 20-T are added per 1 ml of sorbitol solution.

1 M Tris-HCl (pH 7.4)

Dissolve 121.1 gm Tris-HCl in 800 ml of deionized distilled water. Adjust pH with concentrated HCl to pH 7.4. Autoclave solution.

20x yeast nitrogen base (YNB), without amino acids

Dissolve 13.4 gm YNB w/o amino acids in 100 ml of ddH$_2$O. Autoclave solution.

Zymolaze 20-T (20,000 U/gm)

Dissolve zymolaze 20-T at a final concentration of 10 mg/ml in 1 M sorbitol and 50 mM sodium phosphate, pH 7.5. Aliquot into small tubes and store at -20°C.

Appendix 3

Marker	Our	Copeland	Mit	EUCIB	JXN BSS	MRC	MGD
D11Mit74	**0.00**		2.20			2.00	0.00
D11Xrf285					0.00		
D11Ggcle					0.00		
D11Bwg0414e					0.00		
D11Bwg0572e					0.00		
D11Bwg1392e					0.00		
D11Bwg1548e					0.00		
D11Ncvs74					0.00		
code335					0.00		
D11Mcg1 (Nf2)	**0.25**					3.00	1.00
D11Mit72	**0.25**	3.30*	2.20	0.00			1.00
D11Mit304	**0.25**		2.20				1.00
D11Mit16	**0.25**		2.20	4.00		3.00	1.00
D11Mit106	**0.25**		3.30*				1.00
Lif	**0.25**	0.00				4.00*	1.00
D11Mit1	**0.25**		2.20	4.29	0.00	3.00	1.00
D11Mit73			2.20				1.00
Camk2b	**0.50**	0.00				4.00	1.00
Igfbp1		0.50			0.00		2.00
Igfbp3		0.50					2.00
Gk					0.00	3.00	5.00*
lapls1-25					0.00	4.00	
lapls3-26					0.00	4.00	
Pmv2					0.00	4.00	5.00
Pmv22					1.00	5.00	8.00
brl	**1.25**						
D11Mit71		3.30	0.00*			1.00*	1.00
D11Mit129			2.20	4.87			1.00
D11Mit62	**1.50**		2.20				1.00
D11Mit226	**1.50**		2.20	5.15			1.00
JKMV80				5.15			
JKPAV190				5.15			
JKAV380				5.35			
Ikaros		3.30					7.00
D11Bir2					2.00		
D11Bir3					2.00		
D11Mit259		3.30	5.50*	5.44			5.00
D11Mit150			4.40	5.44			2.00
D11Mit204	**2.16**		4.40	5.44			2.00
D11Mit2	**2.38**	3.30	4.40	6.02			2.00
D11Mit133	**2.82**		4.40	5.73 *			2.00
D11Mit148	**3.26**	3.30					1.00*

Marker	Our	Copeland	Mit	EUCIB	JXN BSS	MRC	MGD
D11Mit162		3.30	6.60*				8.00
ERBB		4.00					
D11Mit371		6.60					
D11Mit228			4.40				2.00
D11Mit75			4.40	6.60			2.00
D11Mit76			4.40	6.89			2.00
D11Mit78	**8.79**		4.40	7.75			2.00
D11Mit77	**8.79**		4.40	8.04			2.00
D11Mit227			4.40	8.04			2.00
D11Mit305			4.40	8.04			2.00
D11Mit295				9.48			13.00
D11Mit306				9.77			
D11Mit294				10.64			
D11Mit152		9.40		10.64			
D11Mit81				11.50			
D11Mit19		9.40		11.79		14.00	
D11Mit151				11.79			
D11Mit83				12.37			
D11Mit82				12.37			
D11Mit149			2.20	20.00			1.00

Appendix 3. A composite map in the proximal region of the mouse chromosome 11. Data was compiled from different published maps as described earlier in chapter 3. Markers are listed based on data generated in our laboratory (bold) followed by the Copeland, Whitehead Institute (Mit), EUCIB, Jackson backcross (JXN BSS), Oxford (MRC), and lastly mouse genome database (MGD). Numbers represent the position of the loci in cM. * represents discrepancy in the position of this marker with regard to other published maps.

Appendix 4

No.	Name	Sequence	B6 Size	C3H Size
1 -	*D1Mit1* Left *D1Mit1* Right	GGG TCT CTG AAG GCT TTG TG TGA ATA CAG AAG CCA CGG TG	153	153
2 -	*D1Mit2 Left* *D1Mit2 Right*	TCC CAG AGG TCT CCA AGA CA CCA CAG TGT GTG ATG TCT TC	122	137
3 -	*D1Mit16* Left *D1Mit16* Right	CAG CTA GAA ATG GCA ATG AGG CTT GTT CTA CAC CCA GCA AGC	120	120
4 -	*D1Mit62* Left *D1Mit62* Right	GAA TAA CCC ATG TTT ATA TCG GTG CTC TGG ACT TGT GTT CTA TGC C	148	160
5 -	*D1Mit71* Left *D1Mit71* Right	GCC ATA CCT GGT AGC GTG TT AAT TTT CAG ATG TAG CCA TAA GCC	214	238
6 -	*D1Mit72* Left *D1Mit72* Right	TGA GTG GCA TCC CTA ATT CC GTG TGT GTC ACT ATT CTT GGT TCC	160	160
7 -	*D1Mit73* Left *D1Mit73* Right	TCG AAT TTT GAT CAT GAA GGC GTT ACC GCA ATC ACA GCA GA	190	190
8 -	*D1Mit74* Left *D1Mit74* Right	AAA ACC TGA GTT CGA CCC CT ATA AAG CCT CAT CTA CAT GGG C	214	216
9 -	*D1Mit106* Left *D1Mit106* Right	TGT CTC TCC GAG TCT GTC TCT G AGA AAC TGT TCC ACC CCC TT	130	130
10 -	*D1Mit129* Left *D1Mit129* Right	TAT GAT TCT GAG GGC TTG GG CCC CCA AAA TAA AAG TAG ATT GG	140	138

No.	Name	Sequence	B6 Size	C3H Size
11 -	*D11Mit148* Left *D11Mit148* Right	GGAAAGAGAAAAGACTTAACAGAACA TCC CAG TAA AAC TGC CTT CTG	145	147
12 -	*D11Mit149* Left *D11Mit149* Right	AGA CGG ATG ATC TCT GCC C TTT GAA TTT TAT CCT TTG CAA GC	145	147
13 -	*D11Mit150* Left *D11Mit150* Right	GGT CAG ACA CTG AGT GAA GAT ATA GC TCC TCT GAC ACC CAT AAG TTC A	194	153
14 -	*D11Mit162* Left *D11Mit162* Right	AGC ATT ACT GTA AAT TCT GTT TCC G AAG GTG ATT TTA AAG CAA AAG CC	123	123
15 -	*D11Mit204* Left *D11Mit204* Right	CTACTTAAATGTAGGGAGAGGTAGTGG GTC TAG ATT GAT CTC TGC AAC CTG	138	136
16 -	*D11Mit226* Left *D11Mit226* Right	AGG TGA ACT CTT TTG AAG TTT GTG AAAGGAGTGACTGAGAAAGACACC	142	126
17 -	*D11Mit228* Left *D11Mit228* Right	GAA CCT AGA TGA AAA TGG GTG C CTACCCTGAATA AA AGATA TGTGTG	134	114
18 -	*D11Mit259* Left *D11Mit259* Right	GTATAGAGAGAGAGATGCATGGATACA AAT CTC TCT CCT GCT TTC ATG C	116	116
19 -	*D11Mit304* Left *D11Mit304* Right	ACT CAT CAT AAA CAA AGG CAT GC ATTTCAAATACATTAGTGGAAACATCA	90	-1
20 -	*D11Mit305* Left *D11Mit305* Right	TTCTATGAGGAAATTCAGTAGATACCA TTTAGTTTACTTCAGGTCAACACACA	114	114

No.	Name	Sequence	B6 Size	C3H Size
21 -	*Dl1Dal6* Forward 1 *Dl1Dal6* Reverse 1	TGC TTA GAA CAA GGC AGT CT GCT TTG GTT ACA CAA TCA GC	154	154
22 -	*Dl1Dal6* Forward 2 *Dl1Dal6* Reverse 2	CAG AAA GCA GGA GAT GAA AT CAC GGA AAA AGA AAA GAA CTC	231	231
23 -	*Dl1Dal7* Forward *Dl1Dal7* Reverse	GCA CAG ACA CCC AGA ACT TC CAG CAC ATT GAG GAA CTT CA	110	110
24 -	*Ikaros* Forward *Ikaros* Reverse	GGA GGC ACA AGT CTG TTG AT ATC CCC TTC ATC TGG AGT GT	116	116
25 -	*Dl1Dal9* Forward *Dl1Dal9* Reverse	AGG AGG AAG AGG AGG ACT CA GCT CGC CTT TAT CCA TTT TC	224	224
26 -	*Tcn-2* Forward *Tcn-2* Reverse	GCA CCA GCA AGT GAC AAG TT ATC CAT CCA AGG TAA GAG ACG	210	210
27 -	*Dl1Dal10* Forward *Dl1Dal10* Reverse	ACA CCC AGA ATA GCC AAA GA GAA ATG GAC TTC AGT GGA GAG T	534	534
28 -	*Dl1Dal2* Forward *Dl1Dal2* Reverse	TCA ATG GCA GCG CCA ATG CCT TGA GCT GTG TAC TGC	606	606
29 -	*Dl1Dal8* Forward *Dl1Dal8* Reverse	TGG TGA AAG CAT ACA GAG AA GAA GCA GAG AAC AGA GTA AGC	520	520

Appendix 5

1 M Glycylglycine, pH 7.5

glycylglycine	66.05 gm
deionized distilled water	350 ml

Adjust pH to 7.5 with 6N NaOH. Complete the final volume to 500 ml with deionized distilled water. Store at 4°C.

Homogenizing buffer (0.25 M sucrose, 0.1 M glycylglycine (pH 7.5), 2 mM MgCl₂, 1 mM EDTA and 3 mM DTT)

sucrose	42.79 gm
1 M glycylglycine	50 ml
500 mM MgCl$_2$.6H$_2$O	2 ml
500 mM EDTA (pH 8.0)	1 ml
dithiothrietol (DTT)	0.23 gm

Adjust the final volume to 500 ml with deionized distilled water. Store at 4°C.

10% Lubrol

Dissolve 10 gm of Lubrol in 100 ml of deionized distilled water. Heat solution while stirring until it is completely dissolved. Store at 4°C.

10 mM IBMX

Dissolve 0.0222 gm of IBMX in a total volume of 10 ml of deionized distilled water. Add few drops of 6 N NaOH to get it in solution. Store in small aliquots at -20°C.

100 mM ATP

Dissolve 0.5511 gm of ATP in a final volume of 10 ml of deionized distilled water. Store in small aliquots at - 70°C.

1% Bovine serum albumin (BSA)

Dissolve 0.1 gm of BSA in a final volume of 10 ml of deionized distilled water. Store in small aliquots at -20°C.

0.1 M DTT

Dissolve 0.3084 gm of DTT in a final volume of 20 ml of deionized distilled water.

200 mM Creatine phosphate (CP)

Dissolve 0.5102 gm in a final volume of 10 ml of deionized distilled water. Store in small aliquots at -20°C.

Creatine phosphokinase (CPK)

Dissolve 1 mg in a final volume of 500 µl deionized distilled water. This solution is prepared fresh every time.

24 mM CaM (55,000 U/ mg solid, 66,000 U/mg protein)

Dissolve 0.1 mg in a final volume of 0.245 ml of deionized distilled water.

Bibliography

Abdel-Majid R. M., Leong W. L., Schalkwyk L. C., Smallman D. S., Wong S. T., Storm D. R., Fine A., Dobson M. J., Guernsey D. L., and Neumann P. E. (1998) Loss of adenylyl cyclase I activity disrupts patterning of mouse somatosensory cortex. *Nature Genet.* **19:** 289-291.

Abdel-Majid R. M., Willis B. S., Katsnelson A., Kind P. C., McKnight G. S., Neumann P. E. (1999) Involvement of protein kinase A in patterning of the mouse somatosensory cortex. Submitted to *Nature Neurosci.*

Agmon A., and Connors B. W. (1992) Correlation between intrinsic firing patterns and thalamocortical synaptic responses of neurons in mouse barrel cortex. *J. Neurosci.* **12:** 319-329.

Agmon A., and O'Dowd D. K. (1992) NMDA receptor-mediated currents are prominent in the thalamocortical synaptic response before maturation of inhibition. *J. Neurophysiol.* **68:** 345-349.

Agmon A., Yang L. T., Jones E. G., and O'Dowd D. K. (1995) Topological precision in the thalamic projection to neonatal mouse barrel cortex. *J. Neurosci.* **15:** 549-561.

Agmon A., Yang L. T., O'Dowd D. K., and Jones E. G. (1993) Organized growth of thalamocortical axons from the deep tier of terminations into layer IV of developing mouse barrel cortex. *J. Neurosci.* **13:** 5365-5382.

Aitken A. R., and Tork I. (1988) Early development of serotonin-containing neurons and pathways as seen in wholemount preparations of the fetal rat brain. *J. Comp. Neurol.* **274:** 32-47.

Akaneya Y., Tsumoto T., Kinoshita S., and Hatanaka H. (1997) Brain-derived neurotrophic factor enhances long-term potentiation in rat visual cortex. *J. Neurosci.* **17:** 6707-6716.

Akers R. M., and Killackey H. P. (1978) Organization of corticocortical connections in the parietal cortex of the rat. *J. Comp. Neurol.* **181:** 513-537.

Albers K. M., Wright D. E., and Davis B. M. (1994) Overexpression of nerve growth factor in epidermis of transgenic mice causes hypertrophy of the peripheral nervous system. *J. Neurosci.* **14:** 1422-1432.

Al-Ghoul, W. M. and Miller M. W. (1989) Migration of neurones to the trigeminal principal sensory nucleus of the rat. *Soc. Neurosci. Abstr.* **15:** 588.

Amieux P. S., Cummings D. E., Motamed K., Brandon E. P., Wailes L. A., Le K., Idzerda R. L., and McKnight G. S. (1997) Compensatory regulation of RIα protein levels in protein kinase A mutant mice. *J. Biol. Chem.* **272:** 3993-3998.

Angevine J. B. Jr. (1970) Time of neuron origin in the diencephalon of the mouse. An autoradiographic study. *J. Comp. Neurol.* **139:** 129-187.

Arakawa Y., Sendtner M., and Thoenen H. (1990) Survival effect of ciliary neurotrophic factor (CNTF) on chick embryonic motoneurons in culture: comparison with other neurotrophic factors and cytokines. *J. Neurosci.* **10:** 3507-3515.

Ardelt A. A., Flaris N. A., and Roth K. A. (1994) Neurotrophin-4 selectively promotes survival of striatal neurons in organotypic slice culture. *Brain Res.* **2:** 340-344.

Arvidsson J., Rice F. L., Fundin B. T., Albers K. M., Silos-Santiago I., Fagan A. M., Barbacid M., Ernfors P., and Davis B. M. (1995) Effects of NT-3 and TrkC manipulations on developing Merkel innervation in the mystacial pad of the mouse. *Soc. Neurosci. Abstr.* **21:** 1540.

Augustine G. J., Charlton M. P., and Smith S. J. (1987) Calcium action in synaptic transmitter release. *Ann. Rev. Neurosci.* **10:** 633-693.

Baier H., Bonhoeffer F. (1992) Axon guidance by gradients of a target-derived component. *Science* **255:** 472-475.

Bailey C. H., and Kandel E. R. (1993) Structural changes accompanying memory storage. *Annu. Rev. Physiol.* **55:** 397-426.

Bailey C. H., and Chen M. (1989) Structural plasticity at identified synapses during long term memory in Aplysia. *J. Neurobiol.* **20:** 356-372.

Bakalyar H. A., and Reed R. R. (1990) Identification of a specialized adenylyl cyclase that may mediate odorant detection. *Science* **250:** 1403-1406.

Bansal V. S., and Majerus P. W. (1990) Phosphatidylinositol-derived precursors and signals. *Ann. Rev. Cell Biol.* **6:** 41-67.

Barbacid M. (1995a) Neurotrophic factors and their receptors. *Curr. Opin. Cell. Biol.* **7:** 148-155.

Barbacid M. (1995b) Structural and functional properties of the Trk family of neurotrophin receptors. *Annu. N. Y. Acad. Sci.* **766:** 442-458.

Barbe M. F., and Levitt P. (1991) The early commitment of fetal neurons to the limbic cortex. *J. Neurosci.* **11:** 519-533.

Barbe M. F., and Levitt P. (1992) Attraction of specific thalamic input by cerebral grafts depends on the molecular identity of the implant. *Proc. Natl. Acad. Sci. U.S.A.* **89:** 3706-3710.

Barde Y. A. (1989) Trophic factors and neuronal survival. *Neuron* **2:** 1525-1534.

Barnstable C. J. (1993) Cyclic nucleotide-gated nonselective cation channels: a multifunctional gene family. *EXS.* **66:** 121-133.

Bates B., Rios M., Trumpp A., Chen C., Fan G., Bishop J. M., and Jaenisch R. (1999) Neurotrophin-3 is required for proper cerebellar development. *Nature Neurosci.* **2:** 115-117.

Bates C. A., and Killackey H. P. (1985) The organization of the neonatal rat's brainstem trigeminal complex and its role in the formation of central trigeminal patterns. *J. Comp. Neurol.* **240:** 265-287.

Bayer S. A., and Altman J. (1991) *Neocortical Development.* Raven Press, New York.

Beck K. D., Powell-Braxton L., Widmer H. R., Valverde J., and Hefti F. (1995) Igf1 gene disruption results in reduced brain size, CNS hypomyelination, and loss of hippocampal granule and striatal parvalbumin-containing neurons. *Neuron* **14:** 717-730.

Belford G. R., and Killackey H. P. (1979a) Vibrissae representation in subcortical trigeminal centers of the neonatal rat. *J. Comp. Neurol.* **183:** 305-321.

Belford G. R., and Killackey H. P. (1979b) The development of vibrissae representation in subcortical trigeminal centers of the neonatal rat. *J. Comp. Neurol.* **188:** 63-74.

Bennett M. K., and Kennedy M. B. (1987) Deduced primary structure of the β subunit of brain type II Ca^{2+}/ calmodulin-protein kinase determined by molecular cloning. *Proc. Natl. Acad. Sci. U.S.A.* **84:** 1794-1798.

Bennett M. K., Erondu N. E., and Kennedy M. B. (1983) Purification and characterization of a calmodulin-dependent protein kinase that is highly concentrated in brain. *J. Biol. Chem.* **258:** 12735-12744.

Bennett-Clarke C. A., Chiaia N. L., and Rhoades R. W. (1996) Thalamocortical afferents in rat transiently express high-affinity serotonin uptake sites. *Brain Res.* **733:** 301-306.

Bennett-Clarke C. A., Chiaia N. L., Crissman R. S., and Rhoades R. W. (1991) The source of the transient serotonergic input to the developing visual and somatosensory cortices in rat. *Neuroscience* **43**: 163-183.

Bennett-Clarke C. A., Lane R. D., and Rhoades R. W. (1995) Fenfluramine depletes serotonin from the developing cortex and alters thalamocortical organization. *Brain Res.* **702**: 255-260.

Bennett-Clarke C. A., Leslie M. J., Chiaia N. L., and Rhoades R. W. (1993) Serotonin 1B receptors in the developing somatosensory and visual cortices are located on thalamocortical axons. *Proc. Natl. Acad. Sci. U.S.A.* **90**: 153-157.

Bennett-Clarke C. A., Leslie M. J., Lane R. D., and Rhoades R. W. (1994) Effect of serotonin depletion on vibrissa-related patterns of thalamic afferents in the rat's somatosensory cortex. *J. Neurosci.* **14**: 7594-7607.

Benshalom G., White E. L. (1986) Quantification of thalamocortical synapses with spiny stellate neurons in layer IV of mouse somatosensory cortex. *J. Comp. Neurol.* **253**: 303-314.

Bernardo K. L., and Woolsey T. A. (1987) Axonal trajectories between mouse somatosensory thalamus and cortex. *J. Comp. Neurol.* **258**: 542-564.

Berninger B., and Poo M-m. (1996) Fast actions of neurotrophic factors. *Curr. Opin. Neurobiol.* **6**: 324-330.

Berry M. and Rogers A. W. (1965) The migration of neuroblasts in the developing cerebral cortex. *J. Anat.* **99**: 691-709.

Bliss T. V. P. and Collingridge G. L. A. (1993) A synaptic model for memory: Long term potentiation in the hippocampus. *Nature (London)* **361**: 31-39.

Blitzer R. D., Wong T., Nouranifar R., Iyengar R., and Landau E. M. (1995) Postsynaptic cAMP pathways gates early LTP in hippocampal CA1 region. *Neuron* **15**: 1403-1414.

Blöchl A., and Thoenen H. (1995) Characterization of nerve growth factor (NGF) release from hippocampal neurons: evidence for a constitutive and an unconventional sodium-dependent regulated pathway. *Eur. J. Neurosci.* **7**: 1220-1228.

Blöchl A., and Thoenen H. (1996) Localization of cellular storage compartments and sites of constitutive and activity-dependent release of nerve growth factor (NGF) in primary cultures of hippocampal neurons. *Mol. Cell. Neurosci.* **7**: 173-190.

Blue M. E., Erzurumlu R. S., and Jhaveri S. (1991) A comparison of pattern formation by thalamocortical and serotonergic afferents in the rat barrel field cortex. *Cereb. Cortex* **1:** 380-389.

Bonhoeffer T. (1996) Neurotrophins and activity-dependent development of the neocortex. *Curr. Opin. Neurobiol.* **6:** 199-126.

Bothwell M. (1995) Functional interactions of neurotrophins and neurotrophin receptors. *Ann. Rev. Neurosci.* **18:** 403-410.

Bouhelal R., Smounya L., and Bockaert J. (1988) 5-HT$_{1B}$ receptors are negatively coupled with adenylate cyclase in rat substania nigra. *Eur. J. Pharmacol.* **151:** 189-196.

Bourtchuladze R., Frenguelli B., Blendy J., Cioffi D., Schutz G., and Silva A. J. (1994) Deficient long-term memory in mice with a targeted mutation of the cAMP-responsive element-binding protein. *Cell* **79:** 59-68.

Brandon E. P., Gerhold K. A., Qi M., McKnight G. S., and Idzerda R. L. (1995a) Derivation of novel embryonic stem cell lines and targeting of cyclic AMP-dependent protein kinase genes. *Recent Prog. Horm. Res.* **50:** 403-408.

Brandon E. P., Logue S. F., Adams M. R., Qi M., Sullivan S. P., Matsumoto A. M., Dorsa D. M., Wehner J. M. McKnight G. S., and Izerda R. L. (1998) Defective motor behavior and neural gene expression in RIIβ-protein kinase A mutant mice. *J. Neurosci.* **18:** 3639-3649.

Brandon E. P., Zhuo M., Huang Y. Y., Qi M., Gerhold K. A., Burton K. A., Kandel E. R., Mcknight G. S., and Idzerda R. L. (1995b) Hippocampal long-term depression and depotentiation are defective in mice carrying a targeted disruption of the gene encoding the RIβ subunit of cAMP-dependent protein kinase. *Proc. Natl. Acad. Sci. U.S.A.* **92:** 8851-8855.

Braun S., Croizat B., Lagrange M. C., Warter J. M., and Poindron P. (1996) Neurotrophins increase motoneurons' ability to innervate skeletal muscle fibers in rat spinal cord--human muscle cocultures. *J. Neurol. Sci.* **136:** 17-23.

Brodmann K. (1909) Lokalisationslehre der Groshirnrinde in ihren Pricipen dargestellt aug Grund des Zeellen baue, Barth, Leipzig.

Brooks S. P. J., and Storey K. B. (1992) Bound and determined: A computer program for making buffers of defined ion concentrations. *Analytical Biochemistry* **201:** 119-126.

Brown M. C., Jansen J. K., and Van Essen D. (1976) Polyneuronal innervation of skeletal muscle in new-born rats and its elimination during maturation. *J. Physiol. (London)* **261:** 387-422.

Brunelli M., Castellucci V., and Kandel E. R. (1976) Synaptic facilitation and behavioral sensitization in Aplysia: possible role of serotonin and cyclic AMP. *Science* **194:** 1178-1181.

Brunet L. J., Gold G. H., and Ngai J. (1996) General anosmia caused by a targeted disruption of the mouse olfactory cyclic nucleotide-gated cation channel. *Neuron* **17:** 681-693.

Bruning G., and Liangos O. (1997) Transient expression of the serotonin transporter in the developing mouse thalamocortical system. *Acta. Histochem.* **99:** 117-121.

Buck J., Sinclair M. L., Schapal L., Cann M. J., and Levin L. R. (1999) Cytosolic adenylyl cyclase defines a unique signaling molecule in mammals. *Proc. Natl. Acad. Sci. U.S.A.* **96:** 79-84.

Burgin K. E., Waxham M. N., Rickling S., Westgate S., Mobley W. C., and Kelly P. T. (1990) In situ hybridization histochemistry of Ca^{2+}/calmodulin-dependent protein kinase in developing rat brain. *J. Neurosci.* **10:** 1788-1798.

Burke D. T., Carl G. F., and Olson M. V. (1987) Cloning of large segments of exogenous DNA into yeast by means of artificial chromosome vectors. *Science* **236:** 806-812.

Burton K. A., Johnson B. D., Hausken Z. E., Westenbrock R. E., Idzerda R. L., Scheuer T., Scott J. D., Catterall W. A., and McKnight G. S. (1997) Type II regulatory subunits are not required for the anchoring-dependent modulation of Ca^{2+} channel activity by cAMP-dependent protein kinase. *Proc. Natl. Acad. Sci. U.S.A.* **94:** 11067-10072.

Cabelli R. J., Hohn A., and Shatz C. J. (1995) Inhibition of ocular dominance column formation by infusion of NT-4/5 or BDNF. *Science* **267:** 1662-1666.

Cabelli R. J., Shelton D. L., Segal R. A., and Shatz C. J. (1997) Blockade of endogenous ligands of trkB inhibits formation of ocular dominance columns. *Neuron* **19:** 63-76.

Cadusseau J., and Roger M. (1985) Afferent projections to the superior colliculus in the rat, with special attention to the deep layers. *J. Hirnforsch* **26:** 667-681.

Cali J. J., Zwaagstra J. C., Mons N., Cooper D. M. F., and Krupinski J. (1994) Type VIII adenylyl cyclase: a Ca^{2+}/calmodulin-stimulated enzyme expressed in discrete regions of rat brain. *J. Biol. Chem.* **269:** 12190-12195.

Calia E., Persico A. M., Baldi A., and Keller F. (1998) BDNF and NT-3 applied in the whisker pad reverse cortical changes after peripheral deafferentation in neonatal rats. *Eur. J. Neurosci.* **10:** 3194-3200.

Calikoglu A. S., Gutierrez-Ospina G., D'Ercole A. J. (1996) Congenital hypothyroidism delays the formation and retards the growth of the mouse primary somatic sensory cortex (S1). *Neurosci. Lett.* **213:** 132-136.

Carter B. D., Dechant G., Frade J. M., Kaltschmidt C., Barde Y. A. (1996) Neurotrophins and their p75 receptor. *Cold Spring Harb. Symp. Quant. Biol.* **61:** 407-415.

Carvell G. E., and Simons D. J. (1988) Membrane potential changes in rat SmI cortical neurons evoked by controlled stimulation of mystacial vibrissae. *Brain Res.* **448:** 186-191.

Carvell G. E., and Simons D. J. (1990) Biometric analyses of vibrissal tactile discrimination in the rat. *J. Neurosci.* **10:** 2638-2648.

Cases O., Seif I., Grimsby J., Gaspar P., Chen K., Pournin S., Muller U., Aguet M., Babinet C., Shih J. C., and De Maeyer E. (1995) Aggressive behavior and altered amounts of brain serotonin and norepinephrine in mice lacking MAOA . *Science* **268:** 1763-1766.

Cases O., Vitalis T., Seif I., De Maeyer E., Sotelo C., Gaspar P. (1996) Lack of barrels in somatosensory cortex of Monoamine Oxidase A-deficient mice: role of a serotonin excess during the critical period. *Neuron* **16:** 297-307.

Castelluci V. F., Kandel E. R., Schwartz J. H., Wilson F. D., Nairn A. C., Greengard P. (1980) Intracellular injection of the catalytic subunit of cyclicAMP-dependent protein kinase simulates facilitation of transmitter release underlying behavioral sensitization in Aplysia. *Proc. Natl. Acad. Sci. U.S.A.* **77:** 7492-7496.

Castrén E., Zafra F., Thoenen H., and Lindholm D. (1992) Light regulates expression of brain-derived neurotrophic factor mRNA in rat visual cortex. *Proc. Natl. Acad. Sci. U.S.A.* **89:** 9444-9448.

Catalano S. M., Robertson R. T., and Killackey H. P. (1991) Early ingrowth of thalamocortical afferents to the neocortex of the prenatal rat. *Proc. Natl. Acad. Sci. U.S.A.* **88:** 2999-3003.

Catalano S. M., Robertson R. T., and Killackey H. P. (1996) Individual axon morphology and thalamocortical topography in developing rat somatosensory cortex. *J. Comp. Neurol.* **367:** 36-53.

Caviness V. S. Jr. (1975) Architectonic map of neocortex of the normal mouse. *J. Comp. Neurol.* **164**: 247-263.

Cellerino A., and Maffei L. (1996) The action of neurotrophins in the development and plasticity of the visual cortex. *Prog. Neurobiol.* **49**: 53-71.

Chao M. V. (1992) Neurotrophin receptors: a window into neuronal differentiation. *Neuron* **9**: 583-593.

Chapin J. K., Sadeq M., and Guise J. L. (1987) Corticocortical connections within the primary somatosensory cortex of the rat. *J. Comp. Neurol.* **263**: 326-346.

Chiaia N. L., Bauer W. R., Zhang S., King T. A., Wright P. C., Hobler S. C., and Freeman K. A. (1992a) Effects of neonatal transection of the infraorbital nerve upon the structural and functional organization of the ventral posteromedial nucleus in the rat. *J. Comp. Neurol.* **326**: 561-579.

Chiaia N. L., Bennett-Clarke C. A., and Rhoades R. W. (1992b) Differential effects of peripheral damage on vibrissa-related patterns in trigeminal nucleus principalis, subnucleus interpolaris, and subnucleus caudalis. *Neuroscience* **49**: 141-156.

Chiaia N. L., Bennett-Clarke C. A., Crissman R. S., Zhang S., and Rhoades R. W. (1997) Long-term effects of neonatal axoplasmic transport attenuation on the organization of the rat's trigeminal system. *J. Comp. Neurol.* **381**: 219-229.

Chiaia N. L., Bennett-Clarke C. A., Crissman R. S., Zheng L., Chen M., and Rhoades R. W. (1996) Effect of neonatal axoplasmic transport attenuation in the infraorbital nerve on vibrissae-related patterns in the rat's brainstem, thalamus and cortex. *Eur. J. Neurosci.* **8**: 1601-1612.

Chiaia N. L., Bennett-Clarke C. A., Eck M., White F. A., Crissman R. S., and Rhoades R. W. (1992c) Evidence for prenatal competition among the central arbors of trigeminal primary afferent neurons. *J. Neurosci.* **12**: 62-76.

Chiaia N. L., Fish S. E., Bauer W. R., Bennett-Clarke C. A., and Rhoades R. W. (1992d) Postnatal blockade of cortical activity by tetrodotoxin does not disrupt the formation of vibrissa-related patterns in the rat's somatosensory cortex. *Dev. Brain Res.* **66**: 244-250.

Chiaia N. L., Fish S. E., Bauer W. R., Figley B. A., Eck M., Bennett-Clarke C. A., and Rhoades R. W. (1994) Effects of postnatal blockage of cortical activity with tetrodotoxin upon lesion-induced reorganization of vibrissae-related patterns in the somatosensory cortex of rat. *Dev. Brain Res.* **79**: 301-306.

Chiaia N. L., Rhoades R. W., Bennett-Clarke C. A., Fish S. E., and Killackey H. P. (1991a) Thalamic processing of vibrissal information in the rat. I. Afferent input to the medial ventral posterior and posterior nuclei. *J. Comp. Neurol.* **314:** 201-216.

Chiaia N. L., Rhoades R. W., Fish S. E., and Killackey H. P. (1991b) Thalamic processing of vibrissal information in the rat: II. Morphological and functional properties of medial ventral posterior nucleus and posterior nucleus neurons. *J. Comp. Neurol.* **314:** 217-236.

Chinkers M., and Garbers D. L. (1989) The protein kinase domain of the ANP receptor is required for signaling. *Science* **245:** 1392-1394.

Chmielowska J., Carvell G. E., and Simons D. J. (1988) Spatial organization of corticothalamic cells in the rat SmI vibressa/barrel cortex *Soc. Neurosci. Abstr.* **14:** 222.

Chmielowska J., Carvell G. E., and Simons D. J. (1989) Spatial organization of thalamocortical and corticothalamic projection systems in the rat SmI barrel cortex. *J. Comp. Neurol.* **285:** 325-338.

Choi E. J., Wong S. T., Hinds T. J., and Storm D. R. (1992) Calcium and muscarinic agonist stimulation of type I adenylyl cyclase in whole cells. *J. Biol. Chem.* **267:** 12440-12442.

Chun L. L., Patterson P. H. (1977) Role of nerve growth factor in the development of rat sympathetic neurons in vitro. I. Survival, growth, and differentiation of catecholamine production. *J. Cell. Biol.* **75:** 694-704.

Cline H. T., Debski E. A., and Constantine-Paton M. (1987) N-methyl-D-aspartate receptor antagonist desegregates eye-specific stripes. *Proc. Natl. Acad. Sci. U.S.A.* **84:** 4342-4345.

Coburn C. M., and Bargmann C. I. (1996) A putative cyclic nucleotide-gated channel is required for sensory development and function in *C. elegans. Neuron* **17:** 695-706.

Cohen P. (1988) Protein phosphorylation and hormone action. *Proc. R. Soc. Lond. (B)* **234:** 115-144.

Cohen-Cory S., and Fraser S. E. (1995) Effects of brain-derived neurotrophic factor on optic axon branching and remodelling in vivo. *Nature* **378:** 192-196.

Cohen-Cory S., Dreyfus C. F., and Black I. B. (1991) NGF and excitatory neurotransmitters regulate survival and morphogenesis of cultured cerebellar Purkinje cells. *J. Neurosci.* **11:** 462-471.

Conover J. C., Erickson J. T., Katz D. M., Bianchi L. M., Poueymirou W. T., McClain J., Pan L., Helgren M., Ip N. Y., Boland P., Friedman B., Wiegand S., Vejsada R., Kato A. C., DeChlara T. M., and Yancopoulos G. D. (1995) Neuronal deficits, not involving motor neurons, in mice lacking BDNF and/or NT-4. *Nature* (*London*) **375:** 235-238.

Constantine-Paton M., Cline H. T., and Debski E. (1990) Patterned activity, synaptic convergence, and the NMDA receptor in developing visual pathways. *Annu. Rev. Neurosci.* **13:** 129-154.

Cooper D. M. F., Mons N., and Karpen J. W. (1995) Adenylyl cyclases and the interaction between calcium and cAMP signalling. *Nature* (*London*) **374:** 421-424.

Cooper D. M., Karpen J. W., Fagan K. A., and Mons N. E. (1998) Ca^{2+}-sensitive adenylyl cyclases. *Adv. Second Messenger Phosphoprotein Res.* **32:** 23-51.

Cooper N. G., Steindler D. A. (1986) Monoclonal antibody to glial fibrillary acidic protein reveals a parcellation of individual barrels in the early postnatal mouse somatosensory cortex. *Brain Res.* **380:** 341-348.

Copeland N. G., Gilbert D. J., Jenkins N. A., Nadeau J. H., Eppig J. T., Maltais L. J., Miller J. C., Dietrich W. F., Steen R. G., and Lincoln S. E. (1993) Genome Maps IV. *Science* **262:** 67-82.

Corsi P. (1991) The Enchanted Loom: Chapters in the History of Neuroscience. Corsi P. (ed.) Oxford University Press, New York.

Cox E. C., Muller B., and Bonhoeffer F. (1990) Axonal guidance in the chick visual system: posterior tectal membranes induce collapse of growth cones from the temporal retina. *Neuron* **4:** 31-37.

Cragg B. G. (1975) Absence of barrels and disorganization of thalamic afferent distribution in the sensory cortex of reeler mice. *Exp. Neurol.* **49:** 858-862.

Crair M. C., and Malenka R. C. (1995) A critical period for long-term potentiation at thalamocortical synapses. *Nature* (*London*) **375:** 325-328.

Crossin K. L., Hoffman S., Tan S. S., and Edelman G. M. (1989) Cytotactin and its proteoglycan ligand mark structural and functional boundaries in somatosensory cortex of the early postnatal mouse. *Dev. Biol.* **136:** 381-392.

Crowley C., Spencer S. D., Nishimura M. C., Chen K. S., Pitts-Meek S., Armanini M. P., Ling L. H., MacMahon S. B., Shelton D. L., Levinson A. D., and Phillips H. (1994) Mice lacking nerve growth factor display perinatal loss of sensory and sympathetic neurons yet develop basal forebrain cholinergic neurons. *Cell* **76:** 1001-1011.

Cummings D. E., Brandon E. P., Planas J. A., Motamed K., Idzerda R. L., and McKnight G. S. (1996) Genetically lean mice result from targeted disruption of the RII beta subunit of protein kinase A. *Nature (London)* **382:** 622-626.

Curcio C. A., and Coleman P. D. (1982) Stability of neuron number in cortical barrels of aging mice. *J. Comp. Neurol.* **212:** 158-172.

D'Amato R. J., Blue M. E., Largent B. L., Lynch D. R., Ledbetter D. J., Molliver M. E., and Snyder S. H. (1987) Ontogeny of the serotonergic projection to rat neocortex: transient expression of a dense innervation to primary sensory areas. *Proc. Natl. Acad. Sci. U.S.A.* **84:** 4322-4326.

Dash P. K., Hochner B., and Kandel E. R.(1990) Injection of the cAMP-responsive element into the nucleus of Aplysia sensory neurons blocks long-term facilitation. *Nature (London)* **345:** 718-721.

Davies A. M. (1988a) Role of neurotrophic factors in development. *Trends. Genet.* **4:** 139-143.

Davies A. M. (1988b) The trigeminal system: An advantageous experimental model for studying neuronal development. *Development* **103:** 175-183.

Davies A. M. (1994) The role of neurotrophins in the developing nervous system. *J. Neurobiol.* **25:** 1334-1348.

Davies A. M. (1997) Studies of neurotrophin biology in the developing trigeminal system. *J. Anat.* **191:** 483-491.

Davies A. M., Bandtlow C., Heumann R., Korsching S., Rohrer H., and Thoenen H. (1987) Timing and site of nerve growth factor synthesis in developing skin in relation to innervation and expression of the receptor. *Nature (London)* **326:** 353-358.

Davies A., and Lumsden A. (1984) Relation of target encounter and neuronal death to nerve growth factor responsiveness in the developing mouse trigeminal ganglion. *J. Comp. Neurol.* **223:** 124-137.

Dawson D. R., and Killackey H. P. (1985) Distinguishing topography and somatotopy in the thalamocortical projections of the developing rat. *Brain Res.* **349:** 309-313.

Dawson D. S., Murray A. W., and Szostak J. W. (1986) An alternative pathway for meiotic chromosome segregation in yeast. *Science* **234:** 713-717.

DeCamilli P., Harris S. M. Jr., Huttner W. B. and Greengard P. (1983) Synapsin I (protein I) a nerve terminal-specific phosphoprotein. II. Its specific association with synaptic vesicles demonstrated by immunocytochemistry in agarose-embedded synaptosomes. *J. Cell. Biol.* **96:** 1355-1373.

Dechant G., Barde Y. A. (1997) Signalling through the neurotrophin receptor p75NTR. *Curr. Opin. Neurobiol.* **7:** 413-418.

Dechant G., Rodriguez-Tebar A., Barde Y. A. (1994) Neurotrophin receptors. *Prog. Neurobiol.* **42:** 347-352.

Deckwerth T. L., and Johnson E. M. Jr. (1993) Neurotrophic factor deprivation-induced death. *Ann. N. Y. Acad. Sci.* **679:** 121-131.

Defer N., Marinx O., Stengel D., Danisova A., Iourgenko V., Matsouka I., Caput D., Hanoune J. (1994) Molecular cloning of the human type VIII adenylyl cyclase. *FEBS Lett.* **351:** 109-113.

Donoghue M. J., and Rakic P. (1999) Molecular evidence for the early specification of presumptive functional domains in the embryonic primate cerebral cortex. *J. Neurosci.* **19:** 5967-5979.

Dörfl J. (1985) The innervation of the mystacial vibrissae of the white mouse. A topographical study. *J. Anat. (London)* **142:** 173-184.

Drescher M. J., Khan K. M., Beisel K. W., Karadaghy A. A., Hatfield J. S., Kim S. Y., Drescher A. J., Lasak J. M., Barretto R. L., Shakir A. H., and Drescher D. G. (1997) Expression of adenylyl cyclase type I in cochlear inner hair cells. *Mol. Brain Res.* **45:** 325-330.

Dugich-Djordjevic M. M., Ohsawa F., and Hefti F. (1993) Transient elevation in catalytic trkB mRNA during postnatal development of the rat brain. *Neuroreport* **4:**1091-1094.

Durand G. M., Kovalchuk Y., and Konnerth A. (1996) Long-term potentiation and functional synapse induction in developing hippocampus. *Nature* **381:** 71-75.

Durham D., and Woolsey T. A. (1978) Acute whisker removal reduces neuronal activity in barrels of mouse SmI cortex. *J. Comp. Neurol.* **178:** 629-644.

Durham D., and Woolsey T. A. (1984) Effects of neonatal whisker lesions on mouse central trigeminal pathways. *J. Comp. Neurol.* **223:** 424-447.

Edelhoff S., Villacres E. C., Storm D. R., and Disteche C. M. (1995) Mapping of adenylyl cyclase genes type I, II, III, IV, V and VI in mouse. *Mammal. Genome* **6:** 111-113.

Ernfors P., Lee K. F., and Jaenisch R. (1994) Mice lacking brain-derived neurotrophic factor develop with sensory deficits. *Nature (London)* **368:** 147-150.

Ernfors P., Lee K. F., Kucera J., and Jaenisch R. (1994) Lack of neurotrophin-3 leads to deficiencies in the peripheral nervous system and loss of limb proprioceptive afferents. *Cell* **77:** 503-512.

Ernfors P., Wetmore C., Olson L., and Persson H. (1990) Identification of cells in rat brain and peripheral tissues expressing mRNA for members of the nerve growth factor family. *Neuron* **5:** 511-526.

Erondu N. E., and Kennedy M. B. (1985) Regional distribution of type II Ca^{2+}/Calmodulin-dependent protein kinase in rat brain. *J. Neurosci.* **5:** 3270-3277.

Erzurumlu R. S. and Jhaveri S. (1992) Emergence of connectivity in the embryonic rat parietal cortex. *Cereb. Cortex* **2:** 336-352.

Erzurumlu R. S., and Jhaveri S. (1990) Thalamic axons confer a blueprint of the sensory periphery onto the developing rat somatosensory cortex. *Dev. Brain Res.* **56:** 229-234.

Erzurumlu R. S., and Jhaveri S. (1992) Trigeminal ganglion cell processes are spatially ordered prior to the differentiation of the vibrissa pad. *J. Neurosci.* **12:** 3946-3955.

Erzurumlu R. S., and Killackey H. P. (1980) Diencephalic projections of the subnucleus interpolaris of the brainstem trigeminal complex in the rat. *Neuroscience* **5:** 1891-1901.

Erzurumlu R. S., and Killackey H. P. (1983) Development of order in the rat trigeminal system. *J. Comp. Neurol.* **213:** 365-380.

Erzurumlu R. S., Bates C. A., and Killackey H. P. (1980) Differential organization of thalamic projection cells in the brain stem trigeminal complex of the rat. *Brain Res.* **198:** 427-433.

Fabri M., and Burton H. (1991) Topography of connections between primary somatosensory cortex and posterior complex in rat: a multiple fluorescent tracer study. *Brain Res.* **538:** 351-357.

Fariñas I., Jones K. R., Backus C., Wang X. Y., and Reichardt L. F. (1994) Severe sensory and sympathetic deficits in mice lacking neurotrophin-3. *Nature* **369:** 658-661.

Fawcett J. W. and O'Leary D. D. M. (1985) The role of electrical activity in the formation of topographic maps in the nervous system. *Trends. Neurosci.* **8:** 201-206.

Feany M. B., and Quinn W. G. (1995) A neuropeptide gene defined by the Drosophila memory mutant amnesiac. *Science* **268:** 869-873.

Feinstein P. G., Schrader K. A., Bakalyar H. A., Tang W-J., Krupinski J., Gilman A. G. and Reed R. R. (1991) Molecular cloning and characterization of a Ca^{2+}/calmodulin-insensitive adenylyl cyclase from rat brain. *Proc. Natl. Acad. Sci. U.S.A.* **88:** 10173-10177.

Feldman D. E., Nicoll R. A., Malenka R. C., and Isaac J. T. (1998) Long-term depression at thalamocortical synapses in developing rat somatosensory cortex. *Neuron* **21:** 347-357.

Feldman M. L., and Peters A. A. (1974) A study of barrels and pyramidal dendritic clusters in the cerebral cortex. *Brain Res.* **77:** 55-76.

Feldman S. G., and Kruger L. (1980) An axonal transport study of the ascending projection of medial lemniscal neurons in the rat. *J. Comp. Neurol.* **192:** 427-454.

Figurov A., Pozzo-Miller L. D., Olafsson P., Wang T., and Lu B. (1996) Regulation of synaptic responses to high-frequency stimulation and LTP by neurotrophins in the hippocampus. *Nature* **381:** 706-709.

Firestein S. and Zufall F. (1994) The cyclic nucleotide gated channel of olfactory receptor neurons. *Semin. Cell Biol.* **5:** 39-46.

Forbes D. J., and Welt C. (1981) Neurogenesis in the trigeminal ganglion of the albino rat: a quantitative autoradiographic study. *J. Comp. Neurol.* **199:** 133-147.

Fox K. and Daw N. W. (1993) Do NMDA receptors have a critical function in visual cortical plasticity? *Trends. Neurosci.* **16:** 116-122.

Fox K., Sato H., and Daw N. (1989) The location and function of NMDA receptors in cat and kitten visual cortex. *J. Neurosci.* **9:** 2443-2454.

Fox K., Sclaggar B. L., Glazewski S., and O'Leary D. D. M. (1996) Glutamate receptor blockade at cortical synapses disrupts development of thalamocortical and columnar organization in somatosensory cortex. *Proc. Natl. Acad. Sci. U.S.A.* **93:** 5584-5589.

Friedman W. J., Black I. B., and Kaplan D. R. (1998) Distribution of the neurotrophins brain-derived neurotrophic factor, neurotrophin-3, and neurotrophin-4/5 in the postnatal rat brain: an immunocytochemical study. *Neuroscience* **84:** 101-114.

Fujimiya M., Kimura H., and Maeda T. (1986) Postnatal development of serotonin nerve fibers in the somatosensory cortex of mice studied by immunohistochemistry. *J. Comp. Neurol.* **246:** 191-201.

Fujita S. (1963) The matrix cell and cytogenesis in the developing central nervous system. *J. Comp. Neurol.* **120:** 37-42.

Fukunaga K., Goto S., and Miyamoto E. (1988) Immunohistochemical localization of Ca^{2+}/calmodulin dependent protein kinase II in rat brain. *J. Neurochem.* **51:** 1070-1078.

Fundin B. T., Silos-Santiago I., Ernfors P., Fagan A. M., Aldskogius H., DeChiara T. M., Phillips H. S., Barbacid M., Yancopoulos G. D., and Rice F. L. (1997) Differential dependency of cutaneous mechanoreceptors on neurotrophins, trk receptors, and P75 LNGFR. *Dev. Biol.* **190:** 94-116.

Gao B., and Gilman A. G. (1991) Cloning and expression of a widely distributed (type IV) adenylyl cyclase. *Proc. Natl. Acad. Sci. U.S.A.* **88:** 10178-10182.

Gibson J. M., and Welker W. I. (1983) Quantitative studies of stimulus coding in first-order vibrissa afferents of rats. 2. Adaptation and coding of stimulus parameters. *Somatosens. Mot. Res.* **1:** 95-117.

Gilman A. G. (1987) G proteins: transducers of receptor-regenerated signals. *Ann. Rev. Biochem.* **56:** 615-649.

Gilman A. G. (1989) G proteins and regulation of adenylyl cyclase. *JAMA* **262:** 1819-1825.

Gilman A. G. (1995) G proteins and regulation of adenylate cyclase (Nobel Lecture). *Biosci. Rep.* **15:** 65-97.

Glatt C. E., and Snyder S. H. (1993) Cloning and expression of an adenylyl cyclase localized to the corpus striatum. *Nature* **61:** 536-538.

Glazewski S., Chen C-M., Silva A., and Fox K. (1996) Requirement for α-CaMKII in experience-dependent plasticity of the barrel cortex. *Science* **272:** 421-423.

Goldenring J. R., McGuire J. S. Jr., and DeLorenzo R. J. (1984) Identification of the major postsynaptic density protein as homologous with the major calmodulin-binding subunit of a calmodulin-dependent protein kinase. *J. Neurochem.* **42:** 1077-1084.

Gomperts S. N., Rao A., Craig A. M., Malenka R. C., and Nicoll R. A. (1998) Postsynaptically silent synapses in single neuron cultures. *Neuron* **21:** 1443-1451.

Goodman C. S., and Shatz C. J. (1993) Developmental mechanisms that generate precise patterns of neuronal connectivity. *Cell* **72:** 77-98.

Gottlieb D. I., Rock K., and Glaser L. (1976) A gradient of adhesive specificity in developing avian retina. *Proc. Natl. Acad. Sci. U.S.A.* **73:** 410-414.

Gottschaldt K. M., Iggo A., and Young D. W. (1973) Functional characteristics of mechanoreceptors in sinus hair follicles of the cat. *J. Physiol. (London)* **235:** 287-315.

Götz R., Köster R., Winkler C., Raulf F., and Lottspeich F. (1994) Neurotrophin-6 is a new member of the nerve growth factor family. *Nature (London)* **372:** 266-269.

Green E. L. (1981) *Genetics and Probability in Animal Breeding Experiments.* MacMillan Press, London.

Greenough W. T., and Chang F. L. (1988) Dendritic pattern formation involves both oriented regression and oriented growth in the barrels of mouse somatosensory cortex. *Brain Res.* **471:** 148-152.

Gundersen R. W., and Barrett J. N. (1979) Neuronal chemotaxis: chick dorsal-root axons turn toward high concentrations of nerve growth factor. *Science* **206:** 1079-1080.

Gutierrez-Ospina G., Calikoglu A. S., Ye P., and D'Ercole A. J. (1996) In vivo effects of insulin-like growth factor-I on the development of sensory pathways: analysis of the primary somatic sensory cortex (S1) of transgenic mice. *Endocrinology* **137:** 5484-5492.

Hahnenberger K. M., Baum M. P., Polizzi C. M., Carbon J., and Clarke L. (1989) Construction of functional artificial minichromosomes in the fiddion yeast Achizosaccharomyces pombe. *Proc. Natl. Acad. Sci. U.S.A.* **86:** 577-581.

Haldi M. L., Strickland C., Lim P., Van Berkel V., Chen X., Noya D., Korenberg J. R., Husain Z., Miller J., and Lander E. S. (1996) A comprehensive large-insert yeast artificial chromosome library for physical mapping of the mouse genome. *Mammalian Genome* **7:** 767-769.

Hamburger V., and Levi-Montalcini R. (1949) Proliferation, differentiation and degeneration in the spinal ganglia of the chick embryo under normal and experimental conditions. *J. Exp. Zool.* **111:** 457-501.

Hamburger V., Brunso-Bechtold J. K., and Yip J. W. (1981) Neuronal death in the spinal ganglia of the chick embryo and its reduction by nerve growth factor. *J. Neurosci.* **1:** 60-72.

Hannan A. J., Blakemore C., Shin H-S., and Kind P. (1998a) Phospholipase C-β1 is required for normal development of barrels in mouse somatosensory cortex. *Soc. Neurosci. Abstr.* **24:** 59.

Hannan A. J., Kind P. C., and Blakemore C. (1998b) Phospholipase C-β1 expression correlates with neuronal differentiation and synaptic plasticity in rat somatosensory cortex. *Neuropharmacology* **37:** 593-605.

Hardie D. G. (1990) *Biochemical Messengers: Hormones, Neurotransmitters and Growth Factors.* Chapman and Hall Press, London.

Harris R. M., and Woolsey T. A. (1981) Dendritic plasticity in mouse barrel cortex following postnatal vibrissa follicle damage. *J. Comp. Neurol.* **196:** 357-376.

Harris R. M., and Woolsey T. A. (1983) Computer-assisted analyses of barrel neuron axons and their putative synaptic contacts. *J. Comp. Neurol.* **220:** 63-79.

Harris W. A. (1980) The effects of eliminating impulse activity on the development of the retinotectal projection in salamanders. *J. Comp. Neurol.* **194:** 303-317.

Harris W. A. (1984) Axonal pathfinding in the absence of normal pathways and impulse activity. *J. Neurosci.* **4:** 1153-1162.

Hartikka J., and Hefti F. (1988) Comparison of nerve growth factor's effects on development of septum, striatum, and nucleus basalis cholinergic neurons in vitro. *J. Neurosci. Res.* **21:** 352-364.

Hashimoto E., Frolich L., Ozawa H., Saito T., Maurer K., Boning J., Takahata N., Riederer P. (1998) Reduced immunoreactivity of type I adenylyl cyclase in the postmortem brain of alcoholics. *Alcohol Clin. Exp. Res.* **22:** 88S-92S.

Hawkins R. D., Kandel E. R., and Siegelbaum S. A. (1993) Learning to modulate transmitter release: themes and variations in synaptic plasticity. *Ann. Rev. Neurosci.* **16:** 625-665.

Hayashi H. (1980) Distribution of vibrissae afferent fiber collaterals in the trigeminal nuclei as revealed by intra-axonal injection of horseradish peroxidase. *Brain Res.* **183:** 442-446.

Hellevuo K., Yushimura M., Mons N., Hoffman P. L., Cooper D. M. F., and Tabakoff B. (1995) The characterization of a novel human adenylyl cyclase which is present in brain and other tissues. *J. Biol. Chem.* **270:** 11581-11589.

Henderson T. A., Johnson E. M. Jr, Osborne P. A., and Jacquin M. F. (1994) Fetal NGF augmentation preserves excess trigeminal ganglion cells and interrupts whisker-related pattern formation. *J. Neurosci.* **14:** 3389-3403.

Henderson T. A., Mosconi T. M., Foschini D. R., Silos-Santiago I., Barbacid M., and Jacquin M. F. (1995) Whisker-related patterning in the cerebral cortex of trkA, trkB, trkC knockout mice. *Soc. Neurosci. Abstr.* **21:** 279.

Henderson T. A., Rhoades R. W., Bennett-Clarke C. A., Osborne P. A., Johnson E. M., Jacquin M. F. (1993) NGF augmentation rescues trigeminal ganglion and principalis neurons, but not brainstem or cortical whisker patterns, after infraorbital nerve injury at birth. *J. Comp. Neurol.* **336:** 243-260.

Henderson T. A., Woolsey T. A., and Jacquin M. F. (1992) Infraorbital nerve blockade from birth does not disrupt central trigeminal pattern formation in the rat. *Dev. Brain Res.* **66:** 146-152.

Hersch S. M., and White E. L. (1981) Thalamocortical synapses with corticothalamic projection neurons in mouse SmI cortex: electron microscopic demonstration of a monosynaptic feedback loop. *Neurosci. Lett.* **24:** 207-210.

Higashi S., Crair M. C., Kurotani T., Inokawa H., and Toyama K. (1999) Altered spatial patterns of functional thalamocortical connections in the barrel cortex after neonatal infraorbital nerve cut revealed by optical recording. *Neuroscience* **91:** 439-452.

Hoffman C. S., and Winston F. (1987) A ten-minute DNA preparation from yeast efficiently releases autonomous plasmids for transformation of *Escherichia coli*. *Gene* **57:** 267-272.

Hohmann C. F., Hamon R., Batshaw M. L. and Coyle J. T. (1988) Transient postnatal elevation of serotonin levels in mouse neocortex. *Dev. Brain Res.* **43:** 163-166.

Horton H. L., and Levitt P. (1988) A unique membrane protein is expressed on early developing limbic system axons and cortical targets. *J. Neurosci.* **8:** 4653-4661.

Hubel D. H. and Wiesel T. N. (1970) The period of susceptibility to the physiological effects of unilateral eye closure in kittens. *J. Physiol. (London)* **206:** 419-436.

Hubel D. H., and Wiesel T. N. (1963) Shape and arrangement of columns in cat's striate cortex. *J. Physiol. (London)* **165:** 559-568.

Hubel D. H., Wiesel T. N., and LeVay S. (1977) Plasticity of ocular dominance columns in the monkey striate cortex. *Phil. Trans. R. Soc. Lond.* (B) **278:** 377-409.

Huntley G. W., and Benson D. L. (1999) Neural (N)-cadherin at developing thalamocortical synapses provides an adhesion mechanism for the formation of somatotopically organized connections. *J. Comp. Neurol.* **407:** 453-471.

Huttner W. B., Sciebler W., Greengard P., and DeCamilli P. (1983) Synapsin I (protein I), a nerve terminal-specific phosphoprotein. III. Its association with synaptic vesicles studied in a highly purified synaptic vesicle preparation. *J. Cell. Biol.* **96:** 1374-1388.

Hyman C., Juhasz M., Jackson C., Wright P., Ip N. Y., and Lindsay R. M. (1994) Overlapping and distinct actions of the neurotrophins BDNF, NT-3, and NT-4/5 on cultured dopaminergic and GABAergic neurons of the ventral mesencephalon. *J. Neurosci.* **14:** 335-347.

Ibáñez C. F. (1994) Structure-function relationships in the neurotrophin family. *J. Neurobiol.* **25:** 1349-1361.

Ibáñez C. F., Ernfors P., Timmusk T., Ip N. Y., Arenas E., Yancopoulos G. D., and Persson H. (1993) Neurotrophin-4 is a target-derived neurotrophic factor for neurons of the trigeminal ganglion. *Development* **117:** 1345-1353.

Ikeda K., Araki K., Takayama C., Inoue Y., Yagi T., Aizawa S., and Mishina M. (1995) Reduced spontaneous activity of mice defective in the epsilon 4 subunit of the NMDA receptor channel. *Mol. Brain Res.* **33:** 61-71.

Ip N. Y., and Yancopoulos G. D. (1996) The neurotrophins and CNTF: two families of collaborative neurotrophic factors. *Annu. Rev. Neurosci.* **19:** 491-515.

Isaac J. T., Crair M. C., Nicoll R. A., and Malenka R. C. (1997) Silent synapses during development of thalamocortical inputs. *Neuron* **18:** 269-280.

Isaac J. T., Nicoll R. A., and Malenka R. C. (1995) Evidence for silent synapses: implications for the expression of LTP. *Neuron* **15:** 427-434.

Ishikawa Y., Katsushika S., Chen L., Halnon L., Kawabe J-I., and Homcy C. J. (1992) Isolation and characterization of a novel cardiac adenylyl cyclase cDNA. *J. Biol. Chem.* **267:** 13553-13557.

Ito M. (1995) Barrelfield of the prenatally X-irradiated rat somatosensory cortex: a histochemical and electrophysiological study. *J. Comp. Neurol.* **352:** 248-262.

Iwasato T., Chen D. F., Erzurumulu R. S., Sasaoka T., and Tonegawa S. (1996) Disruption of whisker-specific patterns in the somatosensory cortex and subcortical areas of the rescued NMDAR1 knockout mice. *Soc. Neurosci. Abstr.* **22:** 725.

Iwasato T., Erzurumlu R. S., Huerta P. T., Chen D. F., Sasaoka T., Ulupinar E., and Tonegawa S. (1997) NMDA receptor-dependent refinement of somatotopic maps. *Neuron* **19:** 1201-1210.

Iyengar R. (1993) Molecular and functional diversity of mammalian Gs-stimulated adenylyl cyclases. *FASEB J.* **7**: 768-775.

Jacquin M. F., Renehan W. E., Klein B. G., Mooney R. D., and Rhoades R. W. (1986) Functional consequences of neonatal infraorbital nerve section in rat trigeminal ganglion. *J. Neurosci.* **6**: 3706-3720.

Jeanmonod D., Rice F. L., and Van der Loos H. (1981) Mouse somatosensory cortex: alterations in the barrelfield following receptor injury at different early postnatal ages. *Neuroscience* **6**: 1503-1535.

Jensen K. F., and Killackey H. P. (1987a) Terminal arbors of axons projecting to the somatosensory cortex of the adult rat. I. The normal morphology of specific thalamocortical afferents. *J. Neurosci.* **7**: 3529-3543.

Jensen K. F., Killackey H. P. (1978b) Terminal arbors of axons projecting to the somatosensory cortex of the adult rat. II. The altered morphology of thalamocortical afferents following neonatal infraorbital nerve cut. *J. Neurosci.* **7**: 3544-3553.

Jhaveri S, Erzurumlu R. S., Laywell E. D., Steindler D. A., Albers K. M., Davis B. M. (1996) Excess nerve growth factor in the periphery does not obscure development of whisker-related patterns in the rodent brain. *J. Comp. Neurol.* **374**: 41-51.

Jhaveri S., Erzurumlu R. S., and Crossin K. (1991) Barrel construction in rodent neocortex: role of thalamic afferents versus extracellular matrix molecules. *Proc. Natl. Acad. Sci. U.S.A.* **88**: 4489-4493.

Jhaveri S., Erzurumlu R. S., Chiaia N., Kumar T. R., and Matzuk M. M. (1998) Defective whisker follicles and altered brainstem patterns in activin and follistatin knockout mice. *Mol. Cell. Neurosci.* **12**: 206-219.

Johnson R. A., and Sutherland E. W. (1973) Detergent-dispersed adenylate cyclase from rat brain. *J. Biol. Chem.* **248**: 5114-51121.

Jones K. R., Farinas I., Backus C., and Reichardt L. F. (1994) Targeted disruption of the BDNF gene perturbs brain and sensory neuron development but not motor neuron development. *Cell* **76**: 989-999.

Kaas J. H. (1983) What, if anything, is S-I? The organization of the "first somatosensory area" of cortex. *Physiol. Rev.* **63**: 206-231.

Kaas J. H. (1990) The somatosensory system In: The Human Nervous System. Paxinos G. (ed.) Academic Press, New York, pp: 813-844.

Kaas J. H., and Pons T. P. (1988) The somatosensory system of primates. In: *Comparative Primate Biology*. Steklis (ed.) Vol. 4: Neurosciences Alan R. Liss Inc., New York, pp: 421-468.

Kahn C. R. (1976) Membrane receptors for hormones and neurotransmitters. *J. Cell. Biol.* **70**: 261-286.

Kang H., and Schuman E. M. (1995) Long-lasting neurotrophin-induced enhancement of synaptic transmission in the adult hippocampus. *Science* **267**: 1658-1662.

Kang H., Welcher A. A., Shelton D. and Schuman E. M. (1997) Neurotrophins and time different roles for TrkB signalling in hippocampal long-term potentiation. *Neuron* **19**: 653-664.

Karls U., Muller U., Gilbert D. J., Copeland N. G., Jenkins, and Harbers, K. (1992) Structure, expression, and chromosome location of the gene for the β subunit of brain-specific Ca^{2+}/Calmodulin-dependent protein kinase II identified by transgene integration in an embryonic lethal mouse mutant. *Mol. Cell. Biol.* **12**: 3644-3652.

Katsushika S., Chen L., Kawabe J. I., Nilakantan R., Halnon N. J., Homcy C. J., Ishikawa Y. (1992) Cloning and characterization of a sixth adenylyl cyclase isoform: type V and type VI constitute a subgroup within the mammalian adenylyl cyclase family. *Proc. Natl. Acad. Sci. U.S.A.* **89**: 8774-8778.

Katz L. C., and Shatz C. J. (1996) Synaptic activity and the construction of cortical circuits. *Science* **274**: 1133-1138.

Katz L. C., Gilbert C. D., and Wiesel T.N. (1989) Local circuits and ocular dominance columns in monkey striate cortex. *J. Neurosci.* **9**: 1389-1399.

Kaupp U. B. (1991) The cyclic nucleotide-gated channels of vertebrate photoreceptors and olfactory epithelium. *Trends. Neurosci.* **14**: 150-157.

Kaupp U. B. (1995) Family of cyclic nucleotide gated ion channels. *Curr. Opin. Neurobiol.* **5**: 434-442.

Kawasaki H., Springett G. M., Mochizuki N., Toki S., Nakaya M., Matsudu M., Housman D. E., and Graybiel A. M. (1998) A family of cAMP-binding proteins that directly activate Rap1. *Science* **282**: 2275-2279.

Keller A., and White E. L. (1987) Synaptic organization of GABAergic neurons in the mouse SmI cortex. *J. Comp. Neurol.* **262**: 1-12.

Keller A., White E. L., and Cipolloni P. B. (1985) The identification of thalamocortical axon terminals in barrels of mouse SmI cortex using immunohistochemistry of anterogradely transported lectin (*Phaseolus vulgaris*-leucoagglutinin). *Brain Res.* **343:** 159-165.

Kelly P. T., and Vernon P. (1985) Changes in the subcellular distribution of calmodulin-kinase II during brain development. *Dev. Brain Res.* **18:** 211-224.

Kelly P. T., Shields S., Conway K., Yip R., and Burgin K. (1987) Developmental changes in Calmodulin-Kinase II activity at brain synaptic junctions: Alterations in holoenzyme composition. *J. Neurochem.* **49:** 1927-1940.

Kennedy M. B., Bennett M. K., and Erondu N. E. (1983) Biochemical and immunochemical evidence that the "major postsynaptic density protein" is a subunit of a calmodulin dependent protein kinase. *Proc. Natl. Acad. Sci. U.S.A.* **80:** 7357-7361.

Kidd F. L., and Isaac J. T. (1999) Developmental and activity-dependent regulation of kainate receptors at thalamocortical synapses. *Nature* **400:** 569-573.

Killackey H. P. (1973) Anatomical evidence for cortical subdivisions based on vertically discrete thalamic projections from the ventral posterior nucleus to cortical barrels in the rat. *Brain Res.* **51:** 326-331.

Killackey H. P., and Belford G. R. (1979) The formation of afferent patterns in the somatosensory cortex of the neonatal rat. *J. Comp. Neurol.* **183:** 285-303.

Killackey H. P., and Belford G. R. (1980) Central correlates of peripheral pattern alterations in the trigeminal system of the rat. *Brain Res.* **183:** 205-210.

Killackey H. P., and Erzurumlu R. S. (1981) Trigeminal projections to the superior colliculus of the rat. *J. Comp. Neurol.* **201:** 221-242.

Killackey H. P., and Fleming K. (1985) The role of the principal sensory nucleus in central trigeminal pattern formation. *Brain Res.* **354:** 141-145.

Killackey H. P., and Leshin S. (1975) The organization of specific thalamocortical projections to the posteromedial barrel subfield of the rat somatic sensory cortex. *Brain Res.* **86:** 469-472.

Killackey H. P., Belford G., Ryugo R., and Ryugo D. K. (1976) Anomalous organization of thalamocortical projections consequent to vibrissae removal in the newborn rat and mouse. *Brain Res.* **104:** 309-315.

Killackey H. P., Chiaia N. L., Bennett-Clarke C. A., Eck M., and Rhoades R. W. (1994) Peripheral influences on the size and organization of somatotopic representations in the fetal rat cortex. *J. Neurosci.* **14:** 1496-1506.

Killackey H. P., Jacquin M. F., and Rhoades R. W. (1990) Development of somatosensory structures. In: *Development of Sensory Systems in Mammals.* Coleman Jr. (ed.) Wiley Press, New York, pp: 403-429.

Kim H. G., Fox K., and Conners B. W. (1995) Properties of excitatory synaptic events in neurons of primary somatosensory cortex of neonatal rats. *Cereb. Cortex* **5:** 148-157.

Kim H. G., Wang T., Olafsson P., and Lu B. (1994) Neurotrophin 3 potentiates neuronal activity and inhibits gamma-aminobutyratergic synaptic transmission in cortical neurons. *Proc. Natl. Acad. Sci. U.S.A.* **91:** 12341-12345.

Kim U., and Ebner F. F. (1999) Barrels and septa: separate circuits in rat barrels field cortex. *J. Comp. Neurol.* **408:** 489-505.

Klein R., Silos-Santiago I., Smeyne R. J., Lira S. A., Brambilla R., Bryant S., Zhang L., Snider W. D., and Barbacid M. (1994) Disruption of the neurotrophin-3 receptor gene trkC eliminates la muscle afferents and results in abnormal movements. *Nature (London)* **368:** 249-251.

Klein R., Smeyne R. J., Wurst W., Long L. K., Auerbach B. A., Joyner A. L., and Barbacid M. (1993) Targeted disruption of the trkB neurotrophin receptor gene results in nervous system lesions and neonatal death. *Cell* **75:** 113-122.

Kobayashi T., Nakamura H., and Yasuda M. (1990) Disturbance of refinement of retinotectal projection in chick embryos by tetrodotoxin and grayanotoxin. *Dev. Brain Res.* **57:** 29-35.

Kohara Y., Akiyama K., and Isono K. (1987) The physical map of the whole *E. coli* chromosome: application of a new strategy for rapid analysis and sorting of a large genomic library. *Cell* **50:** 495-508.

Koralek K. A., Jensen K. F., and Killackey H. P. (1988) Evidence for two complementary patterns of thalamic input to the rat somatosensory cortex. *Brain Res.* **463:** 346-351.

Korsching S. (1993) The neurotrophic factor concept: A re-examination. *J. Neurosci.* **13:** 2739-2748.

Krishna G., Weiss B., and Brode B. B. (1968) A simple, sensitive, method for the assay of adenyl cyclase. *J. Pharm. Exper. Therap.* **163:** 379-385.

Kristt D. A. (1979) Development of neocortical circuitry: histochemical localization of acetylcholinesterase in relation to the cell layers of rat somatosensory cortex. *J. Comp. Neurol.* **186:** 1-15.

Krupinski J., Coussen F., Bakalyar H. A., Tang W-J., Feinstein P. G., Orth K., Slaughter C., Reed R. R., and Gilman A. G. (1989) Adenylyl cyclase amino acid sequence: possible channel- or transporter-like structure. *Science* **244:** 1558-1564.

Krupinski J., Lehman T. C., Frankenfield C. D., Zwaagstra J. C. and Watson P. A. (1992) Molecular diversity in the adenylyl cyclase family: evidence for eight forms of the enzyme and cloning of type VI. *J. Biol. Chem.* **267:** 24858-24862.

Kuffler D. P. (1994) Promoting and directing axon outgrowth. *Mol. Neurobiol.* **9:** 233-243.

Kusumi K., Smith J. S., Segre J. A., Koos D. S., and Lander E. S. (1993) Construction of a large-insert yeast artificial chromosome library of the mouse genome. *Mamm. Genome* **4:** 391-392.

Kutsuwada T., Sakimura K., Manabe T., Takayama C., Katakura N., Kushiya E., Natsume R., Watanabe M., Inoue Y., Yagi T., Aizawa S., Arakawa M., Takahashi T., Nakamura Y., Mori H., and Mishina M. (1996) Impairment of suckling response, trigeminal neuronal pattern formation, and hippocampal LTD in NMDA receptor ε2 subunit mutant mice. *Neuron* **16:** 333-344.

Land P. W., and Simons D. J. (1985) Metabolic activity in SmI cortical barrels of adult rats is dependent on patterned sensory stimulation of the mystacial vibrissae. *Brain Res.* **341:** 189-194.

Landers M. S., and Sullican R. M. (1999) Vibrissae-evoked behavior and conditioning before functional ontogeny of the somatosensory vibrissae cortex. *J. Neurosci.* **19:** 5131-5137.

Larin Z., Monaco A. P., Meier-Ewert S., and Lehrach H. (1993) Construction and characterization of yeast artificial chromosome libraries from the mouse genome. *Methods Enzymol.* **225:** 623-637.

Lauder J. M. (1990) Ontogeny of the serotonergic system in the rat: serotonin as a developmental signal. *Ann. N. Y. Acad. Sci.* **600:** 297-313.

Lauder J. M. (1993) Neurotransmitters as growth regulatory signals: role of receptors and second messengers. *Trends. Neurosci.* **16:** 233-240.

Lauder J. M., and Krebs H. (1978) Serotonin as a differentiation signal in early neurogenesis. *Dev. Neurosci.* **1:** 15-30.

Lebrand C., Cases O., Adelbrecht C., Doye A., Alvarez C., Elmestikawy S., Sief I., and Gasper P. (1996) Transient uptake and storage of serotonin in developing thalamic neurons. *Neuron* **17:** 823-835.

Lebrand C., Cases O., Wehrle R., Blakely R. D., Edwards R. H., and Gaspar P. (1998) Transient developmental expression of monoamine transporters in the rodent forebrain. *J. Comp. Neurol.* **401:** 506-524.

Lee K. J., and Woolsey T. A. (1975) A proportional relationship between peripheral innervation density and cortical neuron number in the somatosensory system of the mouse. *Brain Res.* **99:** 349-353.

Lentz S. I., Knudson C. M., Korsmeyer S. J., and Snider W. D. (1999) Neurotrophins support the development of diverse sensory axon morphologies. *J. Neurosci.* **19:** 1038-1048.

Leong W. L., Dobson M. J., Logsdon J. M., Abdel-Majid R. M., Schalkwyk L. C., Guernsey D. L. and Neumann P. E. (1999) ETn insertion in the mouse *Adcy1* gene: transcriptional and phylogenetic analyses. *Mammal. Genome.* In press.

Leslie M. J., Bennett-Clarke C. A., Rhoades R. W. (1992) Serotonin 1B receptors form a transient vibrissa-related pattern in the primary somatosensory cortex of the developing rat. *Dev. Brain Res.* **69:** 143-148.

Lessman V. (1998) Neurotrophin-Dependent modulation of glutamatergic synaptic transmission in the mammalian CNS. *Gen. Pharmac.* **31:** 667-674.

Lessmann V., and Heumann R. (1998) Modulation of unitary glutamatergic synapses by neurotrophin-4/5 or brain-derived neurotrophic factor in hippocampal microcultures: presynaptic enhancement depends on pre-established paired-pulse facilitation. *Neuroscience* **86:** 399-413.

Lessmann V., Gottmann K., and Heumann R. (1994) BDNF and NT-4/5 enhance glutamatergic synaptic transmission in cultured hippocampal neurones. *Neuroreport* **6:** 21-25.

Letourneau P. C. (1978) Chemotactic response of nerve fiber elongation to nerve growth factor. *Dev. Biol.* **66:** 183-196.

LeVay S., Stryker M. P., and Shatz C. J. (1978) Ocular dominance columns and their development in layer IV of the cat's visual cortex: a quantitative study. *J. Comp. Neurol.* **179:** 223-244.

LeVay S., Wiesel T. N., and Hubel D. H. (1980) The development of ocular dominance columns in normal and visually deprived monkeys. *J. Comp. Neurol.* **191:** 1-51.

Levi-Montalcini R. (1964) Growth control of nerve cells by a protein factor and its antiserum. *Science* **143:** 105-110.

Levi-Montalcini R. (1987a) The nerve growth factor 35 years later. *Science* **237:** 1154-1162.

Levi-Montalcini R. (1987b) The nerve growth factor: thirty-five years later. *EMBO J.* **6:** 1145-1154.

Levi-Montalcini R., and Cohen S. (1956) In vitro and in vivo effects of a nerve growth-stimulating agent isolated from snake venom. *Proc. Natl. Acad. Sci. U.S.A.* **42:** 695-699.

Levi-Montalcini R., and Hamburger V. (1951) Selective growth stimulating effects of mouse sarcoma on the sensory and sympathetic nervous system of the chick embryo. *J. Exp. Zool.* **116:** 321-361.

Levi-Montalcini R., and Hamburger V. (1953) A diffusible agent of mouse sarcoma, producing hyperplasia of sympathetic ganglia and hyperneurotization of viscera in the chick embryo. *J. Exp. Zool.* **123:** 233-252.

Levin B. E., Craik R. L., and Hand P. J. (1988) The role of norepinephrine in adult rat somatosensory (SmI) cortical metabolism and plasticity. *Brain Res.* **443:** 261-271.

Levin L. R., and Reed R. R. (1995) Identification of functional domains of adenylyl cyclase using *in vivo* chimeras. *J. Biol. Chem.* **270:** 7573-7579.

Levin L. R., Han P. L., Hwang P. M., Feinstein P. G., Davis R. L., Reed R. R. (1992) The Drosophila learning and memory gene rutabaga encodes a Ca^{2+}/Calmodulin-responsive adenylyl cyclase. *Cell* **68:** 479-489.

Levine E. S., Black I. B., and Plummer M. R. (1998a) Neurotrophin modulation of hippocampal synaptic transmission. *Adv. Pharmacol.* **42:** 921-924.

Levine E. S., Crozier R. A., Black I. B., and Plummer M. R. (1998b) Brain-derived neurotrophic factor modulates hippocampal synaptic transmission by increasing N-methyl-D-aspartic acid receptor activity. *Proc. Natl. Acad. Sci. U.S.A.* **95:** 10235-10239.

Levine E. S., Dreyfus C. F., Black I. B., and Plummer M. R. (1995) Brain-derived neurotrophic factor rapidly enhances synaptic transmission in hippocampal neurons via postsynaptic tyrosine kinase receptors. *Proc. Natl. Acad. Sci. U.S.A.* **92:** 8074-8077.

Levitt P. (1984) A monoclonal antibody to limbic system neurons. *Science* **223:** 299-301.

Levitt P., and Rakic P. (1980) Immunoperoxidase localization of glial fibrillary acidic protein in radial glial cells and astrocytes of the developing rhesus monkey brain. *J. Comp. Neurol.* **193:** 815-840.

Levitt P., Cooper M. L., and Rakic P. (1981) Coexistence of neuronal and glial precursor cells in the cerebral ventricular zone of the fetal monkey: an ultrastructural immunoperoxidase analysis. *J. Neurosci.* **1:** 27-39.

Levitt P., Cooper M. L., and Rakic P. (1983) Early divergence and changing proportions of neuronal and glial precursor cells in the primate cerebral ventricular zone. *Dev. Biol.* **96:** 472-484.

Levitt P., Ferri R. T., and Barbe M. F. (1993) Progressive acquisition of cortical phenotypes as a mechanism for specifying the developing cerebral cortex. *Perspect. Dev. Neurobiol.* **1:** 65-74.

Levitt P., Pawlak-Byczkowska E., Horton H. L., and Cooper V. (1986) Assembly of functional systems in the brain: Molecular and anatomical studies of the limbic system. In *The Neurobiology of Down Syndrome.* Epstein C. J. (ed.) Raven Press, New York, pp: 195-209.

Lewin G. R., and Barde Y. A. (1996) Physiology of the neurotrophins. *Annu. Rev. Neurosci.* **19:** 289-317.

Li Y., Erzurumlu R. S., Chen C., Jhaveri S., and Tonegawa S. (1994) Whisker-related neuronal patterns fail to develop in the trigeminal brainstem nuclei of NMDAR1 knockout mice. *Cell* **76:** 427-437.

Liao D., Hessler N. A., and Malinow R. (1995) Activation of postsynaptically silent synapses during pairing-induced LTP in CA1 region of hippocampal slice. *Nature* (*London*) **375:** 400-404.

Liao D., Zhang X., O'Brien R., Ehlers M. D., and Huganir R. L. (1999) Regulation of morphological postsynaptic silent synapses in developing hippocampal neurons. *Nat. Neurosci.* **2:** 37-43.

Lichtenstein S. H., Carvell G. E., and Simons D. J. (1990) Responses of rat trigeminal ganglion neurons to movements of vibrissae in different directions. *Somatosens. Mot. Res.* **7:** 47-65.

Lidov H. G., and Molliver M. E. (1982) Immunohistochemical study of the development of serotonergic neurons in the rat CNS. *Brain Res. Bull.* **9:** 559-604.

Lidov H. G., Rice F. L., and Molliver M. E. (1978) The organization of the catecholamine innervation of somatosensory cortex: the barrel field of the mouse. *Brain Res.* **153:** 577-584.

Lieske V., Bennett-Clarke C. A., and Rhoades R. W. (1999) Effects of serotonin on neurite outgrowth from thalamic neurons in vitro. *Neuroscience* **90:** 967-974.

Lin C., Lu S. M., and Yamawaki R. M. (1987) Laminar and synaptic organization of terminals from the ventrobasal and posterior thalamic nuclei in rat barrel cortex. *Soc. Neurosci. Abstr.* **13:** 248.

Lin S. Y., Wu K., Levine E. S., Mount H. T., Suen P. C., and Black I. B. (1998) BDNF acutely increases tyrosine phosphorylation of the NMDA receptor subunit 2B in cortical and hippocampal postsynaptic densities. *Mol. Brain Res.* **55:** 20-27.

Lindholm D., Castrén E., Berzaghi M., Blöchl A., and Thoenen H. (1994) Activity-dependent and hormonal regulation of neurotrophin mRNA levels in the brain: implications for neuronal plasticity. *J. Neurobiol.* **25:** 1362-1372.

Lindsay R. M., Wiegand S. J., Altar C. A., and DiStefano P. S. (1994) Neurotrophic factors: from molecule to man. *Trends. Neurosci.* **17:** 182-190.

Lisman J. (1994) The CaM kinase II hypothesis for the storage of synaptic memory. *Trends. Neurosci.* **17:** 406-412.

Livingstone M. S. (1985) Genetic dissection of Drosophila adenylate cyclase. *Proc. Natl. Acad. Sci. U.S.A.* **82:** 5992-5996.

Livingstone M. S., Sziber P. P., and Quinn W. G. (1984) Loss of calcium/calmodulin responsiveness in adenylate cyclase of rutabaga, a Drosophila learning mutant. *Cell* **37:** 205-215.

Lo D. C. (1995) Neurotrophins and neuronal plasticity. *Science* **15:** 979-981.

Lohof A. M., Ip N. Y., and Poo m-m. (1993) Potentiation of developing neuromuscular synapses by the neurotrophins NT-3 and BDNF. *Nature* **363:** 350-353.

Lohof A. M., Quillan M., Dan Y., and Poo M-m. (1992) Asymmetric modulation of cytosolic cAMP activity induces growth cone turning. *J. Neurosci.* **12:** 1253-1261.

Lorente de Nó R. (1922) La corteza cerebral del raton *Trab. Lab. Invest. Biol. (Madrid)* **20:** 41-78.

Lorente de Nó R. (1938) Achitectonics and structure of the cerebral cortex. In: *Physiology of the nervous system.* Fulton J. F. (ed.), Oxford University Press, London, pp: 291-327.

Lorente de Nó R. (1949) In: *Physiology of the Nervous System.* Fulton J. F. (ed.), Oxford University Press, London, pp: 288-315.

Lotto B., Upton L., Price D. J., and Gaspar P. (1999) Serotonin receptor activation enhances neurite outgrowth of thalamic neurones in rodents. *Neurosci. Lett.* **269:** 87-90.

Lu B., and Figurov A. (1997) Role of neurotrophins in synapse development and plasticity. *Rev. Neurosci.* **8:** 1-12.

Lu S. M., and Lin R. C. (1993) Thalamic afferents of the rat barrel cortex: a light- and electron-microscopic study using Phaseolus vulgaris leucoagglutinin as an anterograde tracer. *Somatosens. Mot. Res.* **10:** 1-16.

Lund R. D. and Mustari M. J. (1977) Development of the geniculocortical pathway in rats. *J. Comp. Neurol.* **173:** 289-305.

Lundborg G., Dahlin L., Danielsen N., and Zhao Q. (1994) Trophism, tropism, and specificity in nerve regeneration. *J. Reconstr. Microsurg.* **10:** 345-354.

Luskin M. B., and Shatz C. J. (1985a) Neurogenesis of the cat's primary visual cortex. *J. Comp. Neurol.* **242:** 611-631.

Luskin M. B., and Shatz C. J. (1985b) Studies of the earliest generated cells of the cat's visual cortex: cogeneration of subplate and marginal zones. *J. Neurosci.* **5:** 1062-1075.

Luskin M. B., Pearlman A. L., and Sanes J. R. (1988) Cell lineage in the cerebral cortex of the mouse studied in vivo and in vitro with a recombinant retrovirus. *Neuron* **1:** 635-647.

Lysakowski A., Wainer B. H., Bruce G., Hersh L. B. (1989) An atlas of the regional and laminar distribution of choline acetyltransferase immunoreactivity in rat cerebral cortex. *Neuroscience* **28:** 291-336.

Ma P. M. (1991) The barrelettes-architectonic vibrissal representations in the brainstem trigeminal complex of the mouse. I. Normal structural organization. *J. Comp. Neurol.* **309:** 161-199.

Ma P. M. (1993) Barrelettes--architectonic vibrissal representations in the brainstem trigeminal complex of the mouse. II. Normal post-natal development. *J. Comp. Neurol.* **327:** 376-397.

Ma P. M., and Woolsey T. A. (1984) Cytoarchitectonic correlates of the vibrissae in the medullary trigeminal complex of the mouse. *Brain Res.* **306:** 374-379.

Maier D. L., Mani S., Donovan S. L., Soppet D., Tessarollo L., McCasland J. S., and Meiri K. F. (1999) Disrupted cortical map and absence of cortical barrels in growth-associated protein (GAP)-43 knockout mice. *Proc. Natl. Acad. Sci. U.S.A.* **96:** 9397-9402.

Maier D. L., Meiri K. F., and McCasland J. S. (1998) Absence of cortical barrels in GAP-43 knockout mice. **24:** 631.

Maisonpierre P. C., Belluscio L., Friedman B., Alderson R. F., Wiegand S. J., Furth M. E., Lindsay R. M., and Yancopoulos G. D. (1990) NT-3, BDNF, and NGF in the developing rat nervous system: parallel as well as reciprocal patterns of expression. *Neuron* **5:** 501-509.

Malenka R. C., Kauer J. A., Perkel D. J., Mauk M. D., and Kelly P. T. (1989) An essential role for postsynaptic calmodulin and protein kinase activity in long-term potentiation. *Nature (London)* **340:** 554-557.

Malinow R., Madison D. V., and Tsien R. W. (1988) Persistent protein kinase activity underlying long-term potentiation. *Nature (London)* **335:** 820-824.

Malinow R., Schulman H., and Tsien R. W. (1989) Inhibition of postsynaptic PKC or CaM-KII blocks induction but not expression of LTP. *Science* **245:** 862-866.

Mamounas L. A., Blue M. E., Siuciak J. A., and Altar C. A. (1995) Brain-derived neurotrophic factor promotes the survival and sprouting of serotonergic axons in rat brain. *J. Neurosci.* **15:** 7929-7939.

Mansour-Robaey S., Mechawar N., Radja F., Beaulieu C., and Descarries L. (1998) Quantified distribution of serotonin transporter and receptors during the postnatal development of the rat barrel field cortex. *Dev. Brain Res.* **107:** 159-163.

Marchase R. B., Vosbeck K., and Roth S. (1976) Intercellular adhesive specificity. *Biochim. Biophys. Acta.* **457:** 385-416.

Marin-Padilla M. (1971) Early prenatal ontogenesis of the cerebral cortex (neocortex) of the cat (*Felis domestica*): a Golgi study. I. The promordial neocortical organization. Z. *Anat. Entwicklungsgesch* **134**: 117-145.

Matsouka I., Suzuki Y., Defer N., Nakanishi H., and Hanoune J. (1997) Differential expression of type I, II, and V adenylyl cyclase gene in the postnatal developing rat brain. *J. Neurochem.* **68**: 498-506.

McAllister A. K. Lo D. C., and Katz L. C. (1995) Neurotrophins regulate dendritic growth in developing visual cortex. *Neuron* **15**: 791-803.

McAllister A. K., Katz L. C. and Lo D. C. (1997) Opposing roles for endogenous BDNF and NT-3 in regulating cortical dendritic growth. *Neuron* **18**: 767-778.

McAllister A. K., Katz L. C., and Lo D. C. (1996) Neurotrophin regulation of cortical dendritic growth requires activity. *Neuron* **17**: 1057-1064.

McAllister A. K., Katz L. C., and Lo D. C. (1999) Neurotrophic and synaptic plasticity. *Ann Rev. Neurosci.* **22**: 295-318.

McCandlish C. A., Li C. X., and Waters R. S. (1993) Early development of the SI cortical barrel field representation in neonatal rats follows a lateral-to-medial gradient: an electrophysiological study. *Exp. Brain Res.* **92**: 369-374.

McConnell S. K. (1988a) Fates of visual cortical neurons in the ferret after isochronic and heterochronic transplantation. *J. Neurosci.* **8**: 945-974.

McConnell S. K. (1988b) Development and decision-making in the mammalian cerebral cortex. *Brain Res.* **472**: 1-23.

McConnell S. K., and Kaznowski C. E. (1991) Cell cycle dependence of laminar determination in developing neocortex. *Science* **254**: 282-285.

McFarlane S., McNeill L., and Holt C. E. (1995) FGF signaling and target recognition in the developing Xenopus visual system. *Neuron* **15**: 1017-1028.

McGuinness T. L., Lai N. Y., Ouimett C. C. and Greengard P. (1984) Calmodulin-dependent protein kinases in brain, In *Calcium in Biological Systems* Rubin R. P., Putney J. W., and Weiss E. (eds.), Plenum Press, New York, pp: 291-305.

McGuinness T. L., Lai Y., and Greengard P. (1985) Ca^{2+}/Calmodulin-dependent protein kinase II: isozymic forms from rat forebrain and cerebellum. *J. Biol. Chem.* **260**: 1696-1704.

Menesini-Chen M. G., Chen J. S., and Levi-Montalcini R. (1978) Sympathetic nerve fibers ingrwoth in the CNS of neonatal rodent upon intracerebral NGF injections. *Arch. Ital. Biol.* **116:** 53-84.

Meyer R. L. (1982) Tetrodotoxin blocks the formation of ocular dominance columns in goldfish. *Science* **218:** 589-591.

Meyer R. L. (1983) Tetrodotoxin inhibits the formation of refined retinotopography in goldfish. *Brain Res.* **282:** 293-298.

Miller K. D., Chapman B., and Stryker M. P. (1989) Visual responses in adult cat visual cortex depend on N-methyl-D-aspartate receptors. *Proc. Natl. Acad. Sci. U.S.A.* **86:** 5183-5187.

Miller M. W. (1988) Effect of prenatal exposure to ethanol on the development of cerebral cortex: I. Neuronal generation. *Alcohol. Clin. Exp. Res.* **12:** 440-449.

Miller M. W., and Muller S. J. (1989) Structure and histogenesis of the principal sensory nucleus of the trigeminal nerve: effects of prenatal exposure to ethanol. *J. Comp. Neurol.* **282:** 570-580.

Miller S. G., and Kennedy M. B. (1985) Distinct forebrain and cerebellum isozymes of type II Ca^{2+}/Calmodulin-dependent protein kinase associate differently with the postsynaptic density fraction. *J. Biol. Chem.* **260:** 9039-9046.

Ming G. l., Lohof A. M., and Zheng J. Q. (1997) Acute morphogenic and chemotropic effects of neurotrophins on cultured embryonic Xenopus spinal neurons. *J. Neurosci.* **17:** 7860-7871.

Mitreiter K., Schmidt J., Luz A., Atkinson M. J., Hofler H., Erfle V., and Strauss P. G. (1994) Disruption of the murine p53 gene by insertion of an endogenous retrovirus-like element (ETn) in a cell line from radiation-induced osteosarcoma. *Virology* **200:** 837-841.

Mitrovic N., and Schachner M. (1995) Detection of tenascin-C in the nervous system of the tenascin-C mutant mouse. *J. Neurosci. Res.* **42:** 710-717.

Mitrovic N., Dorries U., and Schachner M. (1994) Expression of the extracellular matrix glycoprotein tenascin in the somatosensory cortex of the mouse during postnatal development: an immunocytochemical and in situ hybridization analysis. *J. Neurocytol.* **23:** 364-378.

Mitrovic N., Mohajeri H., and Schachner M. (1996) Effects of NMDA receptor blockade in the developing rat somatosensory cortex on the expression of the glia-derived extracellular matrix glycoprotein tenascin-C. *Eur. J. Neurosci.* **8:** 1793-1802.

Miyashita-Lin E. M., Hevner R., Wassarman K. M., Martinez S., and Rubenstein J. L. (1999) Early neocortical regionalization in the absence of thalamic innervation. *Science* **285:** 906-909.

Montarolo P. G., Goelet P., Castelluci V. F., Morgan J., Kandel E. R., and Schacher S. (1986) A critical period for macromolecular synthesis in long-term heterosynaptic facilitation in Aplysia. *Science* **234:** 1249-1254.

Mountcastle V. B. (1978) In: *The Mindful Brain.* Mountcastle V. B. and Edelman G. M. (eds.), MIT Press, Cambridge, pp: 7-50.

Nakanishi S. (1992) Molecular diversity of glutamate receptors and implications for brain functions. *Science* **258:** 597-603.

Narisawa-Saito M., Carnahan J., Araki K., Yamaguchi T., and Nawa H. (1999) Brain-derived neurotrophic factor regulates the expression of AMPA receptor proteins in neocortical neurons. *Neuroscience* **88:** 1009-1014.

Nathans D. (1979) Restriction endonucleases, simian virus 40, and the new genetics. *Science* **206:** 903-909.

Nilsson AS, Fainzilber M, Falck P, Ibáñez CF (1998) Neurotrophin-7: a novel member of the neurotrophin family from the zebrafish. *FEBS Lett.* **424:** 285-290.

Nothias F., Peschanski M., and Besson J. M. (1988) Somatotopic reciprocal connections between the somatosensory cortex and the thalamic Po nucleus in the rat. *Brain Res.* **447:** 169-174.

O'Brien T. F., Steindler D. A., and Cooper N. G. (1987) Abnormal glia and glycoconjugate disposition in the somatosensory cortical barrel field of the early postnatal reeler mutant mouse. *Dev. Brain Res.* **32:** 309-317.

O'Leary D. D., and Stanfield B. B. (1989) Selective elimination of axons extended by developing cortical neurons is dependent on regional locale: experiments utilizing fetal cortical transplants. *J. Neuorsci.* **9:** 2230-2246.

Oakley R. A., and Tosney K. W. (1988) Peanut agglutinin (PNA) binds tissues that act as barriers to axon advance in the chick embryo. *Soc. Neursci. Abstr.* **14:** 870.

Olavarria J., Van Sluyters R. C., and Killackey H. P. (1984) Evidence for the complementary organization of callosal and thalamic connections within rat somatosensory cortex. *Brain Res.* **291:** 364-368.

O'Leary D. D. (1989) Do cortical areas emerge from a protocortex? *Trends. Neurosci.* **12:** 400-406.

O'Leary D. D., Ruff N. L., and Dyck R. H. (1994) Development, critical period plasticity, and adult reorganizations of mammalian somatosensory systems. *Curr. Opin. Neurobiol.* **4:** 535-544.

Olson M. V., Dutchik J. E., Graham M. Y., Brodeur G. M., Helms C., Frank M., Maccollin M., Scheinman R., and Frank K. T. (1986) Random-clone strategy for genomic restriction mapping in yeast. *Proc. Natl. Acad. Sci. U.S.A.* **83:** 7826-7830.

O'Rourke N. A., Dailey M. E., Smith S. J., and McConnell S. K. (1992) Diverse migratory pathways in the developing cerebral cortex. *Science* **258:** 299-302.

Ortega S., Ittmann M., Tsang S. H., Ehrlich M., and Basilico C. (1998) Neuronal defects and delayed wound healing in mice lacking fibroblast growth factor 2. *Proc. Natl. Acad. Sci. U.S.A.* **95:** 5672-5677.

Osterheld-Haas M. C., and Hornung J. P. (1996) Laminar development of the mouse barrel cortex: effects of neurotoxins against monoamines. *Exp. Brain Res.* **110:** 183-195.

Osterheld-Haas M. C., Van der Loos H., and Hornung J. P. (1994) Monoaminergic afferents to cortex modulate structural plasticity in the barrelfield of the mouse. *Dev. Brain Res.* **77:** 189-202.

Ouimet C. C., McGuinness T. L., and Greengard P. (1984) Immunocytochemical localization of Calcium/calmodulin-dependent protein kinase II in rat brain. *Proc. Natl. Acad. Sci. U.S.A.* **81:** 5604-5608.

Parnavelas J. G. (1990) Neurotransmitters in the cerebral cortex. *Prog. Brain Res.* **85:** 13-29.

Pastan I. (1972) Cyclic AMP *Sci. Am.* **227:** 97-105.

Pasternak J. R., and Woolsey T. A. (1975) The number, size and spatial distribution of neurons in lamina IV of the mouse SmI neocortex. *J. Comp. Neurol.* **160:** 291-306.

Paterson J. M., Smith S. M., Harmar A. J., and Antoni F. A. (1995) Control of a novel adenlylyl cyclase by calcineurine. *Biochem. Biophys. Res. Commun.* **214:** 1000-1008.

Patterson S. L., Abel T., Deuel T. A. S., Martin K. C., Rose J. C., and Kandel E. R. (1996) Recombinant BDNF rescues deficits in basal synaptic transmission and hippocampal LTP in BDNF knockout mice. *Neuron* **16:** 1137-1145.

Peirce J. C., Sternberg N., and Sauer B. (1992) A mouse genomic library in the bacteriophage P1 cloning system: Organization and characterization. *Mammal. Genome* **3:** 550-558.

Penschuck S., Giorgetta O., and Fritschy J. M. (1999) Neuronal activity influences the growth of barrels in developing rat primary somatosensory cortex without affecting the expression pattern of four major GABAA receptor alpha subunits. *Dev. Brain Res.* **112:** 117-127.

Peschanski M. (1984) Trigeminal afferents to the diencephalon in the rat. *Neuroscience* **12:** 465-487.

Petralia R. S., Esteban J. A., Wang Y. X., Partridge J. G., Zhao H. M., Wenthold R. J., and Malinow R. (1999) Selective acquisition of AMPA receptors over postnatal development suggests a molecular basis for silent synapses. *Nature Neurosci.* **2:** 31-36.

Pierce J. C., and Sternberg N. L. (1992) Using bacteriophage P1 system to clone high molecular weight genomic DNA. *Meth. Enzymol.* **216:** 549-574.

Pitts A. F., and Miller M. W. (1995) Expression of nerve growth factor, p75, and trk in the somatosensory and motor cortices of mature rats: evidence for local trophic support circuits. *Somatosens. Mot. Res.* **12:** 329-342.

Powell T. P. (1981) In: *Brain Mechanisms and Perceptual Awareness*. Pompeiano O. and Ajmone Marsan C. (eds.), Raven Press, pp: 1-19.

Prakash N., Cohen-Cory S., Frostig R. D. (1996) Rapid and opposite effects of BDNF and NGF on the functional organization of the adult cortex in vivo. *Nature* **381:** 702-706.

Premont R. T., Chen J., Ma H-W., Ponnapalli M., and Iyengar R. (1992) Two members of a widely expressed subfamily of hormone-stimulated adenylyl cyclases. *Proc. Natl. Acad. U.S.A.* **89:** 9809-9813.

Premont R. T., Matsouka I., Mattei M-G., Pouille Y., Defer N., and Hanoune J. (1996) Identification and characterization of a widely expressed form of adenylyl cyclase. *J. Biol. Chem.* **271:** 13900-13907.

Price J., and Thurlow L. (1988) Cell lineage in the rat cerebral cortex: A study using retroviral mediated gene transfer. *Development* **104:** 473-482.

Purves D. (1986) The trophic theory of neural connections. *Trends. Neurosci.* **9:** 486-489.

Purves D. (1988) *Body and Brain. A Trophic Theory of Neural Connections.* Oxford University Press, Oxford.

Purves D. and Lichtman J. W. (1985) Trophic effects of targets on neurons In: *Principles of Neural Development.* Sinauer Associates Inc. Press, Sunderland.

Purves D., and Lichtman J. W. (1980) Elimination of synapses in the developing nervous system. *Science* **210:** 153-157.

Purves D., Hadley R. D., and Voyvodic, J. T. (1986) Dynamic changes in the dendritic geometry of individual neurons visualized over periods of up to three months in the superior cervical ganglion of living mice. *J. Neurosci.* **6:** 1051-1060.

Purves D., Riddle D. R., White L. E., and Gutierrez-Ospina G. (1994) Neural activity and the development of the somatic sensory system. *Curr. Opin. Neurobiol.* **4:** 120-123.

Qi M., Zhuo M., Skalhegg B. S., Brandon E. P., Kandel E. R., McKnight G. S. and Izerda R. L. (1996) Impaired hippocampal plasticity in mice lacking the Cβ1 catalytic subunit of cAMP-dependent protein kinase. *Proc. Natl. Acad. Sci. U.S.A.* **93:** 1571-1576.

Rakic P. (1972) Mode of cell migration to the superficial layers of fetal monkey neocortex. *J. Comp. Neurol.* **145:** 61-83.

Rakic P. (1974) Neurons in rhesus monkey visual cortex: systematic relation between time of origin and eventual disposition. *Science* **183:** 425-427.

Rakic P. (1977) Prenatal development of the visual system in rhesus monkey. *Philos. Trans. R. Soc. Lond. (B)* **278:** 245-260.

Rakic P. (1978) Neuronal migration and contact guidance in the primate telencephalon. *Postgrad. Med. J.* **54:** 25-40.

Rakic P. (1981) Developmental events leading to laminar and areal organization of the neocortex. In: *The Organization of the Cerebral Cortex.* Schmitt F. O. (ed.), MIT Press, Cambridge, pp: 7-28.

Rakic P. (1988) Specification of cerebral cortical areas. *Science* **241:** 170-176.

Rall T. W., Sutherland E. W., and Berthet J. (1957) The relationship of epinephrine and glucagon to liver phosphorelase. IV. Effect of epinephrine and glucagon on the reactivation of phosphorylase in liver homogenates. *J. Biol. Chem.* **224:** 463-475.

Redfern P. A. (1970) Neuromuscular transmission in new-born rats. *J. Physiol. (London)* **209:** 701-709.

Renehan W. E., and Munger B. L. (1986) Degeneration and regeneration of peripheral nerve in the rat trigeminal system. I. Identification and characterization of the multiple afferent innervation of the mystacial vibrissae. *J. Comp. Neurol.* **246:** 129-145.

Rhoades R. W., Bennett-Clarke C. A., Chiaia N. L., White F. A., Macdonald G. J., Haring J. H. and Jacquin M. F. (1990) Development and lesion induced reorganization of the cortical representation of the rat's body surface as revealed by immunocytochemistry for serotonin. *J. Comp. Neurol.* **293:** 190-207.

Rhoades R. W., Bennett-Clarke C. A., Shi M. Y., and Mooney R. D. (1994) Effects of 5-HT on thalamocortical synaptic transmission in the developing rat. *J. Neurophysiol.* **72:** 2438-2450.

Rhoades R. W., Chiaia N. L., Lane R. D., and Bennett-Clarke C. A. (1998) Effect of activity blockade on changes in vibrissae-related patterns in the rat's primary somatosensory cortex induced by serotonin depletion. *J. Comp. Neurol.* **402:** 276-283.

Rhoades R. W., Enfiejian H. L., Chiaia N. L., Macdonald G. J., Miller M. W., McCann P., and Goddard C. M. (1991) Birthdates of trigeminal ganglion cells contributing axons to the infraorbital nerve and specific vibrissal follicles in the rat. *J. Comp. Neurol.* **307:** 163-175.

Rhoades R. W., Mooney R. D., Chiaia N. L., Nikoletseas M. M., and Rohrer W. H. (1988) What's in a patch? Examination of the trigeminal projection to the superior colliculus with *Phaseolus vulgaris* leuco-agglutinin and single fiber labelling. *Soc. Neurosci. Abstr.* **14:** 1165.

Rice F. L. (1985b) An attempt to find vibrissa-related barrels in the primary somatosensory cortex of the cat. *Neurosci. Lett.* **53:** 169-172.

Rice F. L. (1993) Structure, vascularization, and innervation of the mystacial pad of the rat as revealed by the lectin Griffonia simplicifolia. *J. Comp. Neurol.* **337:** 386-399.

Rice F. L. (1995) Comparative aspects of barrel structure and development. In: *Cerebral Cortex.* Jones E. G. and Diamond I. T. (ed.), Plenum Press, New York and London, pp: 54.

Rice F. L., Albers K. M., Davis B. M., Silos-Santiago I., Wilkinson G. A., LeMaster A. M., Ernfors P., Smeyne R. J., Aldskogius H., Phillips H. S., Barbacid M., DeChiara T. M., Yancopoulos G. D., Dunne C. E., and Fundin B. T. (1998) Differential dependency of

unmyelinated and A delta epidermal and upper dermal innervation on neurotrophins, trk receptors, and p75LNGFR. *Dev. Biol.* **198:** 57-81.

Rice F. L., and Van der Loos H. (1977) Development of the barrels and barrel field in the somatosensory cortex of the mouse. *J. Comp. Neurol.* **171:** 545-560.

Rice F. L., Gomez C. M., Leclerc S. S., Dykes R. W., Moon J. S., and Pourmoghadam K. (1993) Cytoarchitecture of the ferret suprasylvian gyrus correlated with areas containing multiunit responses elicited by stimulation of the face. *Somatosens. Mot. Res.* **10:** 161-188.

Rice F. L., Gomez C., Barstow C., Burnet A., and Sands P. A. (1985) comparative analysis of the development of the primary somatosensory cortex: interspecies similarities during barrel and laminar development. *J. Comp. Neurol.* **236:** 477-495.

Rice F. L., Henderson T. A., Albers K. M., Davis B. M., Carlson J. N., and Jacquin M. F. (1995) Different effects of fetal NGF injections and transgenic NGF enhancement on the innervation of the whisker pad in neonatal rats and mice. *Soc. Neurosci. Abstr.* **21:** 1540.

Rice F. L., Henderson T. A., Osborne E. M., Johnson E. M., and Jacquin M. F. (1994) Fetal NGF augmentation affects whiskerpad innervation density and patterns at birth. *Soc. Neurosci. Abstr.* **20:** 1095.

Rice F. L., Kinnman E., Aldskogius H., Johansson O., and Arvidsson J. (1993) The innervation of the mystacial pad of the rat as revealed by PGP 9.5 immunofluorescence. *J. Comp. Neurol.* **337:** 366-385.

Rice F. L., Mance A., and Munger B. L. (1986) A comparative light microscopic analysis of the sensory innervation of the mystacial pad. I. Innervation of vibrissal follicle-sinus complexes. *J. Comp. Neurol.* **252:** 154-174.

Riddle D. R., and Purves D. (1995) Individual variation and lateral asymmetry of the rat primary somatosensory cortex. *J. Neurosci.* **15:** 4184-4195.

Riddle D. R., Gutierrez G., Zheng D., White L. E., Richards A., and Purves D. (1993) Differential metabolic and electrical activity in the somatic sensory cortex of juvenile and adult rats. *J. Neurosci.* **13:** 4193-4213.

Riddle D., Richards A., Zsuppan F., and Purves D. (1992) Growth of the rat somatic sensory cortex and its constituent parts during postnatal development. *J. Neurosci.* **12:** 3509-3524.

Ringstedt T., Lagercrantz H., and Persson H. (1993) Expression of members of the trk family in the developing postnatal rat brain. *Dev. Brain Res.* **72:** 119-131.

Robertson R. T. (1987) A morphogenic role for transiently expressed acetylcholinesterase in developing thalamocortical systems? *Neurosci. Lett.* **75**: 259-264.

Rocamora N., Welker E., Pascual M., and Soriano E. (1996) Upregulation of BDNF mRNA expression in the barrel cortex of adult mice after sensory stimulation. *J. Neurosci.* **16**: 4411-4419.

Roger M., and Cadusseau J. (1984) Afferent connections of the nucleus posterior thalami in the rat, with some evolutionary and functional considerations. *J. Hirnforsch* **25**: 473-485.

Ross E. M., and Gilman A. G. (1980) Biochemical properties of hormone-sensitive adenylate cyclase. *Ann. Rev. Biochem.* **49**: 533-564.

Rumpel S., Hatt H., and Gottmann K. (1998) Silent synapses in the developing rat visual cortex: evidence for postsynaptic expression of synaptic plasticity. *J. Neurosci.* **18**: 8863-8874.

Sachdev R. N., Lu S. M., Wiley R. G., and Ebner F. F. (1998) Role of the basal forebrain cholinergic projection in somatosensory cortical plasticity. *J. Neurophysiol.* **79**: 3216-3228.

Sahyoun N., LeVine H. III, Burgess S. K., Blanchard S., Chang K. J., and Cuatrecasas P. (1985) Early postnatal development of calmodulin-dependent protein kinase II in rat brain. *Biochem. Biophys. Res. Commun.* **132**: 878-884.

Salomon Y. (1979) Adenylate cyclase assay. *Advances in Cyclic Nucleotide Research* **10**: 35-55.

Salomon Y., Londos C., and Rodbell M. (1974) A highly sensitive adenylate cyclase assay. *Analytical Biochem.* **58**: 541-548.

Sambrook J., Fritsch E. F., and Maniatis T. (1982) Molecular Cloning: A Laboratory Manual. Cold Spring Harbor Laboratory Press, New York.

Sassone-Corsi P. (1995) Transcription factors responsive to cAMP. *Annu. Rev. Cell. Dev. Biol.* **11**: 355-377.

Sauer F. C. (1935) Mitosis in the neural tube. *J. Comp. Neurol.* **62**: 377-405.

Scarisbrick I. A., and Jones E. G. (1993) NCAM immunoreactivity during major developmental events in the rat maxillary nerve-whisker system. *Dev. Brain Res.* **71**: 121-135.

Scharfman H. E. (1997) Hyperexcitability in combined entorhinal/hippocampal slices of adult rat after exposure to brain-derived neurotrophic factor. *J. Neurophysiol.* **78:** 1082-1095.

Schecterson L. C., and Bothwell M. (1992) Novel roles for neurotrophins are suggested by BDNF and NT-3 mRNA expression in developing neurons. *Neuron* **9:** 449-463.

Schlaggar B. L., and O'Leary D. D. (1991) Potential of visual cortex to develop an array of functional units unique to somatosensory cortex. *Science* **252:** 1556-1560.

Schlaggar B. L., and O'Leary D. D. (1994) Early development of the somatotopic map and barrel patterning in rat somatosensory cortex. *J. Comp. Neurol.* **346:** 80-96.

Schlaggar B. L., Fox K., and O'Leary D. D. (1993) Postsynaptic control of plasticity in developing somatosensory cortex. *Nature (London)* **364:** 623-626.

Schlessinger D. (1990) Yeast artificial chromosomes: tools for mapping and analysis of complex genomes. *Trends. Genet.* **6:** 248, 255-258.

Schmidt J. T. (1990) Long-term potentiation and activity-dependent retinotopic sharpening in the regenerating retinotectal projection of goldfish: common sensitive period and sensitivity to NMDA blockers. *J. Neurosci.* **10:** 233-246.

Schmidt J. T., and Edwards D. L. (1983) Activity sharpens the map during the regeneration of the retinotectal projection in goldfish. *Brain Res.* **269:** 29-39.

Schoups A. A., Elliott R. C., Friedman W. J., and Black I. B. (1995) NGF and BDNF are differentially modulated by visual experience in the developing geniculocortical pathway. *Dev. Brain Res.* **86:** 326-334.

Schramm M., and Selinger Z. (1984) Message transmission: receptor controlled adenylate cyclase system. *Science* **225:** 1350-1356.

Schwartz P. M., Borghesani P. R., Levy R. L., Pomeroy S. L., and Segal R. A. (1997) Abnormal cerebellar development and foliation in BDNF-/- mice reveals a role for neurotrophins in CNS patterning. *Neuron* **19:** 269-281.

Senft S. L., and Woolsey T. A. (1991) Growth of thalamic afferents into mouse barrel cortex. *Cereb Cortex* **1:** 308-335.

Shatz C. (1990) Impulse activity and the patterning of connections during CNS development. *Neuron* **5:** 745-756.

Shatz C. J., and Stryker M. P. (1978) Ocular dominance in layer IV of the cat's visual cortex and the effects of monocular deprivation. *J. Physiol. (London)* **281:** 267-283.

Shatz C. J., and Stryker M. P. (1988) Prenatal tetrodotoxin infusion blocks segregation of retinogeniculate afferents. *Science* **242:** 87-89.

Sherwood N. T., and Lo D. C. (1999) Long-term enhancement of central synaptic transmission by chronic brain-derived neurotrophic factor treatment. *J. Neurosci.* **19:** 7025-7036.

Sikich L., Woolsey T. A., and Johnson E. M. Jr. (1986) Effect of a uniform partial denervation of the periphery on the peripheral central vibrissal system in guinea pigs. *J. Neurosci.* **6:** 1227-1240.

Silva A. J., Paylor R., Wehner J. M., and Tonegawa S. (1992a) Impaired spatial learning in α-Calcium-Calmodulin kinase II mutant mice. *Science* **257:** 206-211.

Silva A. J., Stevens C. F., Tonegawa S., and Wang Y. (1992b) Deficient hippocampal long-term potentiation in α-Calcium-Calmodulin kinase II mutant mice. *Science* **257:** 201-206.

Silver J., Poston M., and Rutishauser U. (1987) Axon pathway boundaries in the developing brain. I. Cellular and molecular determinants that separate the optic and olfactory projections. *J. Neurosci.* **7:** 2264-2272.

Simon D. K., Prusky G. T., O'Leary D. D. M., and Constantine-Paton M. (1992) N-Methyl-D-aspartate receptor antagonists disrupt the formation of a mammalian neural map. *Proc. Natl. Acad. Sci. U.S.A.* **89:** 10593-10597.

Simons D. J. (1978) Response properties of vibrissa units in rat SI somatossensory cortex. *J. Neurophysiol.* **41:** 798-820.

Simons D. J., and Woolsey T. A. (1978) Golgi-cox impregnated barrel neurons in the rat SmI cortex. *Soc. Neurosci. Abstr.* **4:** 80.

Simons D. J., and Woolsey T. A. (1979) Functional organization in mouse barrel cortex. *Brain Res.* **165:** 327-332.

Simons D. J., and Woolsey T. A. (1984) Morphology of Golgi-Cox-impregnated barrel neurons in rat SmI cortex. *J. Comp. Neurol.* **230:** 119-132.

Singh T. D., Mizuno K., Kohno T., Nakamura S. (1997) BDNF and trkB mRNA expression in neurons of the neonatal mouse barrel field cortex: normal development and plasticity after cauterizing facial vibrissae. *Neurochem. Res.* **22:** 791-797.

Siuciak J. A., Boylan C., Fritsche M., Altar C. A., and Lindsay R. M. (1996) BDNF increases monoaminergic activity in rat brain following intracerebroventricular or intraparenchymal administration. *Brain Res.* **710:** 11-20.

Smeyne R. J., Klein R., Schnapp A., Long L. K., Bryant S., Lewin A., Lira S. A., and Barbacid M. (1994) Severe sensory and sympathetic neuropathies in mice carrying a disrupted Trk/NGF receptor gene. *Nature (London)* **368:** 246-249.

Smith R. L. (1973) The ascending fiber projections from the principal sensory trigeminal nucleus in the rat. *J. Comp. Neurol.* **148:** 423-445.

Snider W. D. (1994) Functions of the neurotrophins during nervous system development: what the knockouts are teaching us. *Cell* **77:** 627-638.

Snider W. D., and Johnson Jr. E. M. (1989) Neurotrophic molecules. *Ann. Neurol.* **26:** 489-506.

Snow D. M., Steindler D. A., and Silver J. (1990) Molecular and cellular characterization of the glial roof plate of the spinal cord and optic tectum: a possible role for a proteoglycan in the development of an axon barrier. *Dev. Biol.* **138:** 359-376.

Snyder S. H. (1985) The molecular basis of communication between cells. *Sci. Am.* **253:** 132-141.

Soderling T. R. (1993) Ca^{2+}/Calmodulin-dependent protein kinase II: role in learning and memory. *Mol. Cell. Biochem.* **127-128:** 93-101.

Song H. J., and Poo M. M. (1999) Signal transduction underlying growth cone guidance by diffusable factors. *Curr. Opin. Neurobiol.* **9:** 355-363.

Song H., Ming G., He Z., Lehmann M., McKerracher L., Tessier-Lavigne M., and Poo M. (1998) Conversion of neuronal growth cone responses from repulsion to attraction by cyclic nucleotides. *Science* **281:** 1515-1518.

Song H-j., Ming G-l., and Poo M-m. (1997) cAMP-induced switching in turning direction of nerve growth cones. *Nature* **388:** 275-279.

Spemann H. (1938) In: *Embryonic Development and Induction.* Yale University Press, New Haven.

Spemann H. and Mangold H. (1924) Induction von embryonolanlagen durch implantation artfremder organisatoren. Arch Mikrosk. Anat. Entwicklungsmech. 100: 599-638. English Translation by V. Hamburger reprinted In: *Foundations of Experimental Embryology,*

Willier B. H. and Oppenheimer J. (eds.), 2nd Ed. 1974. Hafner Press, New York, pp: 144-184.

Sperry R. W. (1951) Mechanisms of neural maturation. In: *Handbook of Experimental Psychology*. Stevens S. S. (ed.), Wiley Press, New York, pp: 236-280.

Sperry R. W. (1965) Embryogenesis of behavioral nerve nets. In: *Organogenesis*. DeHaan R. L. and Ursprung H. (eds.), Holt, Rinehart and Winston, New York, pp: 161-171.

Stanfield B. B., and O'Leary D. D. (1985) Fetal occipital cortical neurons transplanted to the rostral cortex can extend and maintain a pyramidal tract axon. *Nature (London)* **313:** 135-137.

Stanfield B. B., O'Leary D. D., and Fricks C. (1982) Selective collateral elimination in early postnatal development restricts cortical distribution of rat pyramidal tract neurons. *Nature (London)* **298:** 371-373.

Steffen H. , and Van der Loos H. (1980) Early lesions of mouse vibrissal follicles: their influence on dendrite orientation in the cortical barrelfield. *Exp. Brain Res.* **40:** 419-431.

Steindler D. A., Cooper N. G., Faissner A., and Schachner M. (1989) Boundaries defined by adhesion molecules during development of the cerebral cortex: the J1/tenascin glycoprotein in the mouse somatosensory cortical barrel field. *Dev. Biol.* **131:** 243-260.

Steindler D. A., O'Brien T. F., Laywell E., Harrington K., Faissner A., and Schachner M. (1990) Boundaries during normal and abnormal brain development: in vivo and in vitro studies of glia and glycoconjugates. *Exp. Neurol.* **109:** 35-56.

Steindler D. A., Settles D., Erickson H. P., Laywell E. D., Yoshiki A., Faissner A., and Kusakabe M. (1995) Tenascin knockout mice: barrels, boundary molecules, and glial scars. *J. Neurosci.* **15:** 1971-1983.

Steinmeyer K., Klocke R., Ortland C., Gronemeier M., Jokusch H., Grunder S., and Jentsch T. J. (1991) Inactivation of muscle chloride channel by transposon insertion in myotonic mice. *Nature* **354:** 304-308.

Stern C. (1968) Developmental genetics of pattern. In: *Genetic Mosaics and Other Essays*. Stern C. (ed.), Harvard University Press, Cambridge, pp: 135-173.

Sternberg N. (1990) Bacteriophage P1 cloning system for the isolation, amplification and recovery of DNA fragments as large as 100 kilobase pairs. *Proc. Natl. Acad. Sci. U.S.A.* **87:** 103-107

Storm D. R., Hansel C., Hacker B., Parent A., and Linden D. J. (1998) Impaired cerebellar long-term potentiation in type I adenylyl cyclase mutant mice. *Neuron* **20:** 1199-1210.

Stryker M. P., and Harris W. A. (1986) Binocular impulse blockade prevents the formation of ocular dominance columns in cat visual cortex. *J. Neurosci.* **6:** 2117-2133.

Stryker M. P., and Strickland S. L. (1984) Physiological segregation of ocular dominance columns depends on the pattern of afferent electrical activity. *Invest. Ophthalmol. Vis. Sci.* **25:** 278.

Sugiura H., and Yamauchi T. (1992) Developmental changes in the levels of Ca^{2+}/Calmodulin-dependent protein kinase II αand β proteins in soluble and particulate fractions of the rat brain. *Brain Res.* **593:** 97-104.

Sur M., Weller R. E., and Kaas J. H. (1980) Representation of the body surface in somatosensory area I of tree shrews, *Tupaia glis. J. Comp. Neurol.* **194:** 71-95.

Sutherland E. W. (1972) Studies on the mechanism of hormone action. *Science* **177:** 401-408.

Sutherland E. W., and Rall T. W. (1958a) Formation of cyclic adenosine ribonucleotide by tissue particles. *J. Biol. Chem.* **232:** 1065-1076.

Sutherland E. W., and Rall T. W. (1958b) Fractionation and characterisation of a cyclic adenosine ribonucleotide formed by tissue particles. *J. Biol. Chem.* **232:** 1077-1091.

Suzuki T. (1994) Protein kinases involved in the expression of long-term potentiation. *Int. J. Biochem.* **26:** 735-744.

Tang W-J., Krupinski J., and Gilman A. G. (1991) Expression and characterization of calmodulin-activated (type I) AC. *J. Biol. Chem.* **266:** 8595-8603.

Taussig R., and Gilman A. G. (1995) Mammalian membrane-bound adenylyl cyclases. *J. Biol. Chem.* **270:** 1-4.

Thoenen H. (1991) The changing scene of neurotrophic factors. *Trends. Neurosci.* **14:** 165-170.

Thoenen H. (1995) Neurotrophins and neural plasticity. *Science* **270:** 593-598.

Thoenen H., Bandtlow C., and Heumann R. (1987) The physiological function of nerve growth factor in the central nervous system: comparison with the periphery. *Rev. Physiol. Biochem. Pharmacol.* **109:** 146-178.

Tobimatsu T., and Fujisawa H. (1989) Tissue-specific expression of four types of rat calmodulin-dependent protein kinase II mRNAs. *J. Biol. Chem.* **264**: 17907-17912.

Tobimatsu T., Kameshita I., and Fujisawa H. (1988) Molecular cloning of the cDNA encoding the third polypeptide (γ) of brain calmodulin-dependent protein kinase II. *J. Biol. Chem.* **263**: 16082-16086.

Tsumoto T. (1990) Excitatory amino acid transmitters and their receptors in neural circuits of the cerebral neocortex. *Neurosci. Res.* **9**: 79-102.

Tsumoto T., Hagihara H., Sato H., and Hata Y. (1987). NMDA receptors in the visual cortex of young kittens are more effective than those of adult cats. *Nature (London)* **327**: 513-514.

Turlejski K., Djavadian R. L., and Kossut M. (1997) Neonatal serotonin depletion modifies development but not plasticity in rat barrel cortex. *Neuroreport* **8**: 1823-1828.

Twitty V. C. (1937) Experiments on the phenomenon of paralysis produced by a toxin occurring in *Trituris* embryos. *J. Exp. Zool.* **76**: 67-104.

Twitty V. C. and Johnson H. H. (1934) Motor inhibition in Amblystoma produced by *Triturus* transplants. *Science* **80**: 78-79.

Ulupinar E., Datwani A., Behar O., Fujisawa H., and Erzurumlu R. (1999) Role of semaphorin III in the developing rodent trigeminal system. *Mol. Cell. Neurosci.* **13**: 281-292.

Valverde F. (1968) Structural changes in the area striata of the mouse after enucleation. *Exp. Brain Res.* **5**: 274-292.

Van der Loos H. (1976) Barreloids in mouse somatosensory thalamus. *Neurosci. Lett.* **2**: 1-6.

Van der Loos H., and Woolsey T. A. (1973) Somatosensory cortex: structural alterations following early injury to sense organs. *Science* **179**: 395-398.

Van Exan R. J., and Hardy M. H. (1980) A spatial relationship between innervation and the early differentiation of vibrissa follicles in the embryonic mouse. *J. Anat.* **131**: 643-656.

Verley R. and Axelrad H. (1975) Postnatal ontogenesis of potentials eliceted in the cerebral cortex by afferent stimulation. *Neurosci. Lett.* **1**: 99-107.

Villacres E. C., Wu Z., Hua W., Nielsen M. D., Watters J. J., Yan C., Beavo J., and Storm D. R. (1995) Developmentally expressed Ca^{2+}-sensitive adenylate cyclase activity is disrupted in the brains of type I adenylate cyclase mutant mice. *J. Biol. Chem.* **270:** 14352-14357.

Villacres E. C., Xia Z., Bookbinder L. H., Edelhoff S., Disteche C. M., and Storm D. R. (1993) Cloning, chromosomal mapping, and expression of human fetal brain type I adenylyl cyclase. *Genomics* **16:** 473-478.

Vincent S. B. (1912) The function of the vibrissae in the behavior of the white rat. *Behavl. Monogr.* **1:** 1-81.

Vitalis T., Cases O., Callebert J., Launay J. M., Price D. J., Seif I., and Gaspar P. (1998) Effects of monoamine oxidase A inhibition on barrel formation in the mouse somatosensory cortex: determination of a sensitive developmental period. *J. Comp. Neurol.* **393:** 169-184.

Volkmar F. R. and Greenough W. T. (1972) Rearing complexity affects branching of dendrites in the visual cortex of the rat. *Science* **176:** 1145-1147.

Vongdokmai R. (1980) effect of protein mulnutrition on development of mouse cortical barrels. *J. Comp. Neurol.* **191:** 283-294.

Vorherr T., Knopfel L., Hoffmann F., Mollner S., Pfeuffer T., and Carafoli E. (1993) The calmodulin binding domain of nitric oxide synthase and adenylyl cyclase. *Biochemistry* **32:** 6081-6088.

Waite P. M., and Cragg B. G. (1982) The peripheral and central changes resulting from cutting or crushing the afferent nerve supply to the whiskers. *Proc. R. Soc. Lond. (B)* **214:** 191-211.

Waite P. M., Marotte L. R., and Mark R. F. (1991) Development of whisker representation in the cortex of the tammar wallaby *Macropus eugeni*. *Dev. Brain Res.* **58:** 35-41.

Waite P. M., Marotte L. R., Leamey C. A., and Mark R. F. (1998) Development of whisker-related patterns in marsupials: factors controlling timing. *Trends. Neurosci.* **21:** 265-269.

Wallach J., Droste M., and Kluxen F. W. (1994) Molecular cloning of a novel type V adenylyl cyclase from rabbit myocardium. *FEBS Lett.* **338:** 257-263.

Walsh C., and Cepko C. L. (1988) Clonally related cortical cells show several migration patterns. *Science* **241:** 1342-1345.

Walsh C., and Cepko C. L. (1992) Widespread dispersion of neuronal clones across functional regions of the cerebral cortex. *Science* **255:** 434-440.

Walter J., Henke-Fahle S., Bonhoeffer F. (1987) Avoidance of posterior tectal membranes by temporal retinal axons. *Development* **101:** 909-913.

Walters E. T., Byrne J. H., Carew T. J., and Kandel E. R. (1983) Mechanoafferent neurons innervating tail of Aplysia. I. Response properties and synaptic connections. *J. Neurophysiol.* **50:** 1522-1542.

Wang Q., and Zheng J. Q. (1998) cAMP-mediated regulation of neurotrophin-induced collapse of nerve growth cones. *J. Neurosci.* **18:** 4973-4984.

Watanabe E., Aono S., Matsui F., Yamada Y., Naruse I., and Oohira A. (1995) Distribution of a brain-specific proteoglycan, neurocan, and the corresponding mRNA during the formation of barrels in the rat somatosensory cortex. *Eur. J. Neurosci.* **7:** 547-554.

Watson P. A., Krupinski J., Kempinski A. M., and Frankenfield C. D. (1994) Molecular cloning and characterization of the type VII isoform of mammalian adenylyl cyclase expressed widely in mouse tissues and in S49 mouse lymphoma cells. *J. Biol. Chem.* **269:** 28893-28898.

Wayman G. A., Impey S., Wu Z., Kindsvogel W., Pritchard L. and Storm D. R. (1994) Synergistic activation of the type I adenylyl cyclase by Ca^{2+} and G_s-coupled receptors *in vivo. J. Biol. Chem.* **269:** 25400-25405.

Weinberger R. P. and Rostas J. A. P. (1986) Subcellular distribution of a calmodulin-dependent protein kinase activity in rat cerebral cortex during development. *Brain Res.* **29:** 37-50.

Weiss P. (1939) *Principles of Development.* Holt, Rinehart and Winston, New York.

Welker C. (1971) Microelectrode delineation of fine grain somatotopic organization of (SmI) cerebral neocortex in albino rat. *Brain Res.* **26:** 259-275.

Welker C., and Woolsey T. A. (1974) Structure of layer IV in the somatosensory neocortex of the rat: description and comparison with the mouse. *J. Comp. Neurol.* **158:** 437-453.

Welker E., Armstrong-James M., Bronchti G., Ourednik W., Gheorghita-Baechler F., Dubois R., Guernsey D. L., Van der Loos H., and Neumann P. E. (1996) Modified tactile

processing in somatosensory cortex of a new mutant mouse, barrelless. *Science* **271:** 1864-1867.

Welker E., Hoogland P. V., and Van der Loos H. (1988) Organization of feedback and feedforward projections of the barrel cortex: a PHA-L study in the mouse. *Exp. Brain Res.* **73:** 411-435.

Welker W. I. (1964) Analysis of sniffing in the albino rat. *Brain Res.* **26:** 223-244.

Weller W. L. (1972) Barrels in somatic sensory neocortex of the marsupial *Trichosurus vulpecula* (brush-tailed possum). *Brain Res.* **43:** 11-24.

Weller W. L. (1993) SmI cortical barrels in an Australian marsupial, *Trichosurus vulpecula* (brush-tailed possum): structural organization, patterned distribution, and somatotopic relationships. *J. Comp. Neurol.* **337:** 471-492.

Weller W. L., and Johnson J. I. (1975) Barrels in cerebral cortex altered by receptor disruption in newborn, but not in five-day-old mice (*Cricetidoe and Muridae*). *Brain Res.* **83:** 504-508.

Welt C., and Steindler D. A. (1977) Somatosensory cortical barrels and thalamic barreloids in reeler mutant mice. *Neuroscience* **2:** 755-766.

Westerfield M., Liu D. W., Kimmel C. B., Walker C. (1990) Pathfinding and synapse formation in a zebrafish mutant lacking functional acetylcholine receptors. *Neuron* **4:** 867-874.

White E. L. (1976) Ultrastructure and synaptic contacts in barrels of mouse SI cortex. *Brain Res.* **105:** 229-251.

White E. L. (1978) Identified neurons in mouse SmI cortex which are postsynaptic to thalamocortical axon terminals: a combined Golgi-electron microscopic and degeneration study. *J. Comp. Neurol.* **181:** 627-661.

White E. L., and DeAmicis R. A. (1977) Afferent and efferent projections of the region in mouse SmI cortex which contains the posteromedial barrel subfield. *J. Comp. Neurol.* **175:** 455-482.

White E. L., and Hersch S. M. (1982) A quantitative study of thalamocortical and other synapses involving the apical dendrites of corticothalamic projection cells in mouse SmI cortex. *J. Neurocytol.* **11:** 137-157.

White E. L., and Keller A. (1987) Intrinsic circuitry involving the local axon collaterals of corticothalamic projection cells in mouse SmI cortex. *J. Comp. Neurol.* **262:** 13-26.

White E. L., Weinfeld L., and Lev D. L. (1997) A survey of morphogenesis during the early postnatal period in PMBSF barrels of mouse SmI cortex with emphasis on barrel D4. *Somatosens. Motor Res.* **14:** 34-55.

Wiesel T. N. (1982) Postnatal development of the visual cortex and the influence of environment. *Nature* **299:** 583-591.

Wiesel T. N. and Hubel D. H. (1965) Comparison of the effects of unilateral and bilateral eye closure on cortical unit responses in kittens. *J. Neurophysiol.* **28:** 1029-1040.

Wilkinson G. A., Rice F. L., Fundin B. T., Silos-Santiago I., Fagan A. M., Smeyne R. J., Glick S. D., Ernfors P. J., Reichardt L. F., and Barbacid M. (1995) Differential effects of various neurotrophin and Trk receptor deletions on the unmyelinated innervation of the epidermis in the mouse whisker pad. *Soc. Neurosci. Abstr.* **21:** 1540.

Williams M. N., Zahm D. S., and Jacquin M. F. (1994) Differential foci and synaptic organization of the principal and spinal trigeminal projections to the thalamus in the rat. *Eur. J. Neurosci.* **6:** 429-453.

Windisch J. M. , Marksteiner R., Lang M. E., Auer B., and Schneider R. (1995) Brain-derived neurotrophic factor, neurotrophin-3, and neurotrophin-4 bind to a single leucine-rich motif of TrkB. *Biochemistry* **34:** 11256-11263.

Wise S. P., and Jones E. G. (1976) The organization and postnatal development of the commissural projection of the rat somatic sensory cortex. *J. Comp. Neurol.* **168:** 313-343.

Wise S. P., and Jones E. G. (1977) Cells of origin and terminal distribution of descending projections of the rat somatic sensory cortex. *J. Comp. Neurol.* **175:** 129-157.

Wise S. P., and Jones E.G. (1978) Developmental studies of thalamocortical and commissural connections in the rat somatic sensory cortex. *J. Comp. Neurol.* **178:** 187-208.

Wolpert L. (1969) Positional information and the spatial pattern of cellular differentiation. *J. Theor. Biol.* **193:** 296-307.

Wolpert L. (1977) *The Development of Pattern and Form in Animals.* Carolina Biological, Burlington, NC.

Wong S. T., Athos J., Figueroa X. A., Pineda V. V., Schaefer M. L., Chavkin C. C., Muglia L. J., and Storm D. R. (1999) Calcium-stimulated adenylyl cyclase activity is critical for hippocampus-dependent long-term memory and late phase LTP. *Neuron* **23:** 787-798.

Wong-Riley M. (1979) Changes in the visual system of monocularly sutured or enucleated cat demonstrable with cyctochrome oxidase histochemistry. *Brain Res.* **171:** 11-28.

Wong-Riley M. T. (1989) Cytochrome oxidase: an endogenous metabolic marker for neural activity. *Trends. Neurosci.* **12:** 94-101.

Wong-Riley M. T., and Welt C. (1980) Histochemical changes in cytochrome oxidase of cortical barrels after vibrissal removal in neonatal and adult mice. *Proc. Natl. Acad. Sci. U.S.A.* **77:** 2333-2337.

Woolsey C. N. (1958) Organization of somatic sensory and motor areas of the cerebral cortex. In: *Biological and Biochemical Basis of Behavior.* Harlow H. F. and Woolsey C. N. (eds.). University of Wisconsin Press, Madison, pp: 63-82..

Woolsey T. A. (1990) Peripheral alteration and somatosensory development. In: *Development of Sensory Systems in Mammals.* Coleman Jr. (ed.), Wiley Press, New York, pp: 461-516.

Woolsey T. A., and Van der Loos H. (1970) The structural organization of layer IV in the somatosensory region (SI) of mouse cerebral cortex. The description of a cortical field composed of discrete cytoarchitectonic units. *Brain Res.* **17:** 205-242.

Woolsey T. A., and Wann J. R. (1976) Areal changes in mouse cortical barrels following vibrissal damage at different postnatal ages. *J. Comp. Neurol.* **170:** 53-66.

Woolsey T. A., Anderson J. R., Wann J. R., and Stanfield B. B. (1979) Effects of early vibrissae damage on neurons in the ventrobasal (VB) thalamus of the mouse. *J. Comp. Neurol.* **184:** 363-380.

Woolsey T. A., Dierker M. L., and Wann D. F. (1975a) Mouse SmI cortex: qualitative and quantitative classification of Golgi-impregnated barrel neurons. *Proc. Natl. Acad. Sci. U.S.A.* **72:** 2165-2169.

Woolsey T. A., Welker C., and Schwartz R. H. (1975b) Comparative anatomical studies of the SmI face cortex with special reference to the occurrence of "barrels" in layer IV. *J. Comp. Neurol.* **164:** 79-94.

Wu Z., Wong S. T., and Storm D. R. (1993) Modification of the Ca^{2+}/Calmodulin sensitivity of the type I adenylyl cyclase by mutagenesis of its calmodulin binding domain. *J. Biol. Chem.* **268:** 23766-23768.

Wu Z-L., Thomas S. A., Villacres E. C., Xia Z., Simmons M. L., Chavkin C., Palmiter R. D., and Storm D. R. (1995) Altered behavior and long-term potentiation in type I adenylyl cyclase mutant mice. *Proc. Natl. Acad. U.S.A.* **92:** 220-224.

Xia Z., and Storm D. R. (1997) Calmodulin-regulated adenylyl cyclases and neuromodulation. *Curr. Opin. Neurobiol.* **7:** 391-396.

Xia Z., Choi E. J., Wang F., Blazynski C., and Storm D. R. (1993) Type I calmodulin-sensitive adenylate cyclase is neural specific. *J. Neurochem.* **60:** 305-311.

Xia Z., Refsdal C. D., Merchant K. M., Dorsa D. M., and Storm D. R. (1991) Distribution of mRNA for the Calmodulin-sensitive Adenylate cyclase in rat brain: Expression in areas associated with learning and memory. *Neuron* **6:** 431-443.

Yamamoto M., Ozawa H., Saito T., Hatta S., Riederer P., and Takahata N. (1997) Ca^{2+}/CaM-sensitive adenylyl cyclase activity is decreased in the Alzheimer's brain: possible correlation to type I adenylyl cyclase. *J. Neural Transm.* **104:**721-732.

Yan Q., Radeke M. J., Matheson C. R., Talvenheimo J., Welcher A. A., and Feinstein S. C. (1997) Immunocytochemical localization of TrkB in the central nervous system of the adult rat. *J. Comp. Neurol.* **378:** 135-157.

Yau K. W. (1994) Cyclic nucleotide gated channels: an expanding new family of ion channels [comment]. *Proc. Natl. Acad. U.S.A.* **91:** 3481-3483.

Yoshimura M., and Cooper D. M. F. (1992) Cloning and expression of a Ca^{2+}-inhibitable adenylyl cyclase from NCB-20 cells. *Proc. Natl. Acad. Sci. U.S.A.* **89:** 6716-6720.

Zacco A., Cooper V., Chantler P. D., Fisher-Hyland S., Horton H. L., and Levitt P. (1990) Isolation, biochemical characterization and ultrastructural analysis of the limbic system-associated membrane protein (LAMP), a protein expressed by neurons comprising functional neural circuits. *J. Neurosci.* **10:** 73-90.

Zafra F., Castrén E., Thoenen H., and Lindholm D. (1991) Interplay between glutamate and gamma-aminobutyric acid transmitter systems in the physiological regulation of brain-derived neurotrophic factor and nerve growth factor synthesis in hippocampal neurons. *Proc. Natl. Acad. U.S.A.* **88:** 10037-10041.

Zhang G., Liu Y., Ruoho A. E., and Hurley J. H. (1997) Structure of the adenyly cyclase catalytic core. *Nature* **386:** 247-253.

Zheng J. Q., Zheng Z., and Poo M-m. (1994) Long-range signaling in growing neurons after local elevation of cyclic AMP-dependent activity. *J. Cell Biol.* **127:** 1693-1701.

Zhou X. F., and Rush R. A. (1994) Localization of neurotrophin-3-like immunoreactivity in the rat central nervous system. *Brain Res.* **643:** 162-172.

Zhu X. O., and Waite P. M. (1998) Cholinergic depletion reduces plasticity of barrel field cortex. *Cereb. Cortex* **8:** 63-72.

Zimmerman S. L. (1995) Cyclic nucleotide gated channels *Curr. Opin. Neurobiol.* **5:** 296-303.

Zucker E. and Welker W. I. (1969) Coding of somatic input by vibrissae neurons in the rat's trigeminal ganglion. *Brain Res.* **12:** 138-156.

Zufall F., Firestein S., and Shepherd G. M. (1994) Cyclic nucleotide-gated ion channels and sensory transduction in olfactory receptor neurons. *Annu. Rev. Biophys. Biomol. Struct.* **23:** 577-607.